



CENOZOIC CONTOURITE DRIFTS AND  
PALAEOCEANOGRAPHIC  
DEVELOPMENT OF THE FAEROE-  
SHETLAND BASIN

MICHAEL WILLIAM HOHBEIN

Submitted in partial fulfilment of the requirements for the  
degree of Ph.D.

Cardiff University

December 2005

UMI Number: U584790

All rights reserved

INFORMATION TO ALL USERS

The quality of this reproduction is dependent upon the quality of the copy submitted.

In the unlikely event that the author did not send a complete manuscript and there are missing pages, these will be noted. Also, if material had to be removed, a note will indicate the deletion.



UMI U584790

Published by ProQuest LLC 2013. Copyright in the Dissertation held by the Author.  
Microform Edition © ProQuest LLC.

All rights reserved. This work is protected against  
unauthorized copying under Title 17, United States Code.



ProQuest LLC  
789 East Eisenhower Parkway  
P.O. Box 1346  
Ann Arbor, MI 48106-1346

*I dedicate this thesis in memory of my grandfathers,  
Ron Hohbein and Maurice Luck, who sparked  
my interest in geology at an early age*

# Summary

This thesis investigated the palaeoceanographic history of the Faeroe Shetland Basin, NE Atlantic, via identification and analysis of contourite drift deposits using petroleum industry seismic and well data. Integration of regional 2D seismic lines, 3D seismic volumes and high resolution seismic profiles with industrial well data permitted full spatial and temporal characterisation of the contourites within the basin, including identification of small scale architectural elements and subtle stratigraphic relationships. In turn, it was possible to make interpretations regarding the palaeoceanographic regime within the basin from the onset and evolution of thermohaline current flow through the basin to correlation with the present day oceanographic situation. Overall, the study serves to highlight the efficacy of industrial seismic and well data for contourite and palaeoceanographic research.

A variety of contourite drift types were identified during seismic-chronostratigraphic division of the Cenozoic succession. Identification of an early middle Eocene contourite drift within the southern Faeroe Shetland Basin dates the onset of southerly flowing deep waters from the Norwegian Greenland Sea into the North Atlantic as part of a North Atlantic Conveyor Belt-style circulation system at approximately 49 million years, predating previous estimates by more than 15 million years. The presence of Oligocene, Miocene and Pliocene contourite drifts within the basin reveals that following initiation in the middle Eocene, southerly flowing deep water circulation through the basin was continuous throughout the late Palaeocene and Neogene to the present day. A gradual increase in deep water flux through the basin throughout this time is hypothesised based on contourite distribution, and is thought to relate to the global greenhouse to icehouse climatic transition that occurred during the Cenozoic. Pulses of increased deep water current velocity related to a combination of climatic and tectonic factors are thought to be responsible for the formation of major deep water erosional unconformities which are associated with the contourite drift successions. A link between contourite deposition and the climatic fluctuations that characterised the late Neogene northern hemisphere is also proposed based on the identification of direct indicators of significant glaciation including iceberg plough marks within the contourite drift units. Contourite drift deposition is interpreted to occur predominantly during climatically warmer episodes, while periods of glaciation are characterised by apparent disruption of ocean current circulation within the basin.



## Acknowledgements

Writing these words fills me with a combination of giddy joy and slight trepidation. After what feels like a long journey, I would like to thank those who helped me along the way, and if I forget anyone to whom thanks are owed, which I fear is inevitable, I thank you too.

First and foremost, I would like to thank Prof. Joe Cartwright with utmost sincerity for giving me the opportunity to undertake this research, and for his continued mentoring and guidance throughout the project, which has been absolutely invaluable. Cheers Joe. I would also like to thank the organisations without whom this project would not have been possible. I am grateful to the Natural Environment Research Council and Shell U.K. Ltd for funding the research. I am also grateful to BP, Conoco Phillips, ExxonMobil, Amerada Hess, Total, Veritas DGC, PGS, Schlumberger, Western Geophysical, Fugro-Geoteam AS, TGS Nopec and the British Geological Survey for providing data which enabled me to complete this study. Schlumberger are thanked for providing the means to interpret the seismic data, in the form of software and hardware. Thanks also to the 3Dlab managers, Neil and Gwen, for providing technical support and advice, and to Gwen for her computer related support.

I would like to acknowledge the staff and students of the earth science department for advice, support and friendship during the course of my study. All of the staff members who's door I have knocked on asking advice are gratefully thanked for their time and input. I thank the members and affiliates of the 3D lab, past and present, for making the 3Dlab such a good place to be. In particular, Paul Knutz is thanked for his input into the project at the beginning, and Richard Davies, Mads Huuse and David James are thanked for their time and advice, which was extremely valuable and is greatly appreciated. Thanks to all of the students of the lab for making it the place it is, in particular Dorthe Hansen for among other things her seemingly inexhaustible knowledge of Geoquest and also Mairi Nelson & Claudia Bertoni. A very special thanks goes to my fellow office-comrades; Andy Robinson, Valente Ricoy, Jose Frey, Rob Evans and Mostyn Wall, for all the work related and non-work related discussions and laughs and helping me survive my stint in 3.16. Cheers guys.

There are a few other people I would like to thank. Thanks to Jon Trueman and BP for being so forthcoming in supplying data and giving his time, Russell Wynn and Doug Masson for their perspectives, thoughts and time, which had a big impact on development of some of my ideas, Dorrik Stow for giving me the opportunity to view contourites in the field and Huw Edwards and Chris Drage for allowing me to visit PGS to look at the FSB mega-merge. Sincere thanks also to Sharon and Terry for all your help and support.

Finally, and perhaps most importantly, I would like to thank my family: Mum, Dad, Chris and my Nans. Without your continued support, both moral and financial, throughout my educational career, I could never have got to here, and so I am entirely indebted to you. Thank you. And of course Lins, without your unfaltering, unconditional support and patience over the past 3 years I seriously doubt whether I could have made it. Thank you so much.

## Note regarding thesis structure

This thesis consists of three main research components, Chapters Two, Three and Four, which have been prepared in the style of scientific papers for submittal to international journals. The status of each chapter at the time of submittal of the thesis is summarised below:

*Chapter Two* is in final preparation for submittal to *Paleoceanography* as '*A Middle-Eocene onset of the North Atlantic Conveyor Belt: evidence from the Faeroe-Shetland Basin*'. Hohbein, M.W. and Cartwright, J.A.

*Chapter Three* is in final preparation for submittal to *Marine Geology* as '*Late Palaeogene-Neogene contourite drifts and palaeoceanographic evolution of the Faeroe Shetland Basin*'. Hohbein, M.W. and Cartwright, J.A.

*Chapter Four* has been submitted to *Marine Geology* as '*3D seismic analysis of the West Shetland Drift system: implications for late Neogene palaeoceanography of the NE Atlantic*'. Hohbein, M.W. and Cartwright, J.A., and is in review.

# Table of contents

Summary.....	i
Acknowledgements.....	ii
Note regarding thesis structure.....	iv
Table of contents.....	v
List of Figures.....	ix
Appendices.....	xx

## Chapter One

<b>1. Introduction.....</b>	<b>1-1</b>
1.1. Rationale.....	1-1
1.2. Aims.....	1-5
1.3. Geological Setting.....	1-6
1.4. Seismic analysis of contourites and their palaeoceanographic significance.....	1-9
1.5. Data and methodology.....	1-13
<i>1.5.1. Database.....</i>	<i>1-13</i>
<i>1.5.2. Methodology.....</i>	<i>1-13</i>
1.6. Thesis layout.....	1-17

## Chapter Two

<b>2. Eocene contourite drifts and initiation of overflow across the Greenland Scotland Ridge.....</b>	<b>2-1</b>
2.1. Abstract.....	2-1
2.2. Introduction.....	2-2
2.3. Regional geological setting and oceanography.....	2-3
<i>2.3.1. Geological setting.....</i>	<i>2-3</i>
<i>2.3.2. Oceanographic circulation.....</i>	<i>2-5</i>
<i>2.3.3. Seismic expression of contourite drifts.....</i>	<i>2-7</i>
2.4. Data and methodology.....	2-9
2.5. Seismic Interpretation.....	2-11
<i>2.5.1. Seismic stratigraphy.....</i>	<i>2-11</i>
<i>2.5.2. High resolution seismic stratigraphic analysis of the southern Judd basin.....</i>	<i>2-14</i>
<i>2.5.2.1. Unit P10.....</i>	<i>2-14</i>
<i>2.5.2.2. Unit P20.....</i>	<i>2-19</i>
<i>2.5.2.3. Unit P30.....</i>	<i>2-24</i>
<i>2.5.2.4. Units P30a and P30b.....</i>	<i>2-28</i>

2.5.2.5. Depositional origin of Unit P30 .....	2-30
2.5.3. Regional seismic stratigraphic analysis .....	2-30
2.6. Biostratigraphic dating of the stratigraphy .....	2-32
2.6.1. Well 204/22-1 .....	2-33
2.6.2. Well 204/23-1 .....	2-33
2.6.3. Well 204/24A-1 .....	2-33
2.6.4. BGS 99/3 .....	2-34
2.6.5. Synthesis of Well results .....	2-34
2.6.6. Regional correlation of Unit P30 .....	2-35
2.7. Tectonostratigraphic evolution of the southern Faeroe Shetland Basin during the Eocene .....	2-35
2.8. Discussion: Palaeoceanographic evolution and the North Atlantic Conveyor Belt .....	2-39
2.8.1. An Eocene North Atlantic Conveyor Belt .....	2-39
2.8.1.1. Depositional current .....	2-39
2.8.1.2. Deep water connection .....	2-40
2.8.1.3. Deep water formation .....	2-44
2.8.2. Previous estimates for the onset of deep water exchange across the Greenland Scotland Ridge .....	2-46
2.8.3. Synthesis of evidence: Middle Eocene onset of the North Atlantic Conveyor Belt .....	2-48
2.9. Conclusions .....	2-49

## Chapter Three

<b>3. Late Palaeogene and Neogene contourites and palaeoceanographic evolution of the Faeroe Shetland Basin .....</b>	<b>3-1</b>
3.1. Abstract .....	3-1
3.2. Introduction .....	3-2
3.3. Geological and oceanographic setting .....	3-3
3.4. Data and methodology .....	3-6
3.5. Seismic stratigraphy .....	3-7
3.5.1. Palaeogene and Neogene sediment distribution .....	3-7
3.5.2. Late Palaeogene-Neogene units and boundaries .....	3-9
3.5.3. Biostratigraphic calibration .....	3-12
3.5.3.1. Seismic-Well correlation .....	3-12
3.5.3.2. Well summary .....	3-14
3.6. Clarification of Neogene seismic stratigraphy within the Faeroe Shetland Basin .....	3-15
3.7. Definition of the Intra-Neogene Unconformity .....	3-19
3.8. Seismic-stratigraphic units .....	3-25
3.8.1. Unit CD10 .....	3-25
3.8.2. Unit CD20 .....	3-28
3.8.3. Unit CD30 .....	3-30
3.8.4. Unit CD40 .....	3-34

3.8.5. Unit CD50.....	3-35
3.8.6. Horizon E.....	3-40
3.8.7. Key observations.....	3-41
3.9. Discussion.....	3-42
3.9.1. Deep water unconformities.....	3-42
3.9.1.1. Erosional magnitude.....	3-42
3.9.1.2. Mechanism of formation.....	3-46
3.9.2. Sedimentary and palaeoceanographic development.....	3-49
3.10. Conclusions.....	3-54

## Chapter Four

<b>4. 3D Seismic analysis of the late Neogene West Shetland Drift.....</b>	<b>4-1</b>
4.1. Abstract.....	4-1
4.2. Introduction.....	4-2
4.3. Regional setting.....	4-6
4.3.1. Basin evolution and stratigraphy.....	4-6
4.3.2. Shetland margin subsidence.....	4-8
4.4. Data and methodology.....	4-9
4.5. The West Shetland Drift Slope section.....	4-9
4.5.1. Areal distribution.....	4-10
4.5.2. Internal seismic-stratigraphic division.....	4-13
4.6. Internal unit analysis.....	4-15
4.6.1. Basal surface.....	4-15
4.6.2. Unit 1.....	4-17
4.6.2.1. Unit 1a.....	4-17
4.6.2.2. Unit 1b.....	4-19
4.6.2.3. Sediment wave field.....	4-21
4.6.3. Horizon PL40.....	4-26
4.6.3.1. Seismic character and areal distribution.....	4-26
4.6.3.2. Iceberg plough-marks.....	4-27
4.6.4. Unit 2.....	4-30
4.6.5. The Glacial Unconformity and Unit 3.....	4-31
4.7. Discussion.....	4-32
4.7.1. Sedimentary processes and slope evolution.....	4-33
4.7.1.1. Downslope processes.....	4-33
4.7.1.2. Alongslope processes.....	4-35
4.7.1.3. Glacial influences.....	4-38
4.7.2. Palaeoceanographic development of the West Shetland Margin.....	4-40
4.8. Conclusions.....	4-42

## Chapter Five

<b>5. Discussion</b>	<b>5-1</b>
5.1. Introduction	5-1
5.2. Results summary	5-2
5.2.1. Chapter Two	5-2
5.2.2. Chapter three	5-2
5.2.3. Chapter Four	5-4
5.3. Cenozoic evolution of the Faeroe Shetland Basin	5-4
5.3.1. Summary of alongslope current sedimentation	5-4
5.3.2. Correlation with Cenozoic global change	5-7
5.3.2.1. Development of the Faeroe Shetland Basin as an oceanic gateway	5-7
5.3.2.2. Palaeoceanographic evolution	5-8
5.3.2.3. Formation of the Intra-Neogene Unconformity	5-11
5.4. Utilisation of industrial data for contourite research	5-12
5.4.1. Advantages of industrial seismic data	5-12
5.4.2. Previous studies within the Faeroe-Shetland Basin	5-14
5.4.3. Advances made by this study	5-16
5.5. Limitations and further study	5-20
5.5.1. Limitations of industrial data	5-20
5.5.1.1. General limitations of industry data	5-20
5.5.1.2. Limitations of industry data within the Faeroe Shetland Basin	5-21
5.5.2. Future study	5-22
5.5.2.1. Investigation of onset of the North Atlantic Conveyor Belt	5-22
5.5.2.2. Further study within the Faeroe Shetland Basin	5-23

## Chapter Six

<b>6. Conclusions</b>	<b>6-1</b>
6.1. General conclusions	6-1
6.2. Concluding remarks from Chapter Two	6-2
6.3. Concluding remarks from Chapter Three	6-3
6.4. Concluding remarks from Chapter Four	6-4
<b>7. Bibliography</b>	<b>7-1</b>
<b>Appendix 1. Seismic database</b>	<b>A1-1</b>
<b>Appendix 2. Well database</b>	<b>A2-1</b>

# List of Figures

## Chapter One: Introduction

Figure No.	Figure Caption	Page No.
1.1.	<p>(a) Map to illustrate Global ocean circulation, modified from Rahmstorf (2002). Warm surface currents are represented in red, cold deep water currents in blue and Antarctic sourced bottom waters in purple. The flow direction is given by white arrows, and areas of major deep water generation and down welling are represented by yellow markers. Generation of deep waters in the Northern North Atlantic and Nordic Seas is clearly linked to the global ocean circulatory system.</p> <p>(b) Regional bathymetric features associated with the Faeroe Shetland Basin (FSB). Most significant is the Greenland Scotland Ridge comprised of the Iceland-Greenland Ridge (IGR), Iceland, Iceland-Faeroe Ridge (IFR) and the FSB. Deep water is permitted to cross the ridge at three locations, the Denmark Strait (DS), the IFR and the FSB, and deep water fluxes are represented by arrows (<math>1\text{ Sv}=1\text{ million m}^3\text{ s}^{-1}</math>). Image modified from <a href="http://topex.uscd.edu">http://topex.uscd.edu</a> using Bott (1983) and Hansen and Osterhus (2000). Abbreviations: RP, Rockall Plateau; RT, Rockall Trough; AR, Aegir Ridge; NGS, Norwegian Greenland Sea; JMFZ, Jan Mayan Fracture Zone.</p> <p>(c) Bathymetry of the Faeroe Shetland Basin. Main structural elements which define the basin are represented, schematically illustrated in Figure 1.2. Faeroe Shetland Channel refers to present day bathymetric expression of tectonic Faeroe Shetland Basin. Simplified ocean circulation through the basin represented by coloured arrows; red arrows represent warm surface inflow waters; blue arrows represent cold Norwegian Sea Overflow Water (simplified from Turrell et al., 1999). Abbreviations: MKR, Munkagrunnar Ridge, FBC, Faeroe Bank Channel; WTR, Wyville Thompson Ridge; JA, Judd Anticline; WR, Westray Ridge; RR, Rona Ridge; SSF, Shetland Spine Fault; CR, Corona Ridge; EFR, East Faeroes Ridge; FR, Fugloy Ridge. Map populated with data from Boldreel and Andersen (1993), Andersen et al. (1995), Naylor et al. (1999), Turrell et al. (1999). Please note that figure numbering applies to this chapter only, and therefore 'Figure 2' refers to Figure 1.2.</p>	1-2
1.2.	Schematic cross section across the Faeroe Shetland Basin to illustrate the underlying structure of the basin and the nature of the Cenozoic sediment fill (line location Figure 1.1). The basin is bounded by large NW dipping normal faults on the Shetland margin, and a combination of probable fault blocks combined with Palaeocene lavas on the Faeroese margin. The thick lava succession on the Faeroese margin hampers imaging of underlying Mesozoic stratigraphy and structure. Figure modified from Doré et al. (1999).	1-7
1.3.	Schematic illustration of the key seismic characteristics of contourite drifts. Re-drawn from Stow et al. (2002).	1-10
1.4.	Contourite drift types and their typical seismic reflection configurations and key diagnostic criteria. Infill drifts are generally similar to sheeted drifts, and are therefore not defined separately. Contourite drift geometries can be used to draw inferences upon the locus of depositional current. Modified from Faugères et al. (1999); Stow et al. (2002).	1-12
1.5.	Map of the Faeroe Shetland Basin illustrating the dataset available to the study. The seismic data consists of 13 2D surveys of varying vintages combined with 8 3D surveys (one reprocessed survey not shown) and a high resolution 2D seismic grid. Petroleum exploration wells are represented by red crosses. Note the bias in data coverage toward the Shetland Margin, resulting from a combination of existing discoveries and play fairway distribution, shallow water, and absence of thick basalt coverage which blights exploration of the Faeroese Margin (see Fig 1.2).	1-14
1.6.	Representative 2D seismic profile to illustrate reduction in vertical resolution with increased depth. Sonic velocities calibrated by correlation with well 213/23-1. Note	1-16



increase in velocity with depth, likely due to increased compaction, coupled with decrease in frequency as a result of attenuation, resulting in a decrease in vertical resolution. Interval of interest to this study predominantly lies within the upper resolution interval, with vertical resolutions of c. 10-15m. Abbreviations: V= velocity; F= frequency; VR=vertical resolution;  $\lambda$ = wavelength.

## Chapter Two: Eocene contourite drifts and initiation of overflow across the Greenland Scotland Ridge

Figure No.	Figure Caption	Page No.
2.1.	Map of the North Atlantic and Norwegian Greenland Sea. Contours show bathymetry in metres. Arrows and Sv values ( $1 \text{ Sv} = 1 \text{ Sverdrup} = 10^6 \text{ m}^3 \text{ s}^{-1}$ ) represent deep water overflow volumes across the Greenland Scotland Ridge (Hansen and Osterhus, 2000). Abbreviations: IGR, Iceland-Greenland Ridge; IFR, Iceland-Faeroe Ridge; F, Faeroe Islands; S, Shetland Islands; DS, Denmark Strait; RT, Rockall Trough. Figure references refer to figures within chapter e.g. 'Fig 2' refers to Figure 2.2.	2-4
2.2.	Bathymetry map of the Faeroe-Shetland Basin illustrating location of seismic profiles and seismic datasets. The study focuses on the Judd Basin area, approximately defined by high resolution seismic survey (black grid at southern end of basin). Coloured arrows represent present day oceanographic circulation: red arrows- warm saline inflow waters into the Norwegian Greenland Sea; blue arrows - cold deep water outflow waters. Black line illustrates areal extent of the Unit P30 contourite drift. Abbreviations: FBC, Faeroe-Bank Channel; MKR, Munkagrunnar Ridge. Inset map displays data available to this study. Thin grey lines = 2D seismic database; black lines = high resolution 2D seismic survey; red boxes = 3D data sets; red dots = available wells; 5 key wells used in this study are named. Figure labels refer to Figures within this chapter, e.g. Figure 3 represents the location of Figure 2.3.	2-6
2.3.	Regional strike-orientated 2D seismic profile along the axis of the Faeroe Shetland Basin (line location Fig. 2.2) illustrating spatial distribution of key units. Note shallowing of the Top Balder reflection to the SW, and the dominance of Palaeogene strata toward the SW, thus defining the Palaeogene and Neogene (including Oligocene) depocentres. Note also progressive SW onlap of reflections within Unit P30. Inset panel shows 2D line 20km to SE and details the calibration of late Eocene ( <i>A. michoudii</i> - Priabonian) within well 213 23-1. Figure references refer to figures within chapter e.g. 'Fig 4' refers to Figure 2.4.	2-8
2.4.	Regional 2D seismic profile across the basin (line location Fig. 2.2). The line illustrates the domination of the post-Balder stratigraphy of the southern Faeroe Shetland Basin by Unit P30, which is seen to influence present day seabed topography. Internal reflections exhibit NW directed onlap onto the IEC (Intra-Eocene unconformity) on the Faeroes margin, and SE directed intercalation with and onlap onto the base of slope fans (B.o.s. fans) and the IEC, revealing the mounded depositional geometry. Figure references refer to figures within chapter e.g. 'Fig 3' refers to Figure 2.3.	2-12
2.5.	Chronostratigraphic, biostratigraphic and seismic-stratigraphic scheme for the Eocene of the Faeroe Shetland Basin, with the addition of the late Neogene to illustrate the occurrence of the INU. First and last occurrence datums of Palaeogene dinocyst index events allow dating of the stratigraphy. The stratigraphic top of Unit P30 remains undefined. $\delta^{18}\text{O}$ curve for the Eocene reveals steady increase in isotopic values in relation to global cooling following the Early Eocene Climatic Optimum (EECO, Zachos et al., 2001). Biostratigraphy abbreviations: (B)- Bujak and Mudge (1994); (H)- Hardenbol et al. (1998); (W)- Williams et al. (2004); (NML)- Northern Hemisphere mid-latitudes.	2-13
2.6.	High resolution composite 'dogleg' 2D seismic profile (line location Fig. 2.2). Profile illustrates the stratigraphy devised for this study. Note bi-directional downlap of Unit P30a across the Judd Anticline, and significant S-SW directed onlap formed by Unit P30b. Profile also clearly illustrates erosional truncation of stratigraphy beneath the INU. BGS	2-15

	Borehole 99 3 is located at SE limit of this profile.	
2.7	High resolution 2D seismic profile oriented perpendicular to the basin margins (line location Fig. 2.2). Line illustrates stratigraphic division of this study. Note prograding clinoforms and topset incision within Unit P10, turbidite lenses and stratigraphic thinning toward the SE onto the Judd Anticline within unit P20. Well 204/22-1, 15km to the SW of the profile lithologically calibrates the base of slope fan (Fig. 2.11).	2-17
2.8.	Isopach maps of Units P10 (8a), P20 (8b) and P30 (8c). (a) Isopach map of Unit P10. Unit exhibits approximately circular thickness distribution with no sign of stratigraphic thinning across the Judd Anticline, suggesting that the feature exhibited little or no topography during deposition. Figures 2.9 and 2.10 reveal internal prograding clinoforms, with the general northerly progradation represented by arrows. Lithologically the unit is calibrated by each of the wells. (b) Isopach map of Unit P20. Figures 2.6 and 2.7 reveal that the Unit thins onto the Judd Anticline prior to truncation beneath the IEU toward the SE, and Figure 2.3 reveals stratigraphic thinning to the SW onto the Judd anticline and toward the NE. Turbidite accumulation is restricted to the area NE of the Judd Anticline and thinning onto the Shetland and Faeroese margins and toward the NE suggests that the Unit was limited in all directions by topographic control. (c) Isopach map of Unit P30 reveals broad elongate mounded thickness distribution with internal reflection onlap downlap toward the SE, SW and NW (Figs. 2.4, 2.6 & 2.14) represented by open arrows. Unit is calibrated biostratigraphically and lithologically by BGS borehole 99 3 and Well 213 23-1. 'Fig' references refer to the location of seismic profiles within this Chapter, e.g. 'Fig 9' refers to Figure 2.9.	2-18
2.9.	Regional dip 2D seismic profile (line location Fig. 2.2) to illustrate prograding clinoforms of Unit P10, now tilted, on the Faeroese Margin. Clinoforms are associated with aggradational topsets, suggesting continued subsidence during deposition of Unit P10.	2-20
2.10.	High resolution strike directed 2D seismic profile (line location Fig. 2.2). Profile illustrates the stratigraphy defined by this study. The location of the Judd Deep toward the crest of the Judd Anticline which limits SW extent of Units P10, P20 and P30. Northward prograding clinoforms within Unit P10 are clearly visible. Also note incorporation of turbidite lenses on limb of Judd Anticline, suggesting growth of the fold following deposition of the turbidites.	2-21
2.11.	Well correlation panel of 4 key wells (locations Fig. 2.2). Figure illustrates lithology of stratigraphic succession defined here. Key biostratigraphic marker taxa (dinocyst) are identified (LOD –last occurrence datum), with taxon ranges provided in Fig. 2.5. The IEU which divides the contourite deposition of Unit P30 from underlying units is marked on each well, and is found to consistently be underlain by Ypresian markers and overlain by Lutetian markers. Well 204 22-1 calibrates the base of slope fan from Fig. 2.7 at depths of 1310-1350m, recording coarse rounded quartzose sand overlain and underlain by mudstone. All depths are total vertical depth sub sea level (TVDSS) in metres.	2-23
2.12.	Isochron maps of Unit P30 and associated packages. (a) Illustrates the overall thickness of Unit P30 as mapped using only the high resolution 2D data grid. Note thinning over the Judd Anticline. Thickening on the Shetland slope represents the coeval Shetland margin progradation system. Open arrows represent slope clinoform progradation, solid arrows represent onlap of P30 internal reflections onto the basal IEU surface. (b) Shows the thickness distribution of the base of slope fans which interdigitate with the P30 contourite drift at the base of slope. Individually the fans thin proximally and distally (Fig. 2.13) but when mapped collectively they exhibit greatest thickness at the base of the slope and thin basinward. Arrows represent direction of sedimentation. (c) Reveals the thickness distribution of Unit P30a. The unit is characterised by bi-directionally downlapping reflections that do not exhibit stratal condensation onto the Judd Anticline toward the SE (Fig. 2.6), unlike the overlying Unit P30b (Fig. 2.6). The limits of the unit are defined by depositional lapout to the SE and the NW, and onto the Judd Anticline toward the SW (Figs. 2.6 & 2.7). (d) Illustrates the thickness distribution of Unit P30b, and includes translation of the	2-25

	horizon from the high resolution data to standard 2D data to the NW. The internal reflections continue the onlap configuration of Unit P30a (Figs. 2.6 & 2.11), represented by arrows, resulting in a greater areal extent than Unit P30a. Apparent thinning across the c.N/S fold structure is created by erosion by the INU (Fig. 2.3). The 'Fig' references refer to the location of seismic profiles within this Chapter, e.g. 'Fig 7' refers to Figure 2.7.	
2.13.	High resolution 2D seismic profile to show detail of interdigitation of the P30 contourite drifts and the base of slope fans (line location Fig. 2.2). Note onlap of the contourite reflections onto the stacked fan bodies, and onlap onto the IEU. The SE directed onlap of Unit P30 reflections confirm that the unit consists of bi-directionally downlapping reflections creating 'mounded' internal reflections.	2-27
2.14.	3D seismic strike line parallel to the basin axis to illustrate the increase in onlap angle of the P30 reflections onto the IEU (line location Fig. 2.2). The lapout of internal reflections evolves from an onlap with angular discordance of c.1° with the IEU into downlap exhibiting angular discordance of c.1.5° with the IEU. The intense polygonal faulting of Unit P30 is also clearly displayed.	2-29
2.15.	Schematic seismic facies map to illustrate the evolution of the southern Faeroe Shetland Basin during the Eocene. (a): Early Ypresian northward prograding deltaic system into water depths of c.300m (Smallwood, 2004). Emergent landmass south and east of the Judd Anticline evidenced by coals and delta top facies in wells 204/22-1, 204/23-1 and 204/24-1a. Landmass to south provided sediment. The Judd Anticline exerted no topographic control on sedimentation. Deep water conditions present within basin axis to north (location of deep water on map not geographically constrained in this study). (b): During the Ypresian, deltaic sedimentation ceased and turbidite deposition commenced, representing subsidence of the basin and the establishment of marine conditions throughout the area represented by a southward marine transgression. Restriction of turbidite accumulation to the north of the Judd Anticline evidences initial growth of the fold during this time, as suggested previously (Robinson, 2004; Smallwood, 2004). Input direction of the turbidites is unknown and no channels have been identified, but active fold growth may have triggered seabed instability. (c): During the Lutetian the Judd anticline was breached by SW flowing bottom currents resulting in formation of the IEU and deposition of the P30 contourite body, calibrated by BGS borehole 99/3. Breaching of the Judd anticline was associated with subsidence of the basin axis to water depths of c.450m, resulting in development of coeval Shetland margin progradation, calibrated by wells 204/22-1, 204/23-1 and 204/24-1a. Base of slope fan deposition associated with the Shetland slope system occurred in conjunction with contourite sedimentation, resulting in contourite-fan intercalation. Downslope-sourced sediment may have been reworked by bottom currents. Sedimentation from the Faeroese margin appears to have been minimal, likely due to a lack of a significant proximal land mass.	2-36

### Chapter Three: Late Palaeogene and Neogene contourites and palaeoceanographic evolution of the Faeroe Shetland Basin

Figure No.	Figure Caption	Page No.
3.1.	(a) Seabed bathymetry map of the Faeroe Shetland Basin, with inset regional location map. The Neogene depocentre lies within dotted line, with the Palaeogene depocentre located within the basin axis to the SW. Arrows represent ocean current circulation through the basin, with large red arrows indicating the path of North Atlantic Water, small red arrows representing Modified North Atlantic Water, and the blue arrows representing Norwegian Sea Overflow Water (simplified from Turrell et al., 1999). Seismic profile locations illustrated with figure number circled. Path of correlation panel in Fig 7 also detailed.	3-4

	<b>(b)</b> Map showing data utilised during this study: light grey lines = 2D seismic data; black lines = high resolution 2D seismic data; red boxes = 3D seismic volumes; red dots = industry wells. Key industry well 214/4-1 is indicated. Abbreviations: FBC, Faeroe Bank Channel; MKR, Munkagrunnar Ridge. The circled 'Fig' references refer to the location of seismic profiles within this Chapter, e.g. 'Fig 7' refers to Figure 3.7.	
3.2.	Composite strike oriented 2D seismic profile and corresponding geoseismic section along the basin axis (line location Fig. 3.1). The profile outlines the seismic stratigraphic division produced as part of this study, and its variation along strike. Neogene strata are concentrated toward the NE of the basin, and onlap the Palaeogene strata toward the SW, delineating the Palaeogene and Neogene depocentres. The inset panel consists of a seismic profile situated 10km NW of the composite line (shorter line marked Fig. 2 on base maps), which details the relationship of the Neogene stratigraphy to the middle Eocene Caledonia Fan. Note the significant onlap of unit CD30 reflections into the OL2 reflection across the fan. Abbreviations: E = Horizon E; SB = seabed.	3-8
3.3.	Regional composite 2D seismic profile and geoseismic section across the northern end of the Faeroe Shetland Basin (line location Fig. 3.1). Line details the seismic stratigraphic division of the Palaeogene-Neogene stratigraphy. Note truncation of units beneath the INU on the basin margins. Well 214/4-1 forms the key lithologic and biostratigraphic calibration for the Neogene succession within the basin. Inset box documents stratigraphic division of Ritchie et al. (2003). Abbreviations: E = Horizon E; LEU = Late Eocene Unconformity (Davies and Cartwright 2002); TPL = Top Palaeogene Lavas (Naylor et al., 1999).	3-10
3.4.	Stratigraphic nomenclature for the Faeroe Shetland Basin. The figure provides the stratigraphic division of this study, which is in turn related to existing stratigraphic schemes. A late Miocene-early Pliocene and a middle Miocene event are common to most or all of the studies, and note array of names applied to each event by each study. Abbreviations/acronyms as follows: INU – Intra Neogene Unconformity; C – Cenozoic; FSN – Faeroe Shetland Neogene; FSP – Faeroe Shetland Palaeogene; LOEMU – Late Oligocene Early Miocene Unconformity; EPU – Early Pliocene Unconformity; MMU – Middle Miocene Unconformity; LEU – Late Eocene Unconformity; IMU – Intra Miocene Unconformity; TPU – Top Palaeogene Unconformity; PU – Pliocene Unconformity; IMU – Intra Miocene Unconformity.	3-11
3.5.	Summary of the lithologic and biostratigraphic data from well 214/4-1 from unpublished well reports, some of which were published by Davies et al. (2001) and Davies and Cartwright (2002). Biostratigraphic analysis allows the stratigraphy to be dated based on microfossil assemblages. Lithologically the succession consists of intercalated claystones (grey) and sandstones (yellow). The black zone represents Horizon E. Depth conversion of the seismic reflections that bound the units provides dating and lithologic calibration of the stratigraphy. All depths are TVDSS (sub sea level).	3-13
3.6.	2D seismic profile and geoseismic section orientated orthogonal to the base of the Shetland slope (line location Fig. 3.1). The profile highlights detail of unit relationships on the Shetland margin, and location of Well 214/4-1. Units CD10-CD40 and bounding reflections subcrop the INU at the base of the slope. Note onlap onto the OL1 and OL2 reflections. Seismic resolution is significantly diminished beneath Horizon E. Abbreviations as in Fig. 3.2.	3-16
Table 3.1	Sources of information used by previous studies to the date middle Miocene and early Pliocene erosion events within the Faeroe Shetland Basin.	3-18
3.7.	Correlation panel of industrial wells revealing stratigraphic preservation throughout the basin in order to highlight the erosional hiatus associated with the INU (location Fig. 3.1). Excluding Wells 214/4-1, 208/15-1A and 214/17-1, a stratigraphic break is recorded at the base of the Pliocene, representing the INU erosion event. The presence of late Miocene strata within Well 214/17-1 is based on the occurrence of one example of an upper Miocene microfossil within an assemblage that ranges into the Pliocene and thus is not deemed particularly reliable. Similarly, the late Miocene record of 218/15-1A is part of a broad early Oligocene-Miocene sample and does not provide a defined late Miocene datum.	3-21

3.8.	Schematic seismic profile across the Faeroese margin and corresponding chronostratigraphic chart to highlight the basin-centric locus of Neogene stratal preservation and the significance of erosion associated with formation of UC1 and the INU. The INU truncates progressively older strata toward the shelf. At the point of truncation of the UC1 reflection the INU becomes a composite unconformity, incorporating the hiatal range of the UC1 unconformity. However, it is not possible to define the basinward extent over which the INU can be classified as a composite unconformity. The cross-cutting nature of Horizon E is clearly revealed. The ages and durations placed on the units and hiatuses are approximate due to the resolution of the dating, and the figure is intended to illustrate the distribution of erosion and stratal preservation within the basin and not precise unit ages and hiatal ranges. See section 3.8.6. for explanation of Horizon E.	3-23
3.9.	Seismic profile across the Faeroese margin (line location Fig. 3.1). Line illustrates the distribution of the seismic stratigraphic units on the Faeroese margin. The East Faeroes Ridge forms a significant anticlinal structure on the margin, across which Units CD20, CD30 and CD40 are truncated beneath the INU. Upslope prograding contourite reflection configurations are present within Unit CD10 on the basinward limb of the fold. Erosion associated with the UC1 reflections is most obvious along the base of the Faeroese slope, and estimated at >90m based on stratal truncation (inset). Deposition of CD20 and CD30 by bottom currents was concentrated along the base of the slope and is characterised by broad bidirectional baselap toward the southern end of the slope and upslope progradation toward the north (inset). Stratal projection above the INU toward the upper slope allows estimation of >200m of erosion in this area during formation of the INU. The INU also exhibits incisional features 120m deep on the upper slope.	3-24
3.10	<p><b>(a)</b> Time structure map of the OL1 reflection. The surface extends from the basin axis onto the Faeroese Slope, and the white line represents the boundary between the smooth (Fig. 3.6) and rugose (Fig. 3.9) character of the reflection. Contours are in metres below sea level. Fine dotted line represents limit of data, and dot-dash line represents UK-Faeroese Political border (as applies for all other isochrons).</p> <p><b>(b)</b> Isochron map of Unit CD10. Area of thickened conformable strata present upslope of the East Faeroes Ridge while a mounded upslope prograding reflection configuration was developed on the basinward limb (Fig. 3.9), the boundaries between which are represented by the white lines. Internal reflections also exhibit conformity in the northern axis of the basin (Fig. 3.2), and onlap the OL1 reflection onto the Shetland margin (Fig. 3.6). Open arrows represent onlap of internal reflections onto underlying OL1 reflection. Contours in metres. Dotted and dashed line represents UK-Faeroese Political border.</p> <p><b>(c)</b> Time structure map of the UC1 reflection. Evidence of erosional truncation in the form of angular subcrop is restricted to a strike-parallel band along the base of the Faeroese slope (Fig. 3.9), delineated by white lines. Throughout the remainder of the reflection the underlying reflections of Unit CD10 exhibit conformity and a lack of angular subcrop (Fig. 3.6), with the boundaries between areas of erosion and conformity represented by white lines. FSIB refers to Faeroes slope break. Dotted and dashed line represents UK-Faeroese Political border.</p> <p><b>(d)</b> Isochron map of Unit CD20 (location outline on Fig. 3.10c). To the NE of the Caledonia fan the unit exhibits relatively uniform thickness (Figs. 3.2, 3.3 &amp; 3.6), with upslope prograding undulatory reflections on the Faeroese margin (Fig. 3.9 inset), while to the SW of the fan the internal reflections exhibit bidirectional downlap and a mounded thickness distribution (Fig. 3.9). Dotted and dashed line represents UK-Faeroese Political border. The 'Fig' references refer to the location of seismic profiles within this Chapter, e.g. 'Fig 9' refers to Figure 3.9.</p>	3-26
3.11.	<p><b>(a)</b> Time structure map of the OL2 reflection. The depositional limits of the reflection are defined by onlap onto the UC1 reflection toward the SW (Fig. 3.2), and truncation beneath the INU on the basin margins (Fig. 3.3). Contours are in metres below sea level. Dotted line represents limit of data. Dotted and dashed line represents UK-Faeroese Political border.</p> <p><b>(b)</b> Isochron map of Unit CD30, which reveals a bi-modal thickness distribution separated by the Caledonia fan, onto which the internal reflections onlap (Fig. 3.2). To the NE of the fan, the unit exhibits onlap onto the basin margins and fold structures (Fig. 3.3 &amp; 3.6). SW</p>	3-31

	<p>of the fan the unit exhibits bi-directional downlap at the base of the Faeroese slope (Fig. 3.9). Open and filled arrows represent onlap and downlap respectively. Curved filled arrows represent bi-directional downlap. Contours are in metres. Dotted line represents limit of data. Dotted and dashed line represents UK-Faeroese Political border.</p> <p><b>(c)</b> Time structure map of the OL3 reflection. The surface shallows toward the SW and is locally truncated across the Caledonia fan (Fig. 3.2). Contours are in metres below sea level. Dotted line represents limit of data. Dotted and dashed line represents UK-Faeroese Political border.</p> <p><b>(d)</b> Isochron map of Unit CD40, which exhibits a mounded thickness distribution with bi-directional downlap (closed arrow) onto the basal OL3 reflection throughout the northern FSB (Fig. 3.3), and onlap (open arrows) at its SW limit (Fig. 3.2), coincident with the Caledonia fan, across which it is truncated (Fig. 3.2) reflections are conformable in the basin axis – delimited by the white line. Contours are in metres, dotted line represents limit of data. Dotted and dashed line represents UK-Faeroese Political border. The ‘Fig’ references refer to the location of seismic profiles within this Chapter, e.g. ‘Fig 9’ refers to Figure 3.9.</p>	
3.12	3D visualisation of the OL2 reflection in the vicinity of Well 214/4-1 (Fig. 3.1) to illustrate nature of hummocky deformation of units CD30 and CD40 associated with formation of Horizon E. The seismic section also clearly illustrates onlap of unit CD30 internal reflections onto the fold structures and Shetland slope.	3-33
3.13	<p><b>(a)</b> Time structure map of the INU reflection. The map reveals the palaeo- bathymetry of the INU reflection, which is extremely similar to that of the present day basin. The unconformity exhibits angular subcrop of underlying strata throughout the majority of its extent, except in the basin axis where low angle truncation is prevalent, defined by the white line. Clear evidence for erosion is identified on the Faeroese margin (Fig. 3.9), the southern basin axis (Fig. 3.14) and is inferred on the northern West Shetland Margin (Fig. 3.15). Contours in metres below sea level. Limits of map defined by limits of data.</p> <p><b>(b)</b> Map of subcrop distribution beneath the INU, revealing Palaeogene-Neogene depocentres. Basin-axis centric preservation of pre-INU Neogene strata also revealed. The distribution of Horizon E is wider in extent than the preserved pre-INU Neogene strata. Contours in metres below sea level.</p> <p><b>(c)</b> Isochron map of Unit CD50, revealing bimodal sediment accumulation during the Pliocene-Recent. Prograding wedge deposition from the Faeroese margin resulted in formation of the East Faeroes Wedge, while bottom currents deposited the West Shetland Drift System in the basin axis and on the Shetland Margin (Fig. 3.2, 3.3 &amp; 3.15). The internal reflection configuration is characterised by baselap onto the Shetland slope, with conformable reflections restricted to the basin axis (Fig. 3.2) delimited by the white line. Elsewhere, in the basin unit CD50 is extremely thin (Fig. 3.15). Contours in metres, limits of map defined by limits of data.</p> <p>The ‘Fig’ references refer to the location of seismic profiles within this Chapter, e.g. ‘Fig 9’ refers to Figure 3.9.</p>	3-36
3.14	High resolution 2D seismic profile orthogonal to the Shetland margin at the southern end of the basin (line location Fig. 3.1), revealing erosional truncation of Palaeogene strata beneath the INU. Stratal projection allows estimation of c.180m of erosion in the area during formation of the INU. The high resolution of the data also reveals the pervasive polygonal faulting that characterises the Cenozoic succession within the basin.	3-39
3.15	2D seismic profile across the northern end of the Shetland Slope (line location Fig 3.1). From the basin axis Horizon E is truncated beneath the INU at the base of the Shetland slope, and is preserved in a mid-slope position. In the basin axis Horizon E clearly tracks the OL3 reflection (black line). The OL3 reflection is also truncated beneath the INU at the base of the Shetland Slope, and is thought to originally have continued upslope, forming the pre-INU erosion palaeo-seabed beneath which Horizon E formed. A pre-INU erosion seabed was reconstructed by subtraction of 250ms from Horizon E. The reflection reveals a close match to the OL3 reflection in the basin axis, and upslope of the point of truncation of OL3 is interpreted to give a good approximation of the pre-INU erosion Shetland slope seabed bathymetry. Consequently, at least 200m of erosion on the Shetland Margin is proposed to have occurred during formation of the INU.	3-45

## Chapter Four: 3D Seismic analysis of the late Neogene West Shetland Drift

Figure No.	Figure Caption	Page No.
4.1.	Location map of the Faeroe Shetland Basin illustrating the key 3D and 2D data used in this study (3D:1) and by Knutz and Cartwright (2004) (3D:2). Also indicated are the locations of seismic profiles (figure number circled, number refers to the location of seismic profiles within this Chapter, e.g. 'Fig 3' refers to Figure 4.3.), the spatial distribution of Figures 4.10 (dotted line) and 4.11 (solid line), and the location of well 214/4-1. Yellow filled contours represent 500m, 250m and 50m thickness distribution of WSD Slope section. Coloured arrows represent present day ocean currents: red arrows = surface inflow waters; blue arrows = SW flowing deep waters. Note location of Eocene slope progradation system and influence on WSD Slope thickness distribution. Abbreviations: 2DHR = high resolution 2D data; FBC = Faeroe Bank Channel; MKR = Munkagrinnar Ridge.	4-4
4.2.	Chronostratigraphic chart illustrating various divisions of the Neogene stratigraphy of the Faeroe-Shetland Basin for the purposes of chronostratigraphic correlation between studies. The dashed line of surface PL40 of this study represents the age uncertainty within the early Pliocene. Late Neogene eustatic sea level fluctuations are highlighted (Haq et al., 1987). INU = Intra-Neogene Unconformity; GU, Glacial Unconformity; N1, Lower Nordland Unit; N2, Middle Nordland Unit; N3, Upper Nordland Unit (Stoker, 1999). Time scale from Berggren et al. (1995).	4-7
4.3	Regional 2D seismic profile orthogonal to the Shetland slope (line location Fig. 4.1). The INU surface is seen to truncate underlying strata (arrows), and exhibits an undulating morphology toward the base of slope. WSD Basin and WSD Slope sections are separated by thinned 'transition zone'. Note INU is truncated by the Glacial Unconformity (GU) toward the upper slope, which itself is overlain by Pleistocene glacial prograding wedge deposits. SBM -seabed multiple. Resolution in the shelf region is also reduced by normal move out effects (Bulat, 2005).	4-11
4.4.	Geoseismic schematic and seismic profile illustrating the stratigraphic relationship between WSD Slope and WSD Basin sections (see Fig. 4.1 for profile location). When correlated through the transition zone, the Top B1 reflection (dotted line - dated as Pliocene in age, Knutz and Cartwright, 2003) is found to lie above the PL40 reflection. This is used to assign a preliminary Pliocene age to Unit 1, PL40 and at least part of Unit 2, and a Pliocene to Pleistocene age for the remainder of Unit 2, the GU and Unit 3. The Figure is modified from Knutz and Cartwright (2003) and adds detail to their initial interpretation of the WSD system.	4-12
4.5.	3D seismic profile and line drawing perpendicular to the West Shetland slope to illustrate seismic-stratigraphic division of the WSD Slope section (line location Fig. 4.1). Accumulation of the WSD Slope section is seen to occur at a subtle break of slope on the INU surface. Line drawing summarises reflection termination relationships marked by arrows. Inset panel shows detail of upslope prograding moat system within Unit 2. SB-seabed.	4-14
4.6.	3D seismic profile and line drawing parallel to the West Shetland slope to illustrate the strike-orientated seismic-stratigraphic division of the WSD Slope Section (line location Fig. 4.1). Channel to the right of the profile shows complex internal geometry and deformation of overlying strata due to differential compaction. Channel levee deposit shows lateral downlap. Reflection X exhibits SW downlap onto the levee, and correlates to a series of subtle and interspersed reflections that progressively downlap toward the SW and are interpreted as alongslope current deposits intercalated with the downslope channels. Note progressive SW downlap of reflections within Unit 2 onto the PL40 reflection. SB- seabed.	4-16
4.7.	(a) Isochron map of Unit 1, illustrating time thickness between the INU and seismic marker PL40. Note slope parallel thickness distribution with thinning both upslope and downslope. Fig. 4.5 illustrates downslope prograding internal reflections within Unit 1a	4-18

	<p>while Fig. 4.6 illustrates cross sectional geometries of downslope channels and associated levees.</p> <p><b>(b)</b> Isochron map of Unit 2 illustrating time thickness distribution between seismic marker PL40 and the GU. Unit 2 attains greatest thickness at the northern end of the study area, and thins toward the SW as well as thinning up and down slope. Internal reflections exhibit SW downlap (Fig. 4.6). Figure 5 inset panel illustrates the upslope aggrading bottom current moat system as well as the erosional nature of the upper contact of Unit 2.</p> <p><b>(c)</b> Isochron map of Unit 3, illustrating time thickness distribution between the GU and the seabed. The maximum thickness of Unit 3 is attained near the present day shelf break, from where it thins downslope. Localised thickness increases are related to glacial prograding wedges deposited following onto the GU (Fig. 4.3). The 'Fig' references refer to the location of seismic profiles within this Chapter, e.g. 'Fig 5' refers to Figure 4.5.</p>	
4.8.	3D visualisation of seismic reflection PL10 (stratigraphic location Fig. 4.5) looking toward Shetland shelf reveals the presence of mildly sinuous downslope channels and associated levee deposits within Unit 1a. Subsequent to channel formation, differential compaction has deformed overlying sediments of Units 1a, 1b and 2. Terminal fan deposition is not apparent, and the channels die out downslope.	4-20
4.9.	3D visualisation of the PL20 reflection looking along the West Shetland slope toward the NE, revealing a surface adorned with large sediment waves within the contourite drift body. Wave crests are orientated obliquely to the slope, mildly sinuous and occasionally bifurcating. Wave dimensions die out up and down slope.	4-22
4.10	Analysis of PL20 sediment wave field. A time slice through the PL20 reflection generated from a smoothed and flattened overlying reflection illustrating wave crest geometry and relation to slope contours. The seismic profile X-X' illustrates the cross-sectional geometries of the waves, with the higher amplitude reflections on the NE flank of the waves interpreted to reveal a NE migration direction. From the inferred migration direction of the waves (upcurrent toward the NE) a SW flow direction and migration of the waves to the right of the current and downslope is proposed.	4-24
4.11	Time structure map of the PL40 reflection revealing a surface crisscrossed by iceberg plough marks. Linear plough marks are predominantly orientated parallel to the slope (see Fig. 4.12), although some are aligned at a high angle to the slope. Overlapping curvilinear plough marks may be related to tidal processes. The seismic profile relates the line A-A' across the zoomed box and illustrates the plough marks cross sectional geometry. Plough marks vary from clearly visible, wide V shaped impressions (No. 2) to narrow and subtle features (No. 3&4). The seismic profile also shows deformation of the reflections beneath the plough marks. Zoomed section highlights bulbous termination of linear plough marks. The survey footprint forms an artefact on the time structure map.	4-28
4.12	Rose plot based on orientation measurements of 61km of plough marks. Dominant trend is NE/SW alongslope (044-224°) although a variety of subordinate trends are also present.	4-29
4.13	<p>Schematic summarising the proposed evolution of the WSD Slope section. Water depth (mbsl) on each panel represents present day values and not depositional water depths, which are thought to have been a maximum of 500m shallower than the present day water depths.</p> <p><b>(a)</b> Accumulation of Unit 1a at a break in slope on the INU surface via downslope processes during the early Pliocene. It is likely that alongslope currents were active resulting in subordinate contourite deposition and the possible entrainment of downslope sediments resulting in a lack of fan deposition.</p> <p><b>(b)</b> Deposition of Unit 1b by SW flowing Northern Component Water (NCW) during the early Pliocene, resulting in the formation of the sediment waves and contourite drift deposits and representing the onset of SW flowing alongslope currents as the dominant depositional force on the West Shetland margin. The formation of seismic marker PL40 by alongslope current erosion was followed by iceberg turbation of the seabed, interpreted to represent a period of glaciation during which it is proposed alongslope current flow was disrupted. Sea level fluctuation would be expected with growth and decay of large ice sheets deemed to have been the source of the icebergs.</p> <p><b>(c)</b> Continued flow of Northern Component Water during the Pliocene-early Pleistocene, resulting in the deposition of Unit 2 combined with the development of base of slope and</p>	4-34



	<p>upper slope moat systems. Occasional iceberg presence is also recorded during this interval. Arrows pointing downslope from the upslope moat system represent Coriolis related deflection of SW flowing alongslope currents, potentially distributing sediment supplied by nepheloid layers further upslope.</p> <p>(d) Final phase of the WSD evolution, represented by the shelf transgression of ice sheets to form the Glacial Unconformity (GU), and the subsequent deposition of Unit 3 during the mid-Pleistocene to Recent. Unit 3 shows no seismically identifiable evidence of alongslope currents, and it is proposed that that this time (440-18Ka, Stoker, 1999) alongslope current activity on the West Shetland Slope was reduced, and if any, limited to the deep basin. Significant sea level fall would have accompanied the growth of regional ice sheets.</p>	
--	--	--

## Chapter Five: Discussion

Figure No.	Figure Caption	Page No.
5.1.	<p>Palaeogeographic map time series to illustrate sedimentological and palaeoceanographic history of the Faeroe Shetland Basin. Abbreviations: WTR, Wyville Thompson Ridge; MKR, Munkagrunnar Ridge; EFR, East Faeroes Ridge.</p> <p>(a) Southwesterly flow of Northern Component Water through the basin as part of the North Atlantic Conveyor Belt began in the mid-Eocene (Lutetian) and resulted in the deposition of the P30 elongate mounded contourite drift (Chapter 2) within the southern basin axis. Contemporaneous slope progradation from the Shetland Margin resulted in intercalation of contourite drift and base of slope fans (B.O.S fans). The depositional currents are thought to have exited through the Faeroe Bank Channel with potentially significant overflow of the nascent Wyville Thompson Ridge.</p> <p>(b) Oligocene early Miocene contourite sedimentation was concentrated on the Faeroese margin (CD10, Chapter 3), characterised by combined upslope prograding contourite drifts with sheeted drifts. Note restriction of bottom currents to the Faeroese margin. Overflow across the Wyville Thompson Ridge may have been reduced due to growth on the structures during the Oligocene.</p> <p>(c) During the mid-late Miocene, both upslope prograding and mounded elongate contourite drifts were deposited on the Faeroese margin (CD20 and CD30, Chapter 3), with sedimentation and currents influenced by the newly formed East Faeroes Ridge. Rapid middle Miocene bottom currents caused erosion of the base of the Faeroes slope (UC1, Chapter 3), particularly in the area of the East Faeroes Ridge. CD40 was deposited as a mounded elongate drift in the basin axis during the mid-late Miocene, signifying the increase in distribution of SW flowing bottom currents within the basin as far as the base of the Shetland slope.</p> <p>(d) During the Pliocene, following the formation of the INU during the late Miocene-early Pliocene, SW flowing bottom currents reached the mid-Shetland Slope, and deposited the West Shetland Drift (WSD, Chapter 4). The WSD basin section was characterised by sheeted, infilling drifts, while the WSD slope section formed a tapering elongate plastered drift. During this time rapid, non depositional SW current flow is envisaged on the Faeroese margin. At intermittent periods, icesheets discharged icebergs into the basin, during which times alongslope current activity was reduced.</p>	5-3
5.2.	<p>Cenozoic event history diagram summarising sedimentological and palaeoceanographic evolution of the Faeroe Shetland Basin and key associated tectonic and climatic events. Note that the Faeroe Shetland Basin was present in a form similar to its modern day expression prior to contourite deposition. The two erosion events within the basin (UC1 and INU, represented by red wavy lines at the mid Miocene and the late Miocene-early Pliocene respectively) correspond to tectonic events (subsidence and folding) and climatic events revealed by the <math>\delta^{18}\text{O}</math> curve. Note also that the distribution of SW flowing deep waters within the basin increases throughout the Cenozoic in relation to global climatic cooling. Abbreviations: FSB- Faeroe Shetland Basin; FBC- Faeroe Bank Channel; GSR- Greenland Scotland Ridge. References for all events are documented throughout text.</p>	5-5

5.3.	Comparison of imaging of upslope migrating sediment waves at the base of the Shetland Slope. Damuth and Olsen (1993, 2001) utilised BGS seismic profiles to identify the features (Fig. 5.3a), but were unable to interpret the features in detail or make maps of the seabed or subsurface reflections. The utilisation of 3D seismic data by Knutz and Cartwright (2004) allowed the mapping and 3D visualisation of the sediment waves (Fig. 5.3b), in addition to detailed mapping of the seabed expression (Fig. 5.3c) allowing a more confident interpretation of the features.	5-15
5.4.	Comparison of the quality and resolution of the standard 2D, 3D and high resolution 2D seismic data used in this study. The profile images the discrete onlap surface exhibited by the Eocene contourite drift within the basin (Unit P30, Chapter 2), and clearly shows that without the high resolution data it would not have been possible to identify the reflection configuration and thus interpret the contourite drift with such a high level of confidence.	5-17
5.5	Previous identification of the Eocene contourite drift Unit P30 (Chapter 2), indicated by red arrow. Smallwood (2004) identifies the upslope prograding onlap relationship exhibited by the contourite drift, but fails to identify it as such (Fig. 5.5a). Howe et al. (2002) identify the relationship as indicative of contourite drift deposition (Fig. 5.5b), but do not comment further on the age of the drift body and therefore its significance.	5-18

## Appendices

Appendix 1. Seismic database available to this study.

Appendix 2. Well and borehole database available to this study.

## Chapter One: Introduction

### 1.1. Rationale

This study utilised petroleum industry seismic and well data to identify and analyse contourite drifts within the Faeroe Shetland Basin. A combination of internal drift architecture and temporal and spatial evolution were used to assess the history of the Faeroe Shetland Basin as an oceanic gateway throughout the Cenozoic.

At present the Faeroe Shetland Basin forms a key oceanic gateway that facilitates water mass circulation between the Norwegian Greenland Sea and the North Atlantic which in turn plays a fundamental role within the global climate system by providing a mechanism for the transport of energy around the planet (Schnitker, 1980; Thiede and Eldholm, 1983; Broecker and Denton, 1990; Schmitz, 1995; Hansen and Østerhus, 2000; Rahmstorf, 2002). This is illustrated by the action of the Gulf Stream and North Atlantic Drift surface currents which form part of the North Atlantic Conveyor Belt circulation (Fig. 1.1, Broecker, 1991). Heat energy is transported northward by these currents from the equatorial Atlantic into the Norwegian Greenland Sea and released to the atmosphere, resulting in the formation of cool deep waters (Fig. 1.1, Bigg, 1996; Bacon, 1997; Rossby, 1996). The energy released during this process supplements yearly insolation in the region by about 25%, and results in amelioration of winter climatic conditions in western Europe (Broecker and Denton, 1990; Bigg, 1996; Johnson, 1997; Moron et al., 1998). This thermohaline circulation thus forms a critical component of the northern hemisphere climate and in addition significantly influences the global climate (Crowley, 1992; Wright, 1998; Vellinga and Wood, 2002).

The Faeroe Shetland Basin constitutes a deep water passageway that is significant to this ocean-climate system because it facilitates the exchange of water masses between the North Atlantic and the Norwegian Greenland Sea which is otherwise restricted by the shallow Greenland Scotland Ridge that stretches from SE Greenland to Scotland (Fig. 1.1, Bott, 1983; Nilsen, 1983; Wright and Miller, 1996; Wright, 1998; Turrell et al., 1999; Hansen and Østerhus, 2000). The Denmark Strait and the Iceland Faeroe Ridge also permit deep water

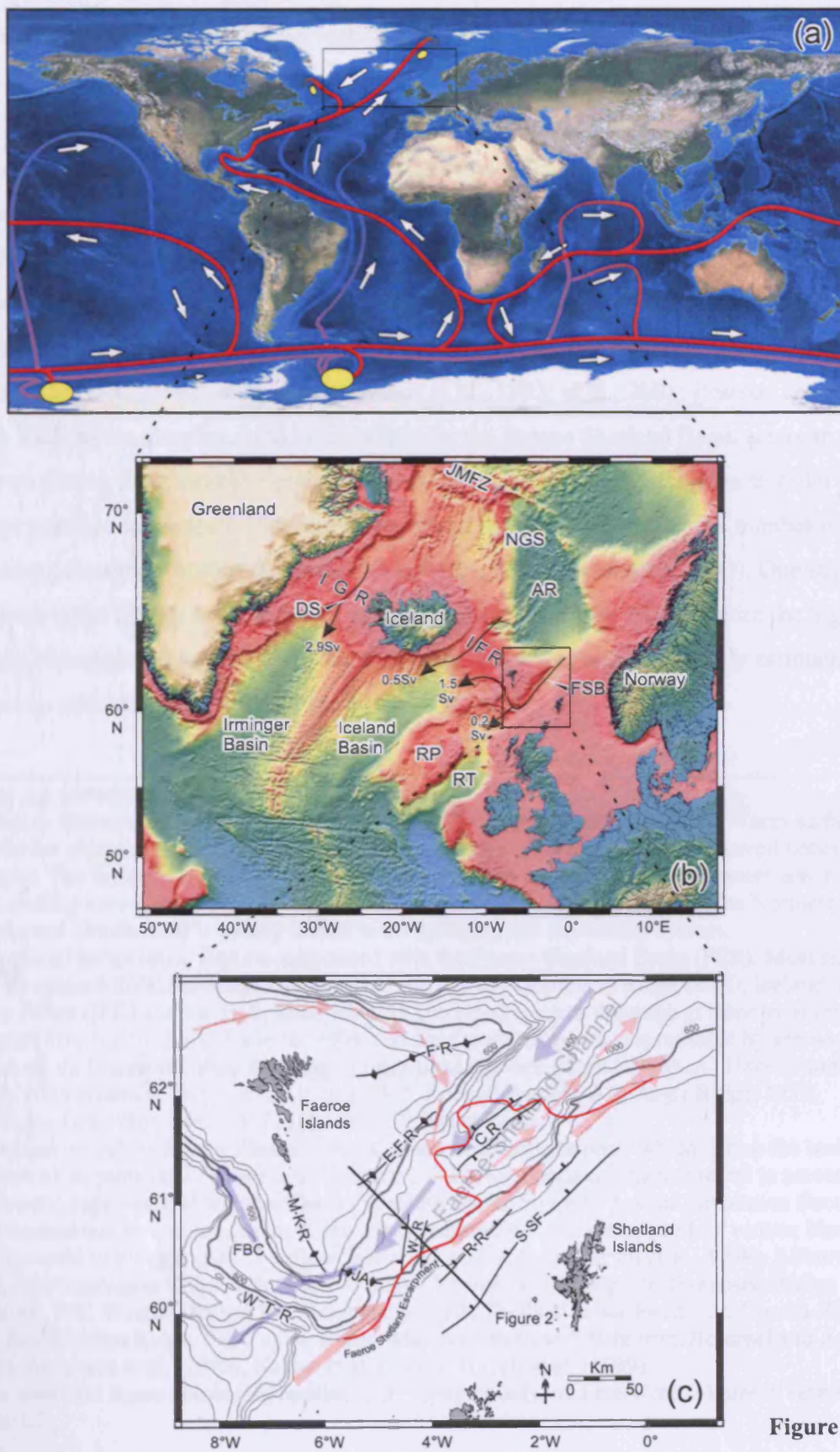


Figure 1.1

exchange, and the deep water (Norwegian Sea Arctic Intermediate Water + Norwegian Sea Deep Water) flux of  $1.7 \text{ million m}^3 \text{ s}^{-1}$  through the Faeroe Shetland Basin (Fig. 1.1, Hansen and Østerhus, 2000) illustrates that along with the Denmark Strait, the Faeroe Shetland Basin forms a critical ocean gateway and constitutes a fundamental component necessary for the functioning of the present day North Atlantic Conveyor Belt. However, the evolution of the global climate system from 'greenhouse' conditions during the Palaeocene and early Eocene into 'icehouse' conditions that characterised the late Neogene (Shackelton and Kennett, 1975; Kennett and Shackelton, 1976; Shackelton and Boersma, 1981; Barron, 1987; Miller et al., 1991; et al., 1998; Zachos et al., 1993; et al., 2001; Pearson and Palmer, 2000) leads to the question as to what extent did the Faeroe Shetland Basin act as an oceanic gateway during this climatic transformation? Efforts to model past climates in order to better predict possible scenarios of future climate change are complicated by the number of unknown parameters within the models (Marotzke, 2000; Rahmstorf, 2002). One such unknown is the timing of initiation of a connection of the North Atlantic with the high latitude Norwegian Greenland Sea and the Arctic Ocean, at present variably estimated to be Eocene to mid Miocene (Berggren and Hollister, 1974;

---

**Figure 1.1 (previous page)**

(a) Map to illustrate Global ocean circulation, modified from Rahmstorf (2002). Warm surface currents are represented in red, cold deep water currents in blue and Antarctic sourced bottom waters in purple. The flow direction is given by white arrows, and areas of major deep water generation and down welling are represented by yellow markers. Generation of deep waters in the Northern North Atlantic and Nordic Seas is clearly linked to the global ocean circulatory system.

(b) Regional bathymetric features associated with the Faeroe Shetland Basin (FSB). Most significant is the Greenland Scotland Ridge comprised of the Iceland-Greenland Ridge (IGR), Iceland-Faeroe Ridge (IFR) and the FSB. Deep water is permitted to cross the ridge at three locations, the Denmark Strait (DS), the IFR and the FSB, and deep water fluxes are represented by arrows ( $1 \text{ Sv} = 1 \text{ million m}^3/\text{s}$ ). Image modified from <http://topex.uscd.edu> using Bott (1983) and Hansen and Østerhus (2000). Abbreviations: RP, Rockall Plateau; RT, Rockall Trough; AR, Aegir Ridge; NGS, Norwegian Greenland Sea; JMFZ, Jan Mayan Fracture Zone.

(c) Bathymetry of the Faeroe Shetland Basin. Main structural elements which define the basin are represented, schematically illustrated in Figure 1.2. Faeroe Shetland Channel refers to present day bathymetric expression of tectonic Faeroe Shetland Basin. Simplified ocean circulation through the basin represented by coloured arrows; red arrows represent warm surface inflow waters; blue arrows represent cold Norwegian Sea Overflow Water (simplified from Turrell et al., 1999). Abbreviations: MKR, Munkagrunnar Ridge, FBC, Faeroe Bank Channel; WTR, Wyville Thompson Ridge; JA, Judd Anticline; WR, Westray Ridge; RR, Rona Ridge; SSF, Shetland Spine Fault; CR, Corona Ridge; EFR, East Faeroes Ridge; FR, Fugloy Ridge. Map populated with data from Boldreel and Andersen (1993), Andersen et al. (1995), Naylor et al. (1999), Turrell et al. (1999). Please note that figure numbering applies to this chapter only, and therefore 'Figure 2' refers to Figure 1.2.

Thiede and Eldholm, 1983; Eldholm, 1990; Davies et al., 2001; Stoker, 2003). Therefore, an understanding of the existence of the Faeroe Shetland Basin as a deep water connection throughout the Cenozoic would add a further constraint to models which attempt to explain the Cenozoic greenhouse to icehouse transition and possibilities of future climate changes.

The objective of this study is therefore to characterise the history of the Faeroe Shetland Basin as an oceanic gateway throughout the Cenozoic. This is to be accomplished by the identification, dating and analysis of sediments deposited or significantly reworked by the deep water currents, known as contourite drifts (see section 1.4), within the Faeroe Shetland Basin. Analysis of these deposits provides a record of the history of the depositional current, and thus the history of thermohaline current flow through the basin. The contourite drifts within the Faeroe Shetland Basin are identified and interpreted using a very large seismic reflection and well database acquired originally for the purpose of hydrocarbon exploration. The study builds upon previous seismic based studies which investigated the palaeoceanographic history of the basin (e.g. Davies et al., 2001; Knutz and Cartwright, 2003; Knutz and Cartwright, 2004; Stoker, 2005). However, rather than concentrating on specific time intervals or events as in previous examples, the aim of this study is to define the onset of contourite deposition and characterise the entire history of the basin as a conduit for thermohaline currents.

This chapter provides an introduction to the project aims and objectives along with a brief summary of the geological evolution of the study area. The identification of contourites using seismic data and their conceptual use as a source of palaeoceanographic information is briefly commented upon. The dataset available for this study and the methods used to interpret it are also described. Finally, the structure of the thesis is outlined.

## 1.2. Aims

The aims of this research are as follows:

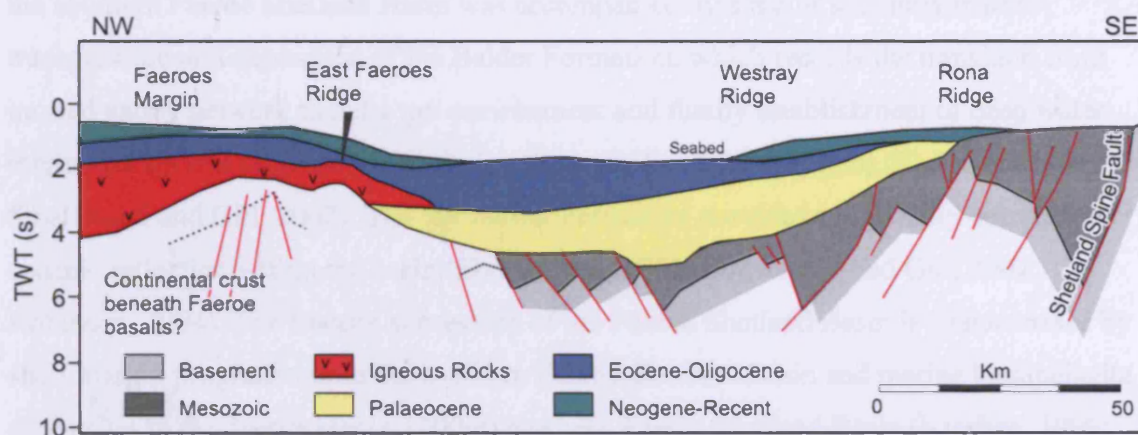
1. Identify and date the earliest contourite drift body within the Faeroe Shetland Basin, thereby dating the onset of deep water circulation.
2. Characterise the extent of contourite deposition within the basin, both spatially and temporally, in order to evaluate the function and significance of the Faeroe Shetland Basin as an oceanic gateway throughout the Cenozoic.
3. Date the Cenozoic contourite drifts via correlation with key wells. Particular attention will be paid to validation of biostratigraphic information from the wells where possible in order to produce a chronostratigraphic division which is as accurate as possible with the data available.
4. Devise a seismic-stratigraphic nomenclature based on the identification and dating of individual contourite bodies which is in turn fully correlated with existing stratigraphic nomenclatures where possible in order to provide a unified seismic stratigraphic base for future work.
5. Draw inferences regarding the currents responsible for the contourite drift deposition such as flow direction, current locus, intensity and evolution through time via analysis of gross depositional morphologies and distribution of smaller scale architectural elements and discrete internal reflection configurations.
6. Investigate the formation of deep water unconformities by alongslope flowing currents.
7. Attempt to relate variation in circulation through the basin to potentially causal factors, both local and global.
8. Investigate the interaction of contourite depositional processes with other depositional systems, particularly downslope processes, and in particular characterise the transition between downslope processes of the Palaeocene- Eocene and contourite sedimentation of the late Palaeogene and Neogene.
9. Demonstrate the expediency of petroleum industry seismic data as a tool for contourite and palaeoceanographic research.



### 1.3. Geological setting

The Faeroe Shetland Basin, geographically demarcated by the Faeroe and Shetland Islands, is located on the NW European continental margin and forms the study area for this project (Fig. 1.1) The Faeroe-Shetland Channel is the modern bathymetric expression of the Faeroe-Shetland Basin, which consists of a series of Mesozoic tilted fault blocks overlain by a thick Cenozoic post rift sedimentary succession (Fig. 1.2, Bott et al., 1984; Mudge and Rashid, 1987; Doré et al., 1999; Roberts et al., 1999). Multiple rift episodes between the Triassic and the Palaeocene were responsible for generation of the basin, with the final rift episode resulting in significant thinning of the crust and generation of a deep water marine basin prior to the opening of the North Atlantic (Skogseid et al., 1992; Dean et al., 1999). Structurally, the SE limit of the basin is defined by the Shetland Spine Fault which closely underlies the Shetland slope break, while the Faeroese margin is defined by a thick basalt succession which has been folded by compressional forces to form a series of large anticlines including (from north to south) the Fugloy Ridge, the East Faeroes Ridge, and the Munkagrunnar Ridge among others (Figs. 1.1 & 1.2, Waagstein, 1988; Hitchin and Ritchie, 1987; Boldreel and Andersen, 1993; Boldreel and Andersen, 1995; Nadin et al., 1997; Naylor et al., 1999).

A brief account of the Cenozoic development of the basin is documented in order to summarise the geological evolution of the basin that is relevant to this study. During the Palaeocene, thick sandstones were shed into the deep water Faeroe Shetland Basin from highlands to the south as a result of tectonic uplift associated with the impingement of the proto-Iceland plume at the base of the crust (White, 1989; Mitchell et al., 1993; White and Lovell, 1997; Lamers and Carmichael, 1999; Jolley and Bell, 2002). Effusion of voluminous flood basalts and intrusion of igneous sills and dykes at this time associated with the mantle plume resulted in creation of the 5km thick Faeroese Platform, and definition of the Faeroese margin of the basin, the limit of which is represented by the Faeroe-Shetland Escarpment (Fig. 1.1, Waagstein, 1988; Nadin et al., 1997; Naylor et al., 1999). During the early Eocene, N-S oriented compression associated with the initiation of spreading on the Aegir Ridge to the north of the Faeroe Shetland Basin in association with opening of the northern North Atlantic resulted in generation of significant compressional structures including the Wyville Thompson Ridge, which consists of a ramp anticline underlain by a northerly dipping fault



**Figure 1.2**

Schematic cross section across the Faeroe Shetland Basin to illustrate the underlying structure of the basin and the nature of the Cenozoic sediment fill (line location Figure 1.1). The basin is bounded by large NW dipping normal faults on the Shetland margin, and a combination of probable fault blocks combined with Palaeocene lavas on the Faeroese margin. The thick lava succession on the Faeroese margin hampers imaging of underlying Mesozoic stratigraphy and structure. Figure modified from Doré et al. (1999).

plane (Boldreel and Andersen, 1993). Withdrawal of the plume and associated subsidence of the southern Faeroe Shetland Basin was accompanied by a major southerly marine transgression and deposition of the Balder Formation, which records the transition from incised valley network to delta top environment and finally establishment of deep water marine conditions (at least 300m) during the early Eocene (Ypresian) (Ebdon et al., 1995; Smallwood and Gill, 2002). The top Balder Formation provides a regionally correlatable seismic reflection within the basin (Ebdon et al., 1995; Smallwood and Gill, 2002; Robinson, 2004). The Eocene succession of the Faeroe Shetland Basin is characterised by shelf margin progradation in the southern Faeroe Shetland Basin and marine hemipelagite deposition in the deep water (c.1000m) northern Faeroe Shetland Basin (Kjørboe, 1999; Robinson, 2004). During the middle Eocene, three large clastic fans sourced from canyons on the Shetland slope were deposited into the basin axis, later to act as hydrocarbon reservoirs sealed by the associated hemipelagite (Robinson, 2004).

In contrast to the early Palaeogene succession within the basin, the Oligocene-Recent succession is dominated by contourite drift deposits (Damuth and Olsen 2001; Davies et al., 2001; Stoker, 2003; Stoker et al., 2005). The earliest contourite deposits within the basin were identified using industrial seismic profiles across the Faeroese slope and dated as early Oligocene by correlation to industry well data (Davies et al., 2001). During the Oligocene, compression resulted in further development of the Wyville Thompson Ridge and associated folds (Boldreel and Andersen, 1993). During the Miocene the basin was characterised by widespread contourite accumulation resulting from a well established alongslope current regime (Stoker, 2003; Laberg et al., 2005). Erosion by deep water currents is thought to have formed deep water unconformities during the mid Miocene, and is thought to be associated with the growth of NE/SW trending folds which formed as a result of middle Miocene compression (Cloke et al., 1999; Andersen et al., 2000; Davies and Cartwright, 2002; Davies et al., 2004). The formation of the Intra-Neogene Unconformity during the late Miocene-early Pliocene represents the most significant deep water erosion event within the Cenozoic succession, and is interpreted to be the result of deep water current erosion related to climatic changes and tectonic adjustment (Stoker 1999; Knutz and Cartwright, 2003; Stoker, 2003; Knutz and Cartwright, 2004; Stoker et al., 2005). During the Pliocene, contourite deposition continued, succeeded by formation of shelfal unconformities and deposition of large scale

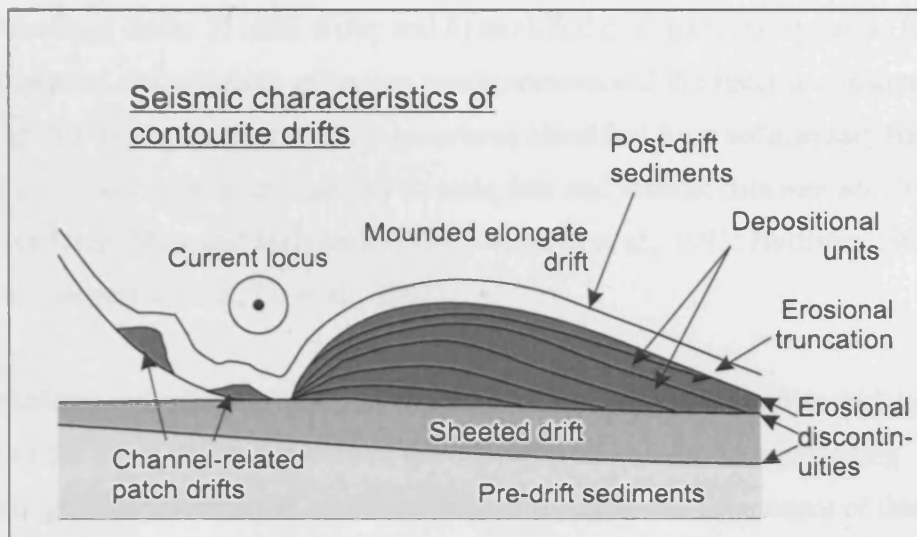
glacial prograding wedge deposits as a result of progradation of ice sheets onto the shelf during the Pleistocene (Stoker et al., 1998; Damuth and Olsen, 2001; Knutz and Cartwright, 2003, Knutz and Cartwright, 2004).

#### 1.4. Seismic analysis of contourites and their palaeoceanographic significance

This section is intended to define the term contourite and to introduce the most important characteristics of contourite drifts with regards to palaeoceanographic and seismic study. Sediment deposition by 'contour currents' was first unequivocally demonstrated by Heezen et al. (1966), some 30 years after the phenomenon was first proposed by George Wüst (Stow et al., 2002). The term contourite was coined for the deposits by Hollister and Heezen (1972), which were most recently defined as 'sediments deposited by or significantly affected by the action of bottom currents' (Hollister, 1993; Stow et al., 2002). In turn, bottom currents are defined as 'currents that operate in deep water and that are part either of the normal thermohaline or of the major wind-driven circulation pattern of the oceans and their marginal seas' (Stow et al., 2002), and are also variably referred to as alongslope currents, thermohaline currents and contour currents.

Contourite drifts are characterised by a variety of facies and a range of diagnostic morphologies have been defined, largely through the use of seismic data (Faugères et al., 1999; Rebesco and Stow, 2001; Stow et al., 2002). Seismic data is particularly applicable to contourite research due to the predominantly large scale and subtle internal structure of contourite drifts, which thus require a method of study which is both regional in coverage and capable of subsurface imaging. As a result, seismic data has become an integral part of the definition and classification of contourite drifts.

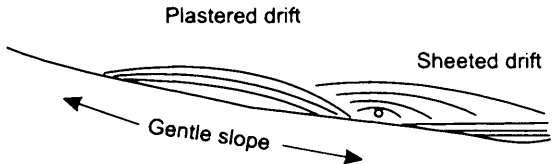
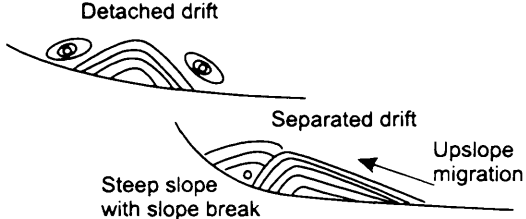

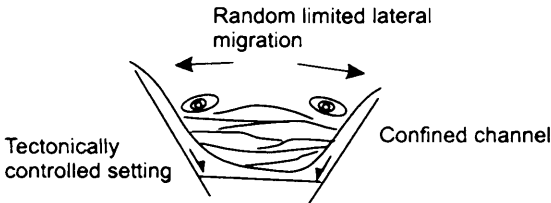
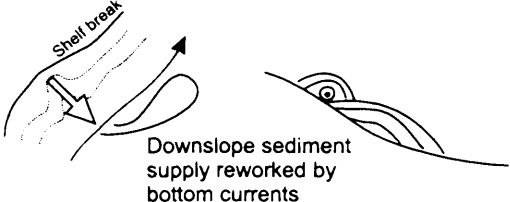
The seismic study of contourite drifts has led to the definition of a variety of diagnostic geometries which are summarised in Figure 1.3 (Faugères et al., 1999; Rebesco and Stow, 2001; Stow et al., 2002). In addition to these general diagnostic reflection geometries which are used to differentiate contourite drifts from other seismic facies, a number of distinct drift

**Figure 1.3**

Schematic illustration of the key seismic characteristics of contourite drifts. Re-drawn from Stow et al. (2002).

morphologies have been identified which have been used to divide contourite drifts into six main types: 1) contourite sheeted drifts; 2) elongate mounded drifts; 3) channel-related drifts; 4) confined drifts; 5) infill drifts; and 6) modified drift-turbidite systems (Fig. 1.4). Using the general characteristic reflection configurations and the specific characteristics of the varying drift types, contourite drifts have been identified from sedimentary basins around the world using both petroleum industry seismic data and seismic data sets acquired for academic use (e.g. Stow and Holbrook, 1984; Faugères et al., 1993; Hollister, 1993; Stow et al., 2002 and papers therein; Lu et al., 2003).

The morphology and internal reflection character of the various contourite drift types allows inference of the locus and parameters of the depositional current, thus providing palaeoceanographic information, and constitutes a fundamental component of this study. One of the most desirable pieces of information is the direction of the current flow. The bottom current flow direction is revealed by contourite drift migration, which in turn is identified by internal reflection progradation (Faugères et al., 1999). Significantly, contourite drifts typically migrate alongslope and down current (Faugères et al., 1999), and therefore, the identification of alongslope prograding internal reflections within contourite drifts reveals the depositional current flow direction (e.g. Howe, 1996; Damuth and Olsen, 2001; Davies et al., 2001; Knutz and Cartwright, 2003; Knutz and Cartwright, 2004). Seismic profiles orthogonal to the long axis of a drift body can also be used to determine the locus of depositional current (Fig. 1.4). The identification of contourite drifts using seismic data also allows postulation of the depositional current velocity. Contourite drift composition depends on the sediment source and the current strength, with deposition of fine grained sediment (silt) from bottom currents with velocities less than 7-15cm/s, while velocities of 30cm/s or greater required to deposit winnowed quartz sand contourite drifts (Heezen et al., 1966; Stow and Holbrook, 1984; Gorsline, 1985; Pickering et al., 1986; McCave, 1995a; McCave, 1995b). The identification of erosion surfaces, which are commonly associated with drifts, provides further insight into the behaviour of bottom currents (Faugères et al., 1999; Stow et al., 2002). Erosion of fine grained (silt sized) particles by bottom currents requires mean current speeds of 15-20cm/s, while considerably higher velocities are required to erode cohesive clay, sand or lithified sediments (McCave, 1995b). Therefore combined with interpretations of depositional current direction, locus and speed responsible for associated

Drift type	Seismic Character	Key criteria
Contourite sheeted drift	 <p>Plastered drift</p> <p>Sheeted drift</p> <p>Gentle slope</p>	<ul style="list-style-type: none"> <li>- Alongslope, downcurrent migration</li> <li>- Downslope and upslope migration</li> <li>- Sheeted drifts infill topography</li> <li>- e.g. Gardar Drift</li> </ul>
Elongate mounded drift	 <p>Detached drift</p> <p>Separated drift</p> <p>Upslope migration</p> <p>Steep slope with slope break</p>	<ul style="list-style-type: none"> <li>- Lateral margins flanked by moats containing depositional current flow axis</li> <li>- Alongslope downcurrent migration</li> <li>- Long axis parallel to slope</li> <li>- Separated drift - upslope migration e.g. Faro Drift</li> </ul>
Channel related drift	 <p>Contourite 'fan'</p> <p>Lateral and axis patch drifts</p>	<ul style="list-style-type: none"> <li>- Formed in deep channels, passageways &amp; gateways</li> <li>- Predominant downcurrent migration</li> <li>- Random lateral migration</li> <li>- Drift morphologies can include contourite 'fans' and lateral and axial patch drifts</li> <li>- e.g. Vema contourite fan</li> </ul>
Confined drift	 <p>Random limited lateral migration</p> <p>Tectonically controlled setting</p> <p>Confined channel</p>	<ul style="list-style-type: none"> <li>- Typical of small tectonically confined basins</li> <li>- Lateral moat development common</li> <li>- e.g. Sumba drift in the Sumba forearc basin</li> </ul>
Modified drift - turbidite systems	 <p>Shelf break</p> <p>Downslope sediment supply reworked by bottom currents</p>	<ul style="list-style-type: none"> <li>- Downslope sediment input reworked by alongslope currents</li> <li>- Common intercalation of turbidite, debrite and contourite facies</li> <li>- e.g. West Antarctic Peninsula</li> </ul>

**Figure 1.4**

Contourite drift types and their typical seismic reflection configurations and key diagnostic criteria. Infill drifts are generally similar to sheeted drifts, and are therefore not defined separately. Contourite drift geometries can be used to draw inferences upon the locus of depositional current. Modified from Faugères et al. (1999) and Stow et al. (2002).

contourite deposits, the identification of erosion surfaces can be interpreted as representation of fluctuations in the ocean current flow regime, which may in turn be linked to changes in circulation or climate identified using other proxies (e.g. stable isotopes).

## 1.5. Data and methodology

### *1.5.1. Database*

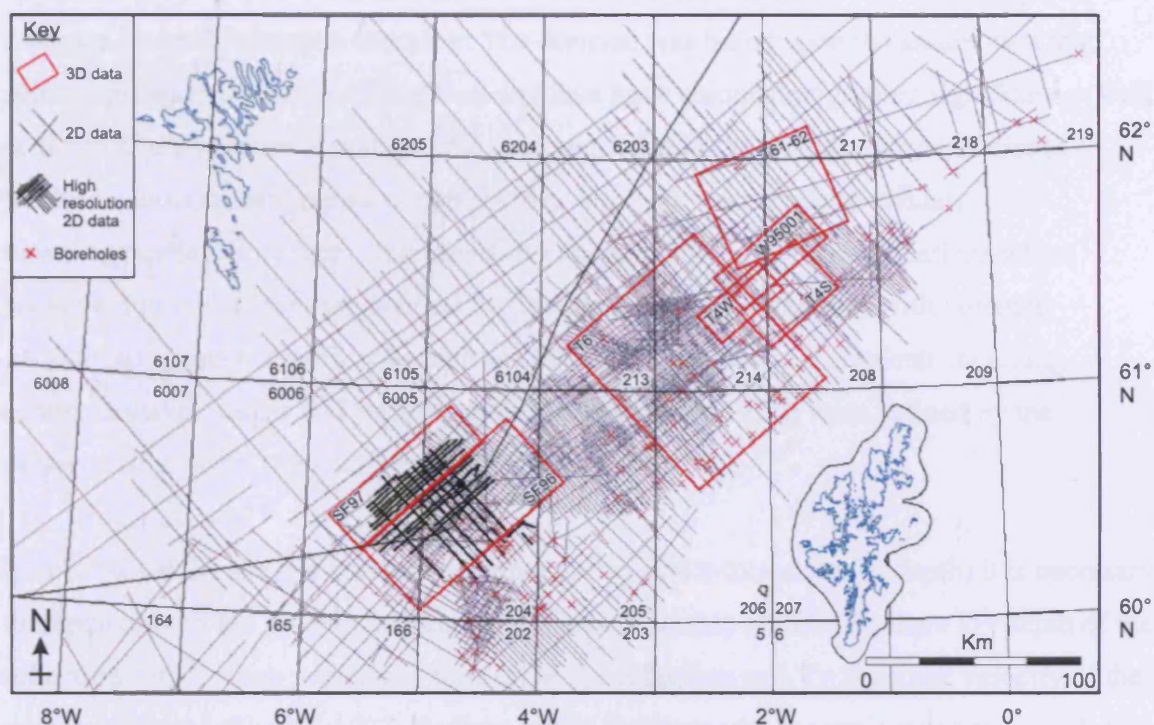
The study utilises a large seismic database consisting multi-channel 2D and 3D seismic data and high resolution 2D seismic site survey data (Appendix 1), most of which has been released from proprietary ownership from petroleum exploration and seismic acquisition companies although some remain proprietary and are available to the study under agreement of confidentiality. The seismic data are combined with 91 petroleum exploration boreholes and two British Geological Survey boreholes which provide lithological and biostratigraphic information (Appendix 2). With the exception of the high resolution 2D seismic survey, which was sourced as part of the study, the data set was pre-collated and loaded into Schlumberger's Geoquest seismic interpretation software prior to commencement.

The database provides seismic coverage of the entire Faeroe Shetland Basin, and comprises c. 32000 line km of 2D multi-channel seismic data from 13 surveys, c.21000km<sup>2</sup> of 3D multi-channel seismic data in 8 surveys and more than 1000km of high resolution 2D multi-channel seismic data (Fig. 1.5). The well database comprises 91 exploration boreholes (Fig. 1.5) some of which provide lithological and biostratigraphic information, the availability and quality of which is highly variable. Some wells are complete with biostratigraphic reports and digital geophysical logs and associated data, while others are only represented by printed reports and composite logs (Appendix 2). The two BGS boreholes recovered core from the shallow section (c. upper 200m) and thus provide robust high resolution biostratigraphic and lithologic calibration.

### *1.5.2. Methodology*

In order to analyse the stratigraphic succession of the basin the seismic data were interpreted using standard seismic-stratigraphic methods detailed by Mitchum et al. (1977). The





**Figure 1.5**

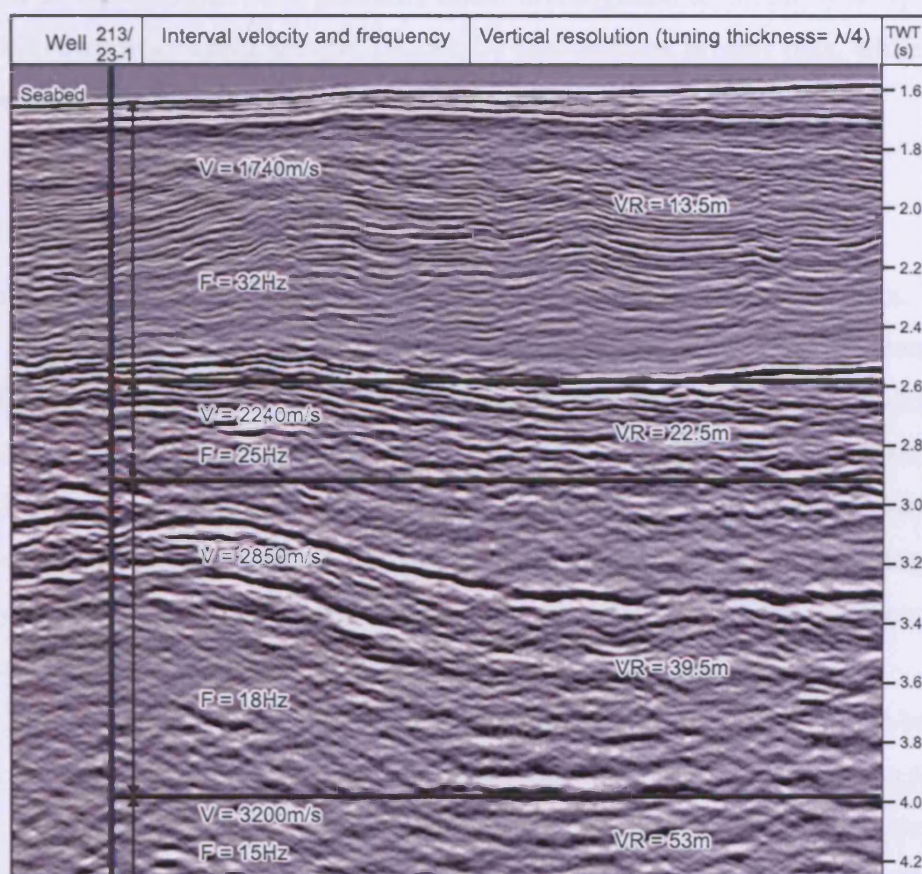
Map of the Faeroe Shetland Basin illustrating the dataset available to the study. The seismic data consists of 13 2D surveys of varying vintages combined with 8 3D surveys (one reprocessed survey not shown) and a high resolution 2D seismic grid. Petroleum exploration wells are represented by red crosses. Note the bias in data coverage toward the Shetland Margin, resulting from a combination of existing discoveries and play fairway distribution, shallow water, and absence of thick basalt coverage which blights exploration of the Faeroese Margin (see Fig 1.2).

stratigraphic succession was divided into units on a regional and local scale based on the identification of key reflections which formed correlatable markers and/or packages of common internal reflection character. The division was based upon the assumption that seismic reflections represent time lines and thus have chronostratigraphic significance (Vail et al., 1977). The seismic stratigraphic units were tied to the well database in order to produce a chronostratigraphic nomenclature. Attempts were made to validate biostratigraphic dating from well reports by comparison to published zonations where possible. Particular attention was paid to the identification of features with potential palaeoceanographic significance such as small scale architectural elements including sediment waves, moats and furrows and erosion surfaces which were defined by the presence of subcrop of underlying reflections.

In order to tie the seismic markers (in time) to the well information (in depth) it is necessary to depth-convert the seismic domain using the relationship  $D=T/2 \cdot V$  where  $D$ = depth of the reflection (m),  $T$ = two way travel time (s) of the reflection and  $V$ = the sonic velocity of the succession (m/s) (Sheriff, 1977; Badley, 1985). Estimates for the sonic velocity were derived from check shot data from petroleum wells with the average sonic velocity for the shallow section (c.upper 1000m) of the Faeroe Shetland Basin found to be c.1800m/s, although more precise values were used where available i.e. around wells with check shot data.

Knowledge of the sonic velocity of the succession is also critical for estimation of the vertical and horizontal resolution of the data, as is estimation of the frequency of the data. The vertical resolution of seismic data can be considered in two ways: firstly as the limit of separation which represents the minimum distance between two reflectors where the reflections from each do not overlap and are distinct, calculated as  $\lambda/2$  (wavelength/2); and secondly as the tuning thickness which is defined as the minimum distance between two reflectors before interference of their reflections becomes destructive, and is equivalent to  $\lambda/4$  (Badley, 1985). The wavelength is determined by the relationship  $\lambda=V/F$  where  $V$ = the sonic velocity and  $F$ = the frequency of the data. Figure 1.6 illustrates the resolution of a representative 2D seismic line within the Faeroe Shetland Basin, and reveals a significant decrease in resolution with depth as a result of frequency attenuation with depth combined with increased sonic velocities, likely due to increased compaction and lithification. The



**Figure 1.6**

Representative 2D seismic profile to illustrate reduction in vertical resolution with increased depth. Sonic velocities calibrated by correlation with well 213/23-1. Note increase in velocity with depth, likely due to increased compaction, coupled with decrease in frequency as a result of attenuation, resulting in a decrease in vertical resolution. Interval of interest to this study predominantly lies within the upper resolution interval, with vertical resolutions of c. 10-15m. Abbreviations: V= velocity; F= frequency; VR=vertical resolution;  $\lambda$  = wavelength.



horizontal resolution of migrated seismic data is also equivalent to  $\lambda/4$ . The profile also shows that the stratigraphic level primarily under investigation in this study is typically imaged with a vertical resolution of c.10-15m by conventional seismic data, while the high resolution seismic data grid return vertical stratigraphic resolutions of c.5m.

## 1.6. Thesis layout

Following the introductory chapter, the thesis is divided into a further 5 chapters. The research component of the thesis comprises 3 chapters written in the style of scientific papers (*Chapters 2, 3 and 4*). The main chapters therefore each include an introductory section and a detailed interpretation and discussion of the results, thus forming semi-independent work packages. Due to the inclusive nature of the main chapters, the thesis concludes with a short discussion of the main results and the data and methodology employed (*Chapter 5*) and a summary of the main scientific conclusions (*Chapter 6*). Each chapter is structured as follows:

*Chapter 2* investigates the onset of contourite drift deposition within the basin, therefore providing an estimate for the initiation of the Faeroe Shetland Basin as an oceanic gateway. The transition between early Palaeogene slope progradation and delta development and contourite deposition within the southern Faeroe Shetland Basin is investigated using high resolution 2D seismic data coupled to detailed analysis and synthesis of biostratigraphic data from key petroleum and BGS boreholes within the area in order to chronologically constrain this critical event in the basin's history. The chapter concludes with a reassessment of the onset of deep water circulation from the Norwegian Greenland Sea across the Greenland Scotland Ridge into the North Atlantic via the Faeroe Shetland Basin, which in turn is related to changes in global climate and ocean circulation during that time.

*Chapter 3* forms a continuation from chapter 2 and charts the development of the Faeroe Shetland Basin as an oceanic gateway throughout the late Palaeogene and Neogene. Division of the stratigraphic succession based on identification of key seismic marker reflections and packages of characteristic reflection configuration is in turn fully correlated with published stratigraphic nomenclatures in order to clarify the late Palaeogene and Neogene succession of the Faeroe Shetland Basin. Analysis of the stratigraphic succession allows reconstruction of the flow of deep waters from the Norwegian Greenland Sea through

the Faeroe Shetland Basin throughout the interval of interest. Furthermore, deep water unconformities present within the basin are documented and interpreted in detail. The chapter concludes with a synthesis of the late Palaeogene and Neogene sedimentary and oceanographic development of the basin.

*Chapter 4* uses 3D data to focus on the characterisation of the Pliocene-Pleistocene West Shetland Drift in order to establish constraints on the palaeoceanographic development of the West Shetland slope throughout the late Neogene. Particular emphasis is placed on the identification and interpretation of smaller scale architectural elements such as sediment waves in order to add detail to the understanding of the development of contourite systems within the basin which cannot be ascertained using 2D seismic profiles. The chapter includes interpretation of the interaction between contourite deposition and alongslope current activity with episodes of glaciation during the late Neogene, and concludes with a model for the palaeoceanographic development of the West Shetland margin.

*Chapter 5* synthesises the main results of each of the 3 studies into a proposed evolution of the Faeroe Shetland Basin as an oceanic gateway. The advantages of the use of industrial seismic data as a tool for contourite research are then briefly investigated, with comment on previous application of this method specifically within the Faeroe Shetland Basin, and the advances that have been made during this study. Finally, the general limitations of seismic data in contourite research both within the Faeroe Shetland Basin and in general are touched upon before the chapter concludes with proposals for future avenues of study.

*Chapter 6* lists the main scientific results and conclusions of this study.

## Chapter Two: Eocene contourite drifts and initiation of overflow across the Greenland Scotland Ridge<sup>1</sup>

### 2.1. Abstract

Using a combination of regional and high resolution 2D seismic and borehole data, a new early middle Eocene contourite drift body has been discovered within the southern Faeroe Shetland Basin. A spectacular climbing disconformity relationship exhibited by the drift onto a basal unconformity surface is confidently interpreted as an indicator of a southerly flowing depositional current, and, combined with other evidence for the structural and sedimentological development of the Faeroe Shetland Basin, is used to suggest that the drift body represents the onset of southerly flowing deep waters from the Norwegian Greenland Sea through the Faeroe Shetland Basin and into the North Atlantic. Therefore, the drift body is interpreted to date the timing of the initiation of the Faeroe Shetland Basin as an oceanic gateway as early middle Eocene, predating previous estimates by more than 15Ma. In turn, the southerly flow of deep waters through the Faeroe Shetland Basin is interpreted to represent the earliest overflow of waters formed in the Norwegian Greenland Sea into the North Atlantic across the Greenland Scotland Ridge as part of a North Atlantic Conveyor Belt-style circulation similar to that which characterises the North Atlantic at present, and which has a major influence on the climate of western Europe. The onset of the circulation system during the middle Eocene is thought to be the result of a combination of factors including generation of deep waters north of the Greenland Scotland Ridge as a result of cooling climate conditions at high latitudes combined with tectonic development of the basin as a deep water passageway across the Greenland Scotland Ridge following the withdrawal of the proto-Icelandic plume. The study highlights the value of industrial seismic and well data to contourite and palaeoceanographic research.

---

<sup>1</sup> In preparation for submittal to *Palaeoceanography* as:

*'A Middle-Eocene onset of the North Atlantic Conveyor Belt: evidence from the Faeroe-Shetland Basin'*. Hohbein, M.W. and Cartwright, J.A.

## 2.2. Introduction

Present day alongslope bottom current circulation through the Faeroe Shetland Basin plays a critical role in the North Atlantic Conveyor Belt circulation (Broecker, 1991) which in turn comprises a critical element of the global thermohaline circulation (Schnitker, 1980; Schmitz 1995; Rahmstorf, 2002). The widespread occurrence of Oligocene-Neogene contourites, sediments deposited by or significantly influenced by bottom currents (Stow et al., 2002), within the Faeroe Shetland Basin suggests an oceanic circulatory regime prevailed within the basin throughout that time. Estimates for the onset deep water circulation through the Faeroe Shetland Basin range from the early Oligocene (Davies et al., 2001) to mid Miocene (Schnitker, 1980; Eldholm, 1990; Stoker, 2003; Stoker et al., 2005). The North Atlantic Conveyor Belt results from thermal densification of surface waters in the Norwegian Greenland Sea in order to produce deep waters which then flow through the Faeroe Shetland Basin into the North Atlantic, and is reliant on a latitudinal temperature gradient between the tropics and the high latitude polar regions (Broecker and Denton, 1990; Broecker, 1991; Hansen and Østerhus, 2000). Multi-proxy investigations reveal that the global climate began to cool during the early Eocene and continued to do so throughout the Neogene, with the development of northern hemisphere ice sheets during the Late Miocene-Pliocene (Shackelton and Kennett, 1975; Raymo, 1992; Thiede et al., 1998 Lear et al., 2000; Pearson and Palmer, 2000; Zachos et al., 2001). However, it has recently been proposed that large northern hemisphere ice sheets existed in the northern hemisphere during the middle Eocene (Tripathi et al., 2005), a claim supported by the identification of ice rafted debris within middle Eocene sediments on the Lomonosov Ridge (ACEX, 2005), while sea surface temperature proxies for the tropics indicate temperatures similar or slightly below modern values (Shackelton and Boersma 1981; Barron 1987; Zachos et al., 2001). The existence of this latitudinal temperature gradient during the middle Eocene (e.g. Zachos et al., 1994) provides the potential for deep water formation in the Norwegian Greenland Sea at this time. In contrast to the Oligocene-Neogene contourite deposition, the Eocene succession of the Faeroe Shetland Basin is largely characterised by slope margin progradation from the Shetland Margin and basalt eruption from the Faeroese Margin, with deep water fan deposition in the deep basin axis (Naylor et al., 1999; Robinson, 2004; Robinson et al., 2004). Therefore, a significant change in dominant depositional process within the basin is apparent between the Eocene and Oligocene, resulting in a distinct change in the

sedimentary succession. It is this period of transition from downslope processes to contourite deposition that forms the focus of this study.

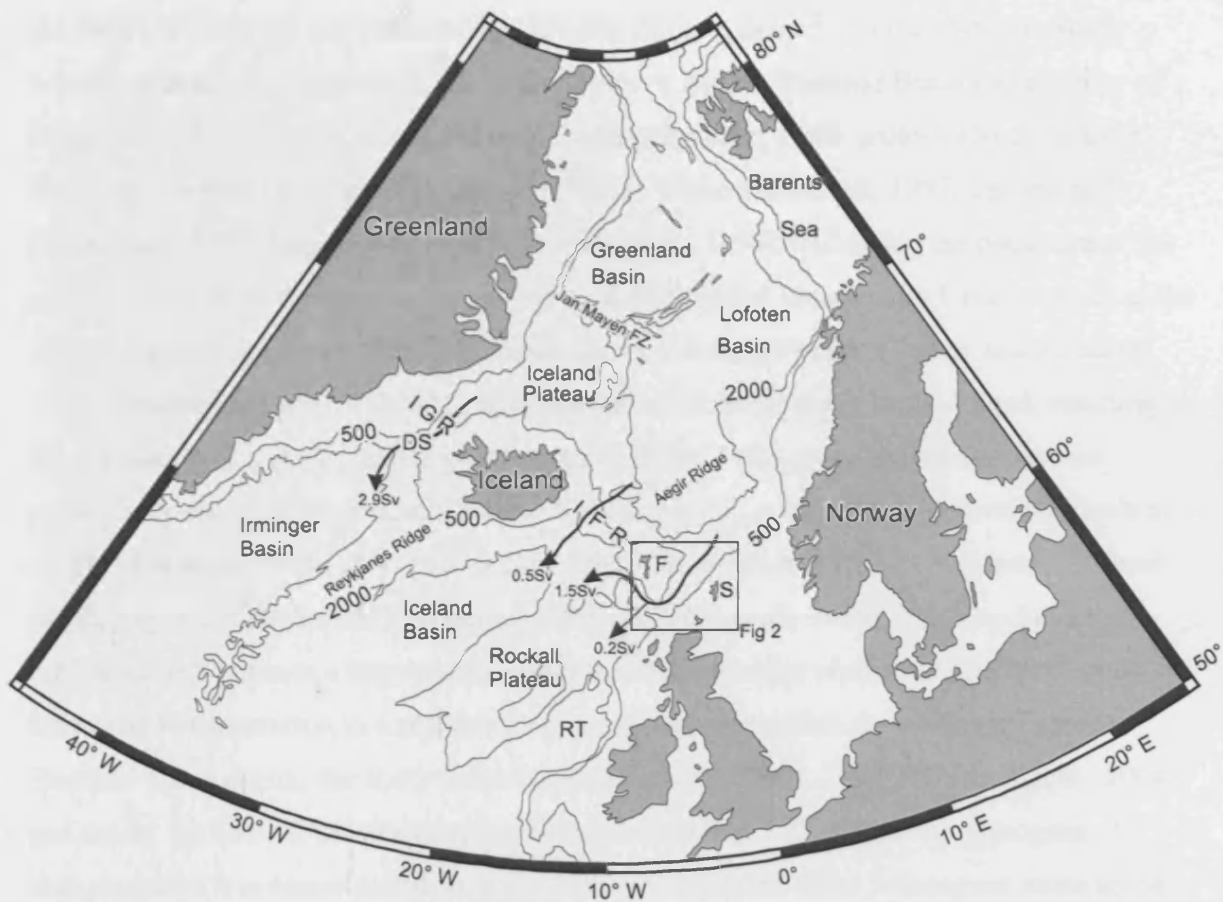
The discovery of commercial hydrocarbon reserves in the Faeroe Shetland Basin has resulted in the acquisition of large quantities of seismic and well data within the basin by the petroleum industry over the past 3 decades that were used during this study used to analyse the Cenozoic succession. The aim of this study is to establish the earliest evidence for contourite deposition within the basin, and to place these deposits in a regional palaeoceanographic framework. Specifically, the transition between the down-slope processes that dominated deposition during the early Eocene (Robinson et al., 2004) and contourite deposition during the Oligocene (Davies et al., 2001) is analysed in detail, using data that was only recently released for academic study. The interpretation of this data has necessitated a re-appraisal of palaeocirculation within the key gateway of the Faeroe Shetland Basin, with the result that onset of deep water exchange of Nordic waters with the North Atlantic commenced much earlier than is widely accepted. This in turn raises questions over the pace of climatic deterioration in the northern hemisphere following from the thermal maximum at the Palaeocene/Eocene boundary (Pearson and Palmer, 2000; Zachos et al., 2001; Bice and Marotzke, 2002), and the significance of the recent claims for ice sheet presence in the northern hemisphere during the middle Eocene (Tripathi et al., 2005). Finally, the paper has a broader underlying aim of extending the approach adopted by Knutz and Cartwright (2003; 2004) in highlighting the potential value of petroleum industry multichannel seismic data for contourite and palaeoceanographic research.

## 2.3. Regional geological setting and oceanography

### *2.3.1. Geological setting*

The Faeroe Shetland Basin is located on the northwestern European margin, and lies between the Shetland and the Faeroe Islands (Fig. 2.1). The basin is the southernmost and deepest passageway across the Greenland-Scotland Ridge (GSR) (Bott, 1983), which forms a major bathymetric ridge that stretches from Eastern Greenland through Iceland and the Faeroes to NW Scotland (Fig. 2.1 – Bott, 1983; Nilsen, 1983). The Faeroe Shetland Basin consists of a series of Mesozoic tilted fault blocks formed through multiple rift episodes





**Figure 2.1**

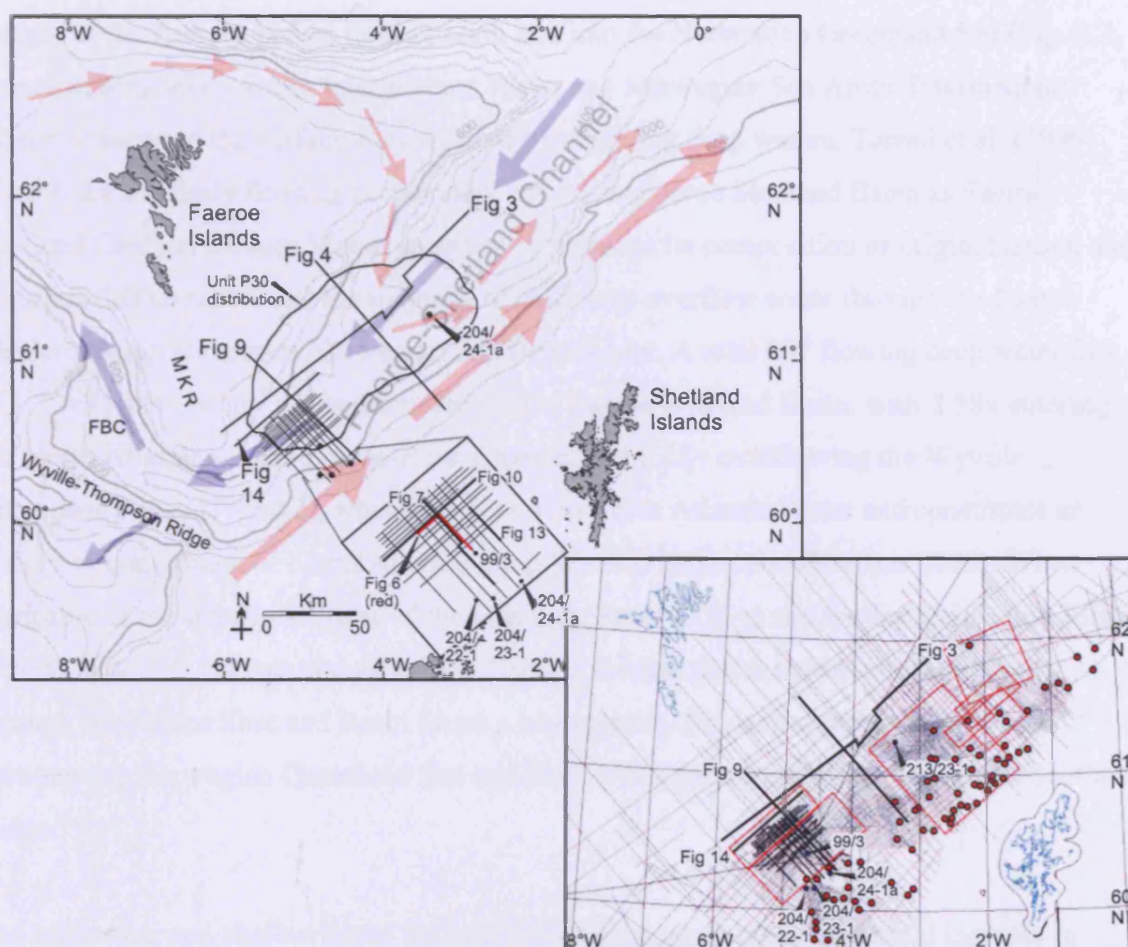
Map of the North Atlantic and Norwegian-Greenland Sea. Contours show bathymetry in metres. Arrows and Sv values ( $1 \text{ Sv} = 1 \text{ Sverdrup} = 10^6 \text{ m}^3 \text{ s}^{-1}$ ) represent deep water overflow volumes across the Greenland-Scotland Ridge (Hansen and Østerhus, 2000).

Abbreviations: IGR, Iceland-Greenland Ridge; IFR, Iceland-Faeroe Ridge; F, Faeroe Islands; S, Shetland Islands; DS, Denmark Strait; RT, Rockall Trough. Figure references refer to figures within chapter e.g. 'Fig 2' refers to Figure 2.2.

which preceded the initiation of seafloor spreading in the northern North Atlantic during the Palaeogene (Hitchen and Ritchie, 1987; Doré and Lundin, 1996; Dean et al., 1999; Naylor et al., 1999). During the late Palaeocene and early Eocene, opening of the northern North Atlantic was accompanied by uplift of the southern Faeroe Shetland Basin and effusion of voluminous flood basalts associated with the impingement of the proto-Icelandic mantle plume on the base of the crust (Waagstein, 1988; White and Lovell, 1997; Lamers and Carmichael, 1999; Naylor et al., 1999; Roberts et al., 1999). Following the departure of the mantle plume from the area and drowning of the sub-aerial Base Balder Unconformity at the southern end of the Faeroe Shetland Basin during the early Eocene (Turner and Scrutton, 1993; Smallwood and Gill, 2002), rapid thermal subsidence of the basin ensued, resulting in the deposition of a thick Cenozoic sedimentary cover. Palaeogene sedimentation was particularly active in the southern Faeroe Shetland Basin, with a thick (several hundreds of metres) Eocene succession accumulating in the Judd basin area (southern Faeroe Shetland Basin, Fig. 2.2, Lamers and Carmichael, 1999; Roberts et al., 1999). The Top Balder Formation reflection is a key seismic-stratigraphic datum that represents the transition from terrestrial sedimentation to a shallow marine environment within the southern Faeroe Shetland Basin during the Early Eocene (Smallwood and Gill, 2002; Robinson et al., 2004), and marks the base of the stratigraphy for this study (Fig. 2.3). Oligocene – Neogene sedimentation was concentrated further north, onlapping the older Palaeogene strata to the south. In consequence, it is possible to define crude southern Palaeogene and northern Neogene depocentres within the basin (Fig. 2.3). The boundary between the Faeroe Shetland Basin and the Rockall Trough to the south is defined by the Wyville-Thompson Ridge and associated structures (Fig. 2.2), which formed as a result of N-S compression during the early Eocene (Boldreel and Andersen, 1995).

### 2.3.2. *Oceanographic circulation*

The Faeroe Shetland Basin forms a major conduit for the present day communication of water masses between the Norwegian-Greenland Seas and the North Atlantic (Turrell et al., 1999; Hansen and Østerhus, 2000; Kuijpers et al., 2002). The present day oceanographic regime within the basin consists of inflow of warm saline waters above c.400-600m and a return outflow of deep, cold waters below 400-600m (Hansen and Østerhus, 2000; Masson et al., 2002). The surface inflow water is composed predominantly of North Atlantic Water



**Figure 2.2**

Bathymetry map of the Faeroe-Shetland Basin illustrating location of seismic profiles and seismic datasets. The study focuses on the Judd Basin area, approximately defined by high resolution seismic survey (black grid at southern end of basin). Coloured arrows represent present day oceanographic circulation: red arrows- warm saline inflow waters into the Norwegian Greenland Sea; blue arrows - cold deep water outflow waters. Black line illustrates areal extent of the Unit P30 contourite drift. Abbreviations: FBC, Faeroe-Bank Channel; MKR, Munkagrunnar Ridge. Inset map displays data available to this study. Thin grey lines = 2D seismic database; black lines = high resolution 2D seismic survey; red boxes = 3D data sets; red dots = available wells; 5 key wells used in this study are named. Figure labels refer to Figures within this chapter, e.g. Figure 3 represents the location of Figure 2.3.

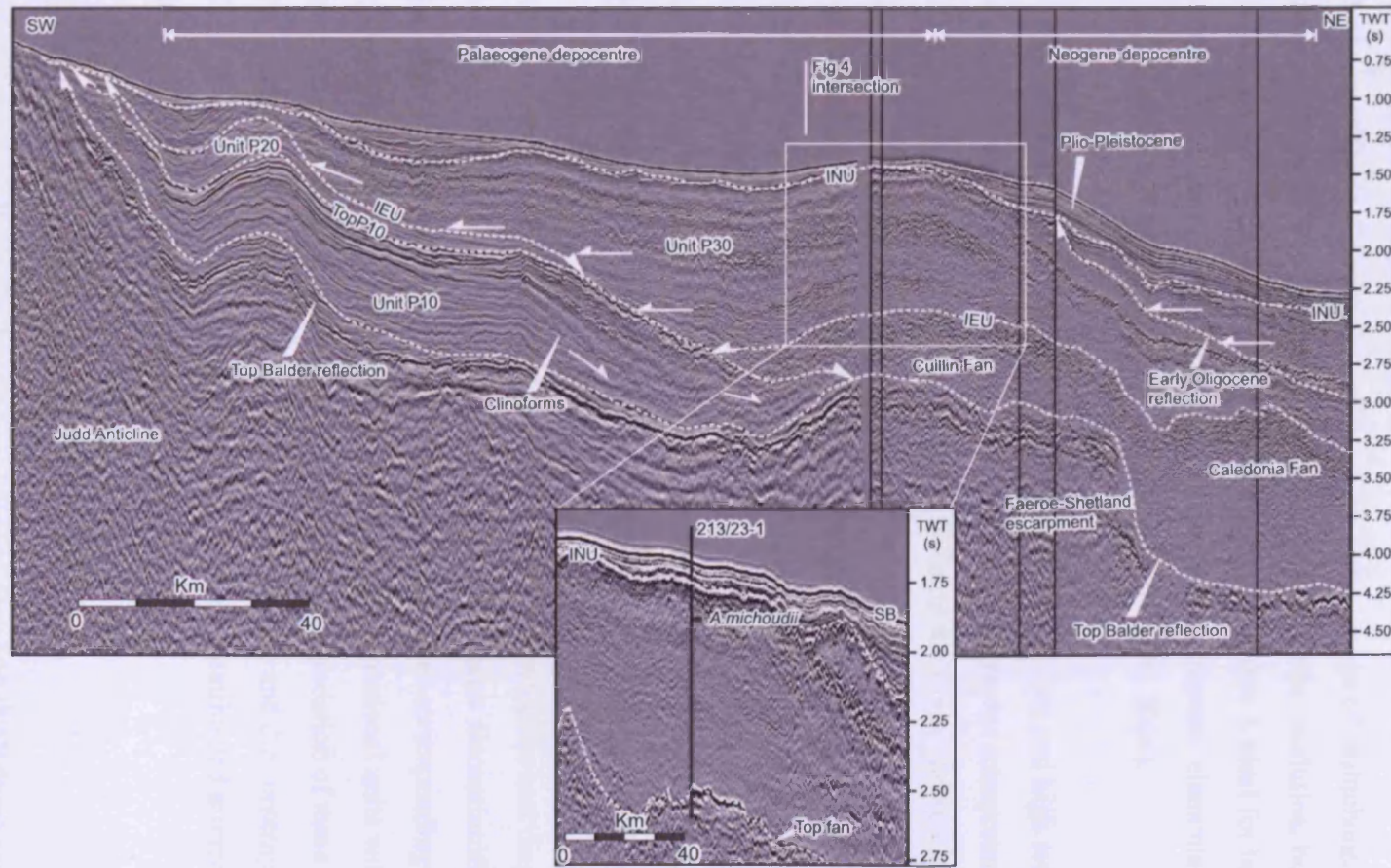
which flows along the Scottish Slope and into the Norwegian Greenland Sea, and modified North Atlantic Water, a branch of the North Atlantic Current that flows around the northern margin of the Faeroes before turning north and into the Norwegian Greenland Sea (Fig. 2.2, Turrell et al., 1999). Arctic Intermediate Water and Norwegian Sea Arctic Intermediate Water lie between the surface waters and the underlying deep waters. Turrell et al. (1999) refer to the southerly flowing deep waters within the Faeroe Shetland Basin as Faeroe-Shetland Channel Bottom Water, so as not to prejudge its composition or origin. Hansen and Østerhus (2000) report that the majority of cold deep overflow water through the Faeroe Shetland Basin comprises Norwegian Sea Deep Water. A total SW flowing deep water flux of 1.7Sv ( $1\text{Sv} = 10^6 \text{ m}^3 \text{ s}^{-1}$ ) is estimated for the Faeroe Shetland Basin, with 1.5Sv entering the North Atlantic via the Faeroe-Bank Channel and 0.2Sv overflowing the Wyville Thompson Ridge (Fig. 2.2), where it mixes with North Atlantic Water and constitutes an important component of North Atlantic Deep Water (Hansen and Østerhus 2000). When compared to the overflow fluxes of the Denmark Strait (2.9Sv) and the Iceland Faeroe Ridge (0.5Sv) (Fig. 2.1, Hansen and Østerhus, 2000), it is clear that the passage of deep water through the Faeroe Shetland Basin forms a key gateway for deep water mass exchange between the Norwegian Greenland Sea and the North Atlantic across the Greenland Scotland Ridge.

The narrowing and shallowing of the basin toward the south causes a tenfold increase in deep water current velocity (Smallwood, 2004), resulting in widespread non-deposition/erosion of the seafloor (Masson et al., 2005). Within the open channel toward the north of the basin, the effect of the Coriolis Force results in SW flowing deep water currents impinging primarily on the Faeroese side of the basin, while toward the south deep water currents fill the bottom of the channel (Turrell et al., 1999; Hansen and Østerhus, 2000; Masson et al., 2005).

### 2.3.3. *Seismic expression of contourite drifts*

Field study of ancient contourite drifts is notoriously difficult on account of the drift size and subtle sedimentological character in relation to associated/interbedded sediments (Stow et al., 2002). One-dimensional study of ancient and modern contourite drifts from core samples faces the same problem. Various geophysical techniques can be employed to study modern





**Figure 2.3**

Regional strike-orientated 2D seismic profile along the axis of the Faeroe Shetland Basin (line location Fig. 2.2) illustrating spatial distribution of key units. Note shallowing of the Top Balder reflection to the SW, and the dominance of Palaeogene strata toward the SW, thus defining the Palaeogene and Neogene (including Oligocene) depocentres. Note also progressive SW onlap of reflections within Unit P30. Inset panel shows 2D line 20km to SE and details the calibration of late Eocene (*A. michoudii* - Priabonian) within well 213/23-1. Figure references refer to figures within chapter e.g. 'Fig 4' refers to Figure 2.4.

or ancient contourite drifts in the marine environment. High resolution reflection seismic imaging (frequency range from 100's Hz-1000's Hz) gives accurate coverage of seabed morphologies and the potential for shallow (few 10's metres) penetration for internal character analysis. Conversely, the lower frequency range of multichannel seismic data (c.10-100Hz) results in relatively low vertical stratigraphic resolution, but greater penetration, in excess of several kilometres, and this makes it ideal for large scale definition of contourite bodies, and interpretation of internal architectural elements (Davies et al., 2001; Knutz and Cartwright 2003; Knutz and Cartwright, 2004).

Combination of industry standard multichannel seismic data and high resolution data acquired for site surveys is thus ideal for seismic stratigraphic interpretation of contourites. Grid dimensions and spacing are critical in defining the limits and spatial resolution of specific features such as moats, or sediment waves, and the availability of 3D seismic data adds significantly to the seismic stratigraphic toolbox in providing spatial resolution of the order of 25-50m over survey areas that can be up to several tens of thousands of km<sup>2</sup>. Many features of drifts which may be difficult to map uniquely using coarse grids of 2D seismic data can thus be elucidated using 3D seismic data, and this provides added constraints to diagnostic interpretation of contourite systems.

Faugères et al. (1999) outlined 3 key features which provide the best diagnostic criteria for contourite drifts when viewed using seismic data: (1) major discontinuities that can be traced throughout the extent of the drifts and represent timelines corresponding to distinct hydrological events; (2) lenticular, convex-upward depositional units with variable geometries and; (3) a specific style of progradation-aggradation of these units influenced by the interaction of the bottom current with Coriolis force and the contemporaneous seabed. These diagnostic criteria provide a basis for the identification and interpretation of contourite drifts which was employed during this study.

## 2.4. Data and methodology

The data base available for this study comprised over 600 (32000km) conventional 2D seismic profiles, 7 3D seismic surveys (c.21000km<sup>2</sup>) and over 1000km of a high resolution 2D seismic site survey combined with 91 industry wells and 2 BGS boreholes (Fig. 2.2). The

conventional 2D seismic profiles afford regional coverage and allowed interpretation of key reflections throughout the basin. Due to the largely pre-Cenozoic nature of the majority of the exploration targets within the basin, the quality of the data in the shallow section varies. Standard 2D seismic profiles exhibit frequencies of between 30-50Hz and using interval velocities of 1800m/s, result in a maximum vertical stratigraphic resolution of c.11-15m (tuning thickness =  $\frac{1}{4}$  of the dominant wavelength, Badley 1985). Similar frequencies dominate the shallow section (upper 1-2s) of the 3D surveys, which on average yield similar vertical resolutions to the 2-D data. The high resolution 2-D data set, 2DHR, was acquired over a limited area toward the southern end of the Judd Basin (Fig. 2.2). The high resolution data exhibits frequencies of 45-170Hz, with peak frequencies of 90-110Hz in the shallow section, retuning a maximum vertical resolution of c.4-5m, and thus presents the potential for analysis of the stratigraphy in extremely fine detail.

The location of the UK-Faeroese border in the centre of the basin combined with (1) the deep water in the centre of the channel and (2) the fact that the majority of hydrocarbon discoveries to date have been made on the Shetland slope, results in a geographical bias in the data with the majority of the 3D surveys situated close to the Shetland Slope (Fig. 2.2). These factors apply to the distribution of the well database and conventional 2D seismic data, resulting in a comparative lack of stratigraphic calibration in the central basin axis. Four exploration wells that penetrated sequences relevant to this analysis were available for this study (Fig. 2.2). Check-shot velocity data derived from the wells were used for depth conversion and for calibration of biostratigraphic and lithological data to the seismic data.

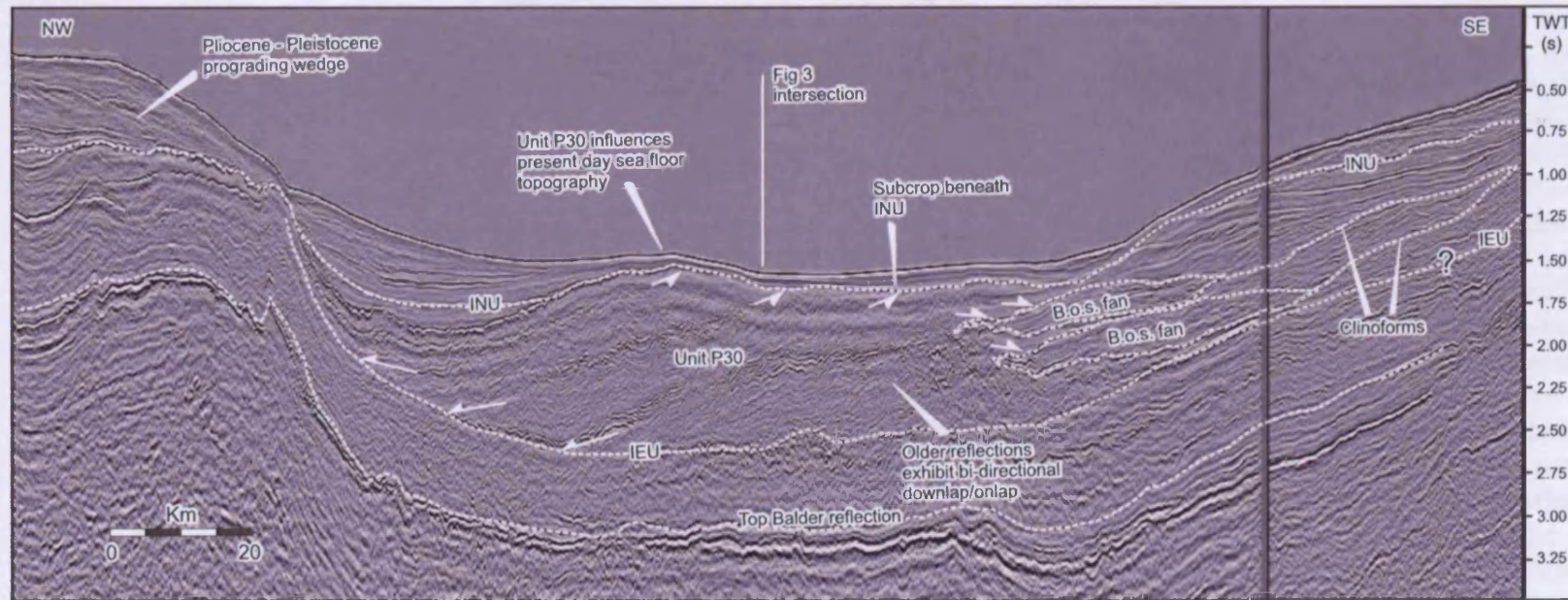
Regional mapping of various reflections was undertaken in order to sub-divide and interpret the post-Top Balder Formation stratigraphy. A detailed stratigraphy was established for the Judd Basin utilising the high resolution data set, which was calibrated with available well and borehole data to support the seismic interpretation. Individual units were identified and defined using the standard seismic-stratigraphic methods outlined by Mitchum et al. (1977).

## 2.5. Seismic Interpretation

### 2.5.1. Seismic stratigraphy

Seismic stratigraphic analysis of the Cenozoic succession within the basin reveals a distinct differential distribution of the Palaeogene and Neogene age strata (Stoker, 2003). Palaeogene strata are distributed throughout the basin, but are concentrated in the southern basin where northerly directed shelf margin and delta progradation during the late Palaeocene and early Eocene resulted in accumulation of a thick Palaeogene succession in the Judd Basin area (Fig. 2.2) (Nadin et al., 1997; Lamers and Carmichael, 1999; Smallwood and Gill, 2002; Robinson, 2004, Robinson et al., 2004). Late Palaeogene and Neogene sedimentation was concentrated toward the northern end of the basin and on the Faeroes margin, and internal packages exhibit reflection onlap onto the Palaeogene strata toward the SW (Fig. 2.3). Therefore, re-analysis of the onset of contourite drift deposition within the basin during this study focuses on the southern basin. A thick post-Top Balder succession is interpreted on regional seismic profiles across the southern end of the basin. This succession attains maximum thickness in the basin axis and thins toward the basin margins (Figs. 2.3 & 2.4). The upper boundary of the post-Balder, Palaeogene succession is marked by the Intra Neogene Unconformity (INU), which forms a significant erosional unconformity throughout the basin and is dated as Late Miocene-Early Pliocene in age (Figs. 2.3, 2.4 & 2.5). It is the thick Palaeogene package between the Top Balder and INU reflections that forms the focus of this study. Detailed seismic interpretation has allowed subdivision of the stratigraphy into 3 main depositional units: Units P10, P20 and P30 (prefix P denotes Palaeogene) (Figs. 2.3, 2.5 & 2.6). Unit P30 is further subdivided into subunits P30a and P30b (Figs. 2.5 & 2.6). Units P10 and P20 are primarily identified using the 2DHR survey, and as a result cannot be mapped for any significant distance beyond the Judd Basin area. Unit P30 forms the most significant of the three units in terms of thickness and depositional extent, and can be correlated from the high resolution data into the regional grid of standard 2D seismic profiles, from which the unit areal extent is defined (Fig. 2.2). These units are firstly defined and described from the sub-area in which 2D high resolution seismic is available (*section 2.5.2*), and subsequently are set within a more regional seismic-stratigraphic context (*section 2.5.3*).





**Figure 2.4**

Regional 2D seismic profile across the basin (line location Fig. 2.2). The line illustrates the domination of the post-Balder stratigraphy of the southern Faeroe Shetland Basin by Unit P30, which is seen to influence present day seabed topography. Internal reflections exhibit NW directed onlap onto the IEU (Intra-Eocene unconformity) on the Faeroes margin, and SE directed intercalation with and onlap onto the base of slope fans (B.o.s. fans) and the IEU, revealing the mounded depositional geometry. Figure references refer to figures within chapter e.g. 'Fig 3' refers to Figure 2.3.

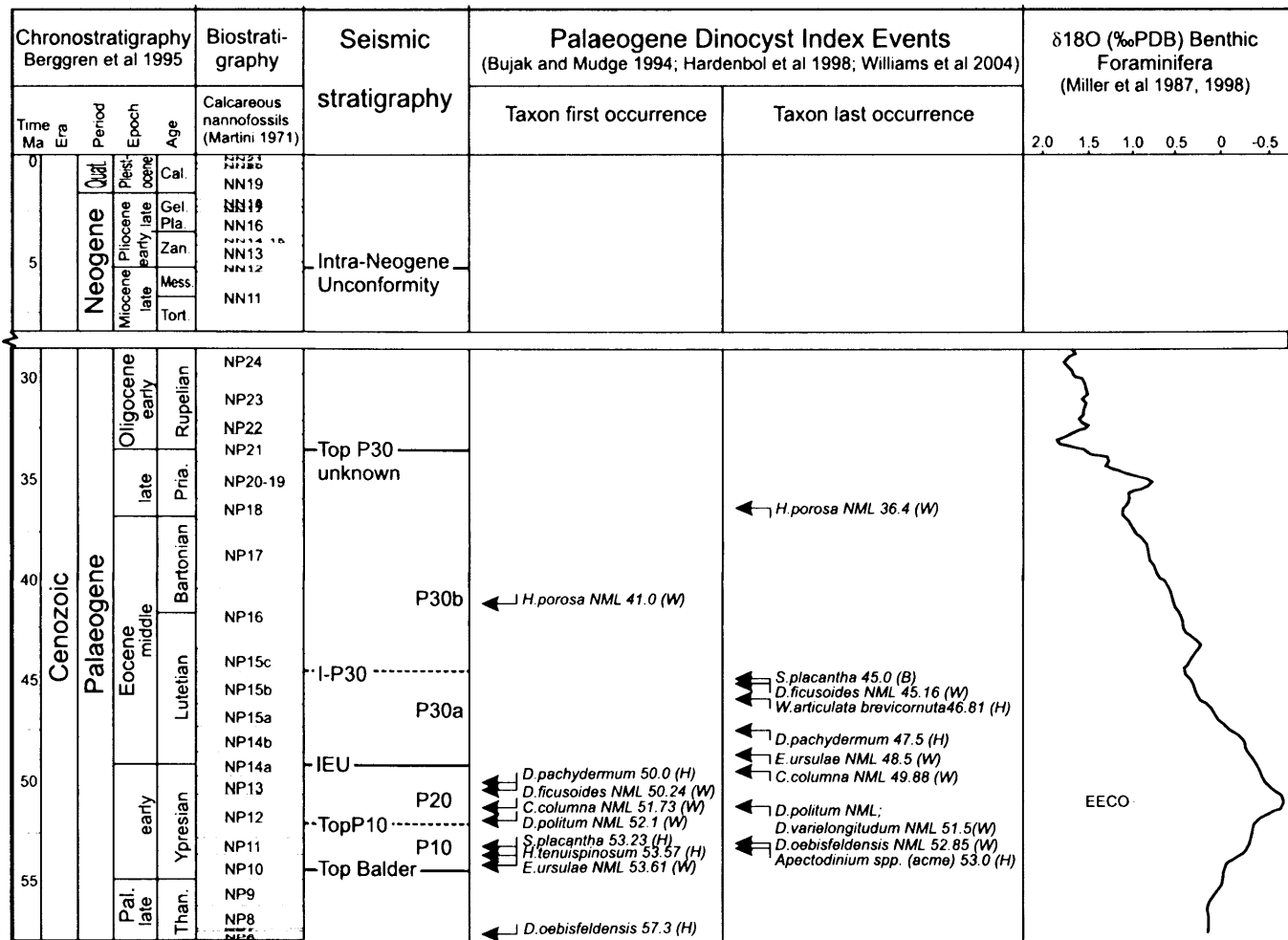


Figure 2.5

Chronostratigraphic, biostratigraphic and seismic-stratigraphic scheme for the Eocene of the Faeroe Shetland Basin, with the addition of the late Neogene to illustrate the occurrence of the INU. First and last occurrence datums of Palaeogene dinocyst index events allow dating of the stratigraphy. The stratigraphic top of Unit P30 remains undefined.  $\delta^{18}O$  curve for the Eocene reveals steady increase in isotopic values in relation to global cooling following the Early Eocene Climatic Optimum (EECO, Zachos et al., 2001). Biostratigraphy abbreviations: (B)- Bujak and Mudge (1994); (H)- Hardenbol et al. (1998); (W)- Williams et al. (2004); (NML)- Northern Hemisphere mid-latitudes.

### *2.5.2. High resolution seismic stratigraphic analysis of the southern Judd basin*

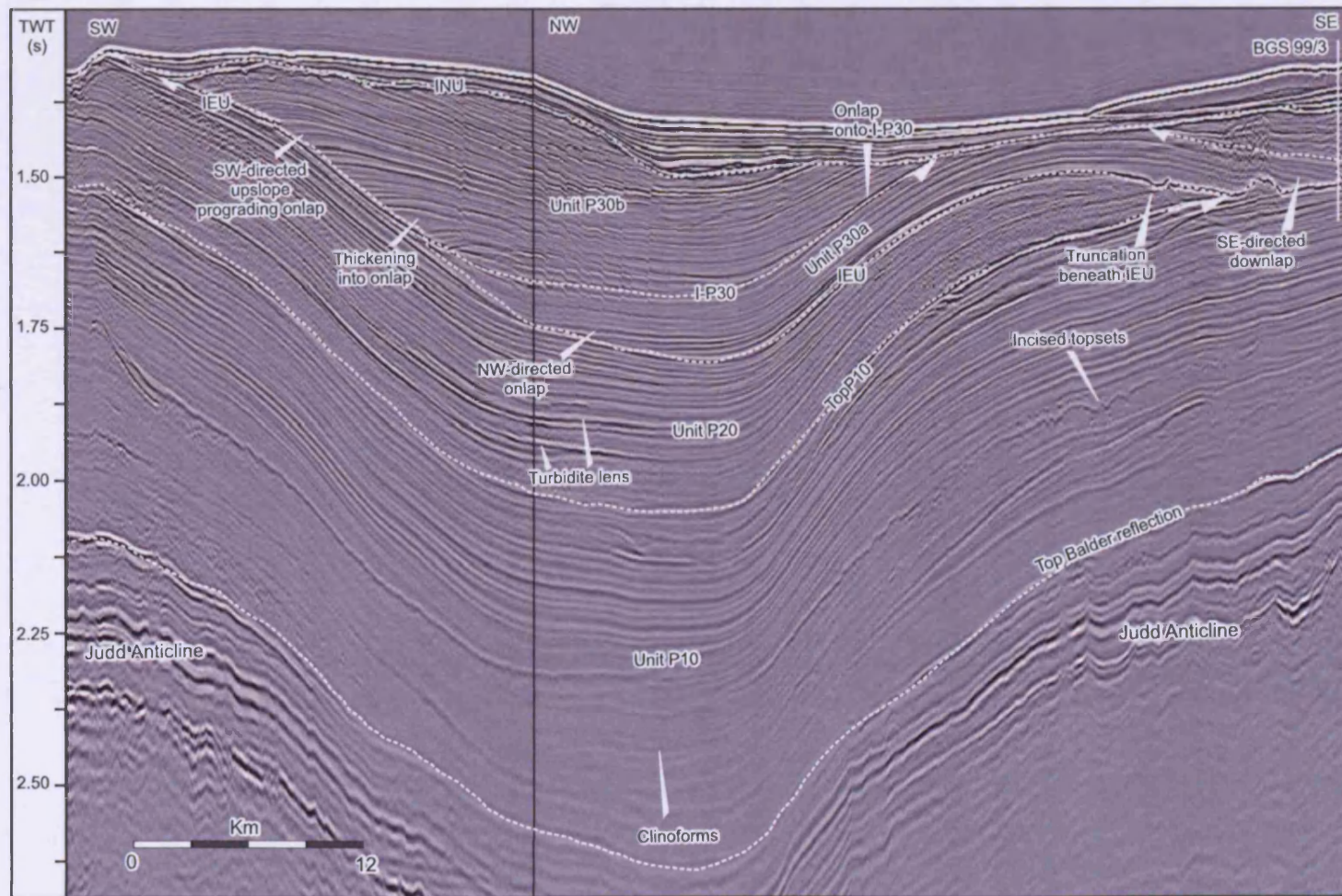
The 2DHR data are used to outline the study interval because of their much higher vertical stratigraphic resolution in comparison to standard seismic data. These data provide additional detail such as reflection terminations and thus allow subtle unconformities to be detected where they would otherwise be uninterpretable if only standard seismic data were available. Each unit defined in this study area is bounded at its top and base by distinctive and laterally correlatable seismic reflections, which separate packages of reflections interpreted to be depositionally distinct from those above and below. Our definition of units is thus based on a depositional package approach (Brown and Fisher, 1977), rather than a strictly sequence stratigraphic approach. A similar package-based approach was employed more regionally in the Eocene of the Faeroe Shetland Basin by Robinson (2004). The unit nomenclature and bounding surfaces are presented in Figure 2.5, and are described in chronological order below.

#### *2.5.2.1. Unit P10*

Unit P10 is bounded at its base by the Top Balder Formation reflection (as identified by Smallwood, 2004), and at its top by reflection TopP10 (approximately equivalent to the I-Lutetian 1 reflection of Smallwood, 2004) (Figs. 2.5 & 2.6). The TopP10 reflection exhibits a variable seismic amplitude and forms a correlatable surface throughout the 2DHR survey and is identified as a bounding surface based on internal reflection character and thickness distributions of the overlying and underlying Units P10 and P20. However, the TopP10 reflection is truncated beneath the Intra Eocene Unconformity (IEU) in the area of the Judd Anticline (Figs. 2.6 & 2.7). Therefore in order to produce a more complete isochron of unit P10, we mapped an immediately underlying (c.20ms below) reflection to the TopP10 reflection that is everywhere concordant to this reflection but has the advantage that it is not truncated beneath the IEU. This subjacent reflection was mapped throughout the high resolution survey, and tied into the standard 2D seismic data where possible. The resulting Unit P10 isopach map reveals a broadly circular thickness distribution over an area of 2200km<sup>2</sup> with greatest thicknesses of up to c.400m occurring toward the SW limit of the map and to c.400m toward the north, north east and east (Fig. 2.8a). The SW limit of the unit is defined by truncation beneath the INU (Fig. 2.3). Regional seismic profiles (Figs. 2.9 &



2-15

**Figure 2.6**

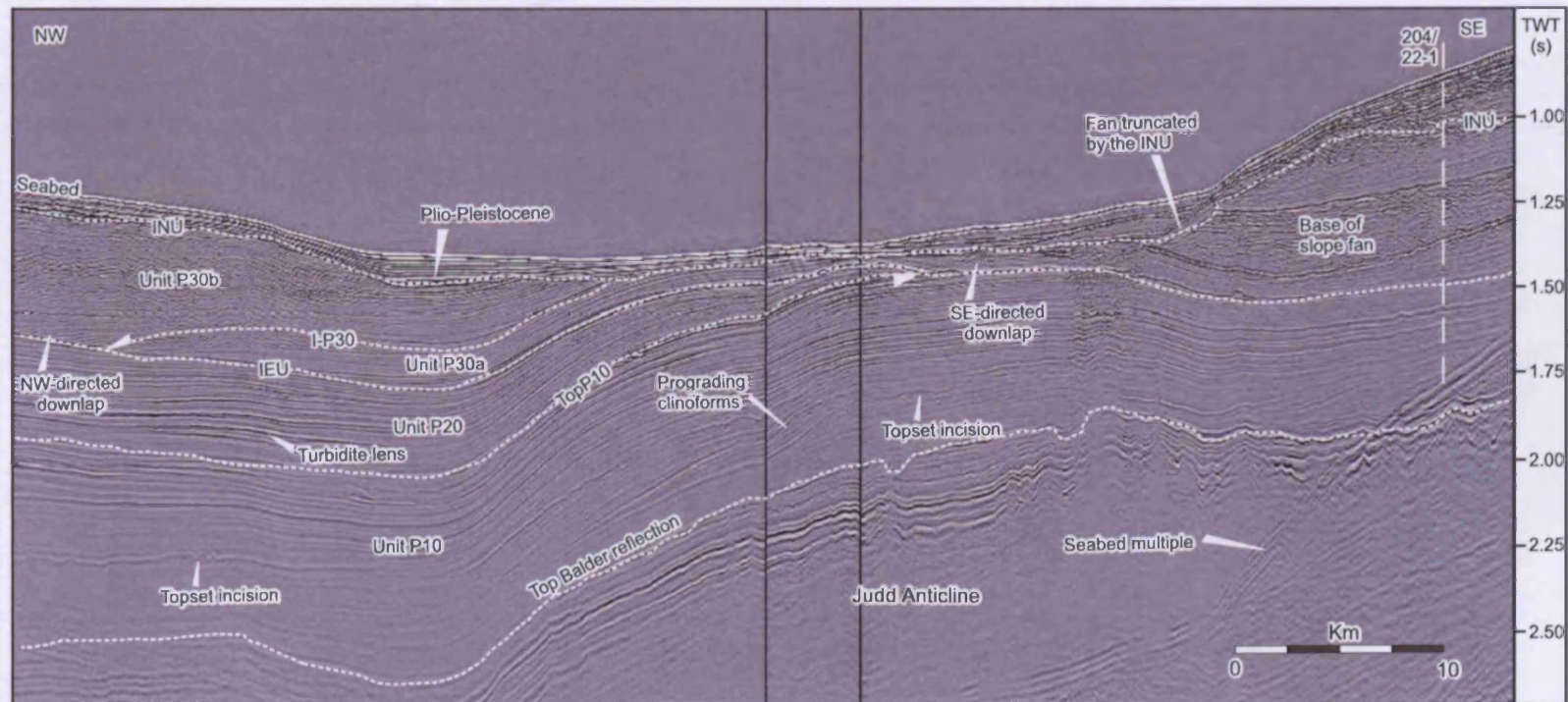
High resolution composite 'dogleg' 2D seismic profile (line location Fig. 2.2). Profile illustrates the stratigraphy devised for this study. Note bi-directional downlap of Unit P30a across the Judd Anticline, and significant S/SW directed onlap formed by Unit P30b. Profile also clearly illustrates erosional truncation of stratigraphy beneath the INU. BGS Borehole 99/3 is located at SE limit of this profile.

2.10) show that the unit consists, in the lower part, of a prograding sigmoidal reflection configuration. The topsets of the individual reflections often exhibit high seismic amplitudes in addition to local incisions which truncate underlying reflections (Fig. 2.6). The prograding reflection configurations combined with the isochron distribution are interpreted as a prograding deltaic system, as previously recognised by Smallwood and Gill (2002) and Robinson (2004). The progradation direction (maximum palaeo-slope) of individual clinoforms was toward the NW, N, and NE (Figs. 2.9 & 2.10), representing an overall northward migration. Apparent lateral progradation is likely a result of delta lobe switching and local topographic/bathymetric controls. The localised thickening of the package at the southwestern edge of the map suggests a close proximity to sediment input and an infilling of accommodation space in that particular area, with distal thinning due to reduction in primary supply and to topographic controls onto the Shetland and Faeroese margins.

Topset aggradation is widely observed within the clinoforms of Unit P10 (Fig. 2.9). This suggests that accommodation space was continually created by a long-term rise in relative sea level during delta progradation. Identification of incision associated with some topsets suggests that this long-term rise was punctuated by periods of relative sea level fall and fluvial channel incision. At least four type-1 sequence boundaries were identified in the same area by Robinson (2004) using lower vertical resolution 3D data.

Well calibration shows that this unit comprises sand and mud dominated facies with abundant woody/coaly debris (204/24a-1; 204/22-1 - Fig. 2.11), supporting the inference of a deltaic depositional environment. Coal horizons, typical of delta topset environments, are also penetrated in each well (204/22-1; 204/23-1 and 204/24-1a – Fig. 2.11). The coal seams tie to high amplitude negative reflections within the seismic data and are confined to the areas interpreted as delta topsets (Fig. 2.7). Significantly, the reflections within unit P10 show now evidence of thickness change across the Judd anticline (Fig. 2.8a), which is implies that the unit was deposited prior to development of the fold as a significant topographic feature.





**Figure 2.7**

High resolution 2D seismic profile oriented perpendicular to the basin margins (line location Fig. 2.2). Line illustrates stratigraphic division of this study. Note prograding clinoforms and topset incision within Unit P10, turbidite lenses and stratigraphic thinning toward the SE onto the Judd Anticline within unit P20. Well 204/22/1, 15km to the SW of the profile lithologically calibrates the base of slope fan (Fig. 2.11).

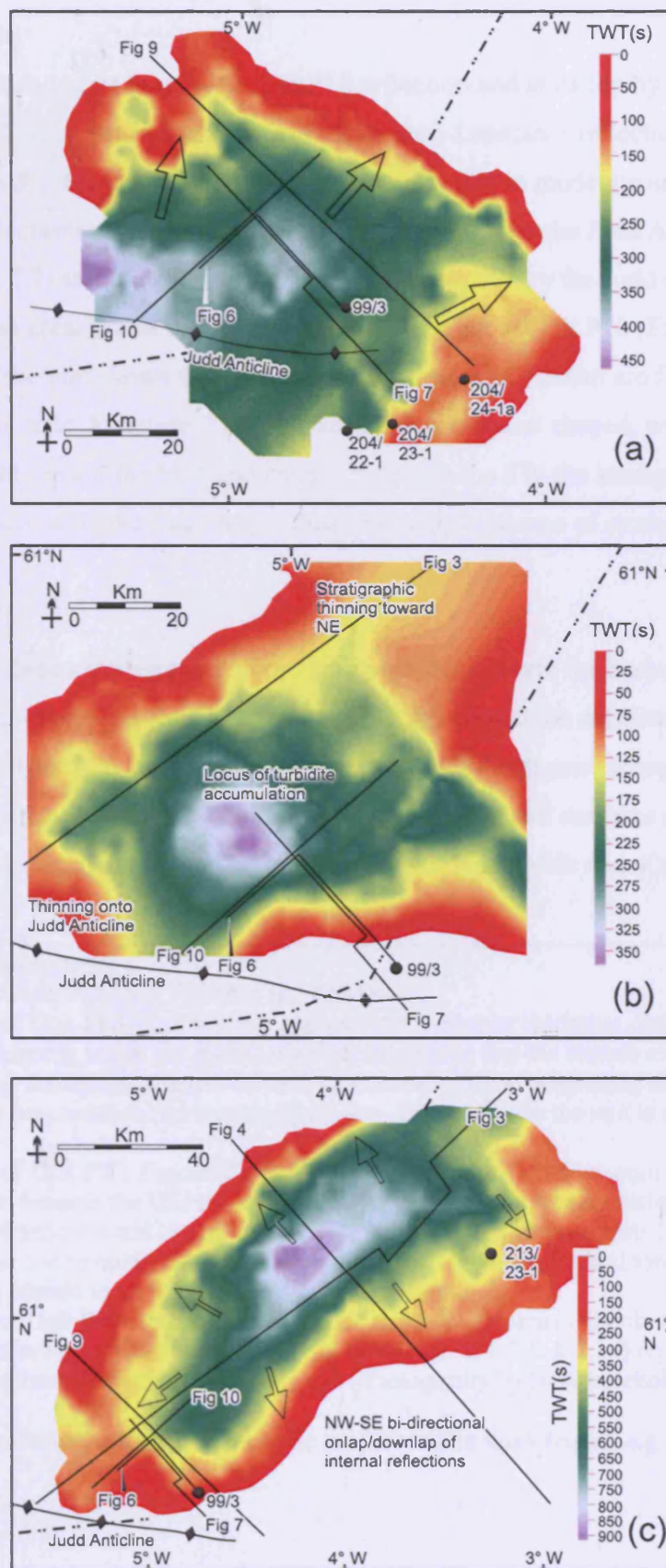


Figure 2.8

### 2.5.2.2. Unit P20

Unit P20 is bounded at its base by the TopP10 reflection and at its top by the Intra-Eocene Unconformity (IEU, approximately equivalent to the I-Lutetian 3 reflection of Smallwood, 2004) (Figs. 2.5 & 2.6). Unit P20 consists of generally low to moderate amplitude parallel to sub-parallel reflections which exhibit stratal convergence onto the Judd Anticline toward the SE (Figs. 2.6 & 2.7) and erosional truncation toward the SW by the Judd deeps (Fig. 2.10), thus reducing the areal extent of Unit P20 when compared to Unit P10 (Fig. 2.8b). The isopach map of the unit shows that maximum thicknesses of c.300m are found to the north of the axis of the Judd Anticline. The Judd anticline is crescent shaped, with thinning of Unit P20 onto the fold toward the Shetland margin, while to the SW the stratigraphy including Unit P20 is truncated by the Judd deeps, thus removing evidence of stratigraphic thinning (Figs. 2.6 & 2.7).

Unit P20 also exhibits stratigraphic thinning toward the NE into the basin (Figs. 2.3 & 2.10). Thinning onto the Faeroese and Shetland margins and toward the northeast suggest that accumulation of Unit P20 was significantly influenced by bathymetric/topographic controls. In the area of increased thickness north of the anticline, the unit contains a series of stacked high amplitude lenses (Figs. 2.6). The lenses are up to 10km wide and 40m thick and in

---

#### Figure 2.8 (previous page)

Isopach maps of Units P10 (8a), P20 (8b) and P30 (8c).

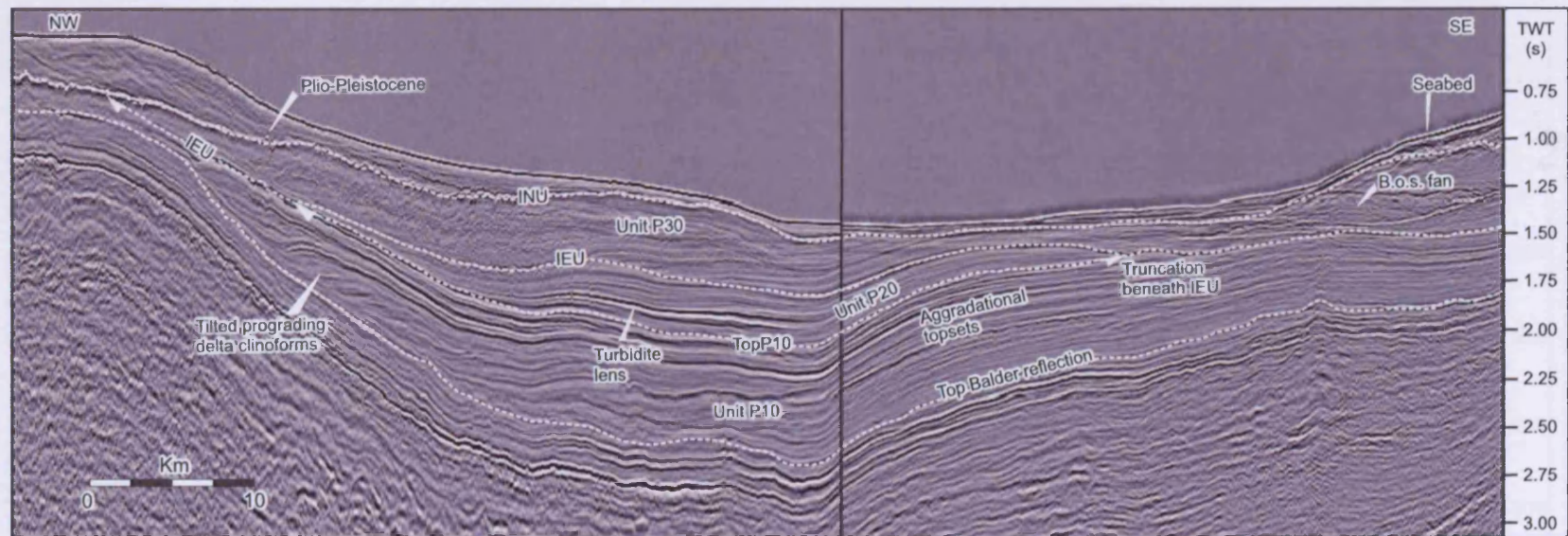
**(a)** Isopach map of Unit P10. Unit exhibits approximately circular thickness distribution with no sign of stratigraphic thinning across the Judd Anticline, suggesting that the feature exhibited little or no topography during deposition. Figures 2.9 and 2.10 reveal internal prograding clinoforms, with the general northerly progradation represented by arrows. Lithologically the unit is calibrated by each of the wells.

**(b)** Isopach map of Unit P20. Figures 2.6 and 2.7 reveal that the Unit thins onto the Judd Anticline prior to truncation beneath the IEU toward the SE, and Figure 2.3 reveals stratigraphic thinning to the SW onto the Judd anticline and toward the NE. Turbidite accumulation is restricted to the area NE of the Judd Anticline and thinning onto the Shetland and Faeroese margins and toward the NE suggests that the Unit was limited in all directions by topographic control.

**(c)** Isopach map of Unit P30 reveals broad elongate mounded thickness distribution with internal reflection onlap/downlap toward the SE, SW and NW (Figs. 2.4, 2.6 & 2.14) represented by open arrows. Unit is calibrated biostratigraphically and lithologically by BGS borehole 99/3 and Well 213/23-1.

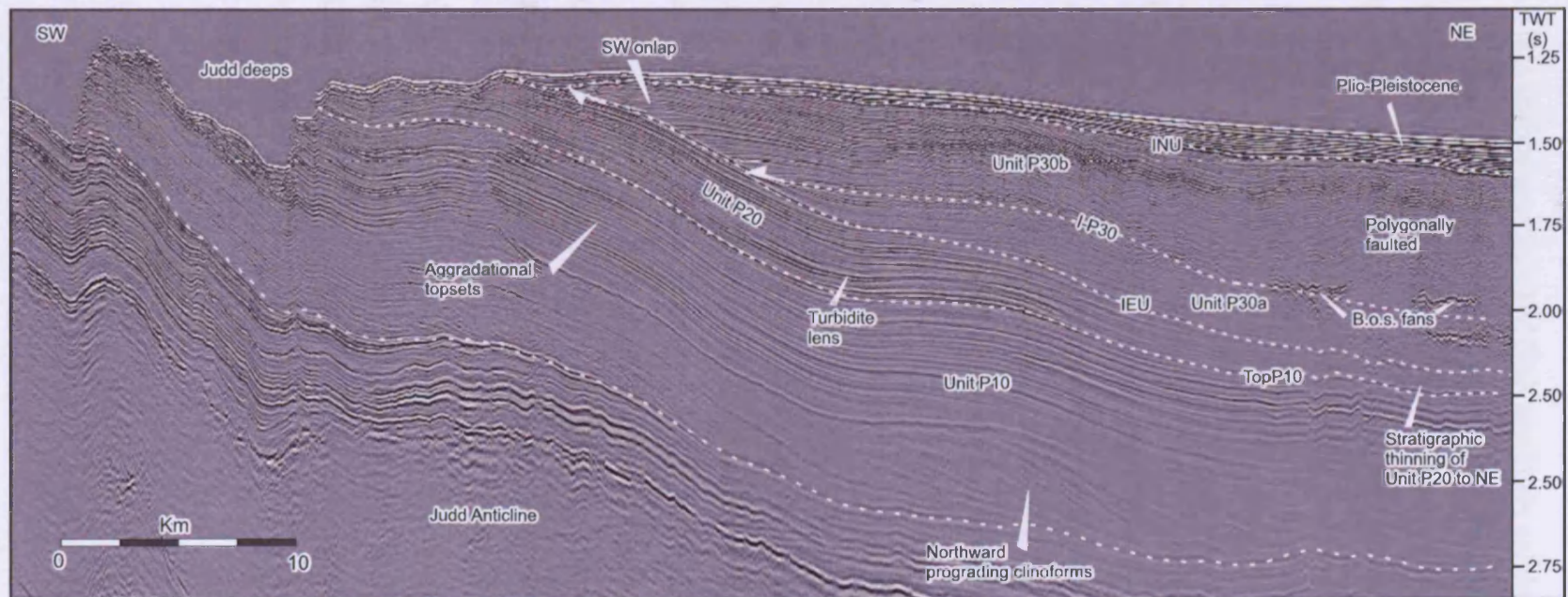
'Fig' references refer to the location of seismic profiles within this Chapter, e.g. 'Fig 9' refers to Figure 2.9.





**Figure 2.9.**

Regional dip 2D seismic profile (line location Fig. 2.2) to illustrate prograding clinoforms of Unit P10, now tilted, on the Faeroese Margin. Clinoforms are associated with aggradational topsets, suggesting continued subsidence during deposition of Unit P10.



**Figure 2.10**

High resolution strike directed 2D seismic profile (line location Fig. 2.2). Profile illustrates the stratigraphy defined by this study. The location of the Judd Deep towards the crest of the Judd Anticline which limits SW extent of Units P10, P20 and P30. Northward prograding clinoforms within Unit P10 are clearly visible. Also note incorporation of turbidite lenses on limb of Judd Anticline, suggesting growth of the fold following deposition of the turbidites.

planform exhibit an elongate geometry which parallels the trend of the anticline. The confined, lens-shaped geometry and high amplitude exhibited by the lenses are typical of the seismic expression of confined turbidite deposits (Reading and Richards, 1994). Unit P20 is therefore interpreted as a series of turbidite lenses and associated hemipelagite deposited in a topographically confined mini-basin. The high amplitude reflections of the turbidites likely reflects a significant acoustic impedance contrast between the interbedded coarse and fine lithofacies.

The thinning of Unit P20 onto the Judd Anticline combined with the topographic control on turbidite distribution suggests that growth of the anticline was initiated during the deposition of Unit P20. The lack of internal onlap surfaces within the convergent Unit P20 further implies that fold growth was in equilibrium with deposition (Cartwright, 1992). Further fold growth subsequent to turbidite deposition is evidenced by inclination of the turbidites on the limb of the fold (Fig. 2.10). Steepening of local slopes during fold growth may have resulted in instability and turbidite deposition. However, it is equally possible that the turbidites were deposited during relative sea level fall. Deposition of turbidites onto the underlying delta topset facies requires a significant increase in palaeobathymetry between deposition of P10 and P20, which likely accompanied the early development of the fold. However, the palaeo-water depth during the deposition of Unit P20 is unknown due to a lack of palaeo-sea level datums. Previous seismic-stratigraphic interpretation of the area has identified features presented above, including the northward prograding deltaic system and that growth of the Judd Anticline post-dated the deltaic deposition (Smallwood and Gill, 2002; Robinson, 2004; Smallwood, 2004). Therefore, although the interpretation was made independently using the previous studies only as references, this section largely confirms previous interpretations of the stratigraphy within the area, and is included in order to clarify the depositional setting of the post-Top Balder Formation Judd basin. However, to the best of the authors knowledge the turbidite deposits of Unit P20 have not previously been identified and documented.



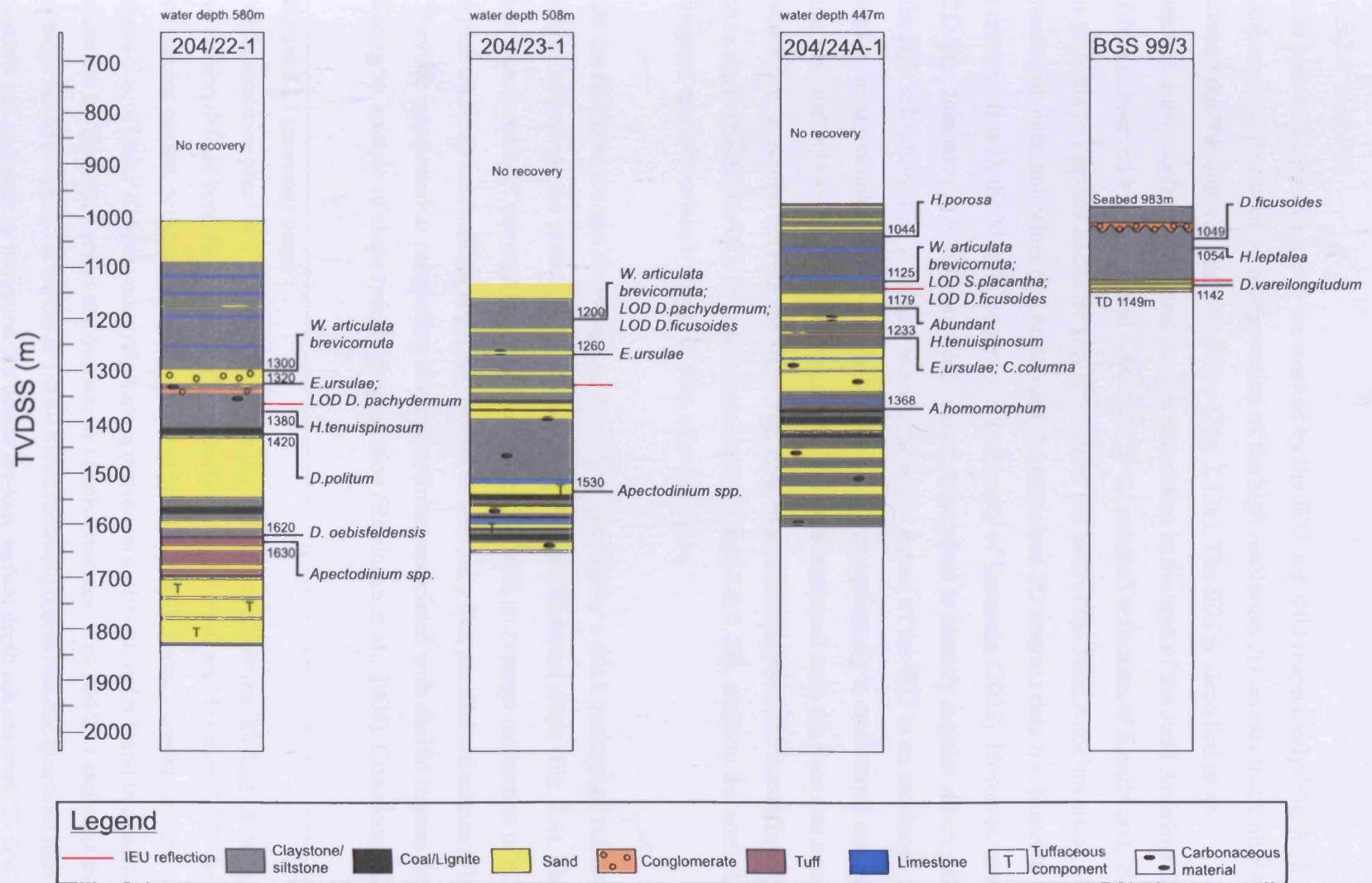


Figure 2.11

### 2.5.2.3. Unit P30

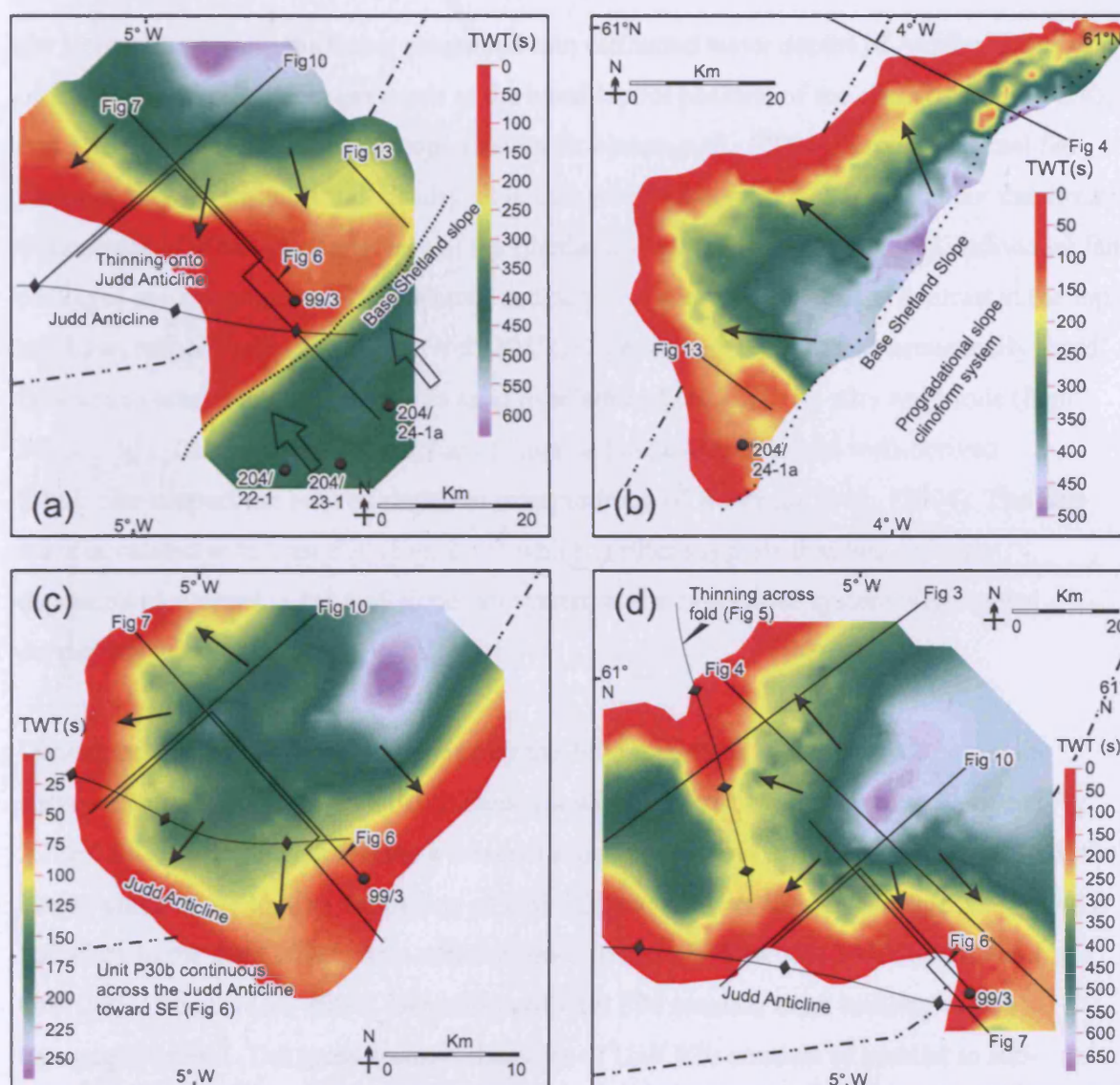
The base and top of Unit P30 are marked by the IEU and INU respectively (Fig. 2.5), and an isopach map produced by interpretation of the high resolution 2D reveals that Unit P30 thins toward the SW onto the Judd Anticline (Fig. 2.12a). The IEU is identified as an unconformity surface with basal angular truncation in the area of the Judd Anticline (Fig. 2.6), as observed by Smallwood (2004) (IEU=I-Lutetian3 reflection of Smallwood, 2004). It is possible to map the unconformity throughout the area of the Judd Anticline using high resolution data, and when tied northward onto standard 2D seismic data it is found to be correlatable with the Middle Eocene Unconformity of Sørensen (2003). However, standard 2D data does not provide the vertical resolution required to identify angular subcrop beneath the IEU reflection (Fig. 2.4), and as such the wider extent of the IEU as an erosional unconformity is unknown. From the basin axis, the unconformity is continuous eastward upslope and onto the Shetland margin (Fig. 2.4), and westward onto the Faeroese margin, where it is truncated beneath the INU (Fig. 2.9). In a strike direction, the unconformity is truncated beneath the INU at its southern limit (Figs. 2.3 & 2.10), while to the north it deepens and is overlain by up to 1300m of overburden.

On the Shetland margin slope region, the IEU is overlain by a thick package of reflections which help shape the present day bathymetry of the west Shetland slope (Fig. 2.4). This package consists of prograding sigmoidal reflections with an average inclination of c.2° and which decrease landward in angle and extend as relatively flat, parallel reflections (Fig. 2.4). They are interpreted as prograding slope clinoforms associated with shelfal topsets deposited during an episode of slope margin progradation (Robinson et al., 2004). Clinoform relief of

---

#### Figure 2.11 (previous page)

Well correlation panel of 4 key wells (locations Fig. 2.2). Figure illustrates lithology of stratigraphic succession defined here. Key biostratigraphic marker taxa (dinocyst) are identified (LOD –last occurrence datum), with taxon ranges provided in Fig. 2.5. The IEU which divides the contourite deposition of Unit P30 from underlying units is marked on each well, and is found to consistently be underlain by Ypresian markers and overlain by Lutetian markers. Well 204/22-1 calibrates the base of slope fan from Fig. 2.7 at depths of 1310-1350m, recording coarse rounded quartzose sand overlain and underlain by mudstone. All depths are total vertical depth sub sea level (TVDSS) in metres.



**Figure 2.12**

Isochron maps of Unit P30 and associated packages.

(a) Illustrates the overall thickness of Unit P30 as mapped using only the high resolution 2D data grid. Note thinning over the Judd Anticline. Thickening on the Shetland slope represents the coeval Shetland margin progradation system. Open arrows represent slope clinoform progradation, solid arrows represent onlap of P30 internal reflections onto the basal IEU surface.

(b) Shows the thickness distribution of the base of slope fans which interdigitate with the P30 contourite drift at the base of slope. Individually the fans thin proximally and distally (Fig. 2.13) but when mapped collectively they exhibit greatest thickness at the base of the slope and thin basinward. Arrows represent direction of sedimentation.

(c) Reveals the thickness distribution of Unit P30a. The unit is characterised by bi-directionally downlapping reflections that do not exhibit stratal condensation onto the Judd Anticline toward the SE (Fig. 2.6), unlike the overlying Unit P30b (Fig. 2.6). The limits of the unit are defined by depositional lapout to the SE and the NW, and onto the Judd Anticline toward the SW (Figs. 2.6 & 2.7).

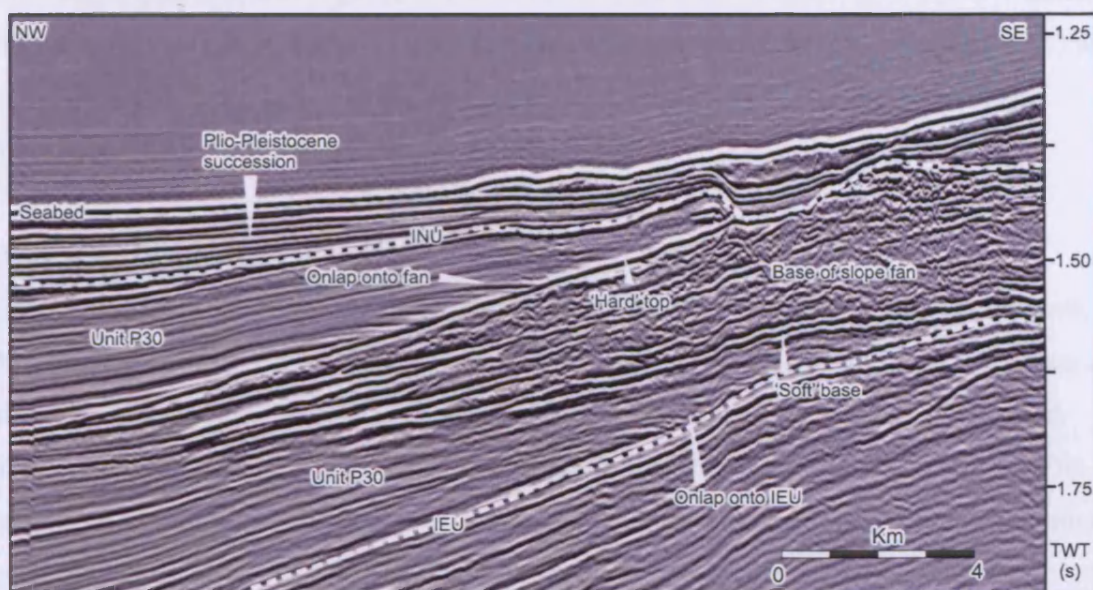
(d) Illustrates the thickness distribution of Unit P30b, and includes translation of the horizon from the high resolution data to standard 2D data to the NW. The internal reflections continue the onlap configuration of Unit P30a (Figs. 2.6 & 2.11), represented by arrows, resulting in a greater areal extent than Unit P30a. Apparent thinning across the c./N/S fold structure is created by erosion by the INU (Fig. 2.3).

The 'Fig' references refer to the location of seismic profiles within this Chapter, e.g. 'Fig 7' refers to Figure 2.7.

the slope system suggests that it prograded into estimated water depths of >450m. A series of stacked reflection packages occur at the basal lapout position of the clinoforms (Fig. 2.4), and were interpreted as base of slope fans by Robinson et al., (2004). Each individual fan package thins proximally and distally, although when grouped the packages attain maximum thicknesses of 400m close the base of the Shetland slope (Figs. 2.12b & 2.13). Individual fan packages are characterised by a positive and negative acoustic impedance contrast at the top and base, respectively (Fig. 2.13). Well 204/22-1 penetrated one of these acoustically ‘hard’ fans which was found to consist of a sand overlain and underlain by silty mudstone (Figs. 2.7 & 2.11). The seismic stratigraphic context, acoustic character and well-derived lithofacies support the base of slope fan interpretation of Robinson et al., (2004). The fans are intercalated with Unit P30 (Fig. 2.13) which further suggests that two separate depositional systems, a base-of-slope fan system and a basin floor system were coeval during this interval.

Deposition of Unit P30 was influenced by the Judd Anticline, which extends across the survey area in a near E-W trend and intersects with the Faeroese and Shetland Slopes (Fig. 2.12a). As a result, the IEU forms a crescent shape shallowing across the southern end of the basin, which at the time of deposition of Unit P30 would have formed a crescent shaped SW boundary to the deep water basin which existed to the NE (Kiørboe, 1999; Smallwood and Gill, 2002; Smallwood, 2004). Deposition of Unit P30 resulted in an infilling of this topographic relief. The gross seismic character of Unit P30 consists of parallel to sub-parallel reflections which become pervasively deformed by a single tier of polygonal faults in a basinward direction (Fig. 2.10). Polygonal faults have been recognised more widely from this interval within the basin and are thought to be linked to very fine grained lithofacies (Cartwright and Dewhurst, 1998). The southerly limit of the Unit P30 reflections is marked by termination against the crescent shaped IEU. This set of reflection terminations forms a spectacular discrete onlap surface (*sensu* Cartwright et al., 1992), suggestive of sediment starvation updip on the slope from the point of onlap. It is noteworthy that individual reflection-bound intervals thicken systematically towards the point of onlap (Fig. 2.6), which results in a progressive increase in the onlap angle from c.1° to a downlap configuration with an angle of c.1.5° (Fig. 2.14). In orthogonal profiles, the onlapping





**Figure 2.13**

High resolution 2D seismic profile to show detail of interdigitation of the P30 contourite drifts and the base of slope fans (line location Fig. 2.2). Note onlap of the contourite reflections onto the stacked fan bodies, and onlap onto the IEU. The SE directed onlap of Unit P30 reflections confirm that the unit consists of bi-directionally downlapping reflections creating 'mounded' internal reflections.



reflections exhibit lateral bi-directional onlap/downlap (Fig. 2.6). These relationships are highly significant and are diagnostic of contourite drifts (see *section 2.3.3*). The SW directed onlap of Unit P30 has previously been identified using the same data (Smallwood 2004) and BGS high resolution seismic data (Howe et al., 2002), although it was not investigated further.

#### 2.5.2.4. Units P30a and P30b

A significant internal onlap surface within unit P30 (I-P30) divides P30 into two subunits, P30a and P30b (Fig. 2.6). Unit P30a is characterised in the vicinity of the high resolution 2D data by bi-directionally downlapping internal reflections that do not exhibit SE directed thinning onto the Judd Anticline, unlike the underlying Unit P20 (Figs. 2.6 & 2.12c). The unit attains a maximum thickness of c.200m and the areal limits are defined by depositional lapout toward the SE, NW and SW (Figs. 2.6 & 2.7). Unit P30b was deposited primarily to the north (basinward) of the Judd Anticline, and is delimited by lateral onlap of internal reflections onto Unit P30a toward the Shetland margin (Fig. 2.6), while the SW and NW reflection termination onto the IEU in the vicinity of the Judd Anticline forms a continuation of the onlap exhibited by reflections of the underlying Unit P30a (Figs. 2.6 & 2.10). The continuation of the onlap relationship exhibited by Unit P30a results in Unit P30b having a greater NW extent than P30a (Fig. 2.12d).

Unit P30b is thicker than unit P30a, reaching a maximum of >580m (Fig. 2.12d). The previously described intercalation of Unit P30 and the Shetland slope progradational system is also most prominently exhibited in unit P30b, which hosts the base of slope fans associated with the Shetland margin progradational system (Fig. 2.13), and exhibits clear onlap of internal reflections onto the fan bodies. The top of Unit P30b is marked by considerable erosional truncation beneath the INU surface (Fig. 2.6), which in some locations has removed several hundred metres of stratigraphy. BGS borehole 99/3 punctuated the southern end of unit P30 (Figs. 2.6 & 2.12a), and revealed that the unit consists of clay and mudstone with thin sand intercalations and a fauna of agglutinated and benthic foraminifera (Fig. 2.11, Riding, 1999). Unit P30 is separated from underlying sandy facies of Unit P10 by the IEU, which consists of mudstone with a rubbly appearance



**Figure 2.14**

3D seismic strike line parallel to the basin axis to illustrate the increase in onlap angle of the P30 reflections onto the IEU (line location Fig. 2.2). The lapout of internal reflections evolves from an onlap with angular discordance of c.1° with the IEU into downlap exhibiting angular discordance of c.1.5° with the IEU. The intense polygonal faulting of Unit P30 is also clearly displayed.

containing a rich faunal assemblage including arenaceous agglutinating foraminifera, shark teeth and glauconite (Riding, 1999).

#### *2.5.2.5. Depositional origin of Unit P30*

From its context on the basin floor, and its relationship with the intercalated slope fans from the Shetland margin, the large lensoid body of Unit P30 could be regarded as a basin plain fan deposit, potentially sourced from along the basin, or from the Faeroese margin. However, our interpretation is that this body represents a large contourite drift. This interpretation derives from the recognition that the progressive onlap and bi-directional downlap of reflections within unit P30 as imaged on the 2DHR data (Figs. 2.6, 2.7 & 2.10) are key seismic stratigraphic features that are widely considered to be diagnostic of contourite drifts elsewhere (Faugères et al., 1993; Faugères et al., 1999; Rebesco and Stow, 2001; Stow et al., 2002). The interpretation of Unit P30 as a contourite drift is supported by the systematic and localised thickening of individual reflection-bound packages approaching the onlap onto the IEU and the progressive steepening of the onlap which gradually transforms into a progressive southerly downlap relationship. This style of onlap is ubiquitous amongst plastered drifts (Faugères et al., 1999), but is not seen in submarine fans. The fine grained sedimentological composition (inferred from widely developed polygonal faulting and locally calibrated in BGS 99/3) is also typical of many deep water contourite drifts (Faugères et al., 1999).

#### *2.5.3. Regional seismic stratigraphic analysis*

The bounding surfaces of Unit P30 were correlated with the regional network of standard 2D seismic profiles in order to ascertain the scale of the unit and to establish any evidence in support of the contourite drift interpretation. The INU forms a regional erosion surface which has been correlated throughout the Faeroe Shetland Basin (Stoker, 1999; Stoker, 2003; Stoker et al., 2005). Therefore, mapping of the basal IEU reflection northward provided a gross isopach map for Unit P30.

At the regional scale of mapping, Unit P30 is found to form a broad elongate mounded depositional body within the southern Faeroe Shetland Basin, lying primarily within UK quads 204, 205 and 213 and Faeroese quads 6005 and 6104 and covering an area of c.8500-

9000km<sup>2</sup> (Fig. 2.8c). The unit extends for c.120km along the basin and reaches a maximum width of c.80km, but most importantly its long axis is oriented parallel to the strike of the basin. The basal reflection of Unit P30 (IEU and its extension) is not clearly visible on the standard 2D data. The southern end of the unit is seen to lie upon the IEU (Fig. 2.10) which, towards the north becomes less well defined due to poor seismic resolution and pervasive polygonal faulting of the succession in the deeper parts of the basin. However, the IEU can be correlated with confidence with the top of a series of middle Eocene fans (Caledonia, Strachan and Cuillin – Robinson, 2004) which were deposited in the basin axis (Fig. 2.3). Continuity of seismic facies within Unit P30 northwards allows the top of the fan bodies to be used as a marker for the base of Unit P30 throughout the rest of its extent. In dip section, the unit exhibits baselap onto the middle Eocene fans, which towards the Faeroese margin is replaced by baselap onto laterally equivalent facies (Fig. 2.4). The northern limit of Unit P30 is marked by a decrease in unit thickness as a result of general convergence of the basal surface with the INU and onlap of Oligocene and Neogene strata onto Unit P30 (Fig. 2.3). The northern limit approximately coincides with the boundary between the Palaeogene and Neogene depocentres (Fig. 2.3).

On the regional scale, the gross internal reflection configuration of Unit P30 consists of a series of polygonally faulted reflections which dip with an average angle of 1.5-2° toward the Faeroese Margin and lap out against a basal surface (IEU equivalent) (Fig. 2.4). The original depositional limit of the reflections to the southeast (Shetland-ward) is largely obscured due to later erosional truncation beneath the INU. However, identification of older, deeper internal reflections which are not truncated by the INU shows that the mounded thickness distribution exhibited by the isopach map was a primary depositional characteristic but this may have been enhanced by erosional sculpting during formation of the INU. Detailed interpretation of internal reflection packages is prevented by polygonal faulting and decreased data resolution. Regional strike profiles exhibit a progressive southerly onlap of internal reflections onto the basal surface, which can be directly correlated with the IEU and the onlap surface identified in the 2DHR data (Fig. 2.3). The IEU surface is thus interpreted to represent a palaeo-seabed which was progressively buried during the deposition of Unit P30. The elongate, basin strike parallel, mounded thickness distribution and deposition onto a flat erosional basal surface are characteristics which together are diagnostic of large

mounded contourite drift bodies (Faugères et al., 1999). In addition, progressive lateral baselap and progressive strike-directed onlap of internal reflections are also key criteria diagnostic of contourite drifts. In summary, the regional interpretation therefore strongly supports the proposed contourite origin of Unit P30 based on detailed analysis of high resolution seismic data, and Unit P30 can be classified as elongate mound contourite drift body *sensu* Faugères et al., (1999).

## 2.6. Biostratigraphic dating of the stratigraphy

As an area of active hydrocarbon exploration, the stratigraphy of the southern Faeroe Shetland Basin has been calibrated by a number of exploration wells and boreholes. Four of these (204/22-1; 204/23-1; 204/24-1a and BGS 99/3) are of particular use in biostratigraphic dating of the stratigraphy presented here, with an additional well which calibrates the northern end of Unit P30 (213/23-1) (Figs. 2.2 & 2.11). For the purpose of this study, the most important event in the history of the Judd Basin requiring biostratigraphic constraint is the onset of contourite deposition, which is represented seismically by the IEU. From the regional interpretation it is also clear that dating this surface will effectively provide a date for the onset of contourite drift deposition within the Faeroe Shetland Basin as a whole.

BGS borehole 99/3 is the only calibration point which penetrates Unit P30 overlying the IEU (Fig. 2.6). The other three wells, 204/22-1; 204/23-1 and 204/24-1a are all found toward the base of the Shetland slope (Fig. 2.2). They penetrate the IEU where it is overlain by a prograding slope margin system, judged as being contemporaneous with unit P30 based on intercalation of the two facies (*section 2.5.2.3*), thus placing useful constraints on the timing of formation of the IEU and the drift body. A correlation panel of the 4 wells (Fig. 2.11) shows the key biostratigraphic marker horizons which are common to all or most of the wells, and also shows the depth of the IEU in each well. The first and last appearance datums of the key biostratigraphic taxa are summarised in Figure 2.5. Synthesis of this well information gives a more precise estimation of the age of the key units and markers than would be possible from any individual well alone. Specific evidence of importance for the age determinations are summarised below for each well in turn.

In each of the wells, the last abundance datum (LAD) of *Apectodinium* spp. (204/22-1; 204/23-1) and the last occurrence datum (LOD) of *Apectodinium homomorphum* (204/24-1a) mark the Late Palaeocene-Earliest Eocene (Bujak and Mudge, 1994; Hardenbol et al., 1998; Williams et al., 2004).

### 2.6.1. Well 204/22-1

The IEU is found at 1372m (Fig. 2.11), and is underlain by abundant *H. tenuispinosum*, characteristic of the Ypresian *Membranilarnacia compressa* Subzone (Bujak and Mudge, 1994) at 1380m. The IEU is also stratigraphically above the LOD of *D. politum* (51.5Ma, Williams et al., 2004) at 1420m, providing further evidence that the IEU is underlain by Ypresian age strata. The units above the IEU are dated with reference to the combination of the LOD of *E. ursulae* and *D. pachydermum* at 1320m indicating a Lutetian age (Bujak and Mudge, Hardenbol et al., 1998; Williams et al., 2004), supported by the LOD of *W. articulata brevicornuta* at 1300m (Lutetian - late NP14 to early NP15, Bujak and Mudge, 1994).

### 2.6.2. Well 204/23-1

Well 204/23-1 lies c.10km to the NE of Well 204/22-1, but lacks Ypresian markers above the *Apectodinium* spp. at 1530m (Fig. 2.11). The IEU is located c.60m below the last occurrence of *E. ursulae*, which itself lies c.60m below the *W. articulata brevicornuta* at 1200m. A confident Lutetian age for the units directly above the IEU is based on the *W. articulata brevicornuta* sample and includes the last occurrence datums of *D. ficusoides* and *D. pachydermum*.

### 2.6.3. Well 204/24A-1

Units beneath the IEU are dated from records of *E. ursulae* in combination with *C. columna* (51.73-49.88Ma, Williams et al., 2004), which constrain an Ypresian age at 1233m, some 90m below the intersection of the IEU with the well at 1145m. Above the IEU, the combination of *W. articulata brevicornuta* with the last occurrence datums of *D. ficusoides* (50.24-45.16Ma – Williams et al., 2004) and *S. placacantha* (LAD Lutetian, mid NP15, Bujak and Mudge, 1994) strongly suggests a Lutetian age for the sample at 1125m. An

upper Eocene age is proven at 1044m by the presence of *H. Porosa* (41.0-36.4Ma – Williams et al., 2004).

#### 2.6.4. BGS 99/3

BGS borehole 99/3 is situated c.20km basinward (NW) of the 3 hydrocarbon exploration wells (Fig. 2.2), and was drilled to test the Eocene succession in the area (BGS 99/3 internal report). As a result of its basinward location, the 99/3 borehole penetrated Unit P30 and underlying deltaic facies of Unit P10 (Fig. 2.6). An Ypresian age for the strata immediately beneath the IEU (Fig. 2.11) is implied by the presence of *D. vareilongitudum* at 158.63m, which has an upper limit to its range in the Ypresian (51.5Ma, Williams et al., 2004). Above the IEU at 143m, the most significant biomarker is *D. ficusoides* at 65.91m. Although *D. ficusoides* is reported to zone entirely within the Lutetian by Powell et al. (1992), Williams et al. (2004) place the first appearance datum of the taxon within the latest Ypresian (50.24Ma), suggesting that Unit P30 could be Ypresian in age at the location of the borehole. However, the presence of *Heteraulacacysta? leptalea* at 73.10m instead argues for an early-mid Lutetian age (BGS 99/3 internal report; Powell 1992), and thus strongly suggests that *Diphyes ficusoides* at 65.91m represents the middle Eocene (Lutetian).

#### 2.6.5. Synthesis of Well results

The close proximity and comparable faunal representation between Wells 204/22-1 204/23-1 and 204/24A-1 and Borehole 99/3 increases confidence in the age determination from the biostratigraphic analysis of the well samples. Figure 2.11 shows that the depth-converted IEU is consistently placed above Ypresian datums and below Lutetian markers within the wells/borehole. This leads to the interpretation presented here that the IEU formed at some time between the Ypresian and Lutetian, although the age of the surface cannot be refined further with the data available. Therefore, it is proposed that units P10 and P20 are Early Eocene (Ypresian) in age and unit P30 and its laterally equivalent slope margin progradation system are Middle Eocene (Lutetian) in age. A Ypresian age for the post-top Balder deltaic facies is consistent with published ages for the stratigraphy in the area (Ebdon et al., 1995; Lamers and Carmichael, 1999; Smallwood and Gill, 2002; Sørensen, 2003). In addition, a middle Eocene age for the IEU would be consistent with age estimates for the Middle

Eocene Unconformity of Sørensen (2003) and the Intra-Lutetian 3 reflection of Smallwood (2004), with which it is correlatable.

#### 2.6.6. Regional correlation of Unit P30

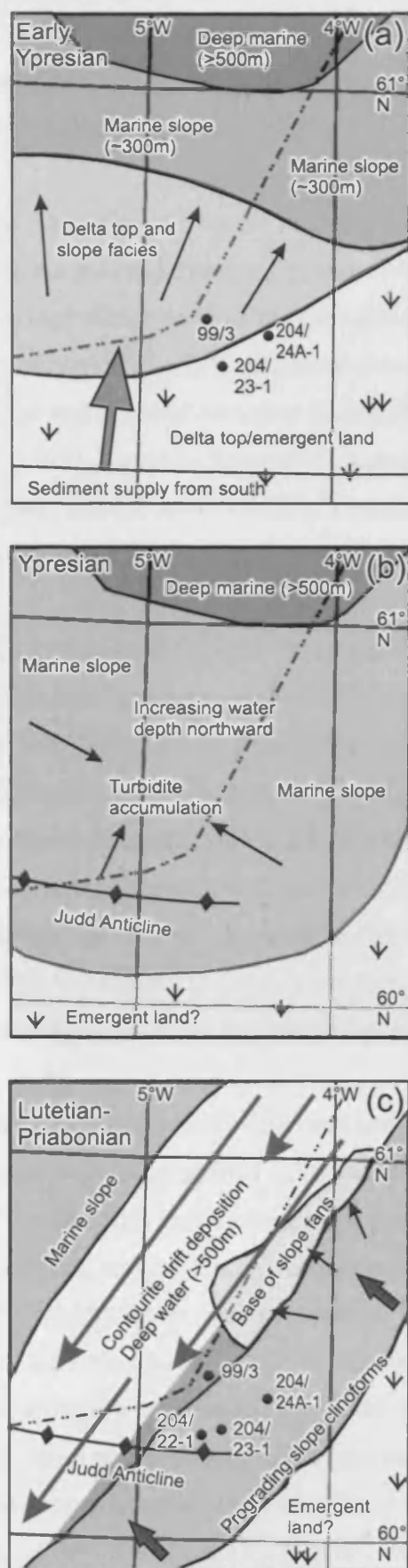
More regionally, the age of the upper limit of Unit P30 is harder to constrain, mainly due to a lack of additional well calibration in a basinal position and by significant erosion of the unit during formation of the INU (locally >300m), a problem encountered by other authors (Sørensen, 2003). However, at its northern limit, Unit P30 is calibrated by hydrocarbon exploration Well 213/23-1 (Fig. 2.8c) where key biostratigraphic taxa also date Unit P30 as Lutetian in age, and record underlying Ypresian strata. In addition, identification of the last occurrence of *Areosphaeridium michoudii* at 1458m (Fig. 2.3) indicates a Priabonian age for the sample (Bujak and Mudge, 1994), showing that deposition of unit P30 continued from the Middle Eocene (Lutetian) into the Upper Eocene (Priabonian).

### 2.7. Tectonostratigraphic evolution of the southern Faeroe Shetland Basin during the Eocene

Integration of seismic and well/borehole data with previously published data has allowed the reconstruction of the Eocene evolution of the southern Faeroe Shetland Basin. This evolution is represented as schematic seismic facies maps in Figure 2.15. Overall, the area evolved from emergent land and associated deltaic sedimentation during the early Eocene (Ypresian, as documented by Robinson, 2004; Smallwood and Gill, 2002; Smallwood, 2004) to marine conditions and contourite sedimentation by the mid-Eocene (Lutetian).

Unit P10 is interpreted as a deltaic complex which prograded northward (Fig. 2.15a) following submergence of the region after formation of the subaerial Base Balder Unconformity and deposition of the Balder Formation (Smallwood and Gill, 2002). Water depths of c.250m at the southern end of the basin are estimated to have been achieved during this time (Smallwood and Gill, 2002), while further north deep water (>500m) conditions were prevalent (Kiørboe et al., 1999; Robinson, 2004) (Fig. 2.15a). Delta topset aggradation within unit P10 is evidence of continued subsidence of the southern Faeroe Shetland Basin during progradation. Subsidence during the early Eocene has been considered as a result of



**Figure 2.15**

Schematic seismic facies map to illustrate the evolution of the southern Faeroe Shetland Basin during the Eocene.

(a): Early Ypresian northward prograding deltaic system into water depths of c.300m (Smallwood, 2004). Emergent landmass south and east of the Judd Anticline evidenced by coals and delta top facies in wells 204/22-1, 204/23-1 and 204/24-1a. Landmass to south provided sediment. The Judd Anticline exerted no topographic control on sedimentation. Deep water conditions present within basin axis to north (location of deep water on map not geographically constrained in this study).

(b): During the Ypresian, deltaic sedimentation ceased and turbidite deposition commenced, representing subsidence of the basin and the establishment of marine conditions throughout the area represented by a southward marine transgression. Restriction of turbidite accumulation to the north of the Judd Anticline evidences initial growth of the fold during this time, as suggested previously (Robinson, 2004; Smallwood, 2004). Input direction of the turbidites is unknown and no channels have been identified, but active fold growth may have triggered seabed instability.

(c): During the Lutetian the Judd anticline was breached by SW flowing bottom currents resulting in formation of the IEU and deposition of the P30 contourite body, calibrated by BGS borehole 99/3. Breaching of the Judd anticline was associated with subsidence of the basin axis to water depths of c.450m, resulting in development of coeval Shetland margin progradation, calibrated by wells 204/22-1, 204/23-1 and 204/24-1a. Base of slope fan deposition associated with the Shetland slope system occurred in conjunction with contourite sedimentation, resulting in contourite-fan intercalation. Downslope-sourced sediment may have been reworked by bottom currents. Sedimentation from the Faeroese margin appears to have been minimal, likely due to a lack of a significant proximal land mass.

the withdrawal of the proto-Iceland Plume at this time (Ebdon et al., 1995; Nadin et al., 1997; White and Lovell, 1997).

The earliest growth on the Judd Anticline is evidenced by stratigraphic thinning of Unit P20 onto the fold and dated as Ypresian. N-S oriented compression as a result of spreading on the Aegir Ridge north of the Greenland Scotland Ridge is thought to have been responsible for formation of c.E-W orientated compressional features, including the Wyville-Thomson Ridge and the Judd Anticline during the early Eocene (Boldreel and Andersen, 1993; Doré et al., 1999). Turbidite deposition accompanied continued growth of the Judd Anticline, which is interpreted to have remained a barrier to deep waters throughout the deposition of Unit P20 (Fig. 2.15b).

The formation of the IEU during the Ypresian/Lutetian is interpreted to represent the breach of the Judd Anticline as a barrier to deep water flow between the Norwegian Greenland Sea and the North Atlantic (Fig. 2.15c). Importantly, the identification in this study of a significant contourite drift body overlying the IEU strongly argues for an alongslope origin for this unconformity surface by the erosive agents of deep water currents. Erosion surfaces overlain by contourite drifts are common within the Neogene succession of the Faeroe Shetland Basin and a common feature of contourite drift sedimentation (Faugères et al., 1999). Subsequent to the erosional phase, the hydrographic regime would have altered such that deposition of the P30 contourite drift ensued during the middle Eocene (Fig. 2.15c).

Unit P30 is confidently dated as Lutetian using the available well and borehole data, and is composed of fine grained siliciclastic sediment, mainly comprising mudstone (BGS borehole 99/3). The early-mid Eocene slope system which was active contemporaneously with drift deposition may have acted as a source for the clastic sediment which forms the drift, being reworked by the alongslope currents. The major internal onlap surface which divides Unit P30 into subunits P30a and P30b is interpreted to represent a shift in depositional locus as a result of growth of the Judd anticline. Deposition of Unit P20 is interpreted to have infilled any major seabed topography associated with the Judd Anticline, and as a result, Unit P30a was deposited across the fold, with no evidence of any contemporaneous seabed topography e.g. in the form of onlap. Onlap of Unit P30b onto the top of the underlying Unit P30a (the I-

P30 reflection, Fig. 2.6) is used as strong evidence for growth of the Judd Anticline following deposition of Unit P30b, resulting in a shift of the deep water currents, and onlap onto the early drift body.

*In summary*, the major Palaeogene events occurring in the southern Faeroe Shetland Basin are:-

- Following regional Palaeocene uplift of the southern Faeroe Shetland Basin, subsidence resulted in a southerly marine transgression and deposition of the Balder Formation in the early Eocene.
- Early Eocene (Ypresian) deltas prograded northward within the southern Faeroe Shetland Basin into water depths of c.250m, while further north the basin was experiencing water depths >500m deep.
- Growth of the Judd Anticline during the early Eocene and concomitant turbidite deposition signify a cessation in delta deposition, and a probable further deepening of the basin. The Judd Anticline grew continuously throughout the deposition of Unit P20
- Formation of the IEU between the early and middle Eocene likely resulted from subsidence of the Judd Anticline to a critical depth which permitted the overflow of deep waters. The IEU was formed in c.450m of water.
- During the middle Eocene, sustained deep water circulation resulted in the onset of contourite deposition within the Faeroe Shetland Basin.
- Unit P30a was deposited onto a flat basal surface (IEU), with little topographic influence of the Judd Anticline apparent (when viewed in dip section). Subsequent growth of the anticline resulted in a shift in depositional locus, and deposition of Unit P30b.

## 2.8. Discussion: Palaeoceanographic evolution and the North Atlantic Conveyor Belt

The recognition of a major contourite drift body of middle Eocene age in the southern Faeroe Shetland Basin that is much older than any previously documented drift in this important gateway raises some fundamental questions that have wider bearing on our understanding of palaeocirculation in the North Atlantic-Arctic region. This area of the northern oceans is critical for the present-day global thermohaline circulation (Broecker, 1991; Rahmstorf, 2002), so it is important to ascertain precisely when this regime became established, and to specify how, if at all, it differed from the modern circulatory regime. The following sections aim to answer these questions, and to set the newly recognised middle Eocene drift in a broader context.

### *2.8.1. An Eocene North Atlantic Conveyor Belt*

Present day contourites within the Faeroe Shetland Basin are deposited by alongslope currents which flow through the basin as part of the North Atlantic Conveyor Belt circulation defined by Broecker (1991). The present day flow of these currents through the basin is driven by four main elements: 1) inflow of warm saline surface waters into the Norwegian Greenland Sea; 2) thermal densification and sinking of the surface waters; 3) outflow of cool deep waters into the North Atlantic; and 4) the presence of a deep water gateway between the Norwegian Greenland Sea and the North Atlantic (Nilsen, 1983; Broecker and Denton, 1990; Broecker, 1991; Schmitz, 1995; Wright and Miller, 1996; Hansen and Østerhus, 2000). The evidence for the existence of each of the components during the Eocene is considered in turn below.

#### *2.8.1.1. Depositional current*

The identification of the middle Eocene drift necessarily implies the action of bottom currents at this time that were part of the thermohaline or major wind driven circulation pattern of the oceans (Stow et al., 2002). The flow direction of the depositional current can be constrained from the tendency for contourite drifts to migrate downstream and alongslope (Faugères et al., 1999), which is represented seismically as a progressive axially directed downlap/onlap (depending on the angle of the surface onto which the reflections lap out). In

a younger drift body (the SE Faeroes Drift) located to the northeast along the base of the Faeroese slope, southerly directed downlap of internal drift reflections has been used to argue for the onset of deep water circulation by southerly flowing currents during the Early Oligocene (Davies et al., 2001). The identification of southerly directed progressive onlap of internal reflections of the P30 drift onto the inclined IEU at the southern end of the Judd Basin is likewise interpreted to have been deposited by a southerly flowing depositional current, but much earlier than suggested by Davies et al., (2001).

This southerly flowing water mass was evidently in place for a long period of relatively stable flow, judging from the consistency of the onlap within the c.800m thick P30 drift body. This drift is interpreted to have been deposited in water depths of >500m, implying that the southwesterly flowing water mass was linked to deepwater circulation rather than wind-driven surface waters. Dating of the P30 drift body shows that deposition initiated during the mid-Eocene (Lutetian – base - 49Ma) and continued until at least the Late Eocene as recorded by the Priabonian taxa *A.Michoudii* within well 213/23-1 (nannofossil zone NP18 dated as 37-36Ma, Berggren et al., 1995). Therefore, the c.800m of sediment were deposited over approximately 12-13Ma, resulting in an average sedimentation rate of 6-7 cm/ka. This value corresponds well to average sediment accumulation rates on elongated mounded drifts of 2-10 cm/ka (Stow et al., 2002).

Having established the onset and longevity of the drift body, the question arises to what extent this drift was the product of localised circulation within the Faeroe Shetland Basin, or a through-going circulatory regime, linking the nascent Norwegian Greenland Sea with the main Atlantic Ocean via the gateway of the Faeroe Shetland Basin? Put differently, was the Faeroe Shetland Basin open as a gateway, and what proportion of deep water exchange between the Norwegian Sea and the Atlantic was routed through this gateway?

#### 2.8.1.2. Deep water connection

A physical connection between the Norwegian Greenland Sea and the North Atlantic is critical for the exchange of deep water masses as part of the North Atlantic Conveyor Belt circulation (Broecker, 1991; Wright and Miller, 1996). At present the Greenland Scotland Ridge (GSR) forms a barrier between the Norwegian Greenland Sea and the North Atlantic,

with the passage of deep waters formed in the Norwegian Greenland Sea permitted in 3 locations: the Denmark Strait, the Iceland-Faeroe Ridge and most significantly the Faeroe Shetland Gateway, comprising the Faeroe Shetland Basin and the Faeroe Bank Channel (Figs. 2.1 & 2.2, Hansen and Østerhus, 2000). Therefore, in order for a modern style through going current circulation to have been responsible for deposition of Unit P30 a physical deep water connection between the basins would have had to existed across the GSR from the middle Eocene onward. To assess this possibility, it is critical to understand the tectonic development of the GSR and the Faeroe Shetland Gateway.

### *Structure and evolution of the Greenland Scotland Ridge*

The GSR extends from the SE continental margin of Greenland to the NW continental margin of Scotland, forming a major bathymetric ridge 4000km long and up to 1500km wide (at the Iceland plateau) which separates the North Atlantic from the Norwegian Greenland Sea (Fig. 2.1, Bott, 1983; Nielsen, 1983). The ridge comprises 3 main sections which are geologically distinct: 1) the Icelandic transverse ridge; 2) the Faeroese Block and 3) the Wyville Thompson Ridge (Bott 1983).

The earliest components of the GSR appear to be the Faeroe Platform and associated minor platforms (Faeroe Bank, Bill Bailey Bank and the Lousy Bank). The arrival of the proto-Icelandic plume at c.62Ma resulted in the onset of extrusive volcanism in the region (White and Lovell, 1997; Sørensen, 2003; Lamers and Carmichael, 1999; Ritchie and Hitchen, 1996; Pearson, 1996; Jolley and Bell, 2002). Peak rift margin magmatism was reached at c.58Ma (Waagstein, 1988; White and McKenzie, 1989; Bell and Jolley, 1997; Jolley, 1997; Sørensen, 2003) with extensive extrusion along the continental margins of central west Greenland, East Greenland, Rockall, Faeroe Platform, Vøring Plateau, NW Scotland, N Ireland and within the Faeroe Shetland Basin (Naylor et al., 1999). The Faeroe platform, which consists of 5km of basalt overlying rifted continental crust, was created between 59-55.5Ma (Waagstein, 1988; Lamers and Carmichael, 1999; Nadin et al., 1999; Naylor et al., 1999; Andersen et al., 2002; Sørensen, 2003).

Full oceanic spreading in the northern North Atlantic commenced in the earliest Eocene (Roberts et al., 1999), with N-S compression associated with spreading on the Aegir ridge

north of the Faeroe Shetland Basin believed to be responsible for formation and early growth of the Wyville Thompson Ridge during that time (Boldreel and Andersen, 1993; Andersen and Boldreel, 1995; Doré et al., 1997). This compression was also responsible for formation of the Munkagrunnar Ridge and the Judd Anticline, among other associated features (Boldreel and Andersen, 1993; Sørensen, 2003), which led to the definition of the Faeroe-Bank Channel in its present day form.

Ridge spreading occurred both south (Reykjanes Ridge) and north (Jan Mayen Ridge) of the GSR from the early Eocene, and formation of the Icelandic transverse ridge is thought to have occurred symmetrically in harmony with the Reykjanes ridge (Bott, 1983). This spreading ridge which formed the Iceland-Greenland and Iceland-Faeroe Ridges probably stood at 1.5-2km above sea level at the time of formation, with the oldest parts sinking below sea level c.20Ma, based on estimation of subsidence rates (Vogt, 1972; Bott, 1983). The Icelandic transverse ridge is thus the youngest part of the ridge, and its formation is dated from magnetic anomaly 24 (55.9-52.36Ma) to present (Bott, 1983; Hardenbol et al., 1998).

*The history of the GSR can be summarised as follows:*

1. Palaeocene volcanism associated with impingement of the Proto-Icelandic Plume began at 62Ma and intensified at 58Ma resulting in extensive basalt extrusion, and formation of the Faeroe Platform
2. Initiation of seafloor spreading north of the Faeroe Shetland Basin during the early Eocene resulted in N-S compression and formation of the Wyville Thompson Ridge, Munkagrunnar Ridge and Judd anticlines in the southern Faeroe Shetland Basin. Creation of the Wyville Thompson Ridge and the Munkagrunnar Ridge defined the newly formed Faeroe-Bank Channel.
3. Spreading of the North Atlantic Ridge which began in the early Eocene and is ongoing resulted in creation of the Iceland-Faeroe-Ridge, which forms the youngest section of the GSR.

*Evolution of Faeroe Shetland Basin*

During the early to mid Palaeocene the Faeroe Shetland Basin existed as a deep water basin at the southern end of the Greenland Scotland Ridge (Lamers and Carmichael, 1999; Smallwood and Gill, 2002). During this time the basin is thought to have been open to the south into the Rockall Trough because Wyville Thompson Ridge did not exist in its present day form. Shoaling of the southern Faeroe Shetland Basin as a result of plume uplift eventually resulted in emergence and formation of the base Balder unconformity during the late Palaeocene/early Eocene (Smallwood and Gill, 2002). The southern Faeroe Shetland Basin was subsequently drowned during the early Eocene, and deep water conditions (>450m) were restored throughout the axis of the basin by the Lutetian. As discussed above, the Faeroe Bank Channel was also defined in the early Eocene.

*The evolution of the Faeroe Shetland Basin can be summarised as follows:*

1. Deep water conditions prevailed throughout the basin during the early to mid Palaeocene
2. Uplift in association with the proto-Icelandic Plume resulted in relative sea level fall and emergence and shallow water conditions prevailed across the southern Faeroe Shetland Basin during the Late Palaeocene and Early Eocene. Meanwhile, deep water conditions (>500m) were maintained toward the north of the basin.
3. Following the initiation of sea floor spreading in the North Atlantic during the Early Eocene, the southern Faeroe Shetland Basin experienced subsidence and relative sea level rise, resulting in the re-establishment of deep water conditions throughout the basin axis by the Middle Eocene.

Therefore, analysis of the development of the Greenland Scotland Ridge and the Faeroe Shetland Basin reveals that by the early Eocene the Faeroe Shetland Basin constituted a deep water gateway across the newly formed Greenland Scotland Ridge. The development of the Wyville Thompson and Munkagrunnar Ridges during the early Eocene provided the Faeroe Bank Channel as a deep water exit for waters flowing into the Faeroe Shetland Basin from the Norwegian Greenland Sea. However, only one of the three phases of compression reported to have created the present day Wyville Thompson Ridge had occurred before the



end of the Eocene, and so it is likely that the ridge was of a lower amplitude than at present, thus potentially allowing the overflow of deep waters across it.

#### *2.8.1.3. Deep water formation*

Deposition of the thick P30 contourite succession over at least 13Ma requires an established southerly flowing deep water current through the Faeroe Shetland Basin during this time. The proposed existence of the Faeroe Shetland Basin as a deep water basin since the early-middle Eocene suggests that from this time onwards a deep water connection between the Norwegian Greenland Sea and the North Atlantic through the Faeroe Shetland Basin was possible. Therefore, Unit P30 is proposed to have been deposited by southerly flowing overflow waters likely exiting the Faeroe Shetland Basin into the North Atlantic through the Faeroe Bank Channel, with the possibility of some breaching of the developing Wyville Thompson Ridge. This water mass is referred to as Northern Component Water (*sensu* Broecker and Peng 1982), and is interpreted as the equivalent of Norwegian Sea Overflow Water that flows south through the Faeroe Shetland Gateway at present.

A prerequisite for the functioning of the North Atlantic Conveyor Belt circulation is a latitudinal temperature gradient so as to permit generation of cool deep waters at high latitudes (Broecker and Denton, 1990; Rahmstorf, 2002). Evidence presented here for a similar circulatory regime in the middle Eocene would thus require a significant latitudinal temperature gradient. The question of deep water production is central to reconstruction of the climatic regime driving the thermohaline circulation in the middle Eocene. Deep water can be generated via halo-thermal processes, where the density of surface waters is increased by evaporation to a point where it sinks into the deep ocean (Brass et al., 1982; Pak and Miller, 1992; Sloan et al., 1995). This method of deep water formation requires restricted marine conditions, low fresh water input and high solar insolation (Kennett and Stott, 1991; Pak and Miller, 1992). However, by the early Eocene the Norwegian Greenland Sea was a significant marine basin that straddled 60-70°N (Doré et al., 1999; Lundin and Doré, 2002), having migrated northward throughout the Mesozoic and early Cenozoic (Knott et al., 1993). Eocene deep water temperatures, and thus polar surface temperatures, are estimated to have been c. 6-8°C during the early to middle Eocene, with near modern tropical sea surface temperatures (Shackelton and Boersma, 1981; Greenwood and Wing, 1995; Huber and

Sloan, 2001; Zachos et al., 2001). The combination of a high northern latitude, open marine basin and a latitudinal temperature gradient suggests that deep water formation north of the Greenland Scotland Ridge during the early to middle Eocene was likely the result of thermal densification as a result of loss of heat to the atmosphere, and not halo-thermal processes. Sinking of surface waters would be most likely to have sustained the southerly deep water flow and contourite deposition in the Faeroe Shetland Basin during the middle Eocene.

In order to sustain the sinking and export of deep waters through the Faeroe Shetland Basin, a northward inflow of surface water into the Norwegian Greenland Sea would be required in order to replenish waters removed from the surface during deep water production, as occurs at present (Hansen and Østerhus, 2000). Eocene contourite deposits identified by seismic stratigraphic analysis of the outer Vøring Marginal High west of Norway are interpreted to have been deposited by northward flowing alongslope currents (Laberg et al., 2005). This is used as evidence to support a northward surface inflow into the Norwegian Greenland Sea during the Eocene, and suggests that all of the criteria, which would have been necessary for a modern style North Atlantic Conveyor Belt circulation to have been operational in the middle Eocene, were present.

Evidence for dramatically shifting climatic and oceanographic regimes during the Eocene has mounted in recent years, and provides support for the notion that the modern-style of thermohaline circulation may have initiated in the Middle Eocene. Major climatic cooling between the middle Eocene and the Oligocene resulting in an increased latitudinal temperature gradient was invoked by Miller and Tucholke (1983) as a potential causal factor in the onset of deep water circulation between the Norwegian Greenland Sea and the North Atlantic during the late Eocene-early Oligocene. Large erratic fluctuations in atmospheric CO<sub>2</sub> levels throughout the Eocene cooling are interpreted as evidence of a less stable climatic regime during the late Palaeogene compared to the Neogene (Pearson and Palmer, 2000), and changes in the palaeoceanographic circulation of the Western North Atlantic during the middle Eocene also point toward fluctuation in oceanic circulation stability (Wade and Kroon, 2002). Furthermore, recent sedimentological and geochemical analysis of Pacific and Southern Atlantic sediment cores has been used to propose the existence of large northern hemisphere ice sheets during the Middle Eocene (Tripathi et al., 2005). This claim is

supported by the discovery of ice rafted debris in mid Eocene cores from the Lomonosov Ridge in the Arctic Ocean (ACEX, 2005). The proposal of northern hemisphere ice sheets during the Middle Eocene is highly controversial (Kump, 2005; C. Lear, pers comm.), but provide potential evidence of polar cooling which can be used to support our inference of cool atmospheric conditions in the region during the middle Eocene.

### *2.8.2. Previous estimates for the onset of deep water exchange across the Greenland Scotland Ridge*

Estimates for the onset of a deep water connection between the Norwegian Greenland Sea and the North Atlantic range from the early-middle Eocene to the mid Miocene. Early estimates of the connection of surface and deep water across the GSR were based on estimates of age and subsidence rate of the crust which constitutes the ridge (Vogt, 1972). Using simple subsidence rate and age estimates it was concluded that a surface water connection was made across the GSR by the late Eocene (37-40Ma), and a deep water connection (several hundred metres) was not established until the mid Miocene (Vogt, 1972). However, the early estimates of thermal subsidence of the GSR did not account for the presence of continental crust underlying the Faeroese block or the Faeroe Shetland Basin (Bott, 1983), or the fact that subsidence of the GSR had been influenced by mantle plume related transient uplift (Miller and Tucholke, 1983; White and Lovell, 1987; Wright and Miller, 1996). In light of these considerations, it is clear that it is no longer appropriate to base estimates for the onset of deep water connection across the GSR on over-simplistic subsidence history models (Miller and Tucholke, 1983).

The estimation of the onset of deep water communication across the GSR is supported by other evidence. The identification of 'Horizon A' in the North Atlantic using seismic profiles, which was found to represent a significant erosional unconformity and in other areas significant biosiliceous ooze and dated as early to middle Eocene in age, was interpreted as evidence for flow of deep waters from the Norwegian Greenland Sea across the GSR and into the North Atlantic (Berggren and Hollister, 1974). Drift bodies of Eocene-Palaeocene age were identified in the Charlie Gibbs Fracture Zone and thought to have possibly been derived from waters overflowing the GSR (Scrutton and Stow, 1984). Other seismic reflections in the North Atlantic variously termed 'R' (Jones et al., 1970; Ruddiman,

1972) and 'R4' (Roberts, 1975; Roberts et al., 1979) and dated as late Eocene to early Oligocene were used as evidence for overflow of deep waters across the GSR and into the North Atlantic (Miller and Tucholke, 1983). The supply of deep water for this Eocene overflow was attributed to flow of cold deep waters from the Arctic Ocean and into the Norwegian Greenland Sea before crossing the GSR through a deep water connection between the Arctic Ocean and the Norwegian Greenland Sea which was thought to have opened at c.50Ma (Talwani and Eldholm, 1977; Miller and Tucholke, 1983). However, more recently it has been shown that although a surface water connection between the Arctic Ocean and the Norwegian Greenland Sea likely existed from 10-15Ma, a deep water connection was unlikely formed before 7.5Ma (Lawver, 1990; Kristofferson, 1990; Thiede and Myhre, 1996). Therefore, if deep water overflow from the Norwegian Greenland Sea was responsible for formation of the unconformities in the North Atlantic which were identified on seismic profiles, the deep water was formed in the Norwegian Greenland Sea and not in the Arctic Ocean.

Another important source of evidence derives from previous studies of drift bodies identified further south from the putative outflow from the Faeroe Shetland Basin, in the Rockall and Porcupine Basins. The onset of deposition of the Feni drift in the North Atlantic is estimated as being Eocene- Oligocene in age, and was used as evidence of onset of flow of deep water across the GSR and deep water circulation in the North Atlantic at this time (Kidd and Hill, 1987). However, Wold (1994) suggested that deep water currents responsible for drift deposition in the North Atlantic during the late Eocene may have formed through evaporation of water on the Rockall Plateau in an arid climate. A number of other studies date the onset of deep water flow across the GSR at the Eocene-Oligocene Boundary (Roberts, 1975; Miller and Tucholke, 1983; Miller and Fairbanks, 1985).

The earliest estimate for deep water flow specifically through the Faeroe Shetland Basin, is dated as early Oligocene based on the identification of the early Oligocene SE Faeroes Drift (Davies et al., 2001). However, the most popular estimate for the onset of deep water flow across the GSR is the mid Miocene (Schnitker, 1980; Eldholm, 1990; Kristofferson, 1990; Lawver, 1990; Wold, 1994; Wright and Miller, 1996; Ramsay et al., 1998; Stoker et al., 2005). This estimate is based on seismic stratigraphic evidence from the Faeroe Shetland

Basin (Stoker, 2003, Stoker et al., 2005), increased deposition on drift bodies in the North Atlantic (Wold, 1994; Wright and Miller, 1996), isotopic evidence (Ramsay et al., 1998) and subsidence estimations of the GSR (Schnitker, 1980; Wright and Miller, 1996). Earlier deep water overflow across the Greenland Scotland Ridge is ruled out in these studies based on the highly suspect assumptions (based on subsidence analyses) that the ridge formed a barrier to deep water mass exchange prior to the early-middle Miocene (Vogt, 1972, Vogt et al., 1981; Schnitker, 1980; Thiede and Eldholm, 1983; Wold, 1994; Wright and Miller, 1996), and that the Faeroe Shetland Basin did not exist as a deep water basin prior to the early Miocene (Thiede and Eldholm, 1983).

### *2.8.3. Synthesis of evidence: Middle Eocene onset of the North Atlantic Conveyor Belt*

Seismic interpretation undertaken as part of this study combined with evidence from previous work suggests that all of the necessary components for a North Atlantic Conveyor Belt style circulation would have been present and active during the middle Eocene. The Unit P30 contourite drift body within the southern Faeroe Shetland Basin is interpreted to have been deposited by southerly flowing deep waters from the middle Eocene over a period of at least 13Ma, requiring a prolonged southerly deep water flow through the basin during this time. We propose that production of the deep water took place in the Norwegian Greenland Sea, north of the Faeroe Shetland Basin, as a result thermal densification facilitated by global cooling and an increase in the latitudinal thermal temperature gradient during the Eocene. Water removed from the surface was replaced by surface inflow of warmer tropical surface waters, which controlled sedimentation on the Outer Vøring Margin, and thus likely took a similar flow path to the present day North Atlantic Water surface inflow. Regional subsidence of the southern Faeroe Shetland Basin during the early Eocene completed the deep water (>500m) gateway across the newly formed Greenland Scotland Ridge, and provided a significant route for the passage of deep waters from the Norwegian Greenland Sea into the North Atlantic. Development of the Wyville Thompson Ridge and the Munkagrunnar Ridge at the southern end of basin during the Early Eocene would have acted as a barrier to southerly flowing deep waters, but the deep water Faeroe Bank Channel

between the two ridges, along with possible overflow across the Wyville Thompson Ridge, would have formed a route for the waters to escape into the North Atlantic.

This study suggests that previous estimates of Oligocene or Neogene timing for the establishment of a deep water connection across the GSR based on identification of the oldest drift bodies (Wold, 1994; Davies et al., 1999) or subsidence rate estimates (Vogt et al., 1981; Miller and Tucholke, 1983) may be much too young. Large hydrodynamic shifts and flux increases have certainly been identified in the Faeroe Shetland Basin during the Oligocene, mid Miocene and early Pliocene (Hohbein and Cartwright (b), in prep; Knutz and Cartwright, 2003, Knutz and Cartwright, 2004), but these are interpreted as changes to a pre-existing circulatory regime which existed within the Faeroe Shetland Basin from the middle Eocene. In the light of the results of this study, further attention should be paid to the original estimates of Eocene connection across the GSR based on studies in the North Atlantic (Jones et al., 1970; Berggren and Hollister, 1974; Roberts, 1975). Our studies support the conclusions from these studies that deep waters from the Norwegian Greenland Sea were able to pass into the North Atlantic from the Eocene onwards, and that the Faeroe Shetland Basin was a significant route for these currents.

## 2.9. Conclusions

1. Sedimentation in the southern Faeroe Shetland Basin evolved from shallow marine deltaic sedimentation to turbidite deposition during the early Eocene (Ypresian), concomitant with early growth of the Judd Anticline.
2. Contourite drift deposition within the Faeroe Shetland Basin was initiated during the middle Eocene (Lutetian), with deposition from southerly flowing deep waters
3. Interdigitation of contourite and base of slope fan deposits reveal coeval alongslope and downslope processes, and mark the transition from domination of Eocene slope process to contourite deposition within the basin.
4. Cool, southerly flowing deep waters are interpreted to have comprised the outflow of deep waters from the Norwegian Greenland Sea, and are thought to have formed part of an Eocene North Atlantic conveyor belt circulation analogous to that active in the North Atlantic at present.

5. A combination of increased latitudinal thermal gradient and subsidence of the southern Faeroe Shetland Basin are thought to be the primary drivers for the onset of deep water flow and contourite deposition.
6. Previous estimates for the onset of deep water communication across the Greenland Scotland Ridge are thought to be too young, with evidence for a deep water gateway across the newly formed Greenland Scotland Ridge by the early Eocene.
7. Re-investigation of early estimates for an Eocene connection across the Greenland Scotland Ridge using large seismic and well databases around the North Atlantic may prove an exciting future avenue of research.
8. Seismic data acquired for the purposes of petroleum exploration have proved to be an extremely useful tool for palaeoceanographic research.



## Chapter Three: Late Palaeogene and Neogene contourites and palaeoceanographic evolution of the Faeroe Shetland Basin<sup>1</sup>

### 3.1. Abstract

The Cenozoic succession within the Faeroe Shetland Basin has been analysed in detail utilising an extensive 2D, 3D and high resolution 2D seismic and well database in order to unravel the palaeoceanographic history of this key oceanic gateway. The identification and detailed interpretation of contourite drift deposits dating from the early Oligocene to Recent is used as evidence for long lived deep water circulation from the Norwegian Greenland Sea into the North Atlantic through the basin as part of a modern style North Atlantic Global Conveyor Belt circulation. The Intra-Neogene Unconformity has also been fully documented for the first time, including regional distribution, magnitude of erosion and mode of formation. The stratigraphic division of this study is fully correlated with previous stratigraphic nomenclatures to increase clarity with regards to the Cenozoic stratigraphic division of the basin. Analysis of contourite drift morphology, age and distribution has allowed reconstruction of the basin palaeoceanographic history, which following onset in the middle Eocene consisted of bottom current sedimentation and erosion largely restricted to the Faeroese margin during the Oligocene and early-mid Miocene and spread to influence the entire basin during the late Miocene –Recent. The study serves to highlight the potential value of industrial seismic data to palaeoceanographic research.

---

<sup>1</sup> In preparation for submittal to Marine Geology as:

*'Late Palaeogene-Neogene contourite drifts and palaeoceanographic evolution of the Faeroe Shetland Basin'*. Hohbein, M.W. and Cartwright, J.A.

### 3.2. Introduction

At present the Faeroe-Shetland Basin forms a crucial gateway for deep water exchange between the Norwegian-Greenland Sea/Arctic Ocean and the North Atlantic as part of the meridional overturning circulation within the North Atlantic (Hansen and Østerhus, 2000). This water mass exchange, dubbed the ‘North Atlantic Conveyor Belt’ (Broecker, 1991), plays a fundamental role in the energy distribution and climate of the Northern Hemisphere (Crowley, 1992; Raymo, 1992; Schmitz, 1995; Rahmstorf, 2000, Rahmstorf, 2002).

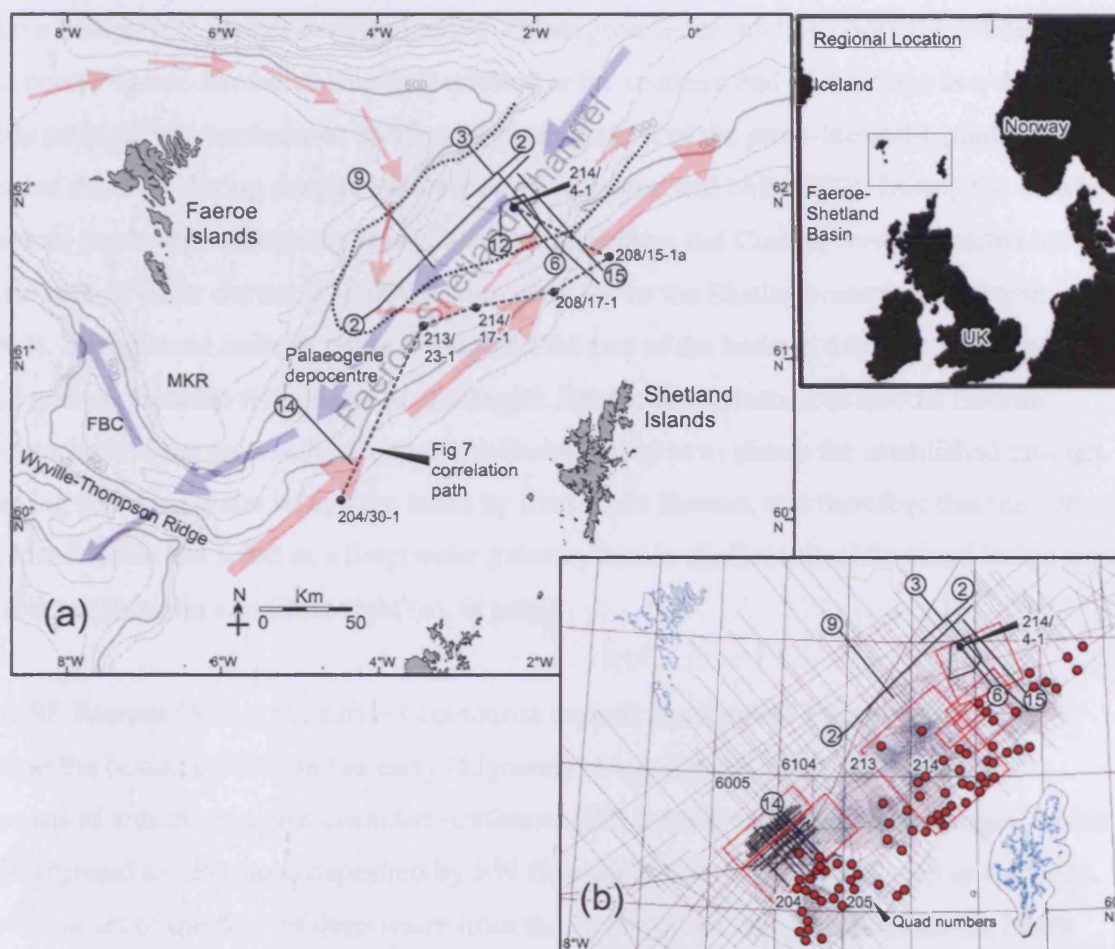
The significance of transport of deep waters through the through the basin at present begs the question to what extent did the basin act as a gateway in the past, particularly throughout the Cenozoic during which time the global climate evolved from the greenhouse conditions of the early Palaeogene to the icehouse world of the Pleistocene (Shackelton and Kennett, 1975; Miller et al., 1991; Zachos et al., 2001). A number of previous studies have analysed the Palaeogene and Neogene stratigraphic succession within the basin (Damuth and Olsen, 1993; Stoker, 1998, Stoker, 1999, Andersen et al., 2000; Damuth and Olsen, 2001; Davies and Cartwright, 2002; Sørensen, 2003; Stoker, 2003, Stoker et al., 2005), resulting in a series of seismic stratigraphic divisions and estimates for the onset of southerly flowing deep water flow through the basin that range between the early Oligocene (Miller and Tucholke, 1983; Davies and Cartwright, 2002) and the mid-Miocene (Wold, 1994; Wright and Miller, 1996; Stoker, 2003). However, recent research by Hohbein and Cartwright (in prep) suggests that the onset of southerly directed deep water flow through the basin dates from the middle Eocene. In spite of these various interpretations of the onset of deep water circulation through the basin, a detailed description and analysis of the basin stratigraphy below megasequence level, with the express aim of estimating the history of bottom current activity through the basin, is presently lacking.

The aim of this study is to analyse the late Palaeogene and Neogene stratigraphy of the through the basin in order to determine the presence and significance of alongslope bottom current activity within the basin throughout that time. This is achieved through interpretation of an extensive database consisting of high quality industrial seismic and well data. Areas of significant bottom current activity are often characterised by contourite accumulation, which are sediments deposited by or significantly affected by the action of bottom currents (Stow et

al., 2002) and/or deep water seabed erosion. Contourite successions display a range of characteristic seismic expressions (Faugères et al., 1999; Rebesco and Stow, 2001; Stow et al., 2002), and therefore can be readily identified using seismic data. As a result this study was based upon identification of contourite drifts within the basin in order to make interpretations and inferences regarding the depositional history of the basin and the degree of influence and characteristics (current direction, pathways) of the depositional currents. An additional aim was to investigate previously documented deep water erosional unconformities. Particular attention was paid to the well referenced but poorly defined Intra-Neogene Unconformity, which forms the most significant erosion surface within the basin, in order to clarify its extent, magnitude of erosion, mode of formation and appropriate definition. Lastly, the study aimed to unify the existing stratigraphic nomenclatures in order to clarify the key seismic stratigraphic events within the basin.

### 3.3. Geological and oceanographic setting

The Faeroe-Shetland Basin forms the deepest passageway across the Greenland-Scotland Ridge, which stretches from SE Greenland to the Scottish Continental Shelf. The basin consists of a series of tilted Mesozoic fault blocks overlain by a Cenozoic post rift succession deposited during thermal subsidence of the basin throughout the Palaeogene-Recent (Nielsen, 1983; Bott, 1984; Roberts et al., 1999). The present day bathymetry of the basin is characterised by a narrow (generally <200km) NE/SW trending channel that deepens from >2000m at the entrance to the Norwegian Sea to <800m at its southern end, flanked by the steeper (3-4°) Faeroese and gentler (1-3°) Shetland slopes. At its southern limit the basin axis turns 90° clockwise and opens into the North Atlantic through the Faeroe Bank Channel which lies between the Wyville Thompson Ridge and Munkagrinnar Ridge (Fig. 3.1). The Faeroese platform was formed as a result of voluminous flood basalt effusion associated with the proto-Iceland Plume during the late Palaeocene and early Eocene (Nadin et al., 1997; Naylor et al., 1999), and the associated initiation of seafloor spreading in the northern North Atlantic during the early Eocene resulted in N-S oriented compression and formation of compressional structures including the Wyville Thompson Ridge and the Munkagrinnar Ridge (Boldreel and Andersen, 1993). Clinoformal relief of early Eocene deltas within the southern Faeroe Shetland Basin suggests water depths of 500m, with the

**Figure 3.1**

(a) Seabed bathymetry map of the Faeroe Shetland Basin, with inset regional location map. The Neogene depocentre lies within dotted line, with the Palaeogene depocentre located within the basin axis to the SW. Arrows represent ocean current circulation through the basin, with large red arrows indicating the path of North Atlantic Water, small red arrows representing Modified North Atlantic Water, and the blue arrows representing Norwegian Sea Overflow Water (simplified from Turrell et al., 1999). Seismic profile locations illustrated with figure number circled. Path of correlation panel in Fig 7 also detailed.

(b) Map showing data utilised during this study: light grey lines = 2D seismic data; black lines = high resolution 2D seismic data; red boxes = 3D seismic volumes; red dots = industry wells. Key industry well 214/4-1 is indicated. Abbreviations: FBC, Faeroe Bank Channel; MKR, Munkagrunnar Ridge.

The circled 'Fig' references refer to the location of seismic profiles within this chapter, e.g. 'Fig 7' refers to Figure 3.7.

basin deepening toward the NE (Kiørboe, 1999; Smallwood and Gill, 2002). Therefore, from the early Eocene onward the Faeroe Shetland Basin existed as a deep water (>500m) basin with a bathymetry similar to that of today. Palaeogene sedimentation consisting of deltaic and coarse clastic fan facies was concentrated at the southern end of the basin as a result of close proximity to landmasses uplifted by impingement of the proto-Icelandic plume at the base of the crust during the late Palaeocene (Smallwood and Gill, 2002). During the middle Eocene, three large submarine fans (Caledonia, Strachan and Cuillin) were deposited into the basin axis in water depths of >1000m from canyons on the Shetland margin (Robinson, 2004). Background sedimentation throughout the rest of the basin at this time consisted of fine grained smectite rich clastic hemipelagite. Recent identification of middle Eocene contourite drifts at the southern end of the basin is used as evidence for established through flowing SW deep water within the basin by the middle Eocene, and therefore that the Faeroe Shetland Basin has acted as a deep water gateway across the Greenland Scotland Ridge since that time (Hohbein and Cartwright (a), in prep).

The SE Faeroes Drift is the earliest contourite deposit documented by previous studies within the basin, and is dated as early Oligocene in age (Davies et al., 2001). The drift consists of a thick elongate mounded contourite drift located on the Faeroese margin, which is interpreted to have been deposited by SW flowing bottom currents and used as evidence for the onset of the flow of deep water from the Norwegian Greenland Sea into the North Atlantic. Contourite drifts of Miocene-Pliocene (Stoker, 2003) and Quaternary age (Stoker et al., 1998; Damuth and Olsen, 2001) are also documented from the basin.

The present day water mass structure within the basin consists of SW flowing, cool deep waters referred to as Norwegian Sea Overflow Water below 400-600m, and warm saline inflow waters comprising North Atlantic Water and Modified North Atlantic Water which flow northward into the Norwegian-Greenland Sea and are described in detail by Turrell et al. (1999) (Fig. 3.1). The circulation is driven by thermal densification and convection of surface waters in the Norwegian Greenland Sea as a result of heat loss from the surface waters to the atmosphere (Broecker, 1991). The sinking of the surface waters is facilitated by their relatively high salinity and thus increased density, reaching a critical density at temperatures of c.2°C (Broecker and Denton, 1990; Hansen and Østerhus, 2000). This

generation of deep water draws warm water northward, creating the surface inflow currents and at depth imparts a lateral pressure gradient, resulting in a southerly return flow of deep water. This system of thermal densification and overturning in the Norwegian Greenland Sea is a fundamental component of the North Atlantic Conveyor Belt circulation (Broecker, 1991), and during periods of extensive sea ice cover north of the Greenland Scotland Ridge is thought to shift south of Iceland (Alley and Clark, 1999; Rahmstorf, 2002), resulting in a lack of deep water formation north of the Faeroe Shetland Basin. Within the Faeroe Shetland Basin the southerly flowing deep waters are focussed on the Faeroese slope as a result of clockwise deflection due to the Coriolis Force. At present the Faeroe Shetland Basin constitutes a volumetrically significant conduit for the passage of southerly flowing deep waters (Norwegian Sea Arctic Intermediate Water + Norwegian Sea Deep Water), with a flux of 1.7Sv ( $1\text{Sv} = 10^6 \text{ m}^3 \text{ s}^{-1}$ ), the majority of which (1.5Sv) exits into the North Atlantic via the Faeroe-Bank Channel, with minor overflow of the Wyville Thompson Ridge (0.2Sv, Hansen and Østerhus, 2000). This compares with flow rates of 2.9Sv through the Denmark Strait and 0.5SV across the Iceland-Faeroe Ridge, which comprise the remaining significant passageways. It is therefore clear that the Faeroe Shetland Basin forms a critical gateway for the circulation of water masses between the North Atlantic and the Norwegian Greenland Sea, and that it appears that this current system was initiated during the middle Eocene. However, what is unclear is the late Palaeogene and Neogene history and evolution of this system.

### 3.4. Data and methodology

The data set available for the study consisted of over 600 (c.32000 line km) conventional 2D seismic reflection profiles, 7 3D seismic surveys (c.21000km<sup>2</sup>) and a high resolution seismic site survey comprising over 1000km of high resolution 2D seismic profiles (Fig. 3.1). These data were correlated where possible with an extensive well database of 91 industry wells, 2 BGS boreholes and associated biostratigraphic and lithostratigraphic data. The conventional 2D seismic data exhibits frequencies of between 30-50Hz and using interval velocities of 1800m/s (based on check shot data from the wells), yields a maximum vertical resolution (tuning thickness,  $\frac{1}{4}$  dominant wavelength, Badley, 1985) of c.11-15m. The 3D data yields similar vertical resolution, but has the added advantage of ‘continuous’ coverage within the dataset, which permits detailed analysis of architectural elements and seismic attribute



analysis. The high resolution 2D data has a bandwidth of 45-170Hz, with peak mean frequencies of 90-110Hz in the shallow section, resulting in maximum vertical resolution (tuning thickness) of c.4-5m ( $\frac{1}{4} \lambda$ ) and affording an exceptional opportunity to study the succession in detail. The quality of the well data was variable, with many showing no recovery through the 'overburden' of recent to Eocene age. However, some wells did collect lithological and biostratigraphic information through the shallow section, and the best, well 214/4-1, utilised a remote operated vehicle to collect samples from the sea floor cuttings pile throughout completion of the Neogene (Davies and Cartwright, 2002), thus providing calibration of the shallow stratigraphy within the basin axis (Fig. 3.1). The seismic data were interpreted following conventional seismic stratigraphic interpretation techniques. The seismic sequence stratigraphy paradigm of Vail et al. (1977) promotes stratigraphical division into a series of genetically related packages based on reflection termination relationships, e.g. truncation, baselap etc.

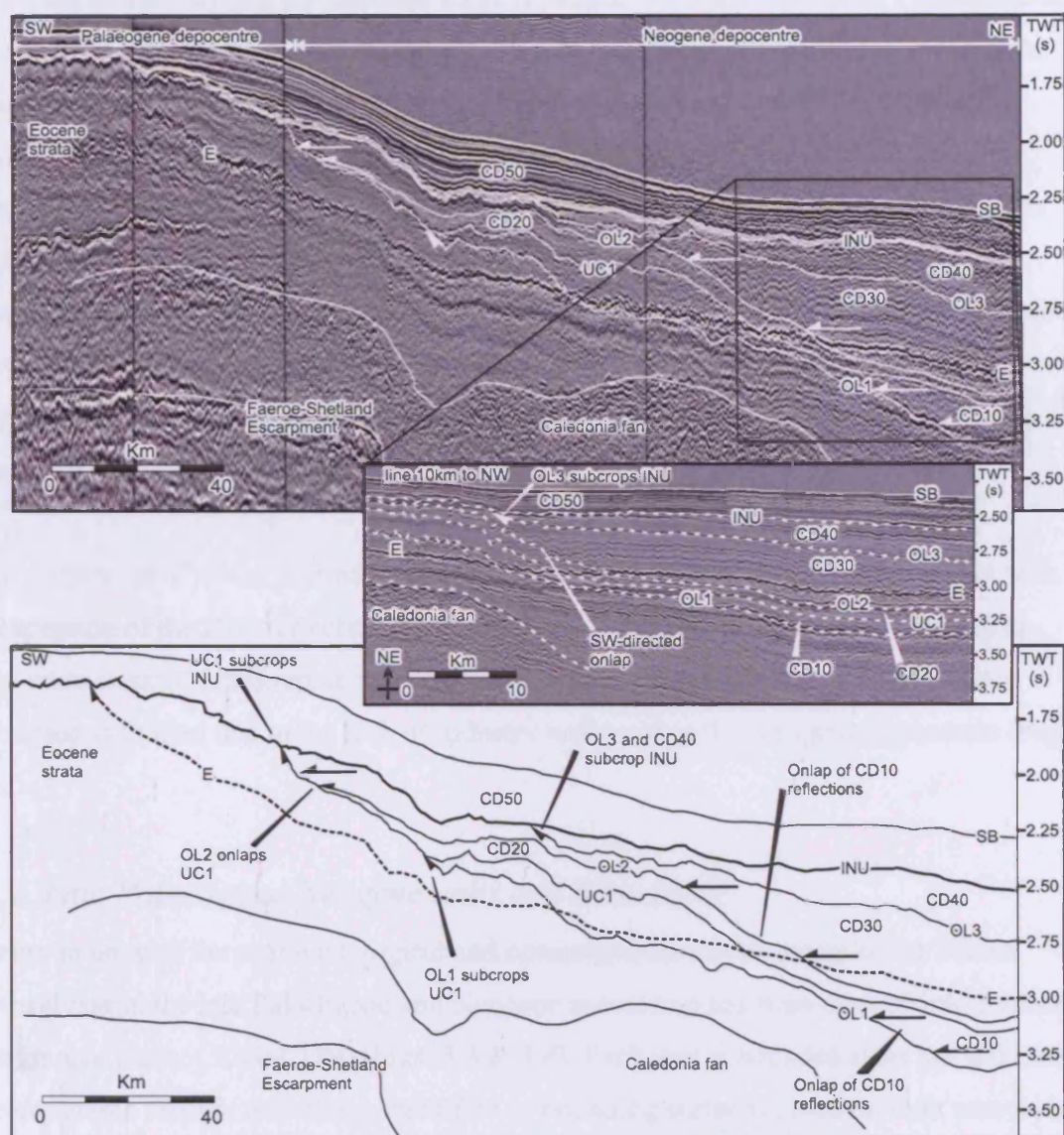
### 3.5. Seismic stratigraphy

The primary emphasis of this study is the analysis, division and interpretation of the upper Palaeogene and Neogene stratigraphic succession within the Faeroe Shetland Basin.

Description of the stratigraphy comprises 4 components: 1, description of regional extent of Neogene sediment preservation within the basin (*section 3.5.1*); 2, outline of the resultant stratigraphical division and biostratigraphic dating (*sections 3.5.2 & 3.5.3*); 3, correlation of the proposed stratigraphic division with existing stratigraphic nomenclatures and definition of the INU (*section 3.5.3 & 3.7*) and 4, detailed description and interpretation of the stratigraphic division devised by this study (*section 3.8*).

#### 3.5.1. Palaeogene and Neogene sediment distribution

Seismic interpretation of the Cenozoic sedimentary succession within the Faeroe Shetland Basin reveals differential gross distribution of Palaeogene and Neogene strata (Fig. 3.2), as previously documented (Stoker, 2003). Although Palaeogene strata are present throughout the basin (Lamers and Carmichael, 1999; Sørensen, 2003; Stoker, 2003; Robinson, 2004, Robinson et al., 2004), the stratigraphic succession within the southern Faeroe Shetland

**Figure 3.2**

Composite strike oriented 2D seismic profile and corresponding geoseismic section along the basin axis (line location Fig. 3.1). The profile outlines the seismic stratigraphic division produced as part of this study, and its variation along strike. Neogene strata are concentrated toward the NE of the basin, and onlap the Palaeogene strata toward the SW, delineating the Palaeogene and Neogene depocentres. The inset panel consists of a seismic profile situated 10km NW of the composite line (shorter line marked Fig 2. on base maps), which details the relationship of the Neogene stratigraphy to the middle Eocene Caledonia Fan. Note the significant onlap of unit CD30 reflections into the OL2 reflection across the fan. Abbreviations: E = Horizon E; SB = seabed.

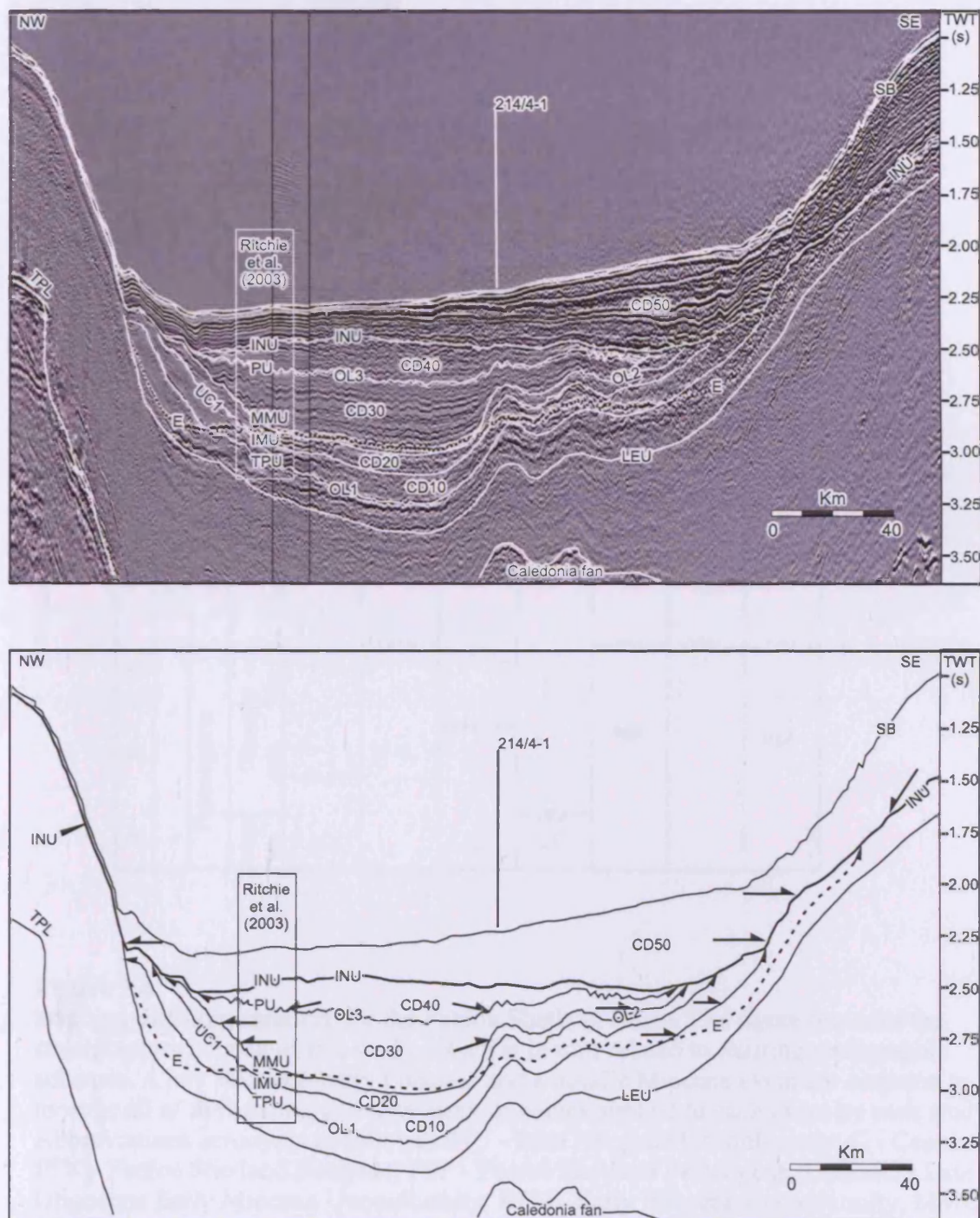
Basin, primarily within UK Quads 204, 205 and 213 and Faeroese Quads 6005 and 6104 (Fig. 3.1b) and underlying the Shetland slope is predominantly composed of Palaeocene and Eocene strata which are unconformably overlain by a thin veneer (<100m) of Pliocene to Recent sediments. This is referred to as the ‘Palaeogene depocentre’ (Figs. 3.1 & 3.2). Conversely, the Neogene strata within the basin, which generally onlap the Palaeogene strata, are largely restricted toward the northern end of the basin and the Faeroese margin (Figs. 3.1 & 3.2), and define the ‘Neogene depocentre’. In order to develop a coherent seismic stratigraphy as part of this study, Oligocene strata are included within the Neogene depocentre. The restriction of Neogene strata to the north of the basin is attributed to topographic relief created by the Palaeogene strata toward the south, evidenced by onlap of Neogene strata (Fig. 3.2).

The significance of this restricted Palaeogene and Neogene stratal distribution is that with the exception of the INU reflection (*section 3.7*), Neogene reflections cannot be used as basin-wide seismic stratigraphic markers. Furthermore, the possibility of well-seismic calibration is limited due to the lack of industry wells within the Neogene depocentre (Fig. 3.1).

### 3.5.2. Late Palaeogene-Neogene units and boundaries

In order to unravel the sedimentological and oceanographic development of the Faeroe Shetland Basin, the late Palaeogene and Neogene succession has been divided into 5 seismic stratigraphic Units, CD10-CD50 (Figs. 3.3 & 3.4). Each unit is bounded at its top and base by correlatable seismic reflections identified as bounding surfaces based on their association with discontinuity of seismic reflections within the units. Three of the five bounding surfaces (OL1, OL2 and OL3) exhibit reflection termination onto them, and are interpreted to represent hiatal surfaces, while the remaining two (UC1 and INU) exhibit reflection termination beneath them in addition to onto them, and are thus interpreted as erosional unconformities (*sensu* Mitchum et al., 1977). Each reflection was identified and interpreted based on overlying and underlying reflection configuration, with no bias from previous studies as to their classification or origin, hence the non-descriptive naming. However the Intra-Neogene Unconformity was a specific focus for this study, and the name originally





**Figure 3.3**

Regional composite 2D seismic profile and geoseismic section across the northern end of the Faeroe Shetland Basin (line location Fig. 3.1). Line details the seismic stratigraphic division of the Palaeogene-Neogene stratigraphy. Note truncation of units beneath the INU on the basin margins. Well 214/4-1 forms the key lithologic and biostratigraphic calibration for the Neogene succession within the basin. Inset box documents stratigraphic division of Ritchie et al. (2003). Abbreviations: E = Horizon E; LEU = Late Eocene Unconformity (Davies and Cartwright 2002); TPL = Top Palaeogene Lavas (Naylor et al., 1999).

Chronostratigraphy Berggren et al 1995				Published stratigraphic nomenclatures for the Cenozoic of the Faeroe Shetland Basin						
Time Ma	Era	Period	Epoch	This Study	Stoker 1999	Andersen et al 2000	Davies & Cartwright 2002	Stratagem 2002	Ritchie et al 2003	Stoker et al 2005
0	Cenozoic	Neogene	Qual.		UNU					
			Pliocene late	CD50	MNU	FPC.D2	C4	FSN-1		FSN-1
5			Pliocene early, late	INU	INU	CN040	EPU	INU	INU	IPB
				CD40					PU	
10			Miocene late	OL3		FPC.D1	C3	FSN-2a		FSN-2a
				CD30						
			Miocene middle	OL2	LNU				MMU	
15				CD20						
				UC1		CN030	MMU	IMU	IMU	IMU
20			Miocene early	CD10		FPC.C		FSN-2b		FSN-2b
25					LOEMU		C2	TPU	TPU	TPU
30		Palaeogene	Oligocene late			CN01		FSP		FSP
			Oligocene early	OL1						
35		Eocene	late				LEU			
							C1			

**Figure 3.4**

Stratigraphic nomenclature for the Faeroe Shetland Basin. The figure provides the stratigraphic division of this study, which is in turn related to existing stratigraphic schemes. A late Miocene-early Pliocene and a middle Miocene event are common to most or all of the studies, and note array of names applied to each event by each study. Abbreviations/acronyms as follows: INU - Intra Neogene Unconformity; C - Cenozoic; FSN - Faeroe Shetland Neogene; FSP - Faeroe Shetland Palaeogene; LOEMU - Late Oligocene Early Miocene Unconformity; EPU - Early Pliocene Unconformity; MMU - Middle Miocene Unconformity; LEU - Late Eocene Unconformity; IMU - Intra Miocene Unconformity; TPU - Top Palaeogene Unconformity; PU - Pliocene Unconformity; IMU - Intra Miocene Unconformity.

proposed by Stoker (1999) was retained following unbiased interpretation of the reflection which was based on first principles.

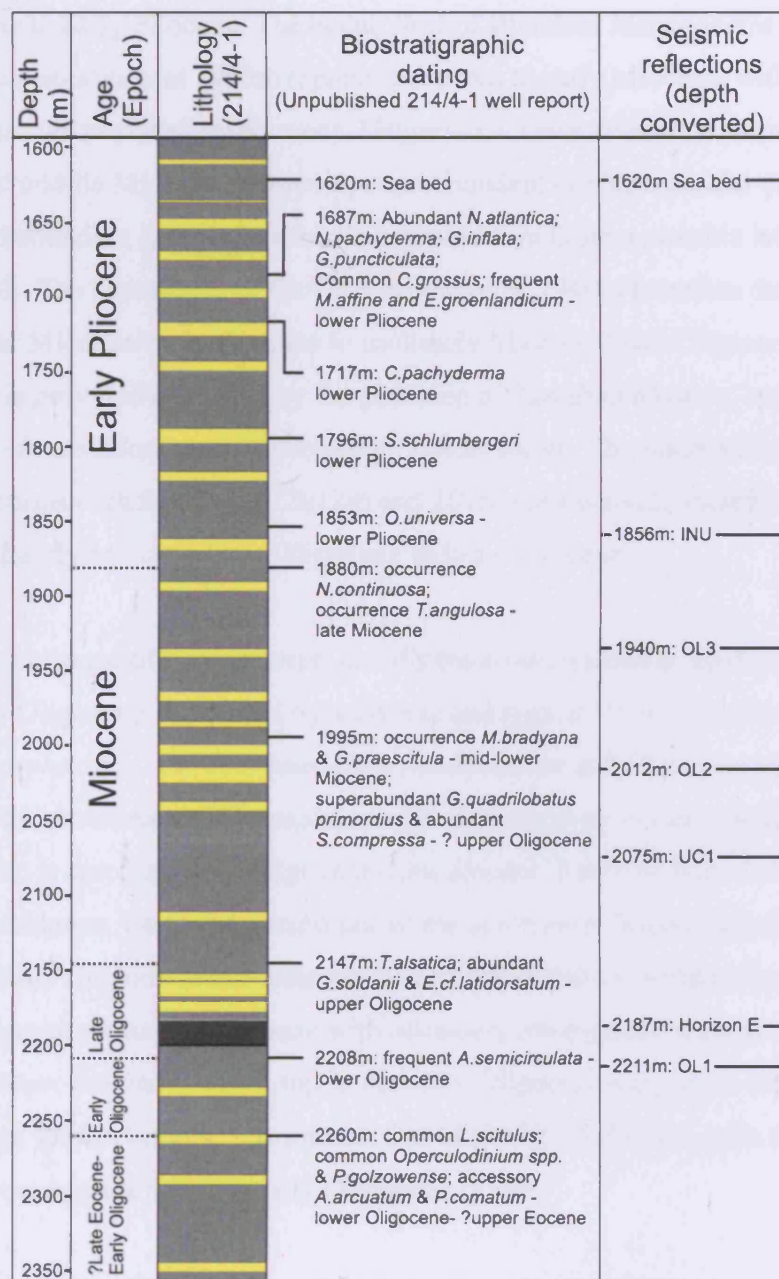
### 3.5.3. Biostratigraphic calibration

Of the 93 petroleum exploration wells and boreholes available to this study, only well 214/4-1 provides a continuous, biostratigraphically calibrated stratigraphic succession through the Neogene and Palaeogene stratigraphy within the Neogene depocentre (Figs.3.1 & 3.5), which thus forms a critical calibration for the stratigraphy established during this study. Acquisition of Neogene and upper Palaeogene samples using a remotely operated vehicle (Davies and Cartwright, 2002) results in some potential uncertainty regarding the depth of origin of the samples and possible mixing during transit. These uncertainties are considered minimised by relatively short transit times within the shallow section (<600m), and dating of samples based on faunal assemblages. Figure 3.5 outlines the correlation of depth converted seismic markers defined in this study with biostratigraphic dating of the Neogene and upper Palaeogene samples, which are described in detail below, and Figure 3.6 shows the relationship of the well to the stratigraphy.

#### 3.5.3.1. Seismic-Well correlation

Biostratigraphic dating of well 214/4-1 presented in this study is sourced from unpublished well reports produced for Mobil North Sea Ltd who were the operator of the well. Some of the data were published by Davies et al. (2001) and Davies and Cartwright (2002). Samples from 1687m, 1717m, 1796m and 1853m (all depths in this section are total vertical depth sub-sea level (TVDSS)) are dated as early Pliocene. The age of the sample from 1687m is based on the occurrence of abundant planktonic foraminifera including *Neogloboquadrina atlantica*, in combination with *Neogloboquadrina pachyderma*, *Globigerina inflata* and *Globigerina puncticulata*. The benthic assemblage contains common *Cibicides grossus*, frequent *Melonis affine* and *Elphidium groenlandicum*, which are characteristic of the Pliocene. The sample from 1717m records the presence of *Cibicidoides pachyderma*, taken to indicate a Pliocene age, and the appearance of *Sigmoilopsis schlumbergeri* at 1796m indicates the lowermost Pliocene. The sample at 1853m records common *Orbulina universa* in addition to a similar faunal assemblage to the overlying samples. The occurrence of *Neoglobigerina continuosa* and *Trifarina angulosa* at 1880m date the sample as late



**Figure 3.5**

Summary of the lithologic and biostratigraphic data from well 214/4-1 from unpublished well reports, some of which were published by Davies et al. (2001) and Davies and Cartwright (2002). Biostratigraphic analysis allows the stratigraphy to be dated based on microfossil assemblages. Lithologically the succession consists of intercalated claystones (grey) and sandstones (yellow). The black zone represents Horizon E. Depth conversion of the seismic reflections that bound the units provides dating and lithologic calibration of the stratigraphy. All depths are TVDSS (sub sea level).



Miocene. Therefore, the intersection of the INU reflection with Well 214/4-1 at 1857m places the reflection between Early Pliocene and Late Miocene datums, and dates the surface as Late Miocene to early Pliocene. The occurrence of abundant *Martinotiella bradyana* and *Globoquadrina praescitula* at 1995m represent the mid to early Miocene, with additional evidence for this age provided by common *Uvigerina acuminata/hosiusi*, which is restricted to the early and middle Miocene. However, superabundant *Globigerinoides quadrilobatus primordius* and abundant *Spirosigmoilinella compressa* indicate a possible late Oligocene age at this depth. The occurrence of the OL3 reflection at 1940m therefore dates the surface between the late Miocene/early Pliocene to mid/early Miocene-?late Oligocene. A late Oligocene age is provided at 2147m by the presence of *Turrilina alsatica*, supported by abundant *Gyroidina soldanii* and *Elphidium cf. latidorsatum*. The intersection of the OL2 and UC1 reflections with the Well at 2012m and 2075m respectively therefore dates the surfaces as mid/early Miocene-?late Oligocene to late Oligocene.

The frequent occurrence of palynomorph *Areoligera semicirculata* at 2208m dates the sample as early Oligocene, supported by a diverse and typical Oligocene taxa including *Deflandrea phosphoritica*, *Cordosphaeridium cantharellum* and *Chirtopteridium mespilanum*. The occurrence of *Cenosphaera spp.* also suggests the early Oligocene. The sample at 2260m is dated as early Oligocene-?late Eocene, based on both foraminiferal and palynological evidence. Common occurrence of the lowermost Oligocene index taxon *Labrispira scitulus* combined with common occurrence of palynomorphs *Operculodinium spp.* and *Palaeocystodinium golzowense* with accessory *Areosphaeridium arcuatum* and *Phthanoperidinium comatum*, which top in the early Oligocene support an early Oligocene-?late Eocene age for the sample. The intersection of the OL1 reflection with the Well at 2211m therefore suggests that it is early Oligocene in age.

#### 3.5.3.2. Well summary

As a result of seismic-well correlation, preliminary age estimates for the units and bounding surfaces of the stratigraphy are summarised below:

#### Bounding reflections

- INU: Late Miocene to Early Pliocene

- OL3: late Miocene to early/mid Miocene-?late Oligocene
- OL2: early/mid Miocene to late Oligocene
- UC1: early/mid Miocene to late Oligocene
- OL1: early Oligocene

#### *Units*

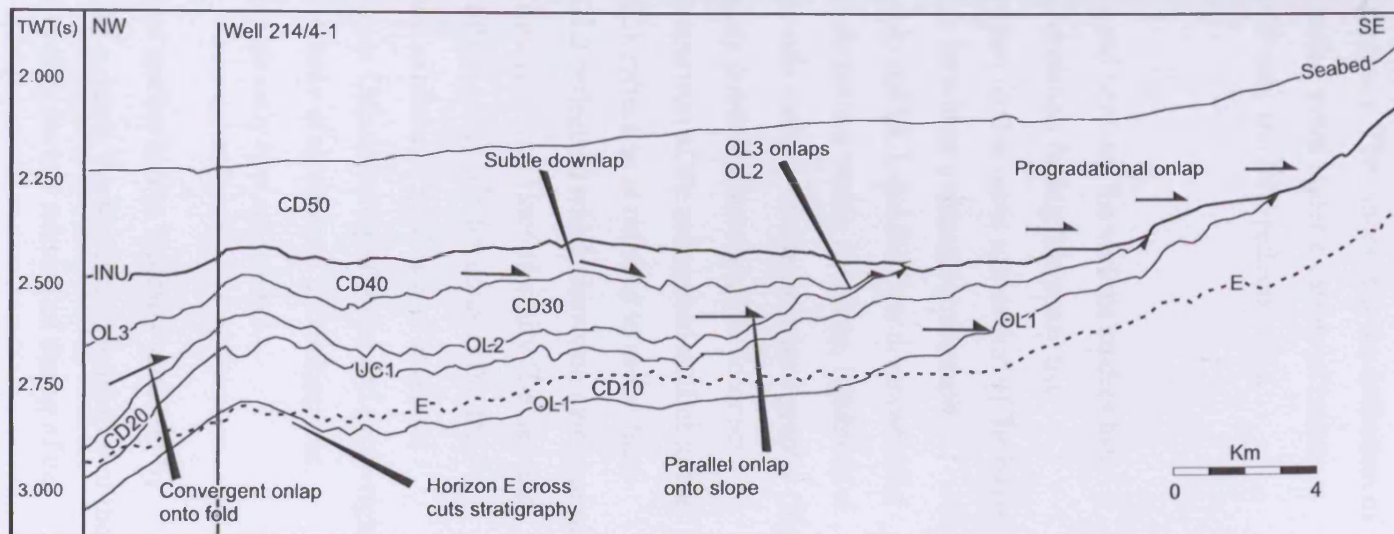
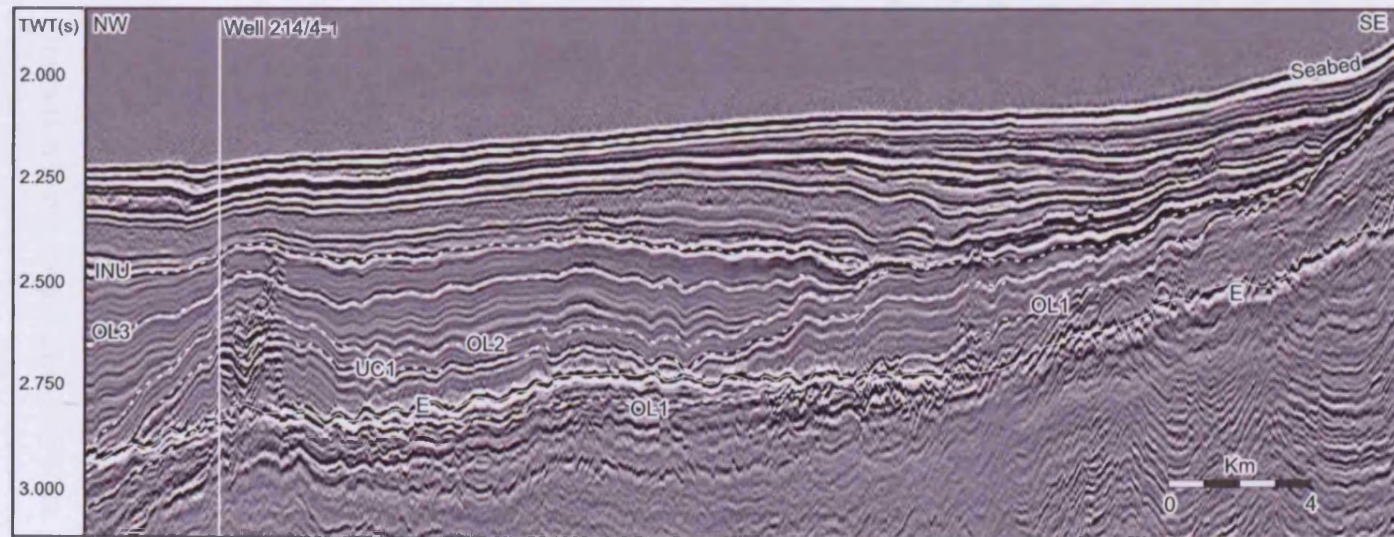
- Unit CD50: early Pliocene to Recent
- Unit CD40: late Miocene
- Unit CD30: early to middle Miocene
- Unit CD20: late Oligocene to early/middle Miocene
- Unit CD10: early Oligocene -?early/middle Miocene

For dating of the units, emphasis was placed upon the more robust age indicative taxa, while possible/questionable age indicators (such as the ?Oligocene datum at 1940m) were judged less reliable. It is therefore acknowledged that the age model proposed here requires testing with higher resolution dating.

### 3.6. Clarification of Neogene seismic stratigraphy within the Faeroe Shetland Basin

A number of stratigraphic nomenclatures have been proposed and published for the Cenozoic of Faeroe Shetland Basin (Stoker, 1999, Andersen et al., 2000; Ritchie et al., 2003; Stoker, 2003, Davies and Cartwright, 2002; Stoker et al., 2005), a summary of which is given in Figure 3.4. As part of this study, each nomenclature has been correlated with the aim of clarifying the Neogene stratigraphy within the basin.

Comparison of the various stratigraphic schemes reveals a number of key seismic-stratigraphic events, namely of early Pliocene, mid Miocene and late Oligocene age, that are common to each of the studies, and which are represented by distinct seismic reflections. However, each study utilises a different set of names and abbreviations for its proposed stratigraphy, leading to the application of an array of names to each distinct reflection. This is best exemplified by the early Pliocene seismic stratigraphic event. An unconformity dated



**Figure 3.6**  
2D seismic profile and geoseismic section orientated orthogonal to the base of the Shetland slope (line location Fig. 3.1). The profile highlights detail of unit relationships on the Shetland margin, and location of Well 214/4-1. Units CD10-CD40 and bounding reflections subcrop the INU at the base of the slope. Note onlap onto the OL1 and OL2 reflections. Seismic resolution is significantly diminished beneath Horizon E. Abbreviations as in Fig. 3.2.

as late Miocene to early Pliocene is identified by each of the referenced studies and variously referred to as the Intra-Neogene Unconformity (Stoker, 1999, Ritchie et al., 2003; Stoker, 2003), the Early Pliocene Unconformity (Davies and Cartwright, 2002), the Pliocene Unconformity (Ritchie et al., 2003), CN040 (Andersen et al., 2000) and most recently the Intra-Pliocene Unconformity (Stoker et al., 2005). Comparison of the published seismic picks for each of these studies reveals that the unconformity is variably picked as one of two reflections, the INU and the OL3 reflections of this study. The outcome is the definition of one of the two reflections as the early Pliocene erosion event under a variety of names, although interpretation during this study shows that only the INU reflection is a demonstrable erosional unconformity.

Inconsistency in the naming of key reflections shared between the various studies has resulted in some confusion. Detailed seismic interpretation during this study has demonstrated that there are 5 major reflections within the Neogene succession of the basin which form obvious candidates for bounding surfaces within a seismic stratigraphic framework (OL1-3, UC1 & INU), out of which only the UC1 and INU are demonstrable erosion surfaces. In their study of contractional deformation within the basin, Ritchie et al., (2003) pick the same 5 seismic reflections used in this study to divide their stratigraphy (Fig. 3.3), which are dated via correlation with previously published stratigraphic schemes (Davies and Cartwright, 2002; Stoker, 2003). Comparison of the referenced studies to the reflections defined in this study shows that the UC1 reflection is referred to as the Intra-Miocene Unconformity (Stoker, 2003), and the OL2 reflection which shows no evidence of erosional subcrop beneath it is referred to as the mid-Miocene Unconformity (Davies and Cartwright, 2002). Likewise, the INU reflection of this study is referred to as the INU (Stoker, 2003) and the OL3 reflection, which again exhibits no evidence of erosional subcrop beneath it is referred to as the Early Pliocene Unconformity (Davies and Cartwright, 2002). Therefore, by reference to earlier studies, Ritchie et al. report 4 unconformities, although when based on seismic stratigraphic analysis only two are present.

Dating of the key seismic markers within published studies is also typically achieved by reference to previously published stratigraphies. As a result, the source and reliability of the age information is not always explicitly clear. To clarify the key sources of dating of the

Neogene succession of the basin, the source data for age estimates of the UC1 and INU surfaces within the key published stratigraphic nomenclatures were collated (Table 3.1).

Study	Reflections	
	UC1 (Miocene)	INU (late Miocene-early Pliocene)
Stoker (1995)	No specific calibration	No specific calibration
Stoker (1999)	N/A	Boreholes including 214/4-1
Andersen et al. (2000)	Analogous studies including Stoker (1995)	Analogous studies including Stoker (1995)
Davies and Cartwright (2002)	214/4-1	214/4-1
Stoker (2002)	N/A	Stoker 1999; Andersen et al. (2000)
Stoker (2003)	Davies and Cartwright (2002); Andersen (2000)	Davies and Cartwright (2002); well database
Ritchie et al. (2003)	MMU: Davies and Cartwright (2002); IMU: Stoker (2003)	INU: Stoker (2003); PU: Davies and Cartwright (2002)
Stoker et al. (2005)	Stoker (2003); Andersen (2000); 77/7, 77/9 and 214/4-1; Stoker et al., in press b; Ritchie et al., (2003)	Davies et al. (2001) (214/4-1); BGS 88/7, 77/9; Stoker (2002)

**Table 3.1.** Sources of information used by previous studies to date the middle Miocene and early Pliocene erosion events within the Faeroe Shetland Basin.

Comparison of each of the studies shows that Well 214/4-1 forms the most important source of chronological constraint on the Neogene succession of the Faeroe Shetland Basin. Each of the studies derives proposed ages either from direct correlation to the well or via correlation with published studies which utilise the well. Although the regional extent of the INU reflection results in greater well constraint, 214/4-1 remains the most important point of chronological constraint.

In summary it has been shown that there are a number of seismic stratigraphic events that are common to each of the various stratigraphic nomenclatures erected for the Faeroe Shetland Basin. However, each event has been assigned a variety of names, and dated using a range of sources all of which stem from Well 214/4-1. Although this study also uses a new set of intentionally non-descript names for the key units and reflections, the stratigraphic subdivision is in turn fully referenced to previous studies to facilitate clarity between the studies. This therefore forms a robust division of the Neogene stratigraphy within the basin, and provides a base for further study and subdivision of the succession.

### 3.7. Definition of the Intra-Neogene Unconformity

Usage of the term Intra-Neogene Unconformity, or INU, has become commonplace, and has been widely used to refer to the youngest major erosional surface, dated as late Miocene/early Pliocene in age, within the Faeroe Shetland Basin (e.g. Knutz and Cartwright, 2003; Ritchie et al., 2003; Sørensen, 2003; Stoker, 2003; Knutz and Cartwright, 2004; Smallwood, 2004). However, section 3.6 demonstrates that at present the INU is not clearly defined and characterised, and that in addition to the name INU, a variety of terminology has been applied to the surface (Early Pliocene Unconformity, Pliocene Unconformity, Early Pliocene Unconformity, Intra-Pliocene Unconformity). Furthermore, the close proximity of the unconformity reflection to other distinctive reflections within basin axis (OL3) has resulted in more than one reflection being labelled as the INU. Therefore, it is important to attempt to clarify the definition of the Intra-Neogene Unconformity, and outline under what circumstances it is appropriate to use the term.

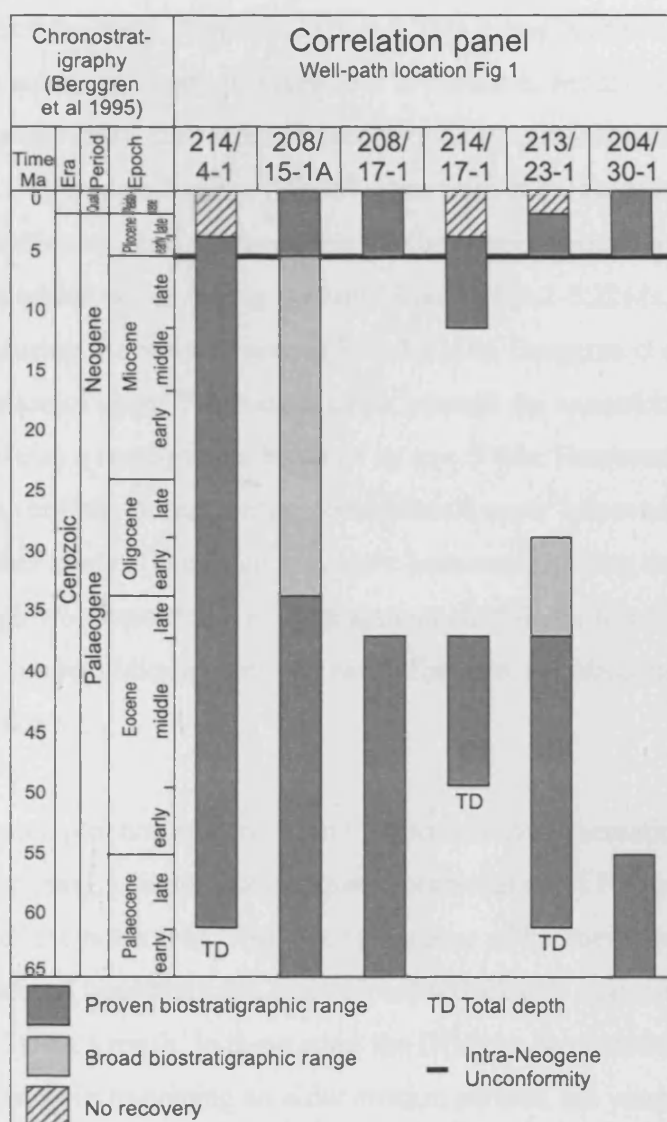
The Intra-Neogene Unconformity was first defined by Stoker (1999) as:

‘A predominantly planar surface which can be traced from the shelf into the basin. On the shelf, it is a seaward tilted, erosive surface, truncating Miocene strata of the Lower Nordland Group, whereas on the slope it is predominantly a downlap/onlap surface. On the outer shelf, it may form part of a composite erosion surface. In the basin the INU appears as a more conformable, draped surface. Borehole and well data suggest a late Miocene-early Pliocene age’.

Identification of the early Pliocene erosion event on the basin margins at the northern end of the basin is unambiguous (Fig. 3.3), but convergence of the unconformity with the OL3 reflection can make identification of the erosion surface within the basin axis problematic (Fig. 3.6). Based on extensive seismic correlation from the Faeroese and Shetland margins into the basin centre during this study (*section 3.8.5*), it has been possible to clarify that the early Pliocene erosion event within the basin axis is represented by the reflection identified as the INU by this study. The OL3 reflection is interpreted as a hiatal surface which was originally continuous for some distance upslope, and was erosionally truncated during formation of the INU (*see section 3.9.1.1* for further explanation).

Throughout the basin the unconformity is punctuated by a number of industry wells and boreholes, which have been used to constrain the timing of the erosion (e.g. Stoker, 2003, Stoker et al., 2005). Estimates of an early Pliocene age for the unconformity are based on the occurrence of early Pliocene microfossils above the unconformity in well 214/4-1 and BGS boreholes 77/7 and 77/9 (Stoker, 2003, Stoker et al., 2005). These data give a date for the cessation of erosion, but do not provide information on the timing of initiation of erosion, for which a late Miocene date is proposed by Stoker (1999). In order to clarify the timing, duration and chronological extent of the INU erosion event, a series of industry wells which penetrate the INU were selected based on well location, the preserved stratigraphic range and the availability of shallow biostratigraphic calibration (Fig. 3.7). In all but one (214/4-1) of the wells a chronostratigraphic break is observed, with Pliocene strata found to overlie strata of upper Miocene (214/4-1) to upper Palaeocene (204/30-1) age. The occurrence of a



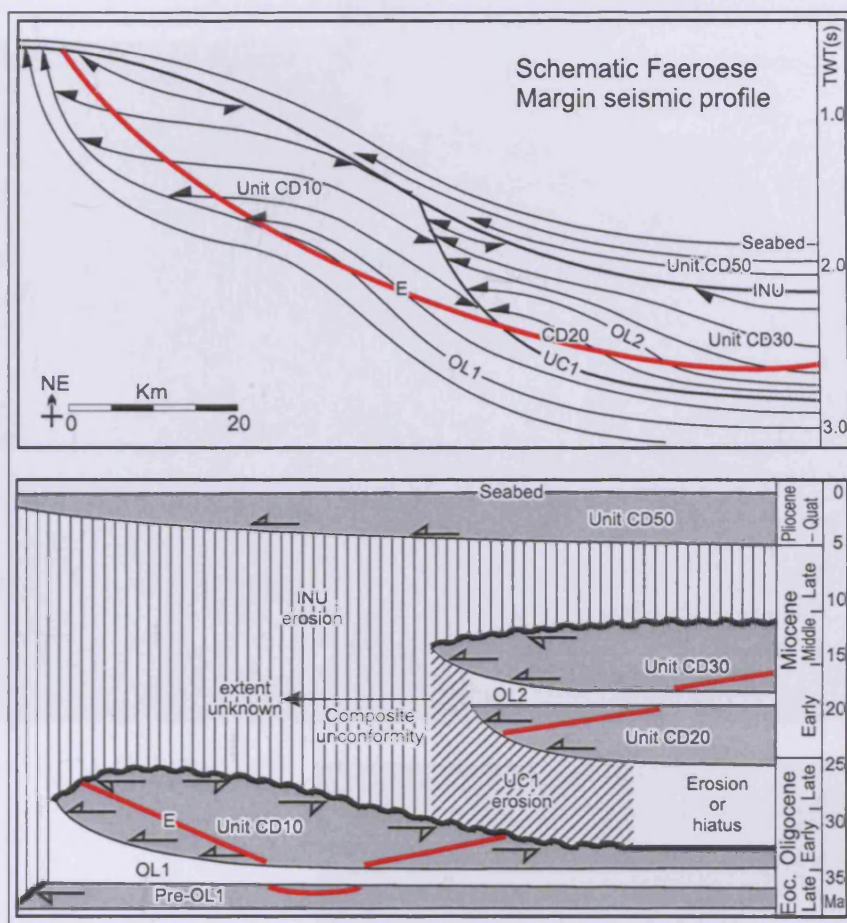
**Figure 3.7**

Correlation panel of industrial wells revealing stratigraphic preservation throughout the basin in order to highlight the erosional hiatus associated with the INU (location Fig. 3.1). Excluding Wells 214/4-1, 208/15-1A and 214/17-1, a stratigraphic break is recorded at the base of the Pliocene, representing the INU erosion event. The presence of late Miocene strata within Well 214/17-1 is based on the occurrence of one example of an upper Miocene microfossil within an assemblage that ranges into the Pliocene and thus is not deemed particularly reliable. Similarly, the late Miocene record of 218/15-1A is part of a broad early Oligocene-Miocene sample and does not provide a defined late Miocene datum.

continuous stratigraphic record in well 214/4-1 including upper Miocene sediments suggests that within the Neogene depocentre, erosion associated with the INU event occurred between the late Miocene and the early Pliocene (11.2- c.3.5Ma, using the timescale of Berggren et al., 1995) over an unknown duration. Elsewhere in the basin, primarily on the Shetland Slope region, Pliocene strata are recorded overlying Oligocene-Miocene (208/15-1a), lower Oligocene (213/23-1), middle Eocene (208/17-1) and upper Palaeocene (204/30-1) strata. From this well correlation, the INU is proposed to have been formed by erosion of an unknown duration which began during the late Miocene (11.2-5.32Ma, Berggren et al., 1995) and ended during the early Pliocene (5.32-3.58Ma, Berggren et al., 1995). The subcrop identification of upper Palaeocene strata beneath the unconformity reveals that the INU locally represents a stratigraphic break of up to c.50Ma. However, the hiatal value of the INU is areally variable, in that during deposition of upper Miocene sediment in the northern basin, other areas of the basin may have been experiencing depositional hiatus. Therefore, although we propose that erosion associated with the formation of the INU occurred between the late Miocene and the early Pliocene, the hiatal range and its spatial distribution are unknown.

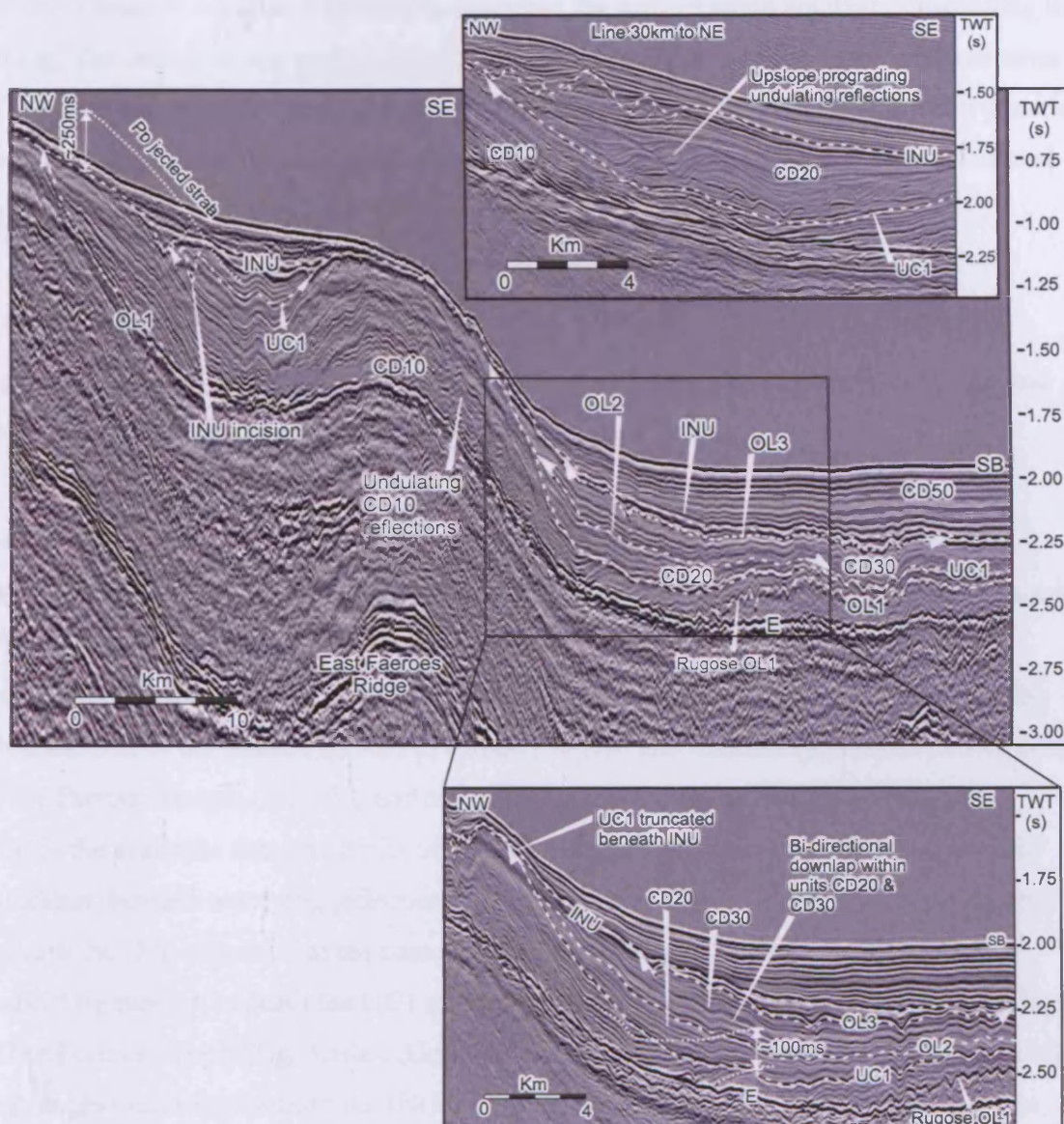
A chronostratigraphic plot constructed from a representative schematic seismic section across the Faeroese margin highlights the spatial preservation of Neogene strata between the axis and margins of the basin (Fig. 3.8). Along the base of Faeroese slope the UC1 reflection consists of an erosional unconformity, and in localised areas is truncated beneath the INU reflection (Fig. 3.9). As a result, in these areas the INU can be characterised as a composite unconformity, because in truncating an older erosion surface, the younger unconformity chronostratigraphically incorporates the older unconformity's hiatus (Fig. 3.8). However, because the original erosional extent of the UC1 unconformity is unknown, the areal extent over which the INU represents a composite unconformity cannot be defined.

In summary, the INU reflection of this study can be confidently correlated with the late Miocene-early Pliocene erosion event identified by previous studies. The INU can be traced throughout the basin and is characterised as an erosional unconformity with erosion occurring between the late Miocene and early Pliocene, resulting in localised erosional vacuity of 50Ma. Based on the timing and unconformable nature of the reflection, the name

**Figure 3.8**

Schematic seismic profile across the Faeroese margin and corresponding chronostratigraphic chart to highlight the basin-centric locus of Neogene stratal preservation and the significance of erosion associated with formation of UC1 and the INU. The INU truncates progressively older strata toward the shelf. At the point of truncation of the UC1 reflection the INU becomes a composite unconformity, incorporating the hiatal range of the UC1 unconformity. However, it is not possible to define the basinward extent over which the INU can be classified as a composite unconformity. The cross-cutting nature of Horizon E is clearly revealed. The ages and durations placed on the units and hiatuses are approximate due to the resolution of the dating, and the figure is intended to illustrate the distribution of erosion and stratal preservation within the basin and not precise unit ages and hiatal ranges. See section 3.8.6. for explanation of Horizon E.





**Figure 3.9**

Seismic profile across the Faeroese margin (line location Fig. 3.1). Line illustrates the distribution of the seismic stratigraphic units on the Faeroese margin. The East Faeroes Ridge forms a significant anticlinal structure on the margin, across which Units CD20, CD30 and CD40 are truncated beneath the INU. Upslope prograding contourite reflection configurations are present within Unit CD10 on the basinward limb of the fold. Erosion associated with the UC1 reflections is most obvious along the base of the Faeroese slope, and estimated at >90m based on stratal truncation (inset). Deposition of CD20 and CD30 by bottom currents was concentrated along the base of the slope and is characterised by broad bidirectional baselap toward the southern end of the slope and upslope progradation toward the north (inset). Stratal projection above the INU toward the upper slope allows estimation of >200m of erosion in this area during formation of the INU. The INU also exhibits incisional features 120m deep on the upper slope.

INU was retained because it accurately describes the surface while not over constraining its timing. The unconformity can be described as a composite unconformity in localised areas of the Faeroese margin, although it is not appropriate to label the unconformity as a generic composite unconformity. The detailed morphology and evolution of the INU is elaborated upon in sections 3.8.5 and 3.9.

### 3.8. Seismic-stratigraphic units

Following the outline and age calibration of the stratigraphic nomenclature, each unit and bounding reflection is described and interpreted in detail below.

#### 3.8.1. Unit CD10

Unit CD10 is marked at its base by the OL1 reflection and its top by the UC1 seismic marker (Figs. 3.3 & 3.4). The OL1 surface is represented by a moderate amplitude positive reflection that varies from a planar/mildly undulatory morphology (predominantly on the Shetland side of the basin, Fig. 3.6) to a highly rugose and undulatory reflection along much of the Faeroes Margin (Fig 3.9), and covers an area in excess of 8000km<sup>2</sup> (Fig. 3.10a). Within the available data, the limits of the reflection are marked on all sides by erosional truncation beneath overlying reflections. The SE limit is marked by slope parallel subcrop beneath the INU reflection at the base of the Shetland slope, while the southern limit is marked by subcrop beneath the UC1 marker along an E/W path across the basin to the base of the Faeroese slope (Fig. 3.10a). Along the majority of the Faeroese margin OL1 exhibits high angle truncation beneath the INU (Fig. 3.9), replaced by depositional onlap onto an underlying surface in the region of the Fugloy Ridge toward the NW limit of the study area (Fig 3.3). Clear identification of reflections underlying OL1 is hampered by the presence of a high amplitude reflection that cross cuts stratigraphy and is identified as Horizon E, of Davies and Cartwright (2002), beneath which seismic resolution is significantly reduced (Fig 3.6). In areas where underlying reflections are identifiable they are generally conformable with OL1, and polygonally faulted, suggesting a fine grained composition (Cartwright and Dewhurst, 1998).



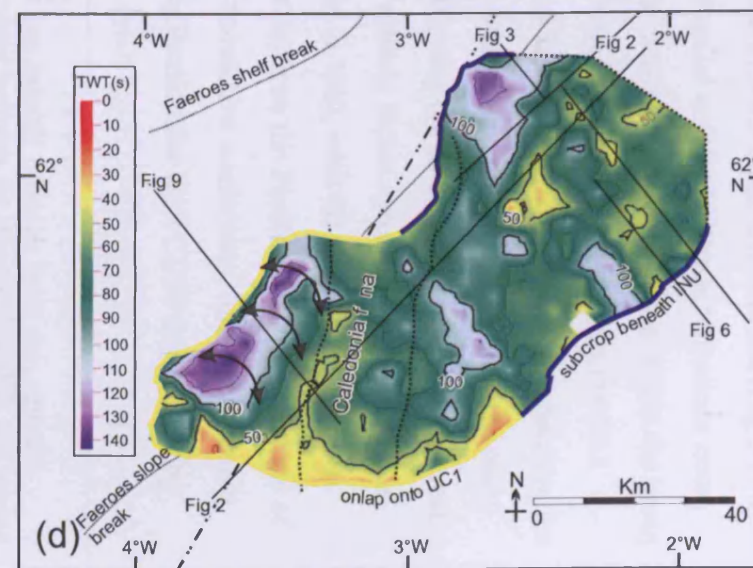
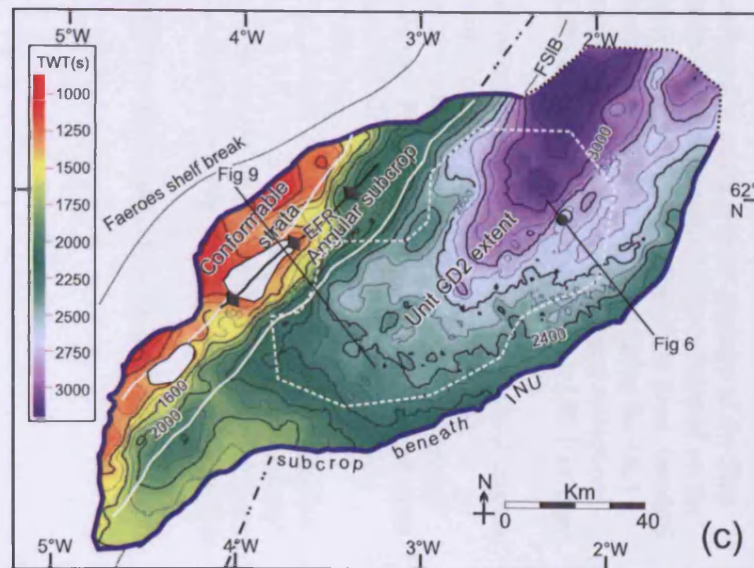
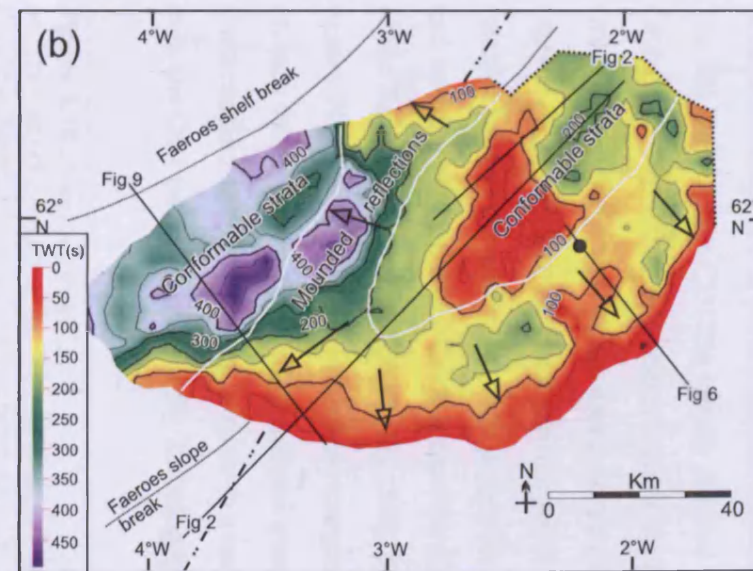
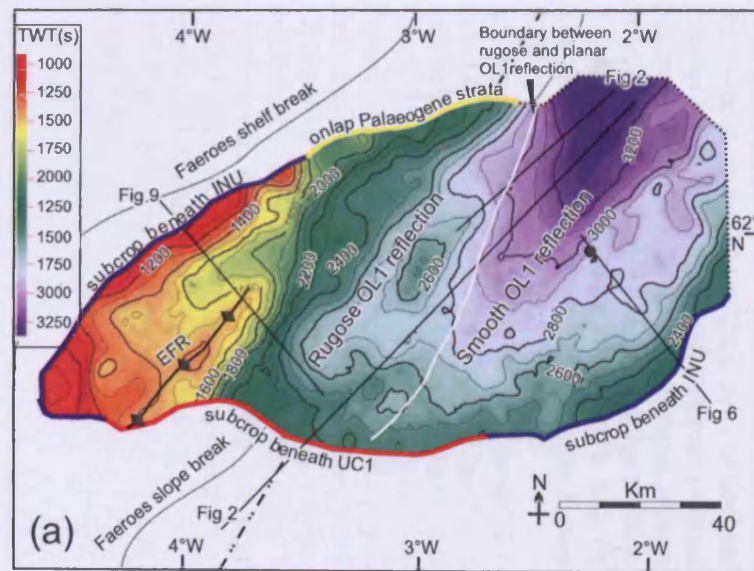


Figure 3.10

Unit CD10 attains maximum thickness of c.425m on the present day Faeroes slope, and exhibits an internal reflection configuration which comprises both discordance (onlap/downlap) and apparent seismic concordance with the basal OL1 surface (Fig 3.10b). The SE limit of unit CD10 is largely defined by parallel onlap of internal reflections onto OL1 (Fig. 3.6). These reflections exhibit conformity with the OL1 reflection within the basin axis at its northern end, which along-strike gives way to subtle SW onlap onto the OL1 surface (Fig. 3.2). On the Faeroese margin, in association with the rugose OL1 reflection, the internal reflections exhibit upslope prograding mounded, bi-directional downlap and onlap and upslope progradation which is best developed along the SE (basinward) limb and crest of the East Faeroes Ridge (EFR) (Fig. 3.9). This seismic facies extends in a slope parallel band c.10km wide along the Faeroese margin (Fig. 3.10b), with the boundaries between seismic facies c. parallel to the structural trend of folds on the Faeroese margin. Upslope of the mounded seismic reflections there is a return to relative conformity, with subtle onlap onto the OL1 reflection (Fig. 3.9). Lithological calibration for Unit CD10 is provided by

---

**Figure 3.10 (previous page)**

**(a)** Time structure map of the OL1 reflection. The surface extends from the basin axis onto the Faeroese Slope, and the white line represents the boundary between the smooth (Fig. 3.6) and rugose (Fig. 3.9) character of the reflection. Contours are in metres below sea level. Fine dotted line represents limit of data, and dot-dash line represents UK-Faeroese Political border (as applies for all other isochrons).

**(b)** Isochron map of Unit CD10. Area of thickened conformable strata present upslope of the East Faeroes Ridge while a mounded upslope prograding reflection configuration was developed on the basinward limb (Fig. 3.9), the boundaries between which are represented by the white lines. Internal reflections also exhibit conformity in the northern axis of the basin (Fig. 3.2), and onlap the OL1 reflection onto the Shetland margin (Fig. 3.6). Open arrows represent onlap of internal reflections onto underlying OL1 reflection. Contours in metres. Dotted and dashed line represents UK-Faeroese Political border.

**(c)** Time structure map of the UC1 reflection. Evidence of erosional truncation in the form of angular subcrop is restricted to a strike-parallel band along the base of the Faeroese slope (Fig. 3.9), delineated by white lines. Throughout the remainder of the reflection the underlying reflections of Unit CD10 exhibit conformity and a lack of angular subcrop (Fig. 3.6), with the boundaries between areas of erosion and conformity represented by white lines. FSIB refers to Faeroes slope break. Dotted and dashed line represents UK-Faeroese Political border.

**(d)** Isochron map of Unit CD20 (location outline on Fig. 3.10c). To the NE of the Caledonia fan the unit exhibits relatively uniform thickness (Figs. 3.2, 3.3 & 3.6), with upslope prograding undulatory reflections on the Faeroese margin (Fig. 3.9 inset), while to the SW of the fan the internal reflections exhibit bidirectional downlap and a mounded thickness distribution (Fig. 3.9). Dotted and dashed line represents UK-Faeroese Political border.

The 'Fig' references refer to the location of seismic profiles within this Chapter, e.g. 'Fig 9' refers to Figure 3.9.



well 214/4-1, which records silty clay-stone with moderately sorted quartzose sandstone intercalations.

Unit CD10 is interpreted as a contourite drift body based on the identification of upslope prograding mounded, bi-directional downlap reflection configurations on the Faeroese slope, which are diagnostic of the seismic expression of ‘separated’ contourite drifts (Faugères et al., 1999). The slope parallel distribution of the contourite seismic facies and the highly rugose seismic geometry exhibited by the OL1 reflection support the interpretation of deposition from an alongslope current. The remainder of Unit CD10 within the basin axis, which consists of largely concordant reflections that lap out onto the Shetland margin and toward the south, could be interpreted as being dominated by sheeted/infilling contourite drifts based on seismic reflection characteristics and lateral association with the interpreted drifts on the Faeroese margin (Faugères et al., 1999; Stow et al., 2002; Rebesco and Stow, 2001). The areas of Unit CD10 more distal from the Faeroese slope may also comprise a significant hemipelagite component, but the lack of features indicative of downslope processes such as channels or fans suggests that CD10 was not influenced by significant slope derived sedimentation.

### 3.8.2. Unit CD20

Unit CD20 is bounded at its base by the UC1 reflection and at its top by the OL2 reflection (Figs. 3.3 & 3.4). The UC1 reflection is characterised by a moderate to high amplitude positive reflection present over an area of c.14000km<sup>2</sup>, but restricted largely to the basin axis and Faeroese margin (Fig. 3.10c). The SE limit of the UC1 reflection is defined by subcrop beneath the INU at the base of the Shetland Slope (Fig. 3.6). The time structure map shows a SW advance of the point of subcrop from north to south, with the SW limit marked by truncation of the UC1 reflection beneath the INU. Similarly, the NW limit of the UC1 reflection is defined by subcrop beneath the INU (Fig. 3.9), and localised truncation of the UC1 reflection beneath the INU also occurs across the crest of the East Faeroes Ridge on the Faeroese margin (Figs. 3.9 & 3.10c).

Reflection UC1 locally exhibits discordant truncation of the underlying reflections of Unit CD10 (Fig. 3.9), and in these areas is interpreted as an erosional unconformity surface. Angular truncation is most clearly observed on the Faeroese margin in the location of the mounded downlap reflections of Unit CD10 (Fig. 3.10c), where localised erosion of c.90m of strata is estimated to have occurred based on projection of truncated reflections above the UC1 surface (Fig. 3.9). Identification of high angle truncation is limited to the mid-lower Faeroese slope, and elsewhere subtle convergence and relative parallelism of the UC1 surface and underlying reflections makes estimation of erosional magnitude difficult. Correlation of the UC1 surface upslope on the Faeroese margin, particularly in the region of the East Faeroes Ridge, reveals conformity of the UC1 surface and the underlying reflections of Unit CD10 (Fig. 3.9). Erosion in a slope parallel zone at a base of slope position is interpreted as evidence for alongslope current erosion (discussed further in *section 3.9.1.2*). The identification of contourite drifts below the unconformity point strongly toward the influence of alongslope current circulation prior to the formation of the unconformity. In addition, the interpreted deep water setting of the basin (*section 3.3*) and lack of features synonymous with subaerial erosion such as incised channels further suggest that the erosion had an alongslope current origin. Both comparison of seismic picks between this and previous studies, and the dating of the UC1 unconformity as likely early-mid Miocene with a possible late Oligocene age lead to the correlation of the UC1 reflection with the unconformity of proposed middle Miocene age identified previously (Andersen et al., 2000; Davies and Cartwright, 2002; Stoker, 2003). However, although the unconformity likely dates from the early-mid Miocene, it is not assigned a name with chronological significance due to the possibility of a late Oligocene age based on the well data available.

Unit CD20 was deposited onto the UC1 surface as a relatively thin unit with an average thickness of c.60-70m and a maximum thickness of c.160m, as illustrated by Figure 3.10d. The influence of the Caledonia fan on Neogene sedimentation is apparent in the isochron distribution of Unit CD20. To the east and northeast of the fan, Unit CD20 consists of a 'drape' of uniform thickness across the UC1 reflection internally comprised of parallel bedded reflections which show little evidence of thickness variation or onlap across anticlinal structures in the area, and subcrop the INU on the Shetland margin (Figs. 3.6 & 3.10d). Lithological calibration by well 214/4-1 shows that the unit consists of a sand rich

facies with clay intercalations, suggesting a depositional process capable of supplying sand to the deep basin. On the Faeroese margin to the west and northwest of the Caledonia fan, Unit CD20 shows greater variation in thickness and internal reflection geometry. Toward the NE end of the Faeroese margin, the internal reflections exhibit upslope prograding onlap/downlap geometries (Fig. 3.9) which are very similar to those identified within Unit CD10, and thus also interpreted as contourite drift deposits. Toward the SW limits of Unit CD20 the reflections become less irregular and simple bi-directional downlap of parallel internal reflections forms a mounded sediment body interpreted as a 'detached' mounded contourite drift (Fig. 3.9, Faugères et al., 1999; Stow et al., 2002). The interpretation of unit CD20 as a contourite drift implies action of bottom currents along the Faeroese margin following the formation of the UC1 surface, and supports the interpreted alongslope current origin for erosion of the Faeroese slope during formation of the UC1 surface. The uniform thickness and lack of typical contourite reflection configurations within unit CD20 in the deep basin suggests that bottom currents were less influential away from the Faeroese margin, although the frequent occurrence of sand identified in 214/4-1 suggests a depositional process capable of transporting sand grade material. A lack of significant evidence for downslope sediment input such as fan development within CD20 suggests that bottom currents may have delivered the coarse fraction. In turn, the lack of onlap onto the anticlinal structures within the basin axis (Fig. 3.6) which formed during the middle Miocene (Davies et al., 2004) suggests deposition of Unit CD20 pre-dates their formation.

### 3.8.3. Unit CD30

The base and top of Unit CD30 are marked by the OL2 and OL3 reflections respectively (Fig. 3.3 & 3.4). The OL2 reflection is characterised by a moderate to low amplitude positive reflection and is less extensive than the previously described surfaces, covering an area of c.5500km<sup>2</sup> (Fig. 3.11a). On the Shetland margin the SE limit of the reflection is marked by erosional truncation beneath the INU (Fig. 3.6 & 3.11a). The depositional limits are preserved toward the south, where the OL2 reflection onlaps onto the UC1 surface (Fig. 3.2). On the Faeroese margin, onlap of the OL2 reflection onto UC1 at the southern end of the Faeroese Margin is replaced by erosional truncation beneath the INU surface toward the NE (Fig. 3.11a).

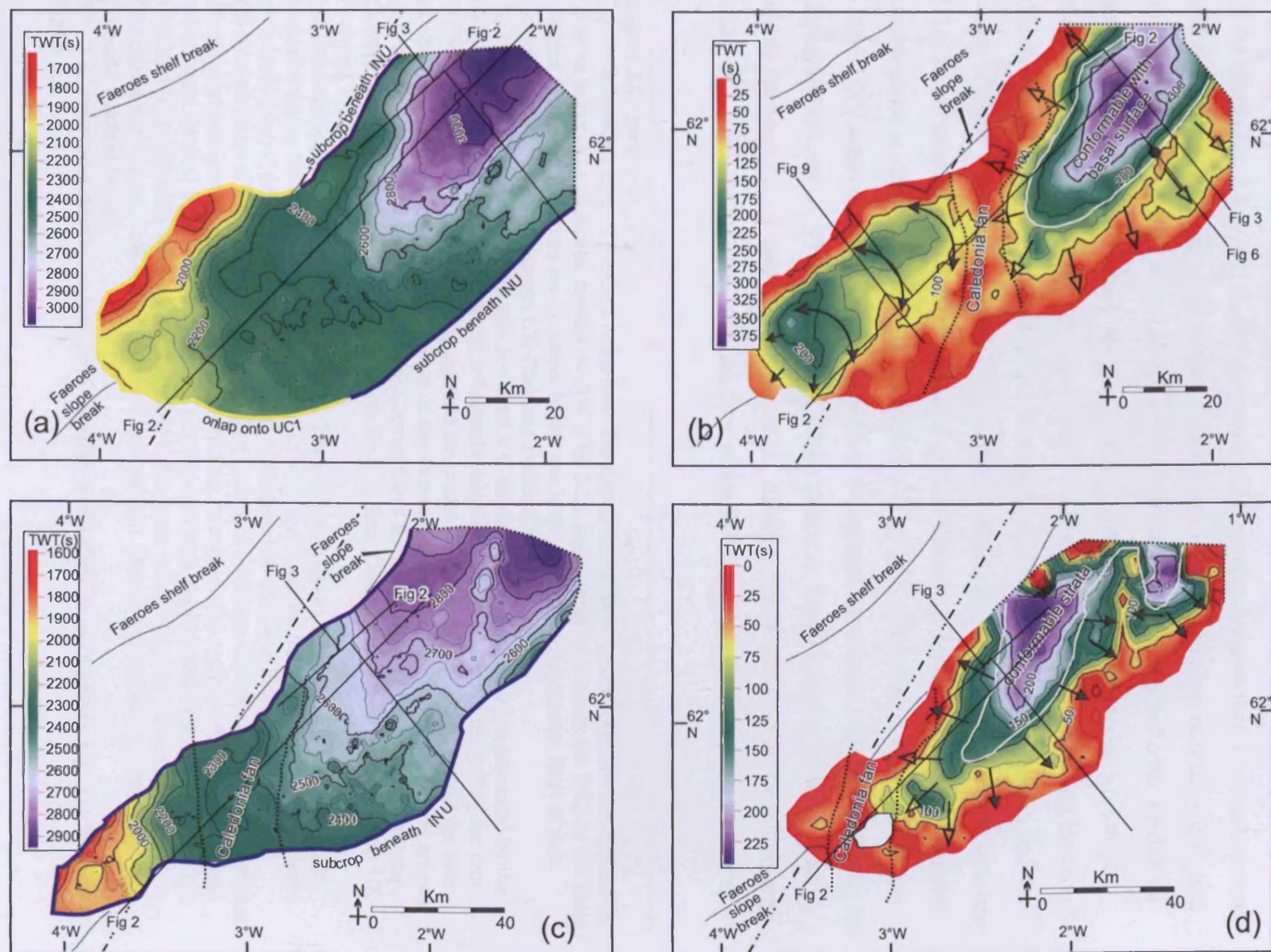


Figure 3.11

Unit CD30 attains thicknesses of >300m in the basin axis (Fig. 3.11b). Unit CD30 is composed of parallel, layer cake seismic reflections which onlap OL2 on the basin margins, to the SW, and onto the basal OL2 surface across the inversion anticlines at the northern end of the basin (Fig. 3.3 & 3.11b). Onlap onto the OL2 surface suggests that it formed a palaeo-seabed which was subsequently buried. Lithologically the unit consists of intercalated sand and mud, as calibrated by well 214/4-1. Over much of their extent the reflections exhibit a hummock-shaped cross section which is related to differential subsidence as a result of biogenic silica diagenesis and resultant compaction, manifest by the cross cutting Horizon E (Davies et al., 2001). Figure 3.12 shows the nature of the hummocky deformation, and the onlap of CD30 reflections onto OL2. Convergence of reflections onto the inversion anticline (Fig. 3.6) is interpreted as evidence for fold growth during the deposition of CD30. Similar convergence is identified onto the Caledonia fan (Fig. 3.2), across which Unit CD30 thins (Fig. 3.11b), suggesting an increase in sea floor topography associated with the fan during the deposition of Unit CD30 through the early-mid Miocene. Tectonic inversion is reported within the basin during this time (Davies et al., 2004), which would account for convergent onlap onto the folds and fans, with the fans which lie above inverted normal faults.

---

**Figure 3.11 (previous page)**

**(a)** Time structure map of the OL2 reflection. The depositional limits of the reflection are defined by onlap onto the UC1 reflection toward the SW (Fig. 3.2), and truncation beneath the INU on the basin margins (Fig. 3.3). Contours are in metres below sea level. Dotted line represents limit of data. Dotted and dashed line represents UK-Faeroese Political border.

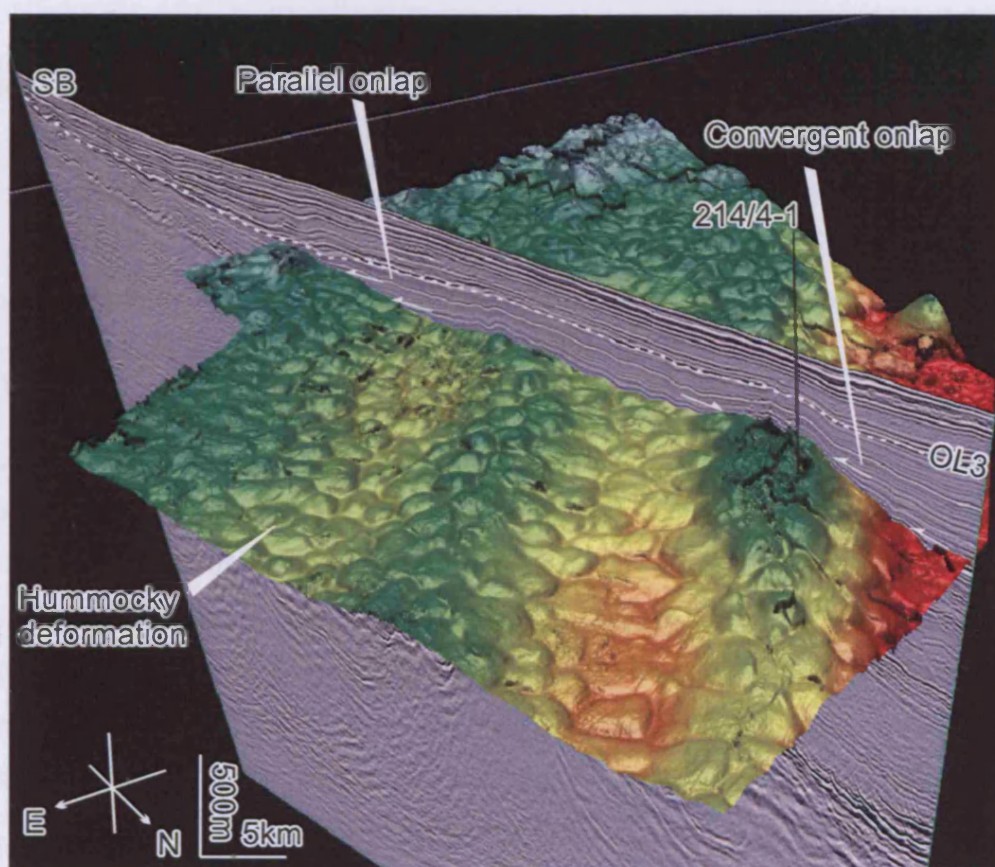
**(b)** Isochron map of Unit CD30, which reveals a bi-modal thickness distribution separated by the Caledonia fan, onto which the internal reflections onlap (Fig. 3.2). To the NE of the fan, the unit exhibits onlap onto the basin margins and fold structures (Fig. 3.3 & 3.6). SW of the fan the unit exhibits bi-directional downlap at the base of the Faeroese slope (Fig. 3.9). Open and filled arrows represent onlap and downlap respectively. Curved filled arrows represent bi-directional downlap. Contours are in metres. Dotted line represents limit of data. Dotted and dashed line represents UK-Faeroese Political border.

**(c)** Time structure map of the OL3 reflection. The surface shallows toward the SW and is locally truncated across the Caledonia fan (Fig. 3.2). Contours are in metres below sea level. Dotted line represents limit of data. Dotted and dashed line represents UK-Faeroese Political border.

**(d)** Isochron map of Unit CD40, which exhibits a mounded thickness distribution with bi-directional downlap (closed arrow) onto the basal OL3 reflection throughout the northern FSB (Fig. 3.3), and onlap (open arrows) at its SW limit (Fig. 3.2), coincident with the Caledonia fan, across which it is truncated (Fig. 3.2) reflections are conformable in the basin axis – delimited by the white line. Contours are in metres, dotted line represents limit of data. Dotted and dashed line represents UK-Faeroese Political border.

The 'Fig' references refer to the location of seismic profiles within this Chapter, e.g. 'Fig 9' refers to Figure 3.9.





**Figure 3.12**

3D visualisation of the OL2 reflection in the vicinity of Well 214/4-1 (Fig. 3.1) to illustrate nature of hummocky deformation of units CD30 and CD40 associated with formation of Horizon E. The seismic section also clearly illustrates onlap of unit CD30 internal reflections onto the fold structures and Shetland slope.

Differential compaction between the sand rich fans and encasing Eocene hemipelagite may also have enhanced relief across the fans (Fisher, 1992). Toward the northern end of the basin, the largely parallel onlap onto the Shetland and Faeroese margins suggests burial of an existing slope. The unit also attains significant thickness to the SW of the fans along the base of the Faeroese slope, where the internal reflections are largely concordant with those within unit CD20, and exhibit NW-SE directed bidirectional onlap/downlap (Fig. 3.9).

The thick succession of Unit CD30 to the east and northeast of the Caledonia fan is interpreted as an infilling sheeted drift (Faugères et al., 1999), deposition of which buried the newly forming topography created by the fold structures. An alongslope current control on deposition is invoked in preference to hemipelagic sedimentation based upon the onlap relationship and the lack of drape (Fig. 3.3), which would be expected if vertical flux was the main source of sedimentation. Deposition appears to have been consistent between units CD20 and CD30 to the SW of the Caledonia fan resulting in continuation of mounded contourite deposition, with a minor hiatus evidenced by onlap of CD30 reflections onto the OL2 surface. Creation of the hiatus could be attributed to a temporary increase in current velocity resulting in non-deposition, as is common in contourite sequences (Faugères et al., 1999). The lateral change from infilling sheeted drifts NE of the Caledonia fan to mounded detached drift deposition to the SW of the fan body corresponds to changing slope angle from the basin axis to the Faeroese slope.

#### 3.8.4. Unit CD40

The upper limit of Unit CD40 is marked by the INU and the base by the OL3 reflection (Figs. 3.3 & 3.4). The OL3 surface is distributed largely within the deep axis of the basin to the NE of the Caledonia fan and is limited in extent by truncation on the basin margins and towards the SW beneath the INU (Fig. 3.11c). Reflection OL3 is conformable with the underlying reflections of Unit CD30 and in the basin axis forms the uppermost reflection which onlaps the OL2 surface on the basin margins and towards the south (Fig. 3.6), thus forming the uppermost reflection of Unit CD30. Downlap of reflections of Unit CD40 onto the OL3 surface define it as a hiatus between the deposition of Units CD30 and CD40.



Unit CD40 attains greatest thickness of around 170m in the basin axis and exhibits stratigraphic thinning to the SE, SW and NW (Fig. 3.11d). In similarity with Unit CD30, Unit CD40 comprises a series of parallel seismic reflections which are deformed in the same hummocky manner (Fig. 3.12), and consist of intercalated clay and sand (Fig. 3.4). Reflections within Unit CD40 exhibit seismic conformity with the OL3 surface over its axial extent, and SE/NW directed bi-directional downlap define the unit margins (Figs. 3.3 & 3.11d). Thus Unit CD40 forms a mounded body which reaches greatest thickness in the basin axis and thins toward the margins. Thinning and localised erosional truncation of Unit CD40 including OL3 beneath the INU is observed across the Caledonia fan (Fig. 3.2 inset panel), defining the units SW limit. Based on seismic reflection configuration and isochron distribution, Unit CD40 is interpreted as a mounded 'detached' contourite drift (Faugères et al., 1999). In addition to the bi-directional downlap, the creation of topography on a flat basal surface is particularly diagnostic of detached contourite drifts (Faugères et al., 1999, Rebesco and Stow, 2001; Stow et al., 2002).

### 3.8.5 Unit CD50

Unit CD50 is bounded at its base by the INU (Fig. 3.3 & 3.4). As documented in section 3.7, the INU reflection is the most widely correlatable reflection of the surfaces mapped, and extends from the basin axis to the upper slopes of both margins throughout the basin (Fig. 3.13a). The regional time structure map of the INU surface, presented here for the first time, reveals a bathymetry comparable to the present day, with a deep basin axis flanked by a shallower SW (Shetland) margin (c.1°), and a slightly steeper NW (Faeroese) margin (c.1-3°), particularly where associated with structures such as the East Faeroes Ridge. The seismic character and subcrop relationships of the INU reflection vary throughout the basin from north to south and from the basin axis onto the margins. The nature and age of the units subcropping the UC1 surface also varies considerably from north to south, due to the distribution of Paleogene and Neogene sediments as described in section 3.5.1 (Fig. 3.13b). As a result, the INU surface is described systematically from north to south.

At the northern end of the basin on the Shetland slope, the INU is manifest as a high negative amplitude, relatively smooth reflection with a basinward dip of c.1°. Angular subcrop of underlying reflections beneath the INU (Fig. 3.6) identifies the surface as an

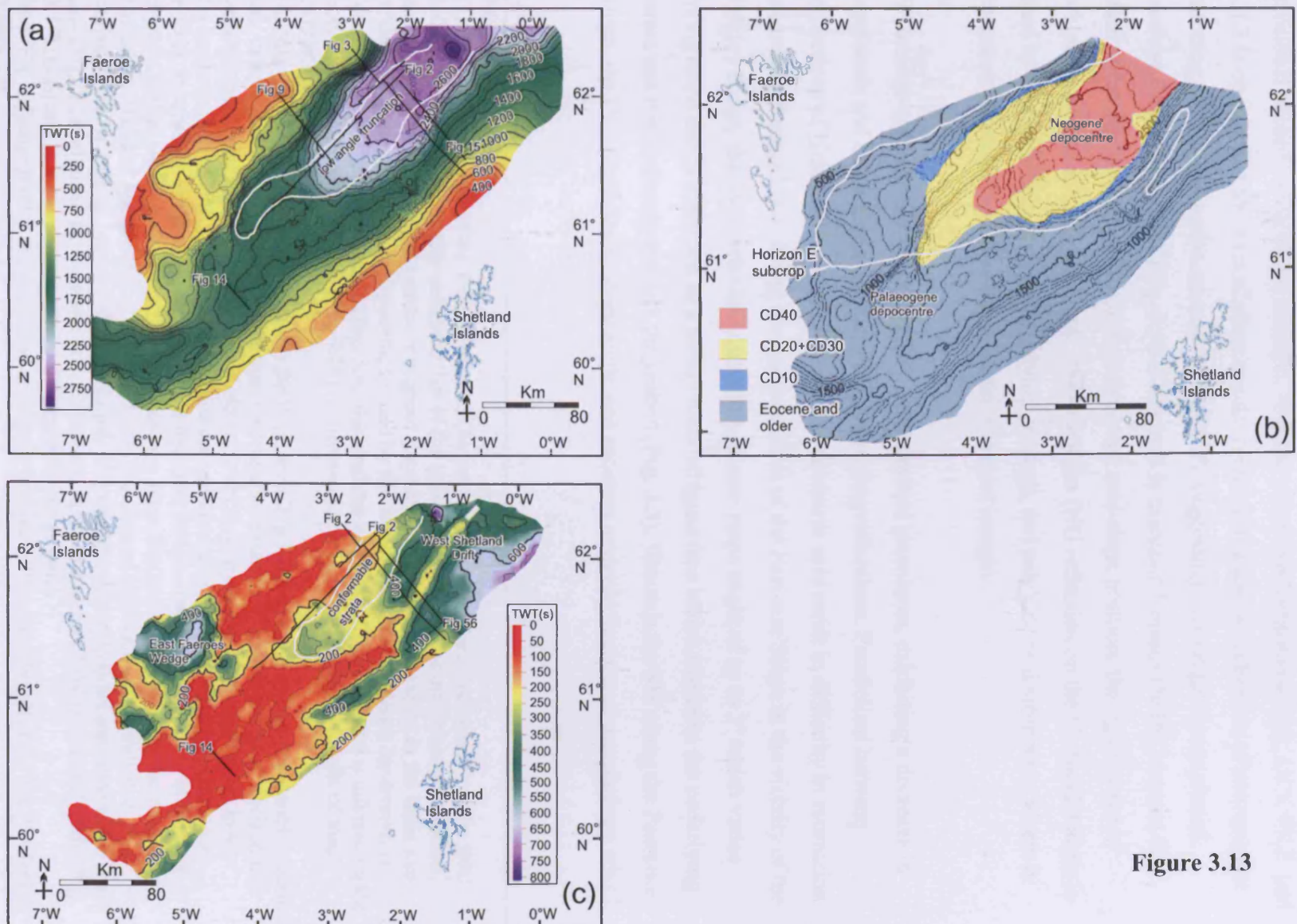


Figure 3.13

erosional unconformity in this location. Angular subcrop of reflections OL1, UC1, OL2, and OL3 is observed at the base of slope and the reflections show no indication of stratigraphic thinning prior to truncation (except CD30/OL3), suggesting they originally continued upslope for some distance (Fig. 3.6). Horizon E is truncated beneath the INU toward the base of the Shetland slope, but is preserved in a mid-slope position, the significance of which is detailed in section 3.9.1.1. The dip of the INU reflection on the Shetland margin is seen to vary with variations in underlying geology, and exhibits local steepening where it intersects Eocene slope clinoforms on the Shetland margin.

Within the northern basin axis the INU becomes less prominent, exhibiting a decrease in amplitude and lower angle truncation of underlying reflections. Parallelism between reflections of Unit CD40 and the INU within the basin axis result in difficulty in estimation of erosional magnitude. Along the northern limit of the Faeroese Slope in the vicinity of the Fugloy Ridge, the INU reflection exhibits a steeper slope angle of up to 3° which varies along slope and is identified as a mildly undulating surface which truncates the underlying strata and lies shallowly beneath the seabed (Fig. 3.3). Towards the SW along the Faeroese slope, the INU decreases in slope angle and acquires a rugose, incisional morphology which

---

### Figure 3.13

**(a)** Time structure map of the INU reflection. The map reveals the palaeo- bathymetry of the INU reflection, which is extremely similar to that of the present day basin. The unconformity exhibits angular subcrop of underlying strata throughout the majority of its extent, except in the basin axis where low angle truncation is prevalent, defined by the white line. Clear evidence for erosion is identified on the Faeroese margin (Fig. 3.9), the southern basin axis (Fig. 3.14) and is inferred on the northern West Shetland Margin (Fig. 3.15). Contours in metres below sea level. Limits of map defined by limits of data.

**(b)** Map of subcrop distribution beneath the INU, revealing Palaeogene-Neogene depocentres. Basin-axis centric preservation of pre-INU Neogene strata also revealed. The distribution of Horizon E is wider in extent than the preserved pre-INU Neogene strata. Contours in metres below sea level.

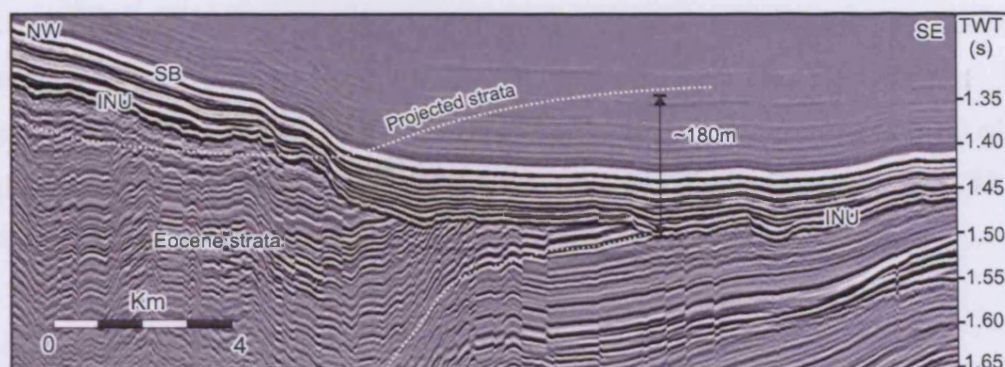
**(c)** Isochron map of Unit CD50, revealing bimodal sediment accumulation during the Pliocene-Recent. Prograding wedge deposition from the Faeroese margin resulted in formation of the East Faeroes Wedge, while bottom currents deposited the West Shetland Drift System in the basin axis and on the Shetland Margin (Fig. 3.2, 3.3 & 3.15). The internal reflection configuration is characterised by baselap onto the Shetland slope, with conformable reflections restricted to the basin axis (Fig. 3.2) delimited by the white line. Elsewhere, in the basin unit CD50 is extremely thin (Fig. 3.15). Contours in metres, limits of map defined by limits of data.

The 'Fig' references refer to the location of seismic profiles within this Chapter, e.g. 'Fig 9' refers to Figure 3.9.

contrasts with the morphology on the Shetland Slope. The incisional character of the INU surface is coincident with the presence tectonic folds, the most significant of which is the East Faeroes Ridge, across which unit CD20, CD30 and CD40 are erosionally truncated, but preserved in the associated synform upslope (Fig. 3.9). Within the synform the INU also exhibits a number of deep, multiphase incisional features >120m deep, which appear to be aligned parallel to the slope (Fig. 3.9). The upslope limit of units CD10, CD20 and CD30 is marked by angular erosional truncation of a succession of reflections c.350m true vertical thickness beneath the INU (Fig. 3.9). Based on the lack of margin-ward convergence of reflections within the truncated units, stratal projection is used to estimate erosion of >250m of strata during formation of the INU. Toward the SW along the basin axis the INU decreases in depth, coincident with the boundary between the Neogene and Palaeogene depocentres (Fig. 3.2). Clear evidence for erosion during the formation of the INU is also present at the southern end of the basin, where high resolution 2D seismic data reveal c.180m of erosion of Palaeogene strata beneath the INU reflection (Fig. 3.14).

In summary, extensive seismic analysis reveals that the INU consists of an erosional unconformity extensive throughout the basin, with erosion particularly evident on the basin margins and throughout the Palaeogene depocentre to the SW. Subtle truncation of strata in the northern basin axis suggests that erosion was least severe at this location. The extent of the INU reflection combined with clear evidence for significant erosion in deep water leads to interpretation that alongslope current erosion was responsible for its formation. Sub-aerial erosion as a result of sea level fall is limited to the shelf and possibly the uppermost portion of the slope, and thus cannot be responsible for erosion of the basin floor in water depths interpreted to have exceeded 1km (Davies and Cartwright, 2002; Robinson, 2004). Other means of generating erosion in deep water such as mass movement, turbidity currents or benthic storms (Shanmugam, 1988) are either too localised or too weak to erode 10's to 100's of metres of sediment on a basinal scale. The fact that a range of sediment types were eroded rules out chemical/diagenetic dissolution as a means of generating the unconformity. Processes responsible for formation of the INU are discussed further in section 3.9.

Unit CD50 is the youngest depositional unit and consists of 2 main depocentres: 1) the West Shetland Drift contourite drift system which lines the basin floor and plasters the Shetland



**Figure 3.14**

High resolution 2D seismic profile orthogonal to the Shetland margin at the southern end of the basin (line location Fig. 3.1), revealing erosional truncation of Palaeogene strata beneath the INU. Stratal projection allows estimation of c.180m of erosion in the area during formation of the INU. The high resolution of the data also reveals the pervasive polygonal faulting that characterises the Cenozoic succession within the basin.



Slope toward the northern end of the Faeroe Shetland Basin (see Knutz and Cartwright 2003, 2004 for detailed interpretation), and 2) the East Faeroes Wedge which consists of a large ( $>3200\text{km}^2$ ) sedimentary prograding wedge which originated from the southern Faeroe Islands and built out across a plateau on the INU surface (Fig. 3.13c). Excluding the East Faeroes Wedge, deposition of Unit CD50 is interpreted as predominantly the result of alongslope current processes (Knutz and Cartwright, 2003, Knutz and Cartwright, 2004), the majority of which occurred within the basin axis and on the Shetland margin.

### 3.8.6. Horizon E

Horizon E is characterised by a high amplitude positive reflection which cross cuts stratigraphy (Figs. 3.3 & 3.8). The reflection is generated by the diagenesis of Opal A to Opal C/T (Davies and Cartwright, 2002; Davies, 2005), which results in an increase in density and thus generation of a positive acoustic impedance contrast resulting in a positive seismic reflection.

The diagenesis of Opal A into Opal CT requires the presence of biogenic Opal A (Hesse, 1990). Therefore, the presence or absence of Horizon E within a unit can be used to make inferences regarding the biogenic silica content of the sediment. In the Neogene depocentre, Horizon E occurs within Units CD10, CD20, CD30 and CD40, and within pre-CD10 strata (Figs. 3.3 & 3.8). The abutment of Horizon E against a late Eocene unconformity is thought to represent the boundary between sediments which contain sufficient amounts of Opal A to undergo diagenesis and those which do not (Davies and Cartwright, 2002), and suggests that there is an increase in the amount of biogenic silica within the sediments between the late Eocene and the Oligocene-Neogene.

Hummocky deformation of the Neogene sediment pile (Fig. 3.12) was generated by differential compaction during the diagenesis of Opal A-CT (Davies, 2005). It is generally observed that in areas where Horizon E is hosted within younger strata (Units CD20 and CD3) hummock generation is more pronounced. This could reasonably be attributed to a higher percentage of Opal A which undergoes diagenesis and thus compaction, resulting in a greater degree of deformation. Sediment samples from well 214/4-1 reveal a four fold increase in the absolute abundance of diatom valves per gram of sediment (dry weight)



between the Oligocene and Middle Miocene (Davies and Cartwright, 2002), which is used as evidence to support the increased biogenic silica content proposed from the seismic data. Therefore, the sediments overlying the late Eocene Unconformity are classified as 'rich' in biogenic silica, which increases in content through the Oligocene and Miocene.

### 3.8.7. Key observations

- Upper Paleogene strata are concentrated at the southern end of the basin and on the Shetland Margin, and Neogene strata (excluding the Plio-Pleistocene section) are concentrated at the northern end and on the Faeroese Margin.
- The Oligocene-Recent stratigraphy can be divided into 5 units based on the identification of distinct seismic boundaries. The boundaries consist of 3 hiatal surfaces defined by supercrop, and two unconformities which are defined by subcrop and supercrop relationships.
- Each unit is interpreted to have been deposited by or significantly influenced by bottom currents.
- Bottom current sedimentation was active during the early Oligocene and continued throughout the Neogene to the present. Bottom current sedimentation was initially focussed on the Faeroese margin during the Oligocene and early-middle Miocene (CD10 and CD20) and subsequently spread to the entire basin (CD30, CD40 and CD50).
- A variety of contourite drift morphologies are observed within the succession. Lower wavelength, upslope prograding mounded drifts are largely restricted to the Faeroese slope, suggesting a link between drift morphology and slope angle. Sheeted and broader mounded drifts accumulated predominantly in the basin axis, and on the lower angle upper Faeroese Slope.
- Erosion associated with the formation of the UC1 reflection was restricted to the Faeroese margin and is interpreted as alongslope current in origin. Erosion is particularly evident in association with East Faeroes Ridge on the Faeroese margin.
- The INU consists of an erosional unconformity of late Miocene-early Pliocene age formed by bottom currents that eroded several hundred metres of stratigraphy from throughout the basin.

- Horizon E formed prior to the INU erosion event, and its presence within the Units CD10, CD20, CD30 and CD40 reveals a significant biogenic silica content, which increased in concentration throughout the Oligocene and Miocene.

## 3.9. Discussion

### 3.9.1 *Deep water unconformities*

The formation of erosional unconformities in marine settings is conventionally regarded as the result of base level fall and sub-aerial erosion (i.e. Vail et al., 1977). However, in this study clear evidence for erosion of several hundreds of metres of strata in hundreds of metres of water demonstrates that significant erosion can occur in deep water settings. In order to investigate the origin of these surfaces, we firstly discuss estimation of the erosional magnitude of the unconformities within the Faeroe Shetland Basin, and secondly comment on the processes responsible for their formation.

#### 3.9.1.1. *Erosional magnitude*

Estimation of thickness of strata removed during erosion is an important element of unconformity analysis, and can be achieved via projection of truncated strata above the unconformity (e.g. Tearpock and Bischke, 2002). In order for this method to be employed, an angular discordance between the truncated strata and the truncation surface is required, provided either by inclined underlying strata or an incisional unconformity (e.g. incised valleys). Where strata are seismically concordant and parallel with an erosion surface, erosional magnitude will be difficult to resolve using seismic data alone. This is particularly relevant in deep water, bottom current dominated areas, where contourite drifts laid down by thermohaline currents are commonly divided by erosion surfaces (Faugères et al., 1999; Rebesco and Stow, 2001; Stow et al., 2002). Within a contourite drift sequence an increase in depositional current velocity may cause hiatus, winnowing and/or erosion of the seabed (McCave and Tucholke, 1986), but non-localised, planar erosion would fail to generate angular discordance at the boundary, resulting in a surface of unconformity separating essentially parallel strata, known as a disconformity (Grabau, 1905). Subsequent slowing of the currents and a resumption of sheeted drift sedimentation would result in an apparently conformable succession when imaged on seismic data.

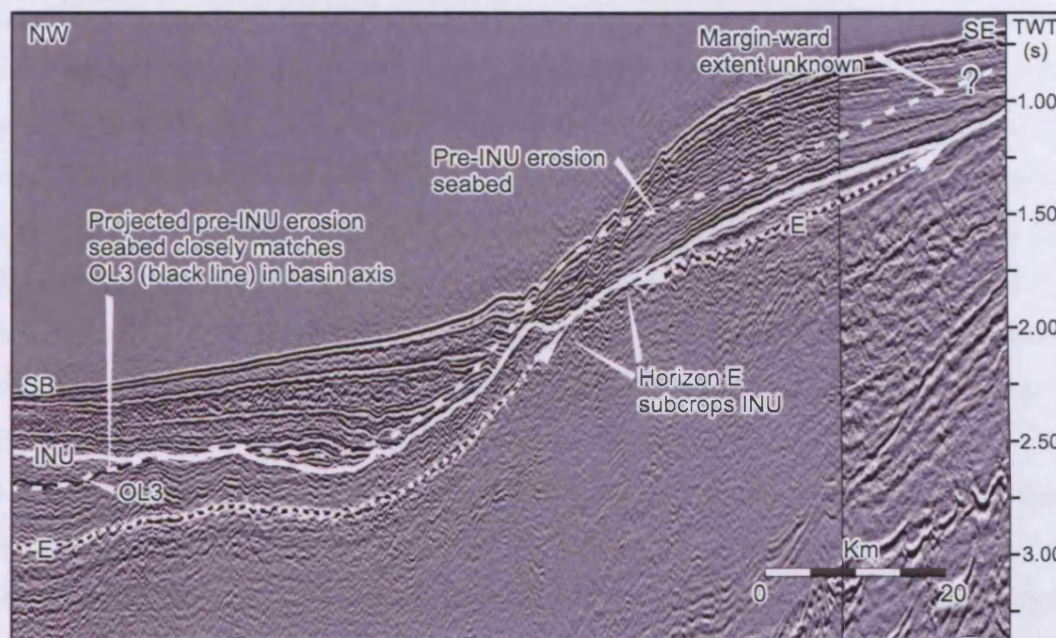
As a result of these factors, conclusive identification of the UC1 surface as an erosional unconformity is limited to the Faeroese margin, and although it is considered very likely that erosion during the formation of the unconformity was more extensive, conformity between the UC1 reflection and underlying strata throughout the rest of the basin makes this difficult to prove. Likewise, erosion of several hundred metres of stratigraphy is evidenced beneath the INU on the Faeroese margin based on projected truncated strata. However, estimation of the erosional magnitude of the INU on the Shetland margin via stratal projection is not possible due to low angle intersection between the unconformity and subcropping reflections and distortion of the sequence by polygonal faults.

The presence of Horizon E beneath the Shetland slope is thought to provide clues to the erosional magnitude of the INU where stratal projection is not possible. The transformation of Opal A-CT is affected by surface area, sediment and pore water chemistry, and temperature, which constitutes the most significant control on the transformation in basins where sediments are compositionally homogeneous (Hesse, 1990), as is the late Palaeogene and Neogene succession of the Faeroe Shetland Basin (214/4-1). The transformation can occur at temperatures ranging from 2-55°C (Davies 2005), although transformation at temperatures below 30-35°C is thought to be rare and exceedingly slow, occurring over 10's of My (Bohrmann et al., 1994; Davies and Cartwright, 2002). Therefore, it is assumed that the transformation of Opal A to Opal CT will occur over a particular temperature range (likely over 30°C) and accordingly track the corresponding temperature isotherms which in the shallow post-rift sections can be assumed to parallel the contemporaneous sea bed (Buntebarth, 1984; Kuramoto et al., 1992). As a result, Opal A-CT transformations are often referred to as bottom-simulating reflections because they generate seismic reflections parallel to either the present day sea bed or an overlying reflection which represents a palaeo-seabed.

Within the basin axis of the Faeroe Shetland Basin, Horizon E is seen to lie parallel to and c.200m below the OL3 reflection, as noted by Davies and Cartwright (2002) who interpreted the OL3 reflection to represent the early Pliocene erosion event (INU) within the basin and therefore proposed that the diagenesis responsible for formation of Horizon E occurred between the late Miocene-early Pliocene. Based on the present day geothermal gradient of

38°C km<sup>-1</sup> within well 214/4-1, if Horizon E had formed the contemporaneous seabed, then the transformation would have formed at temperatures between 8-15°C (Davies and Cartwright, 2002), and in order to account for this apparent low temperature of transformation an elevated geothermal gradient and possible low temperature reaction were invoked (Davies and Cartwright, 2002). However, on the basin margins Horizon E is seen to converge with and subcrop the early Pliocene erosion surface (INU). Therefore, in order for the early Pliocene erosion event to have represented the contemporaneous seabed, the transformation would have had to occur very close to or at the seabed, requiring unfeasibly warm seabed temperatures or transformation at ambient temperature which at present is -0.5-0.5°C, and is also deemed unlikely. However, this problem is solved by the interpretation during this study of the OL3 reflection as an hiatal surface that predates the early Pliocene erosion event, and subcrops the INU at the base of the Shetland margin (Fig. 3.6).

It is therefore proposed that the close proximity of Horizon E and the early Pliocene erosion event on the Shetland margin can be accounted for by inferring significant erosion of a pre-INU erosion Shetland slope seabed bathymetry which overlay Horizon E by at least 200m on the Shetland slope, and is preserved in the basin axis as the OL3 reflection (Fig. 3.15). Subtraction of c.200m (250ms) from Horizon E on a seismic profile across the Shetland Slope in order to produce an estimate of the pre-INU erosion bathymetry produces an extremely close match between Horizon E and OL3 in the basin axis, and margin-ward of the point of subcrop of OL3 is proposed to provide an approximation of the pre-INU slope profile, which was eroded during formation of the INU (Fig. 3.15). The estimation of erosion of 200m from the Shetland slope during formation of the INU based on the relationship of Horizon E to the OL3 reflection fits well within estimates made based on stratal truncation elsewhere in the basin. This method has allowed indirect prediction of erosional magnitude of the INU event on the Shetland margin which was not possible using direct observation of reflection configurations, and resolves the issue of why Horizon E appeared to lie so closely beneath the proposed contemporaneous seabed.



**Figure 3.15**

2D seismic profile across the northern end of the Shetland Slope (line location Fig 3.1). From the basin axis Horizon E is truncated beneath the INU at the base of the Shetland slope, and is preserved in a mid-slope position. In the basin axis Horizon E clearly tracks the OL3 reflection (black line). The OL3 reflection is also truncated beneath the INU at the base of the Shetland Slope, and is thought to originally have continued upslope, forming the pre-INU erosion palaeo-seabed beneath which Horizon E formed. A pre-INU erosion seabed was reconstructed by subtraction of 250ms from Horizon E. The reflection reveals a close match to the OL3 reflection in the basin axis, and upslope of the point of truncation of OL3 is interpreted to give a good approximation of the pre-INU erosion Shetland slope seabed bathymetry. Consequently, at least 200m of erosion on the Shetland Margin is proposed to have occurred during formation of the INU.

### *3.9.1.2. Mechanism of formation*

The formation of erosion surfaces in deep water by alongslope currents has received little attention in comparison to erosion processes associated with sea level fluctuations, which have been extensively studied, particularly since the introduction of the seismic stratigraphic methods by Vail et al. (1977). Alongslope currents are a common cause of erosion in deep water (Stow and Holbrook, 1984; Stow et al., 2002), although gravity driven processes such as mass flow and turbidity currents (Parker et al., 1986; Kneller, 1995) and chemical erosion e.g. carbonate dissolution (Keller et al., 1987) can also cause erosion in deep water settings. Unlike sea-level related unconformity development, the formation of deep water erosion surfaces by alongslope currents does not have an obvious link to sea level fluctuation. However, it is noted here that eustatic fluctuations in sea level caused by the global fluctuations of the volume of ice on land (Vail et al., 1977), are known to influence the global thermohaline circulation system (Alley and Clark, 1999; Clark et al., 2002; Rahmstorf, 2002) with exchange of water masses across the Greenland-Scotland Ridge being most active during interglacials and periods of climatic transition (Rahmstorf, 2002). Therefore, within the Faeroe Shetland Basin, erosion of the shelf and upper slope in conjunction with eustatic sea level fall would likely correspond to a decrease in thermohaline current activity and the potential for formation of deep water unconformities by bottom currents. Conversely interglacial periods corresponding to quiescent highstand deposition on the upper slope and shelf are synonymous with maximum thermohaline current activity, and thus an increased likelihood of deep water erosion. Therefore, there may be an inverse relationship between generation of unconformities on the shelf and upper slope during phases of eustatic sea level fall, and generation of deep water unconformities during interglacial sea level high stands or transgressions.

Erosion associated with the UC1 surface was restricted to a slope parallel zone along the base of the Faeroese slope. At present, a high velocity core of deep water flows from the Norwegian-Greenland Sea through the Faeroe Shetland Basin at speeds of up to and exceeding 1.0m/s, and is concentrated along the Faeroese slope by the westerly deflection caused by the Coriolis Force (Hansen and Østerhus, 2000; Kuijpers et al., 2002; Masson et al., 2005). These modern day southerly flowing deep waters impinge on the Faeroese slope over a similar area to the erosion associated with the UC1 surface, which is thought to have



been caused by a present day style southerly flow of deep waters along the Faeroese margin during the early-mid Miocene. The deep water setting, slope parallel alignment and occurrence of overlying and underlying contourite drifts support the bottom current origin of the UC1 erosion. The shift from deposition of Unit CD10 by alongslope currents on the Faeroese margin to erosion is attributed to an increase in current velocity, which is a common feature of contourite successions (McCave and Tucholke, 1986; Faugères et al., 1999; Stow et al., 2002). Cessation of erosion was coincident with renewed deposition of Units CD20 and CD30, and implies a long lived alongslope current regime on the Faeroese Margin. Erosion of deep marine sediments can be caused by frequent peak current speeds of over 20cm/s (McCave and Tucholke, 1986). Present day current speeds suggest that it is entirely reasonable to invoke frequent current speeds >20cm/s along the Faeroese slope. Slope angle is also known to influence current velocity, with steeper sea beds able to locally support a steeper isopycnal gradient, and thus faster currents (McCave, 1995a & 1995b). This could account for the evidence for increased erosion on the limbs of the East Faeroes Ridge on the Faeroese margin, which exhibits locally steepened seabed gradients. In addition, shallow burial of the contourite drifts (less than 500m) would likely have resulted in preservation of porosities of up to 40% (Velde, 1996) and this relative lack of compaction may facilitate erosion by reducing shear stress required to lift and transport sediment particles.

The regional extent, magnitude and deep water nature of the erosion associated with the INU are interpreted as clear evidence that the unconformity was formed by alongslope current erosion. In common with UC1, an increase in current velocity (with frequent peak current velocities >20cm/s) is proposed to have caused erosion of underlying contourite drifts, followed by the resumption of contourite drift deposition (unit CD50). In contrast to the UC1 surface, the INU surface truncates strata which range from Miocene to Palaeocene in age, although stratal geometries of the Neogene and Palaeogene successions are used as evidence that maximum burial depth of the Neogene and Palaeogene strata would not have exceeded 500m and thus similar preservation of porosity is envisaged for the shallow strata across the basin. In addition, the increased biosiliceous microfossil component within the Neogene deep water sediments would also result in enhanced porosity, due to a large surface area to volume ratio of the microfossils when compared to fine grained siliciclastic or

carbonate sediment particles (Volpi et al., 2003), and may also have facilitated erosion during formation of both the INU and the UC1 reflection. The negative acoustic impedance contrast across the INU across much of the basin (exhibited in Fig. 3.14) is taken as evidence for high biosiliceous content (and thus decreased density) within the Neogene and Upper Palaeogene sediments in comparison to the overlying clastic rich Pliocene succession (resulting in a lower reflection coefficient). This inference is supported by the presence of Horizon E and the switch to a positive acoustic impedance contrast across the INU in areas where it separates Pliocene and Eocene or older strata, which are clastic rich. However, the significant erosion of Eocene and older strata during formation of the INU shows that the biosiliceous component may have enhanced or facilitated erosion in some areas of the basin, but was not a prerequisite. The change in slope angle of the INU on intersection with Eocene strata (*section 3.8.5*) is attributed to differing rheological characteristics between the upper Palaeogene -Neogene strata, and the lower Palaeogene strata, resulting in differing susceptibility to erosion.

The INU is also unique within the stratigraphy for exhibiting erosion so extensively throughout the basin. Evidence for erosion beneath the INU occurs at shallower depths on the Faeroese margin than on the Shetland Margin. Large scale erosion of the Faeroese slope is found within c.550mbpds (metres below present day sea level), whereas significant erosion on the Shetland Margin is only below c.900mbpds. At present, SW flowing deep waters have an asymmetric distribution within the basin, extending to within c.600m of sea level on the Faeroese margin compared with c.900m on the Shetland Margin (Turrell et al., 1999; Hansen and Østerhus, 2000; Kuijpers et al., 2002). The distribution of erosion of the INU could therefore be accounted for by erosion caused by a current similar in distribution to that of the SW current of today. Furthermore, erosion of the crest of the East Faeroes Ridge on the Faeroese slope by the INU suggests that unlike the UC1 surface, where erosion was limited to the base of the Faeroese slope, the currents responsible for formation of the INU were widely distributed across the Faeroese slope, which would fit with a present day style water mass structure.

In summary, the formation of the Neogene deep water erosion surfaces within the Faeroe Shetland Basin is attributed to erosion by alongslope currents as a result of temporal

increases in current velocity, the potential causes of which are discussed in *section 3.9.2*. Significantly, the currents responsible for formation of UC1 and the INU are interpreted to have been flowing to the SW, based on comparison of the locus of erosion with the modern day water mass structure and seabed erosion, combined with reflection geometries within underlying and overlying units. Erosion may have been facilitated by porosity preservation as a result of a lack of compaction due to shallow burial, along with the high biogenic silica content of the Neogene strata, and locally enhanced by increased slope gradients.

### 3.9.2. Sedimentary and palaeoceanographic development

Seismic-stratigraphic interpretation of the upper Palaeogene and Neogene stratigraphy of the Faeroe Shetland Basin has shown that throughout that time, sedimentation within the basin was dominated by alongslope currents. The identification of contourite drifts and unconformities which vary in geometry and locus through time allow us to make an interpretation of the palaeoceanographic development of the basin.

Published estimates of the timing of onset of alongslope current flow through the Faeroe Shetland Basin range from early Oligocene (Miller and Tucholke, 1983; Davies et al., 2001) to mid Miocene (Eldholm, 1990; Wold, 1994; Wright and Miller, 1996; Stoker, 2003), while unpublished work dates the onset during the middle Eocene (Hohbein and Cartwright (a), in prep.). The interpreted formation of the OL1 surface and Unit CD10 by bottom currents from the early Oligocene provides evidence for the flow of bottom currents through the basin during the early Oligocene onwards. Elements which allow present day circulation between the Norwegian-Greenland Sea and the North Atlantic, such as an established latitudinal thermal gradient to promote thermal densification and sinking of surface waters in the Norwegian Greenland Sea (Broecker and Denton, 1990; Thiede and Myhre, 1996), presence of the Faeroe Shetland Basin as a deep water basin open to the North Atlantic (Mitchell et al., 1993; Kjørboe, 1999; Smallwood and Gill, 2002; Robinson, 2004), and limitation of the circum-equatorial thermohaline circulation which characterised the Mesozoic and early Cenozoic by closure of the Tethys Ocean (Ziegler, 1990; Pickering, 2000) were in place by the early Oligocene, thus physically enabling a present day type circulation to have existed at that time. In addition, the Denmark Strait, through which deep

waters are exported at present, did not exist as a seaway until 15-18Ma (Thiede and Eldholm, 1983; Thiede and Myhre, 1996), meaning that the Faeroe Shetland Basin would have been the only deep water gateway across the Greenland Scotland Ridge. High rates of biogenic silica production characterised the Norwegian Greenland Sea during the Palaeogene and much of the Neogene (Thiede and Myhre, 1996; Laberg et al., 2005), and is a likely source for the biogenic silica documented within the upper Palaeogene and Neogene sediments of the Faeroe Shetland Basin by Davies et al., (2001) and Davies and Cartwright (2002), providing further evidence of southerly flowing deep waters through the basin throughout this time. The lack of biogenic silica in Eocene strata within the basin, despite high production rates in the Norwegian Greenland Sea could be accounted for either by weaker southerly flowing deep waters during this time or the dominantly downslope nature of Eocene sedimentation.

Circulation of thermohaline currents through the Faeroe Shetland Basin from the Miocene onward is widely cited, and has been proposed on the basis of increased accumulation rates on sediment drifts in the North Atlantic (Wold, 1994), foraminiferal isotope records (Wright et al., 1992; Wright and Miller, 1996; Ramsay et al., 1999) and seismic stratigraphy (Stoker 2003; Laberg et al., 2005; Stoker et al., 2005). The contourite drifts of Unit CD10 are separated from overlying contourite drifts by the UC1 erosion surface, which is thought to be early to mid Miocene in age, but may date from the late Oligocene. Erosion surfaces and hiatuses of c.middle Miocene age are reported throughout the Western North Atlantic (Shor and Poore, 1979; Miller and Tucholke, 1983; Mountain and Tucholke, 1985; Wold, 1994), and form the basis of  $\delta^{13}\text{C}$  increases in the North Atlantic which are used as evidence for a linkage between the North Atlantic and a deep water source (the Norwegian Greenland Sea), and interpreted as evidence of vigorous early/mid-Miocene alongslope current activity (Miller and Fairbanks, 1985; Miller et al., 1991; Wright and Miller, 1992, Wright and Miller, 1996). The erosion of UC1 within the Faeroe Shetland Basin is therefore likely to correlate with the middle Miocene erosion and hiatal surfaces elsewhere, suggesting major export of deep waters from the Norwegian Greenland Sea into the North Atlantic via the Faeroe Shetland Basin occurred during this time. This supports the interpretation drawn from this study that the erosion of the UC1 surface occurred as a result of a wider oceanographic change in circulation, which is likely to have been locally enhanced by slope topography

around the East Faeroes Ridge. Indeed, tectonic compression in the Faeroe Shetland Basin is reported during the middle Miocene, which would have caused fold growth and locally enhanced erosion (Boldreel and Andersen, 1993; Davies et al., 2004).

Subsidence of the Greenland Scotland Ridge, which controls water mass exchange between the Norwegian Greenland Sea and the North Atlantic (Vogt, 1972; Nilsen, 1983; Wright and Miller, 1996), has been invoked as the cause of middle Miocene erosion within the Faeroe Shetland Basin due to increased flux in the alongslope system (Wright and Miller, 1996). However, the increase in flux through the basin may also have been influenced by step-like changes in global climate and ice volume which occurred around the middle Miocene (Miller et al., 1991; Lear et al., 2003). Evidence for development of northern hemisphere ice sheets during the late Miocene (Fronval and Jansen, 1996; Thiede et al., 1998; ACEX, 2005) signify cold high latitude temperatures which would promote the formation of deep waters in the Norwegian Greenland Sea, and thus increase deep water flux through the via the Faeroe Shetland Basin.

The shift in depositional locus from contourite deposition restricted primarily to the Faeroese margin during the Oligocene-mid Miocene (Units CD10 and CD20) to deposition of the infilling and detached, mounded Unit CD30 and CD40 drift bodies within the basin axis throughout the Miocene is interpreted to represent a hydrodynamic change throughout this time. Depositional morphology of the unit CD40 mounded drift suggests the alongslope currents at the base of the Shetland Margin during the late Miocene, which implies an increased flux of deep water through the basin, and may have been a precursor to basin-wide erosion associated with formation of the INU.

The INU represents the most significant erosion surface within the basin, and is attributed to erosion of the seabed by an increase in alongslope current velocity during the late Miocene-early Pliocene. An increase in current velocity would require an increased volume of SW flowing deep waters flowing through the basin. Late Neogene uplift of the European continental margins (Doré et al., 1999; Japsen and Chalmers, 2000; Stoker et al., 2005) and differential subsidence of basin axes (Cloetingh et al., 1990) could account for increased flux of deep waters through the basin. Strong evidence for a tilting of the basin margins prior to

erosion of the INU is provided by the angular subcrop a thick succession of inclined strata on the basin margins beneath the INU reflection. However, the inclined strata belong to unit CD10, and are thus dated as Oligocene in age and combined with evidence for the presence of a palaeo-slope exhibited by units CD20 and CD30 in the form of upslope prograding drifts, suggests that tilting of the margin occurred during the early Neogene. Stoker (1999) interprets a basinward tilted INU surface on the Shetland margin as evidence for differential subsidence of the Faeroe Shetland Basin which may have promoted erosion and formation of the INU. However, this interpretation relies on the fact that the INU was originally horizontal, for which there is no evidence. Furthermore, tilting during active erosion would result in modification of the unconformity surface, and therefore a tilted planar INU on the basin margins suggests that the differential subsidence occurred post-erosion, and thus cannot have promoted it. As a result of these observations, it is proposed that basin deformation may have enhanced INU erosion, but does not account entirely for it.

Global oceanographic changes during the late Miocene/early Pliocene may have contributed to the formation of the INU. The closure of the Panama Isthmus resulted in extensive changes in ocean circulation and northern hemisphere climate and an increase in volume and velocity of the Gulf Stream (Kaneps, 1979; Schnitker, 1980; Haug and Tiedemann, 1998; Lear et al., 2003). Unusually high Northern Component Water (past equivalent of Norwegian Sea Overflow Water which flows from the Norwegian Greenland Sea into the North Atlantic, Broecker and Peng, 1982) production are also reported to have existed during the Pliocene, prior to the development of glacial/interglacial cycles (Shor and Poore, 1979; Raymo et al., 1992; Wright and Miller, 1996). It therefore is reasonable that an increase in northerly flowing surface waters into the Norwegian Greenland Sea was caused by or may have caused an increased export of deep waters due to cooling and sinking of the warm inflow waters. increased deep water production would generate greater lateral pressure gradients and thus potentially increase the volume and velocity of water mass exchange between the Norwegian Greenland Sea and the North Atlantic. High latitude cooling of surface temperatures is also recorded by deep water  $\delta^{18}\text{O}$  values (Zachos et al., 2001), which provides complimentary evidence for increased cooling of surface inflow waters and thus increased generation of deep waters. Expansion of northern hemisphere ice sheets during the late Miocene and early Pliocene (Raymo et al., 1992; Thiede et al., 1998) may have been



linked to this enhanced cooling of surface waters in the Norwegian Greenland Sea, which would likely have supplied increased moisture and precipitation to fuel ice sheet growth. An increased flux of deep water exchange would also account for the largest growth phase recorded on North Atlantic sediment drifts, which occurred during the late Miocene/early Pliocene (Wold, 1994). Furthermore, late Miocene-early Pliocene erosion surfaces are observed on the Norwegian margin to the north and throughout the Rockall Trough to the south that are correlatable with the INU (Stoker et al., 2005) and which are also attributed a deep water origin. These provide further evidence for a regional erosive deep water circulation at that time.

There appear to be a number of mechanisms which could account for or combine to account for the erosion of the INU during the late Miocene/early Pliocene. Changes in global ocean circulation as a result of factors entirely extraneous to the Faeroe Shetland Basin are likely to have strongly influenced current flow through the basin by changing the nature of the inflow and outflow of the Norwegian Greenland Sea. However, tectonic activity and uplift/subsidence of the NW European margin may have altered the base level of the basin thereby influencing the nature of the water mass circulation. As a result it is thought likely that a combination of factors including the climatic deterioration of the Northern Hemisphere combined with tectonic activity during the late Neogene, were responsible for the formation of the INU surface.

In summary, the Faeroe Shetland Basin is interpreted to have been a conduit for the passageway of deep waters from the Norwegian Greenland Sea into the North Atlantic since at least the early Oligocene, and throughout the Neogene. Bottom current sedimentation and erosion was initially restricted to the Faeroese margin throughout the Oligocene, but an increase in deep water flux during the Miocene resulted in more widespread bottom current sedimentation and erosion, particularly during the late Miocene to recent. Increased current flux during the early-middle Miocene and late Miocene-early Pliocene appear to have been related to local and regional tectonic adjustments in combination with global climatic changes which resulted in development of deep water erosional unconformities within the basin. The distribution of erosion allows the proposal that since at least the early Oligocene, the water mass structure within the basin has been similar to that of today, and combined

with evidence for continued deposition, that a present day style North Atlantic global conveyor circulation has been in operation for at least the past 30Ma.

### 3.10. Conclusions

1. A present day style North Atlantic conveyor belt circulation is interpreted to have been in operation throughout the past 30Ma, with the Faeroe Shetland Basin forming a critical gateway for the passage of deep waters between the Norwegian Greenland Sea and the North Atlantic during that time.
2. The late Palaeogene and Neogene stratigraphy of the basin can be divided into 5 seismic stratigraphic units which range between early Oligocene-Recent. A number of previous stratigraphic nomenclatures for the basin have been correlated with one another and with this study, providing a calibrated reference for further division of the basin stratigraphy.
3. Each unit is interpreted to have been deposited by or significantly influenced by bottom currents. Therefore, contourite deposition within the basin commenced during the early Oligocene and continued throughout the Miocene and Pliocene.
4. Based on the location of contourite drift deposition and erosion, the water mass structure within the Faeroe Shetland Basin throughout the late Palaeogene and Neogene is thought to have been similar to that of the present day.
5. Bottom current sedimentation and erosion was restricted to the Faeroese margin during the early Oligocene to middle Miocene (Units CD10-30). During the late Miocene, detached drift deposition (CD40) in the basin axis suggests a change in water mass structure with a greater distribution of deep waters, and Pliocene sedimentation suggests alongslope currents influenced the majority of the basin.
6. The formation of deep water erosional unconformities within the basin was as a result of increased alongslope current velocity, and was enhanced around areas of increased slope angle and was likely facilitated by moderate-high porosity preservation as a result of shallow burial and a high biogenic silica component.
7. The Intra-Neogene Unconformity is unique within the basin, and formed between the late Miocene and the early Pliocene during which time several hundred metres of strata were removed from a wide area of the basin by SW flowing alongslope

currents. The INU is locally identified as a composite unconformity on the Faeroese margin.

8. The presence of the Opal A-CT transition on the Shetland slope can be used to infer erosional magnitude of an unconformity where traditional stratal projection methods are not possible.

## Chapter Four: 3D Seismic analysis of the late Neogene West Shetland Drift

### 4.1. Abstract

Detailed seismic stratigraphic analysis of the West Shetland Drift, located on the Shetland margin of the Faeroe-Shetland Channel, has been undertaken using commercial 3D seismic data. Emphasis was placed on the interpretation of a significant plastered contourite drift body, with the aim of reconstructing the palaeoceanographic regime of the West Shetland slope during Pliocene-Pleistocene time. Although limited in areal extent, the West Shetland Drift provides a key record of the depositional environment and bottom current activity on the West Shetland slope during the late Neogene. The plastered drift body has been divided into 3 seismic-stratigraphic units and depositional processes responsible for each unit are interpreted. The slope section of the West Shetland Drift evolved from a mixed downslope-alongslope system into a system dominated by alongslope currents and contourite drift deposition during the early Pliocene to mid Pleistocene, during which SW flowing alongslope currents impinged upon the West Shetland slope from the basin floor to a mid-upper slope position. The final stage of deposition consisted of slope wedge progradation associated with mid to late Pleistocene glacial conditions. The late Neogene contourite deposition on the West Shetland Slope was punctuated by periods of glacial activity, during which alongslope current activity was apparently disrupted. Therefore, temporal variations in the depositional environment are attributed, in part, to changes in bottom current activity in association with glacial-interglacial fluctuations. Detailed mapping of key, smaller scale features, including a spectacular bottom current sediment wave field and iceberg plough marks which were identified for the first time during this study, was instrumental in constraining the palaeocurrent regime, and would not have been possible without the high spatial resolution of the 3D seismic data. This study therefore highlights the efficacy of 3D seismic data as a tool for large scale spatial and temporal analysis of contourite drifts and therefore palaeoceanographic research.

---

<sup>1</sup> Submitted to Marine Geology as:

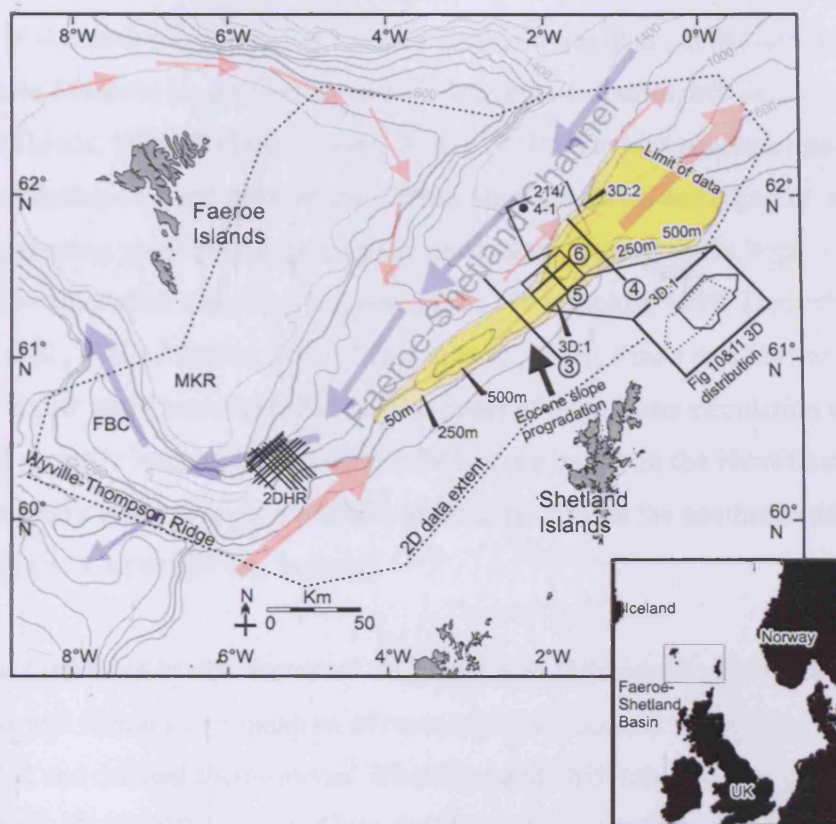
*3D seismic analysis of the West Shetland Drift system: implications for late Neogene palaeoceanography of the NE Atlantic.* Hohbein, M.W. and Cartwright, J.A. In review.

## 4.2. Introduction

Sediments that are deposited by or significantly affected by alongslope flowing bottom currents, known as contourites, provide a valuable source of information regarding the activity of bottom currents of a given area/region during the past, which in turn can be related to changes in global climate (Stow et al., 2002). The recognition of the significant influence of thermohaline bottom currents in the deep ocean basins (Heezen et al., 1966) in combination with an explosion in quantity and quality of offshore seismic and well data associated with increased petroleum exploration has allowed significant advances in the interpretation of contourite drifts, particularly their seismic characteristics (Faugères et al., 1999; Rebesco and Stow, 2001). One of the most valuable characteristics of contourites is that they hold a record of past thermohaline current activity, which in turn provides information about past climatic conditions (Stow et al., 2002). Identifying records of change in thermohaline current activity and climate within these sediments is often achieved via high resolution isotopic and sedimentological analysis of core data, usually for specific events such as glacial-interglacial fluctuations or massive iceberg discharge events (e.g. Raymo et al., 1989; McCave et al., 1995). This high resolution approach allows recognition of current fluctuations to sub-millennial time scales which is clearly of immense value in studies of rapid climate change, but is often limited to the relatively recent past (<100ka, Alley and Clark, 1999; Alley et al., 1999). Core-based studies are also inherently limited by their one-dimensionality, whereas geophysical techniques aimed at defining the internal architecture of drift bodies have the advantage of being able to demarcate loci of enhanced deposition or erosion in three dimensions (e.g. Knutz and Cartwright, 2003, Knutz and Cartwright, 2004). Furthermore, the higher vertical resolution achieved at greater depths by modern seismic data enables current distribution and strength to be inferred over long periods of time (Ma, e.g. Berggren and Hollister, 1974; Davies et al., 2001; Uenzelmann-Neben, 2002; Schut and Uenzelmann-Neben, 2005). High resolution three dimensional multi-channel seismic surveys, particularly in deepwater slope environments, open still greater potential for recognition and analysis of drift bodies, and raise the potential for the 3D analysis of subtle architectural elements in order further constrain spatial and temporal variations in palaeocirculation.

One of the major challenges facing modern palaeoceanography is to reconstruct past water mass geometries and evolution, particularly in key areas of ocean current flow such as 'ocean gateways'. The present day Faeroe Shetland Basin forms a critical oceanic gateway for the exchange of water masses between the North Atlantic and the Norwegian Greenland Sea which in turn plays a crucial role in the mediation of climatic conditions in western Europe (Berggren and Schnitker, 1983; Broecker and Denton, 1990; Rahmstorf, 2002). Previous research suggests that the basin has acted as a key oceanic gateway throughout the late Neogene (Knutz and Cartwright, 2003, Stoker, 2003; Knutz and Cartwright, 2004). The Faeroe Shetland Basin is represented by a deepwater channel, the Faeroe Shetland Channel that separates the Scottish Massif from the Faeroe Platform (Fig. 4.1, Bott, 1984). The Channel forms the deepest conduit across the Greenland-Scotland Ridge, which in turn forms a barrier to exchange of cold deep water masses between the Norwegian-Greenland Sea and the North Atlantic (Nielsen, 1983; Hansen and Østerhus, 2000). The presence of the Greenland Scotland Ridge allows the development of a permanent thermohaline gradient between Nordic Seas and the North Atlantic that is balanced by a near geostrophic flow of northerly sourced deep waters through the Faeroe-Shetland Channel, which constitutes the second most volumetrically significant gateway after the Denmark Strait (1.7Sv Vs 2.9 Sv) (Miller and Tucholke, 1983; Dickson and Brown, 1994; Hansen and Østerhus, 2000). As a result of this circulation, the water mass structure within the channel consists of cold, dense deep waters formed by thermal densification of surface waters in the Norwegian Greenland Sea flowing to the SW below c.400-600m, overlain by warmer surface waters forming the NE return flow (Fig. 4.1, Turrell et al., 1999; Hansen and Østerhus, 2000; Masson, 2001). The warm surface waters consist of North Atlantic Water and Modified North Atlantic Water, while the deep water is largely composed of Norwegian Sea Overflow Water (Turrell et al., 1999; Hansen and Østerhus, 2000). The water masses are distributed asymmetrically within the basin, with southerly flowing deep waters restricted to the Faeroese slope by the Coriolis Force before they enter the North Atlantic via the Faeroe Bank Channel. Measured deep water current velocities can regularly reach 60cm/s but on occasion exceed 100 cm/s in areas where Coriolis force focuses the current at the base of the Faeroes Slope (Hansen and Østerhus, 2000; Masson et al., 2005). The timing of onset of a modern day style thermohaline circulation through the Faeroe Shetland Basin is thought to date from the middle Eocene, based on the identification of the Eocene contourite drifts at the southern end





**Figure 4.1**

Location map of the Faeroe Shetland Basin illustrating the key 3D and 2D data used in this study (3D:1) and by Knutz and Cartwright (2004) (3D:2). Also indicated are the locations of seismic profiles (figure number circled, number refers to the location of seismic profiles within this Chapter, e.g. 'Fig 3' refers to Figure 4.3.), the spatial distribution of Figures 4.10 (dotted line) and 4.11 (solid line), and the location of well 214/4-1. Yellow filled contours represent 500m, 250m and 50m thickness distribution of WSD Slope section. Coloured arrows represent present day ocean currents: red arrows = surface inflow waters; blue arrows = SW flowing deep waters. Note location of Eocene slope progradation system and influence on WSD Slope thickness distribution. Abbreviations: 2DHR = high resolution 2D data; FBC = Faeroe Bank Channel; MKR = Munkagrunnar Ridge.

of the basin (Hohbein and Cartwright (a), in prep). However, early Oligocene and mid Miocene estimates for the onset of modern style circulation have been proposed based on the identification of the early Oligocene Se Faeroes Drift (Davies et al., 2001) and the regionally erosional Middle Miocene Unconformity and subsequent contourite drift deposition (Eldholm and Thiede, 1980; Eldholm, 1990; Wold, 1994). Previous research into the delineation and dating of contourites in the Faeroe Shetland Basin and adjacent areas has been undertaken using geophysical techniques, particularly seabed sonar, high resolution seismic and 2D exploration seismic (Faugères et al., 1984; Stoker, 1999; Damuth and Olsen, 2001; Davies et al., 2001; Masson, 2001, Masson et al., 2002; Knutz and Cartwright, 2003, Stoker, 2003; Knutz and Cartwright, 2004). The onset of deep water circulation through the basin has most recently been estimated as middle Eocene based on the identification of a contourite drift body using of high resolution seismic profiles at the southern end of the basin (Hohbein and Cartwright (a), in prep).

This study was facilitated by the increased availability of 3D seismic volumes located on the Shetland slope, and forms a continuation of research by Knutz and Cartwright (2003, 2004) which identified and defined the bi-modal West Shetland Drift (abbreviated to WSD) contourite deposit. The WSD is divided into the WSD Basin section and the WSD Slope section by Knutz and Cartwright (2003, 2004), with the WSD Basin section described in detail by Knutz and Cartwright (2003, 2004) who were unable to describe the WSD Slope section due to a lack of 3D data coverage. Therefore, the primary objectives of this study are: (1) to describe and analyse in detail the internal anatomy of the slope section of the West Shetland Drift, utilising newly available 3D seismic data; (2) to relate the deposition of the WSD Slope section to that of the basinal section of the West Shetland Drift and (3) to reconstruct the paleoceanographic development of the Shetland slope during the late Neogene. A central theme of this work is to demonstrate more widely the potential of 3D seismic data as a tool for palaeoceanographic research. The high spatial resolution of 3D data has resulted in the discovery of remarkable features including a 1700km<sup>2</sup> field of sediment waves, described here for the first time, that provide invaluable constraints on water mass geometry and flow regime. A further aim of the study is to improve understanding of the interactions of downslope and alongslope processes which are documented from continental margins that host thermohaline currents (e.g. Stoker, 1999,

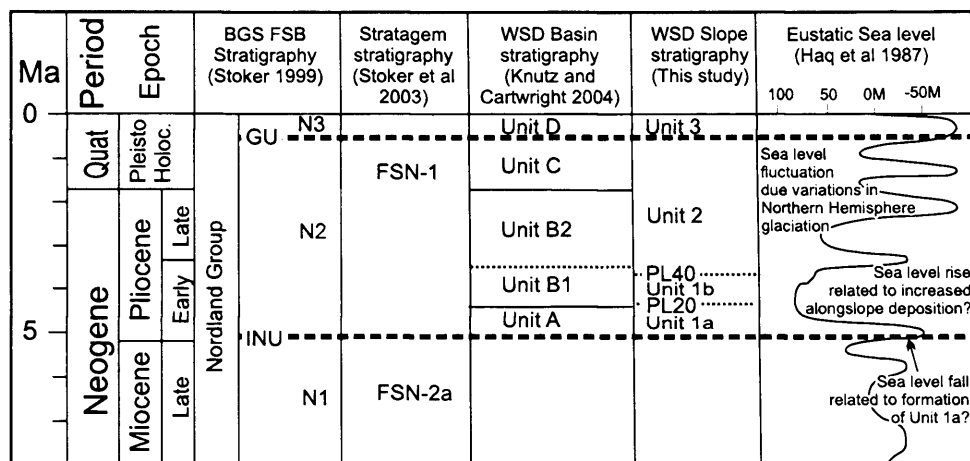
Damuth and Olsen, 1993, Damuth and Olsen, 2001). Finally, this paper also aims to investigate the relationship between the changes in palaeocirculation through the Faeroe Shetland Basin (inferred from 3D seismic-stratigraphic analysis) with fluctuations in the extent of Northern Hemisphere glaciation during the Pliocene-Pleistocene revealed by other proxies (e.g. Raymo et al., 1992; Raymo, 1994; Alley et al., 1999; Billups, 2002).

### 4.3. Regional setting

#### 4.3.1 Basin evolution and stratigraphy

The Faeroe Shetland Basin lies at the SE end of the Greenland Scotland Ridge and consists of a deep water Mesozoic rift basin (Bott, 1984; Hitchen and Ritchie, 1987; Dean et al., 1999) which is divided into a number of sub-basins by large basement faults and transfer zones (Rumph, 1993). The Faeroe-Shetland Channel, which lies in the basin axis, is up to 200km wide (at the 500m isobath) and >1700m deep at the entrance to the Norway Basin, shallowing and narrowing to c.1000m and <40km respectively toward the south (Fig. 4.1). At its southern end the Faeroe Shetland Basin is separated from the Rockall Trough by the Wyville Thompson Ridge, an inversion ramp anticline that was subject to N/S oriented compression during the Eocene, Oligocene and Miocene (Boldreel and Andersen, 1993). NW/SE compression during the mid-Miocene resulted in the formation of at least 17 NE/SW trending anticlines within the basin, and the development of a regional Mid-Miocene Unconformity within the basin (Davies et al., 2001, Davies et al., 2004).

The mid-late Cenozoic stratigraphy of the Faeroe Shetland Basin was divided into groups by Deegan and Scull (1977) who assigned the early-Miocene to Recent sediments to the Nordland Group. This division has been modified by numerous authors (Knox et al., 1988; Isaken and Tonstad 1989; Knox et al., 1992; Knox et al., 1997;) and more recently by Stoker (1999) who divided the Nordland Group into three informal units; the Lower Nordland, Middle Nordland and Upper Nordland dated respectively as Early to Late Miocene, Pliocene to Mid Pleistocene and Mid Pleistocene to Holocene (Fig. 4.2). Most recently, the Neogene stratigraphy of the basin has been divided into 2 unconformity bound mega-sequences, FSN-1 and FSN-2, dated as Miocene and Pliocene to Holocene respectively, for the purpose of correlation with adjacent basins along the NW Atlantic Margin (Fig. 4.2) (Stoker, 2003).

**Figure 4.2**

Chronostratigraphic chart illustrating various divisions of the Neogene stratigraphy of the Faeroe-Shetland Basin for the purposes of chronostratigraphic correlation between studies. The dashed line of surface PL40 of this study represents the age uncertainty within the early Pliocene. Late Neogene eustatic sea level fluctuations are highlighted (Haq et al., 1987). INU = Intra-Neogene Unconformity; GU, Glacial Unconformity; N1, Lower Nordland Unit; N2, Middle Nordland Unit; N3, Upper Nordland Unit (Stoker, 1999). Time scale from Berggren et al. (1995).

Megasequence FSN-2 is interpreted as a mixture of mounded and sheeted contourite drifts with a high biogenic content (Stoker, 2003). The Intra-Neogene Unconformity (INU) marks a significant phase of widespread erosion within the basin and the boundary between the FSN-1 and FSN-2 mega-sequences, and is interpreted to have been formed by intense bottom current erosion associated with regional differential subsidence of the Atlantic European Margin during the late Miocene-early Pliocene (Stoker, 1999; Stoker, 2003). A change in depositional style is reported across the INU, from basinal contourite accumulation to widespread shelf margin progradation accompanied by contourite deposition in the basin axis/base of slope which characterise mega-sequence FSN-1 (Stoker, 1999; Stoker, 2003).

#### *4.3.2 Shetland margin subsidence*

It is important to consider basin subsidence when interpreting the palaeoceanographic history of a particular margin. Analysis of newly available high resolution seismic data located toward the southern end of the basin (2DHR, Fig. 4.1) has resulted in the identification of a package of progradational clinoforms which lie on top of the INU reflection. The clinoform topsets are located 500mbsl at a mid-slope position and exhibit an extremely low  $0.2^\circ$  basinward dip. The identification of topsets can often be assumed to represent palaeo-sea level and paleo-horizontal datums, e.g. deltaic systems (Mitchum et al., 1977; Emery and Myers, 1999), and thus used to estimate basin subsidence. On this basis, the topsets could be interpreted to suggest that up to 500m of subsidence had affected the Shetland slope following the formation of the INU. However, topset identification does not necessarily provide a palaeo-sea level datum. Glacial outwash fans can also exhibit prograding reflection configurations with topsets and prograding clinoforms, but can be deposited in several hundred metres of water at the terminus of tidewater or grounded ice sheets (Benn and Evans, 1998; Stewart, 1991; Crossen, 1991). Significant glacial activity is held responsible for development of large prograding wedges on the Shetland margin following the formation of the INU (Stoker, 1999, Stoker, 2003). Combined with the lack of large, well developed fluvial systems on the Shetland Isles at present, it is thought likely that the prograding system deposited onto the INU is glacial in origin, and thus cannot be confidently used as paleo-sea level datums. Therefore, estimation of post-INU subsidence of the Shetland Margin is not possible with the data available. Accordingly, a value of several

hundred metres (with a maximum of 500m) of Pliocene tectonic subsidence of the Shetland margin is applied to estimates of palaeo-sea level.

#### 4.4. Data and methodology

The data set available for this study consists of commercial 3D seismic data combined with 2D multi channel seismic reflection profiles of varying vintages. The main 3D data set, 3D:1 (Fig 1) covers c.600km<sup>2</sup> and consists of a 12.5m by 12.5m grid with dominant frequencies between 30-50Hz in the Pliocene/Pleistocene section, providing a maximum vertical resolution (tuning thickness,  $\frac{1}{4}$  wavelength, Badley, 1985) of c.10-15m. In addition, more than 32000 line km of 2D seismic profiles with typical vertical resolutions comparable to the 3D data, and the high resolution 2D seismic data grid (2DHR) returning maximum vertical resolution closer to 5m, were available to the study (Fig. 4.1). Interpretation and mapping of these data were undertaken using Schlumberger Geoquest IESX software. Lithological calibration for the late Neogene section is generally poor, with well 214/4-1 providing the sole calibration point for the Neogene succession of the basin (Davies et al., 2001). An average seismic velocity of 1800m/s was used for depth conversion of the shallow section (c. upper 500ms of sediment pile), based on interval velocities derived from borehole check shot data. Key reflections within the WSD Slope section were identified and mapped, using standard seismic sequence stratigraphic criteria of reflection discontinuity (Vail et al., 1977), to reveal their geometry, distribution and internal architecture. The definition of Units 1-3 was based on a combination of internal seismic reflection configurations and terminations, areal distribution and attributes of the bounding surfaces.

#### 4.5 The West Shetland Drift Slope section

On a basinal scale, the post-INU stratigraphy, dated as late Miocene-early Pliocene to Recent (FSN-1, Fig 4.2, Stoker, 2003) consists of two separate depocentres. Firstly, a large prograding wedge extends E and NE from the Faeroes shelf and the Munkagrunnar Ridge over an area of >5000km<sup>2</sup> and reaches a thickness of >500m. This feature is interpreted to result from glacio-marine progradation with sediment derived from the Faeroes platform, and is not discussed further. The second major depocentre is found at the NE end of the



basin, and comprises a large contourite drift accumulation which is called the West Shetland Drift (Fig. 4.1, also see Fig 1 of Knutz and Cartwright, 2004).

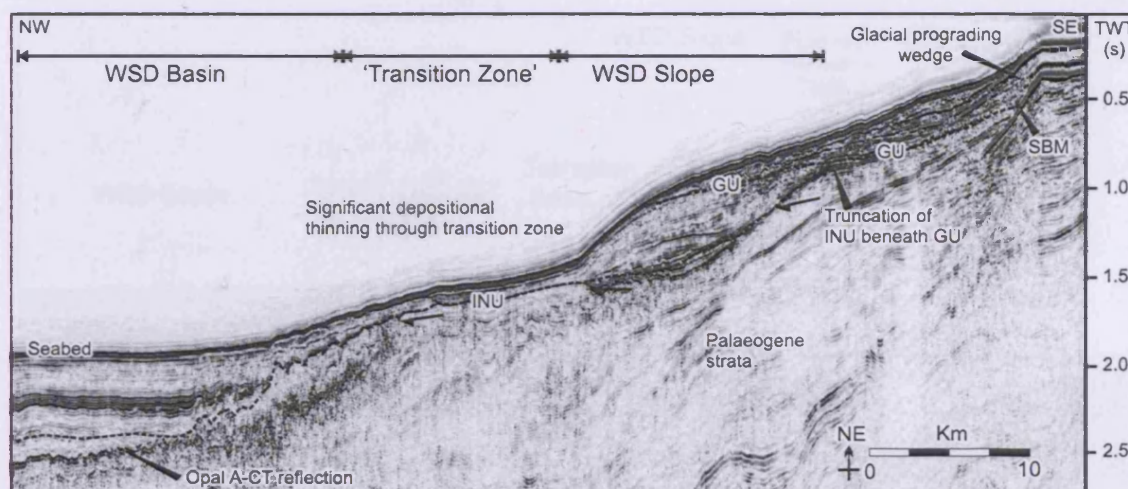
#### 4.5.1. Areal distribution

The WSD covers an area of more than 20,000km<sup>2</sup> and is divided into two main bodies, the WSD Basin and WSD Slope Sections (Fig. 4.3) (Knutz and Cartwright, 2003, Knutz and Cartwright, 2004). The WSD Slope section forms the main focus of this study. The two drift bodies are separated by a zone of condensed deposition, informally referred to here as the 'transition zone', which trends along the base of the Shetland slope (Fig. 4.3). In the study area the transition zone is between 10-15km wide and generally consists of a zone of reduced stratigraphic thickness <100m thick. To the north of the study area the transition zone consists of an upslope prograding moat complex deposited by SW flowing alongslope currents (Knutz and Cartwright, 2004).

The WSD Basin section can be traced from the limits of the data at the NE end of the basin for more than 200km to the SW along the basin axis where it attains thicknesses of up to 300m and consists of sheeted contourite drifts in the basin axis which toward the northern end of the basin grade into aggradational mounded drifts in a base of slope position. The WSD Basin stratigraphy has been divided into 5 contourite units (A-D) interbedded with at least 3 major debris flows (DF1-3) that are interpreted to be the result of failure of contourite drifts sediments deposited on the slope (Fig. 4.4) (Knutz and Cartwright, 2004).

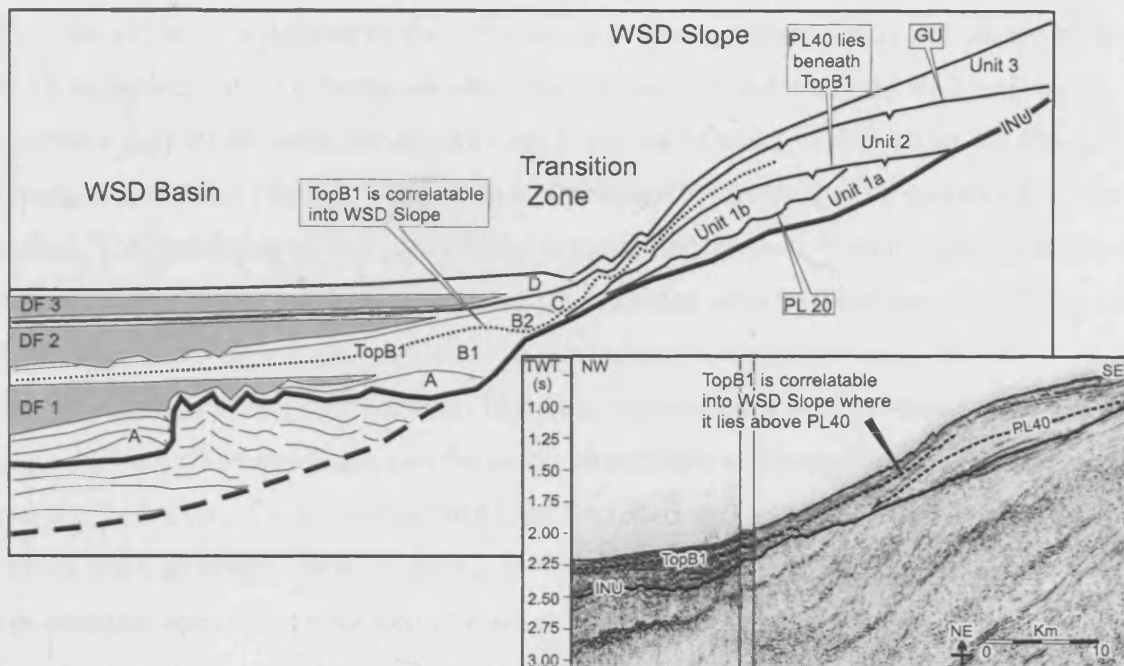
Lithologically, the WSD Basin section comprises a mixture of alternating clay, silt and sand, based on correlation with well 214/4-1. Samples of the late Neogene succession at the well location were collected by remotely operated vehicle and biostratigraphic dating of these samples show the WSD Basin section to be Early Pliocene in age, with no calibration of younger material at the well site (see discussion in Knutz and Cartwright, 2004).

Isochron contours of the WSD Slope reveal a tapering, wedge-like morphology from a thick (locally >540m) accumulation at the NE limit of the data into a thinned 'tail' which extends for more than 180km toward the SW parallel to the mid-slope (Fig. 4.1). Along its extent the WSD slope section also narrows from >40km NE of the study area to <20km wide at its SW limit, combined with a thinning from c.350m to <90m.



**Figure 4.3**

Regional 2D seismic profile orthogonal to the Shetland slope (line location Fig. 4.1). The INU surface is seen to truncate underlying strata (arrows), and exhibits an undulating morphology toward the base of slope. WSD Basin and WSD Slope sections are separated by thinned 'transition zone'. Note INU is truncated by the Glacial Unconformity (GU) toward the upper slope, which itself is overlain by Pleistocene glacial prograding wedge deposits. SBM -seabed multiple. Resolution in the shelf region is also reduced by normal move out effects (Bulat, 2005).

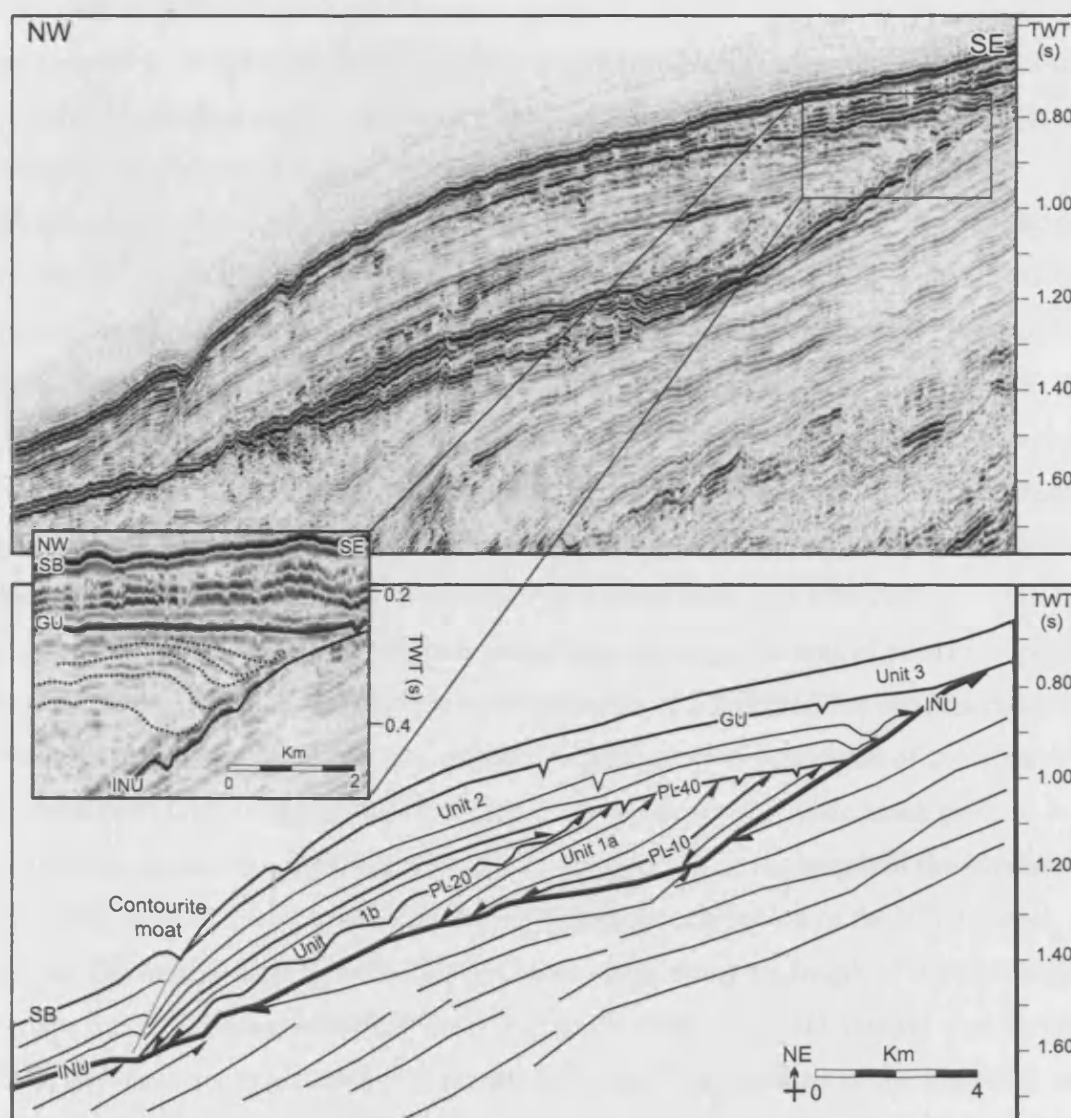


**Figure 4.4**

Geoseismic schematic and seismic profile illustrating the stratigraphic relationship between WSD Slope and WSD Basin sections (see Fig. 4.1 for profile location). When correlated through the transition zone, the Top B1 reflection (dotted line - dated as Pliocene in age, Knutz and Cartwright, 2003) is found to lie above the PL40 reflection. This is used to assign a preliminary Pliocene age to Unit 1, PL40 and at least part of Unit 2, and a Pliocene to Pleistocene age for the remainder of Unit 2, the GU and Unit 3. The Figure is modified from Knutz and Cartwright (2003) and adds detail to their initial interpretation of the WSD system.

#### 4.5.2. Internal seismic-stratigraphic division

During this study the WSD Slope section was divided into 3 Units (Figs. 4.2, 4.5 & 4.6). The base of Unit 1 is defined by the Intra Neogene Unconformity (INU) and the top by the PL40 reflection. Unit 1 is further divided into sub-units 1a and 1b by the PL20 reflection (section 4.6.2). PL40 marks the base of Unit 2, the top of which is defined by the Glacial Unconformity (GU) (Stoker, 1995). Unit 3 is bounded below by the GU and above by the seabed. The correlation of this stratigraphy to previously published stratigraphic schemes is summarised in Figure 4.2. The presence of the transition zone between the WSD Basin and WSD Slope sections hampers correlation between the two sediment bodies due to convergence and tuning of reflections. However, correlation is possible using a combination of the 2D and 3D seismic data, and the oldest identifiable continuous reflection between the two sections is found to be the top Drift Unit B1 reflection from the WSD Basin section (Knutz and Cartwright, 2004) (Figs. 4.2 & 4.4). The reflection is dated as early Pliocene in age based on correlation with well 214/4-1 at which level samples contain *Neogloboquadrina atlantica* in combination with *Neogloboquadrina pachyderma*, *Globigerina inflata*, *Globigerina puncticulata*, *Cibicides grossus*, *Melonis affine* and *Sigmoilopsis schlumbergeri* (Davies et al., 2002). When traced upslope through the transition zone, the TopB1 reflection is found to track into Unit 2 of the WSD Slope section, constraining the age of Unit 2, at least in part, to the early Pliocene (Figs. 4.2 & 4.4). The occurrence of Unit 1 and PL40 stratigraphically below the top B1 reflection suggests that they are also Pliocene and not Pleistocene in age. Therefore, using the preliminary dating of the WSD Basin section, it is proposed that within the WSD Slope section Unit 1 is early Pliocene in age, Unit 2 is partially early Pliocene, while the remainder of Unit 2 and the whole of Unit 3 date from the late Pliocene to Pleistocene, although these post early-Pliocene dates are not directly calibrated by well 214/4-1.



**Figure 4.5**

3D seismic profile and line drawing perpendicular to the West Shetland slope to illustrate seismic-stratigraphic division of the WSD Slope section (line location Fig. 4.1). Accumulation of the WSD Slope section is seen to occur at a subtle break of slope on the INU surface. Line drawing summarises reflection termination relationships marked by arrows. Inset panel shows detail of upslope prograding moat system within Unit 2. SB- seabed.

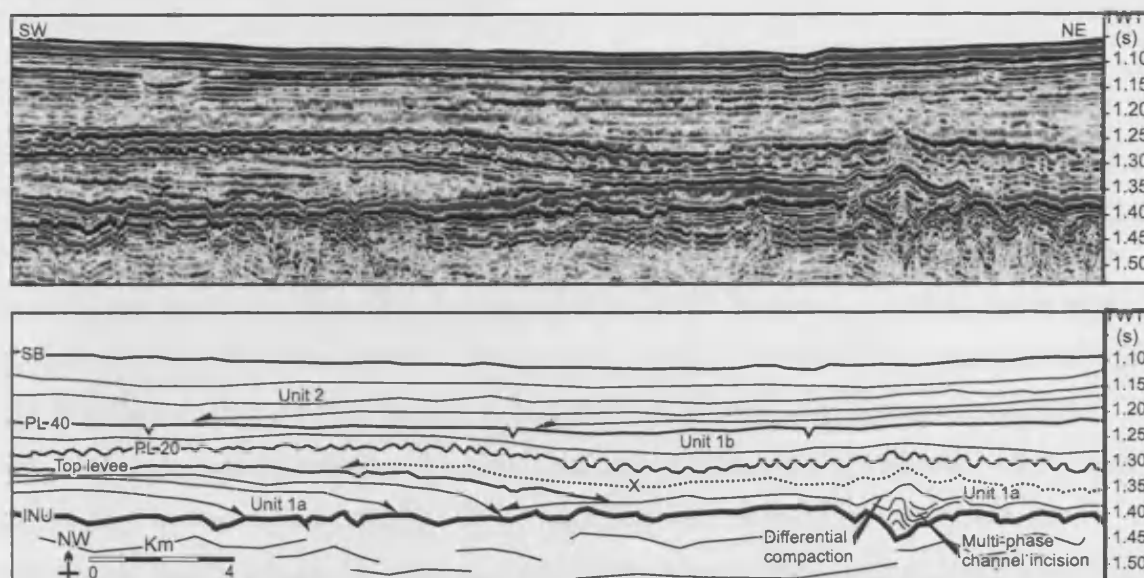
## 4.6. Internal unit analysis

### 4.6.1 Basal surface

The base of the WSD is marked by the INU which is identified as a relatively high amplitude continuous reflection and is interpreted to represent a prominent erosion surface on the West Shetland slope based on angular subcrop of underlying reflections (Fig. 4.3). The unconformity is regionally equivalent to the C10 reflection in the Rockall Trough (Stoker et al., 2002a) and the CN-040 reflection on the East Faeroe Margin (Andersen et al., 2000). The INU is correlatable from the Shetland slope into the basin axis where it becomes less readily identified and appears largely parallel with underlying reflections. In addition, there is no direct evidence of a hiatus in well 214/4-1, which penetrates the INU and records the occurrence of late Miocene and early Pliocene biomarkers. Therefore, erosion during the INU event occurred between the late Miocene and early Pliocene, and resulted in erosional truncation of the Shetland slope, and possibly the basin floor. The morphology of the INU is also apparently affected by variations in underlying geology. An area of positive topographic relief on the INU surface corresponds to the presence of a localised Eocene progradational clinoform complex (Fig. 4.1) which ultimately influenced the deposition of the West Shetland Drift units onto the INU. In addition, an important but subtle break in slope is observed on seismic profiles perpendicular to the slope along the length of the Shetland slope (Fig. 4.5), which formed the locus for subsequent deposition of the WSD Slope section. The overall slope angle of the INU also varies along the length of the Shetland margin, and exhibits a gradient generally  $> 1^\circ$  to the north of the 3D data set used for this study, and shallows to generally  $< 1^\circ$  toward the south. The character of the transition zone in turn is seen to vary laterally with development of upslope prograding moats limited to the northern end of the slope and the thinning and broadening of the transition zone accompanying the decrease in the INU slope angle to the SW.

The geometry of the INU on the West Shetland slope is a critical component of the interpretation of the sequences that were deposited above the INU. Previous workers have used the stratal geometry of the post-INU interval to infer palaeobathymetric evolution and subsidence history of the slope (Stoker, 1999; Knutz and Cartwright, 2003), and any





**Figure 4.6**

3D seismic profile and line drawing parallel to the West Shetland slope to illustrate the strike-orientated seismic-stratigraphic division of the WSD Slope Section (line location Fig. 4.1). Channel to the right of the profile shows complex internal geometry and deformation of overlying strata due to differential compaction. Channel levee deposit shows lateral downlap. Reflection X exhibits SW downlap onto the levee, and correlates to a series of subtle and interspersed reflections that progressively downlap toward the SW and are interpreted as alongslope current deposits intercalated with the downslope channels. Note progressive SW downlap of reflections within Unit 2 onto the PL40 reflection. SB- seabed.

quantification of palaeo-water mass geometry critically depends on an accurate reconstruction of the palaeobathymetry of this slope region.

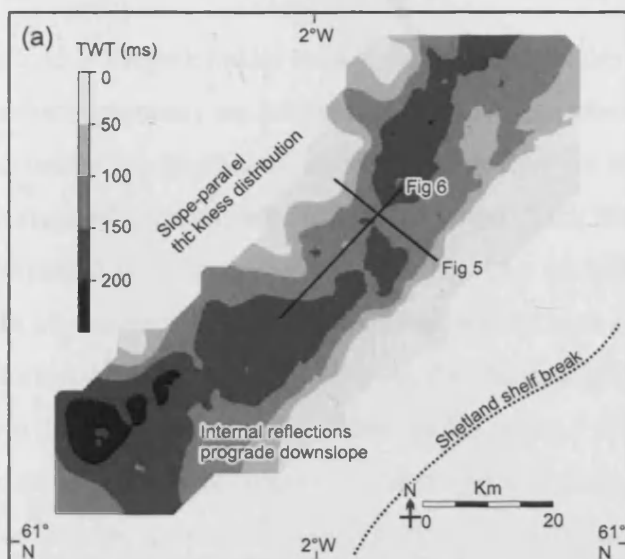
When traced upslope toward the shelf using 2D seismic data, the INU becomes difficult to track due to noise, multiples and normal move-out effects (Bulat, 2005) in the shelf region (Fig. 4.3). Stoker et al. (2002b) report that a seaward dipping INU is observed on the West Shetland shelf is evidence of tilting of the NW European Margin during the Late Neogene, an event proposed by numerous authors (Doré et al., 1999; Stoker et al., 1999, Stoker et al., 2002; Japsen and Chalmers, 2000; Cloetingh et al., 1990). Conversely, Knutz and Cartwright (2003) suggested that the INU had not been significantly affected by tectonic subsidence following its formation, based on the identification of a proposed early Pliocene shelf break datum. As documented in section 4.3.2, we have been unable to support any previous estimates of slope palaeobathymetry, and assign a maximum upper limit of 500m post-INU subsidence to all palaeo-water depth estimates.

#### 4.6.2. Unit 1

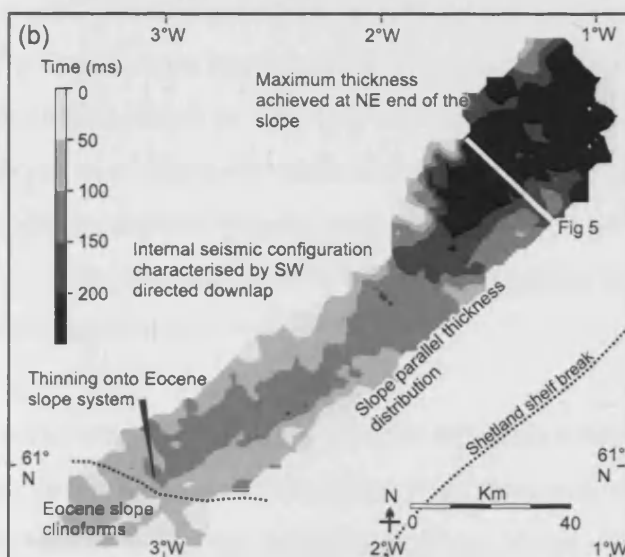
Unit 1 is interpreted as a single seismic-stratigraphic unit on the basis that it is bounded at its top and base by unconformity surfaces PL40 and the INU respectively (Fig. 4.5 & 4.6). Unit 1 is further sub-divided into Sub-Units 1a and 1b based upon changes in the reflection geometry and areal extent between the base and top of the Unit.

##### 4.6.2.1. Unit 1a

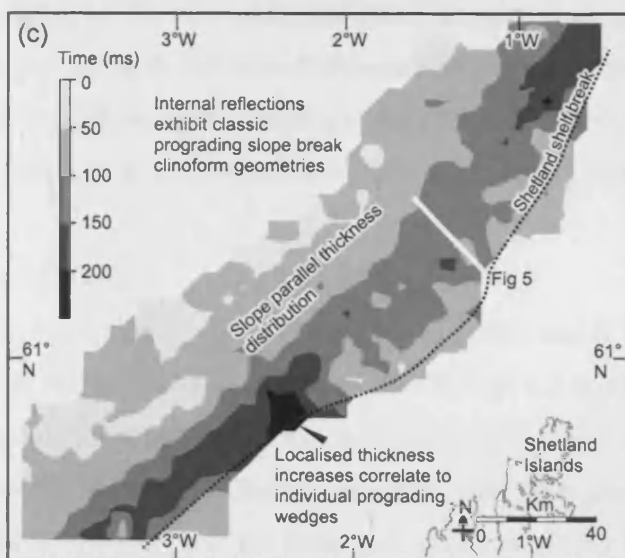
Unit 1a is situated at the break in slope of the INU surface described in section 4.6.1, and comprises the bulk thickness of Unit 1 (Fig. 4.5). The isochron map of Unit 1a (Fig. 4.7a) outlines the thickness distribution which locally attains thicknesses of more than 200m, thins both up and down slope and extends for c.80km along the Shetland slope. The upper and lower limits of Unit 1a are c.750m-1000±100mbsl respectively. Internally, Unit 1a is composed of a series of moderate amplitude, continuous reflections which overlap progressively downslope, with steeper older reflections overlain by progressively shallower reflections (Fig. 4.5). A time structure map of the lower internal reflections within Unit 1a (reflection PL10, Fig. 4.5) reveals NW/SE trending linear features extending from the upslope limit of Unit 1a downslope for at least 15km (Fig. 4.8). In cross section the features

**Figure 4.7**

(a) Isochron map of Unit 1, illustrating time thickness between the INU and seismic marker PL40. Note slope parallel thickness distribution with thinning both upslope and downslope. Fig. 4.5 illustrates downslope prograding internal reflections within Unit 1a while Fig. 4.6 illustrates cross sectional geometries of downslope channels and associated levees.



(b) Isochron map of Unit 2 illustrating time thickness distribution between seismic marker PL40 and the GU. Unit 2 attains greatest thickness at the northern end of the study area, and thins toward the SW as well as thinning up and down slope. Internal reflections exhibit SW downlap (Fig. 4.6). Figure 5 inset panel illustrates the upslope aggrading bottom current moat system as well as the erosional nature of the upper contact of Unit 2.



(c) Isochron map of Unit 3, illustrating time thickness distribution between the GU and the seabed. The maximum thickness of Unit 3 is attained near the present day shelf break, from where it thins downslope. Localised thickness increases are related to glacial prograding wedges deposited following onto the GU (Fig. 4.3).

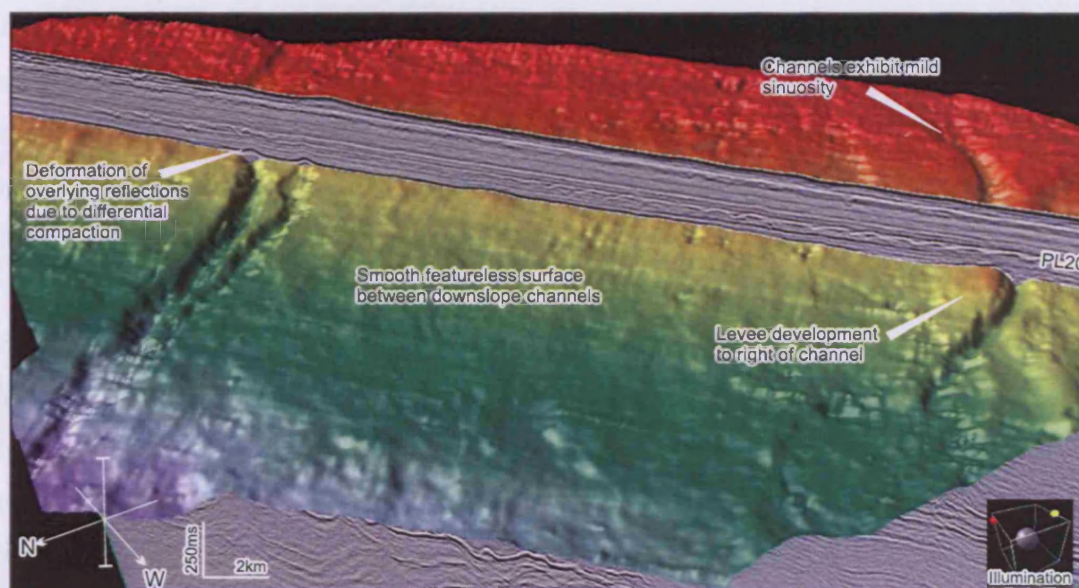
The 'Fig' references refer to the location of seismic profiles within this Chapter, e.g. 'Fig 5' refers to Figure 4.5.

are U to V shaped and up to 2km wide and 150m deep (Fig. 4.6), and combined with their planform geometry are interpreted as downslope channels. Crosscutting incisional internal geometries are interpreted to represent multiple cut and fill phases during channel evolution. Packages of aggradational reflections which flank the channels and downlap laterally are interpreted as constructional levees (Fig. 4.6). At their downslope limit, the channels die out, with no apparent terminal depositional feature such as a base of slope fan. Convex-upward deformation of reflections overlying the channels (Figs. 4.6 & 4.8) is interpreted to result from differential compaction between the channel fill and the surrounding sediment, often the result of a coarse channel fill behaving differently under compaction compared to encasing fine grained sediment (Fisher 1992). Development of downslope channels is restricted to the older reflections within Unit 1a. A series of progressively SW downlapping reflections that are intercalated with and blanket the channel-levee complex (Fig. 4.6) are identified. Alongslope directed reflection downlap is a feature characteristic of the seismic expression of contourite drifts (Faugères et al., 1999), and suggests that downslope and alongslope deposits may be intercalated. The SW limit of Unit 1a is marked by reflection termination onto the area of relict INU topography associated with the underlying Eocene slope progradation system.

In summary, Unit 1a is interpreted to represent a mixed system consisting of an aggradational channel levee system depositing sediment at a break in slope, with possible subordinate alongslope current deposition. Mixed downslope-alongslope systems are common on the Norwegian margin (Dahlgren et al., 2002; O'Grady and Syvitski, 2002). The smooth surfaces and lack of channels of younger reflections within Unit 1a could suggest that the influence of alongslope currents increased during deposition resulting in smoothing of the slope as occurs on the Nova Scotian Slope, Eastern Canada (Stow, 1979).

#### 4.6.2.2. Unit 1b

Unit 1b represents the upper portion of Unit 1 and is bounded at its base by seismic marker PL20 and at its top by reflection PL40 (Figs. 4.5 & 4.6). Overall, Unit 1b consists of parallel aggradational reflections which in dip section are observed to onlap and downlap the underlying INU and Unit 1a (Fig. 4.5). Unit 1b is generally thickest on the lower slope (up to 120m), downslope of the main accumulation of Unit 1a, onto which it thins.



**Figure 4.8**

3D visualisation of seismic reflection PL10 (stratigraphic location Fig. 4.5) looking toward Shetland shelf reveals the presence of mildly sinuous downslope channels and associated levee deposits within Unit 1a. Subsequent to channel formation, differential compaction has deformed overlying sediments of Units 1a, 1b and 2. Terminal fan deposition is not apparent, and the channels die out downslope.

The upper part of Unit 1b consists of a thin (<60m) series of low amplitude, parallel aggradational reflections which progressively onlap PL20 upslope and downlap onto the INU (Figs. 4.5 & 4.6). In strike section, the upper reflections of Unit 1b exhibit configurations suggestive of drape (Fig. 4.6). Based on their acoustic characteristics and dip section stratal geometries, the reflections within the upper portion of Unit 1b could be interpreted as a plastered contourite drift deposit (Faugères et al., 1999; Rebesco and Stow, 2001).

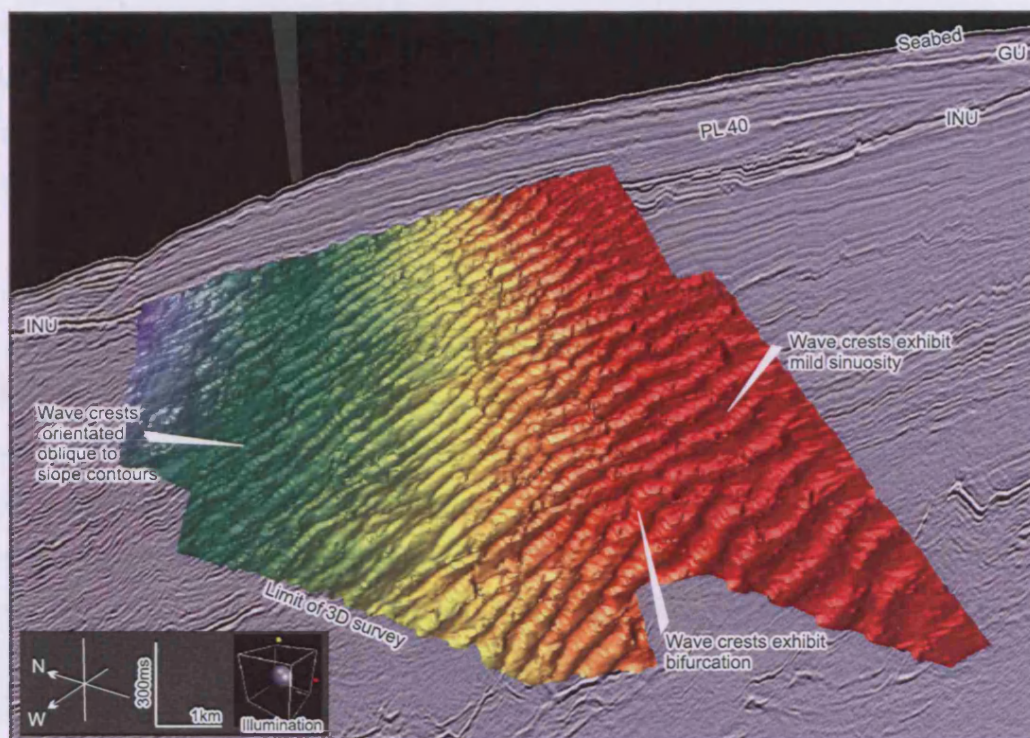
4.6.2.3. Sediment wave field

The lowermost part of Unit 1b is remarkable in that it exhibits the characteristics of a well developed sediment wave field. The event is represented by a seismic ‘doublet’, PL20, with a combined thickness of c.50m and which onlaps the underlying Unit 1a upslope and downlaps the INU at the downslope limit of the WSD Slope section (Fig. 4.5). The upslope and downslope limits of the features are 950-1200±100mbsl respectively. These moderate to high amplitude reflections exhibit an undulating morphology of regularly spaced crests and troughs (Fig. 4.6), and unlike the reflections within Unit 1a, are continuous over the area of high INU bathymetry to the SW for a total of 175km (SW limit coincident with limit of WSD Slope contours, Fig. 4.1).

The undulations of the PL20 reflections have crest to crest separations of 300-700m and heights of between 15 and 25m (average c.18m) (Figs. 4.9 & 4.10). A time structure map of PL20 shows that the crests of the undulations seen in cross section form linear features 6000-8000m in length which are mildly sinuous and exhibit occasional bifurcation (Figs. 4.9). The crests strike obliquely at a variable angle of between 25-50° clockwise to the slope contours, strongly suggesting that the current responsible for their formation flowed either in a SW-NE or a NE-SW direction. The morphology of the crests is also seen to diminish and breakdown toward their upslope and downslope limits (Fig. 4.9). The NE flanks of the individual undulations exhibit higher seismic amplitudes than the SW flank (Fig. 4.10).

Based on the observed planform geometry, the internal reflection configuration and close correspondence with examples described and classified by Wynn and Stow (2002), the undulatory reflections of PL20 are interpreted to represent fine-grained sediment waves





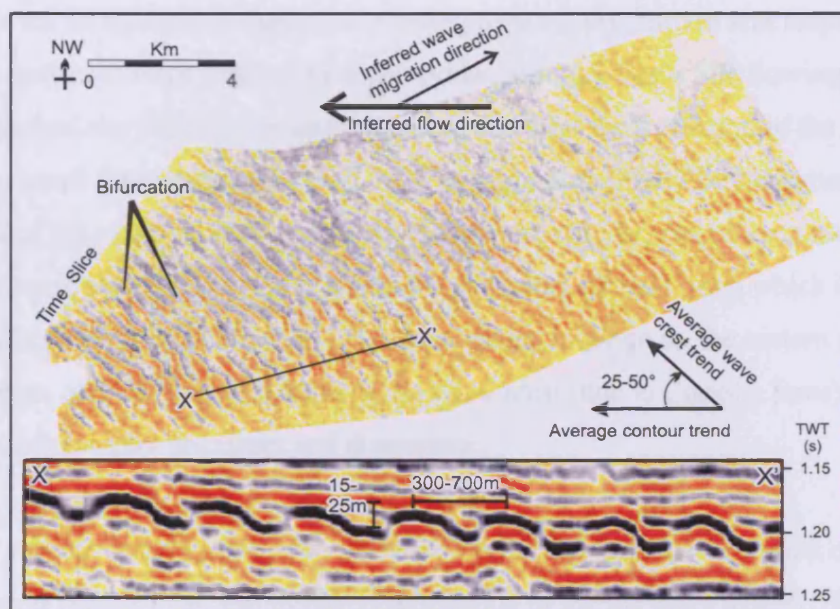
**Figure 4.9**

3D visualisation of the PL20 reflection looking along the West Shetland slope toward the NE, revealing a surface adorned with large sediment waves within the contourite drift body. Wave crests are orientated obliquely to the slope, mildly sinuous and occasionally bifurcating. Wave dimensions die out up and down slope.

deposited by the action of bottom-currents. The waves are distinguished from coarse grained sediment waves that would tend to form isolated, barchan dunes which are smaller (200m wavelength and height of a few metres, Wynn and Stow, 2002). The size of the wave field and their orientation relative to the slope allows us to rule out an origin linked to turbidity currents or slope creep folds (Faugères et al., 1999; Wynn and Stow, 2002; Ercillia et al., 2002).

Sediment wave fields associated with contourite drifts have been extensively documented from around the globe (Embley et al., 1980; Faugères et al., 1993; Flood, 1994; Flood and Giosan, 2002; Wynn and Stow, 2002), and imaged on 3D data (Austin, 2004), but we believe this to be the most laterally extensive drift-related sediment wave field imaged with 3D seismic data. A widely adopted model to explain the development of bottom-current sediment waves is the lee wave model (Flood, 1988). The lee wave model predicts that sediment accumulation is concentrated on the up-current limb of an initial bedform perturbation due to decreased current velocity and bed shear stress. This results in a thickened upcurrent limb and development of a sedimentary bedform which migrates *up-current*. The crests of fine grained bottom-current sediment waves are also observed to be oriented obliquely to slope contours (and flow direction) (Flood, 1994, Wynn and Stow, 2002). In the northern hemisphere, crest rotation will typically be between 10-50° in a clockwise direction (when looking down-current) as a result of the Coriolis Force, and migration will occur upcurrent and upslope, to the right of the flow (Fig. 4.10) (Flood, 1994; Manley and Caress, 1994; Wynn and Stow, 2002).

We attempted to match our observations of the sediment wave field represented by PL20 with the lee wave model. The main limitation with this analysis was the vertical seismic resolution, which was not sufficient to resolve detailed internal stratal geometries within the waves. A 3D seismic section perpendicular to the wave crests (Fig. 4.10) shows inclined, higher amplitude reflections on the NE flank of the sediment waves, which could be interpreted to represent the thickened upcurrent flank of the sediment waves with the higher amplitudes resulting from tuning or coarsening of lithofacies. If this were the case, in the context of the lee wave model, the sediment waves could reasonably be interpreted to have formed by a current flowing from the NE toward the SW. The measured orientation of 25-



**Figure 4.10**

Analysis of PL20 sediment wave field. A time slice through the PL20 reflection generated from a smoothed and flattened overlying reflection illustrating wave crest geometry and relation to slope contours. The seismic profile X-X' illustrates the cross-sectional geometries of the waves, with the higher amplitude reflections on the NE flank of the waves interpreted to reveal a NE migration direction. From the inferred migration direction of the waves (upcurrent toward the NE) a SW flow direction and migration of the waves to the right of the current and downslope is proposed.

50° of the wave crests relative to the depositional slope contours (Fig. 4.10), is within the 10-50° range observed for sediment waves elsewhere (Flood, 1994; Wynn and Stow, 2002) and supports the interpretation that a SW flowing depositional current was responsible for forming the sediment wave field. Additional evidence suggesting a SW flowing depositional current influenced the WSD Slope section before and after the formation of the sediment waves is discussed further in section 4.7.1.2. The migration of the PL20 sediment waves downslope and not upslope, as predicted by the lee wave model, can be accounted for by the fact that the Faeroe Shetland Basin is a relatively narrow, atypical basin which is dominated by thermohaline currents. The result is that deep waters impinge on the eastern as well as western margin, and clockwise rotation of the wave crest (due to Coriolis force) results in bedforms which migrate upcurrent and downslope.

The lack of vertical seismic resolution necessary to identify internal migration of the sediment waves results in an inconclusive application of the lee wave model. The reflection configuration exhibited by seismic marker PL20 could also be interpreted as a diachronous sediment wave progradational system which advanced toward the NE. This may be supported by the lateral extent of the sediment waves, which would suggest that synchronous development of the bedforms may be unlikely, and that a diachronous, progradational series of bedforms may have led to the formation of the sediment wave field. However, the lack of examples of large scale deep water sediment wave fields which migrate down current would also lead us to suggest that if this model were true, the wave field prograded toward the NE, upcurrent, and thus also suggesting deposition by a SW flowing current. High resolution seismic data are required to further our understanding of the wave forming process.

In summary, Unit 1 represents the initial deposition on the West Shetland Margin within the study area following the formation of the INU. The depositional system active throughout the formation of Unit 1 is interpreted to have evolved from an initial mixed system with significant downslope influence to a dominantly alongslope depositional system. The recognition of a laterally extensive sediment wave field allows us to constrain the likely current regime during this depth range to have been flowing to the SW. The mapping of the wave field using the 3D seismic qualifies as an excellent example of the use of 3D seismic to

provide current directional inferences that would have been difficult to derive from conventional 2D seismic profiles.

### 4.6.3. Horizon PL40

#### 4.6.3.1. Seismic character and areal distribution

The upper boundary of Unit 1 is defined by reflection PL40 (Fig. 4.2), which forms a continuous, moderately high amplitude reflection that exhibits minor angular discordance and erosional truncation of the upper reflections of Unit 1 below (Fig. 4.5), and is thus interpreted as an unconformity surface. Both upslope and downslope, PL40 terminates against the INU (Fig. 4.5), and the reflection spans a present day depth range of 750-1250±100mbsl. The depositional areal extent of PL40 is not clear as it cannot be resolved over the entire area due to a combination of incomplete data coverage, thinning below seismic resolution, onlap onto the INU or erosional truncation beneath the Glacial Unconformity.

The minor angular discordance of PL40 with the reflections of Unit 1 beneath, combined with the absence of any downslope process indicators (such as channels) on the PL40 surface, suggests that the limited erosion that occurred during its formation was the result of alongslope currents that had a sufficiently high velocity to remove unlithified surficial sediments of the underlying Unit 1. Any winnowing of the sea floor by alongslope currents would have preferentially removed fine grained sediment and concentrated the coarser fraction, as occurs on the modern day sea floor in the Faeroe Shetland Basin (Masson, 2001; Bulat & Long, 2001; Howe et al., 2001). This may help to explain the higher positive acoustic impedance of PL40 relative to surrounding seismic facies.

Alongslope current erosion is preferred as a mechanism for the formation of PL40 over other possibilities such as base level fall due to a lack of features associated with base level erosion such as a wave cut platforms and lowstand slope channels. Estimation of the magnitude of erosion that PL40 represents is extremely difficult due to the low angle of discordance between PL40 and the underlying strata. The formation of PL40 is therefore interpreted to be the result of a period of increased alongslope current activity leading to probably minor erosion of the seabed.



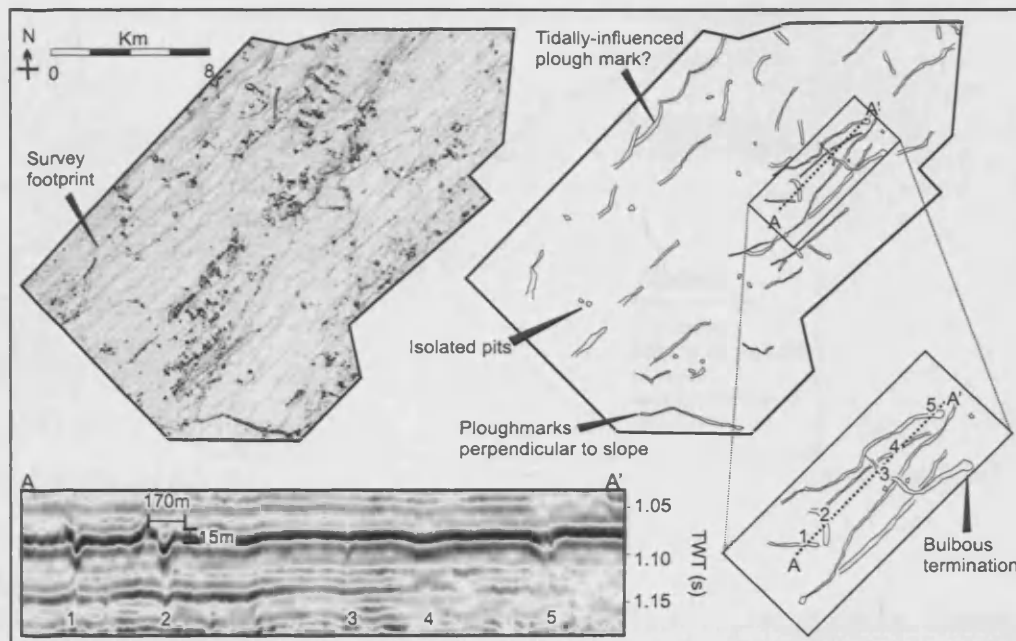
#### 4.6.3.2. Iceberg plough-marks

A time structure map of PL40 reveals the presence of numerous linear features which crisscross the surface (Fig. 4.11). The majority are slope parallel, but some are orientated at high angles to the slope. The features are frequently >10km long and in cross section appear as 'V' shaped features up to 250m wide and up to 20m deep (on average c.10m) resembling small channels (Fig. 4.11). However, the features cross-cut one another in multiple directions suggesting that they are not channels. Instead, the features exhibit characteristics diagnostic of ice berg plough marks resulting from the interaction of icebergs with the seabed (Bass and Woodworth-Lynas, 1988; Todd et al., 1988; Vogt et al., 1994).

In addition to the long, linear scour marks, isolated circular to elliptical 'craters' up to 200m and 20m deep are also observed. Similar circular features are commonly observed in association with linear plough marks, and have been attributed to touch-down of iceberg keels during iceberg melting and re-equilibration (Bass and Woodworth-Lynas, 1988). When viewed in cross section, deformation and apparent lateral displacement of the underlying reflections is observed (Fig. 4.11) which would support the interpretation that the features were related to deformation of the sub-seabed by an impact of an iceberg keel from above. The identification of iceberg plough marks within the main body of a sediment drift raises the possibility of deriving current direction data for use in palaeoceanographic reconstruction.

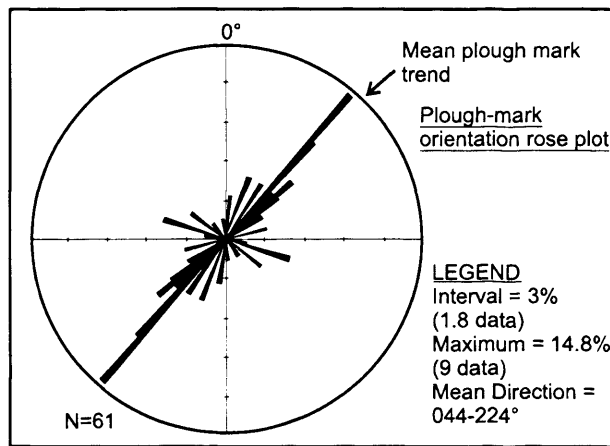
Many of the linear plough marks present on the surface of PL40 are observed to have a bulbous circular depression at one end (Fig. 4.11). Identical features observed on the Labrador Shelf are interpreted to be the result of iceberg grounding after being driven against the slope (Bass and Woodworth-Lynas 1988). The iceberg remains grounded until it melts enough to lift off of the sea bed, and when it does so it leaves behind a linear scour terminating in a pit (Bass and Woodworth-Lynas, 1988; pers comm. David Mosher). Using these palaeo-directional indicators, an attempt was made to derive paleo-transport directions from scour terminations on the PL40 surface. This resulted in mixed directional information with indications of transport along the slope to the NE and the SW. However, the linear plough marks do show a dominant alongslope trend (044°-244°) (Fig. 4.12). Some plough marks show successively overlapping curvilinear patterns (Fig. 4.11), which may be the





**Figure 4.11**

Time structure map of the PL40 reflection revealing a surface crisscrossed by iceberg plough marks. Linear plough marks are predominantly orientated parallel to the slope (see Fig. 4.12), although some are aligned at a high angle to the slope. Overlapping curvilinear plough marks may be related to tidal processes. The seismic profile relates the line A-A' across the zoomed box and illustrates the plough marks cross sectional geometry. Plough marks vary from clearly visible, wide V shaped impressions (No. 2) to narrow and subtle features (No. 3&4). The seismic profile also shows deformation of the reflections beneath the plough marks. Zoomed section highlights bulbous termination of linear plough marks. The survey footprint forms an artefact on the time structure map.

**Figure 4.12**

Rose plot based on orientation measurements of 61km of plough marks. Dominant trend is NE/SW alongslope (044-224°) although a variety of subordinate trends are also present.

result of tidal influences causing an iceberg to take an elliptical transport path as the tide ebbed and flowed (pers comm. P. Knutz). Plough-marks are most evident on the upper two thirds of the PL40 surface, between c.750-1000±100mbsl. It is likely that plough marking occurred further upslope and onto the shelf, although any evidence of this was removed by erosion of the shelf and upper slope region during the formation of the Glacial Unconformity. The significance of the plough-marks is considered further in section 4.7.1.3.

#### 4.6.4. Unit 2

Unit 2 is bounded at its base by PL40 and at its top by the GU, and consists of a succession of parallel, moderately low amplitude discontinuous reflections with a maximum thickness of up to 300m. Upslope the reflections onlap the PL40 and INU reflections, while downslope they downlap onto the INU (Fig. 4.5). In strike section, the reflections are seen to successively downlap onto the PL40 and the INU towards the SW along the West Shetlands margin (Fig. 4.6). The thickness distribution of Unit 2 (Fig. 4.7b) clearly shows the unit thinning up and downslope, and toward the SW. Unit 2 extends for >175km from the study area toward the SW, exhibiting thinning across positive relict topography on the INU (Fig. 4.7b).

Toward their up-dip limit, the Unit 2 internal reflections exhibit a series of U shaped troughs between 1-2km in width and up to 40m deep which prograde/aggrade upslope (Fig. 4.5), and are slope parallel for at least 40km, as revealed by horizon slicing. The features are at c.700±100mbsl, and in both cross section and plan view are extremely similar to the upslope prograding/aggrading moat system present at the base of slope within the study area which was documented by Knutz and Cartwright (2003, 2004). The upslope limit of Unit 2 is therefore interpreted to be marked by an upslope prograding/aggrading moat system which was active during the formation of Unit 2.

The presence of an inferred alongslope moat system, combined with the parallel, aggradational, low amplitude reflections which comprise the rest of Unit 2, are consistent with the seismic character of fine grained plastered contourite deposits (McCave and Tucholke, 1986; Faugères et al., 1999). The lateral continuity of the unit (>175km along the

slope) supports the proposed alongslope origin of the Unit. The rare occurrence of isolated 'V' shaped impressions within Unit 2 which exhibit the same geometry and seismic character as the iceberg plough marks on PL40, suggests intermittent iceberg presence within the Faeroe Shetland Basin during the deposition of Unit 2.

Contourite drifts are observed to exhibit diagnostic alongslope downlapping internal reflections which prograde down current (Faugères et al., 1999). Therefore, the general thinning of Unit 2 to the SW combined with the SW directed downlap of internal reflections are used to argue for a SW flowing depositional current regime during this interval. This is further supported by correlation of Unit 2 with the WSD Basin Section where it correlates with the base of slope moat system which Knutz and Cartwright (2004) interpret to have been deposited by SW flowing depositional currents. This also supports the conclusion of Knutz and Cartwright (2004) that the two sections of the WSD system were active contemporaneously.

#### *4.6.5. The Glacial Unconformity and Unit 3*

The upper limit of Unit 2 is marked by a regionally extensive, prominent, high amplitude reflection which in places shows angular subcropping relationships with underlying strata and is particularly prevalent on the West Shetland shelf (Figs. 4.3 & 4.5). Interpreted as an unconformity, the reflection becomes less prominent downslope, exhibiting a lower seismic amplitude and a lower angle of discordance with the underlying strata. The surface is scored by a number of V shaped impressions with similar cross sectional and plan form geometries to those seen on PL40, and which are thus interpreted as iceberg plough marks. However, imaging of the plough marks on the unconformity is less clear than those on PL40 due to multiples and normal move-out effects in the shallow section (Fig. 4.3). Through correlation with published literature, the reflection is recognised as the Glacial Unconformity, the formation of which has been dated at 0.44Ma in response to the advance of major Pleistocene ice sheets onto the continental shelf (Stoker et al., 1995). The deepest plough marks on the GU are found at 800m  $\pm$  100mbsl. The plough marks appear to exhibit random orientations with an apparent lack of a dominant transport direction.

Unit 3 was deposited on top of the GU, and is continuous along much of the Shetland slope in the form of a series of prograding wedges which are generally around 50-100m thick with localised depocentres reaching 180m thick (Fig. 4.7c). The lithology of this unit is well documented in published literature and consists of a highly variable mixture of diamicts and other glacially derived sediments, resulting from glacially influenced depositional processes including debris flows, glaci-marine and marine sedimentation (Stoker et al., 1993, Stoker, 1999). There are no seismically discernable alongslope current features (such as moats or sediment waves) within Unit 3, which is interpreted as a downslope glacial prograding wedge system.

The present day seabed consists of a mixture of areas of deposition and areas of angular discordance with underlying reflections. Combined with the presence of Holocene boulder lag deposits, this is indicative of dominantly erosive/non-depositional conditions at the seabed during the Holocene (Stoker, 1999; Masson, 2001, 2002; Van Raaphorst, 2001; Bulat & Long, 2001).

## 4.7. Discussion

The main observations made during the detailed seismic mapping and interpretation of the WSD Slope section are summarised below:

- 1) The WSD Slope section is divided into 3 seismic-stratigraphic units, which combined form a SW tapering sediment accumulation at a mid-slope break in the West Shetland slope.
- 2) The base of the WSD is marked by the INU which formed during the Late Miocene/Early Pliocene, and correlation of the WSD Basin and WSD Slope sections allows Unit 1 and part of Unit 2 to be dated as early Pliocene, while the remainder on Unit 2 and Unit 3 are thought to be late Pliocene to Pleistocene in age.
- 3) Early deposition involved a significant downslope component (Unit 1a), which was succeeded by the deposition of sediment waves and contourite drifts (Unit 1b), representing the onset of alongslope current dominance over the deposition of the WSD Slope section. Contourite drift accumulation occurred until the formation of the Glacial Unconformity during the mid-Pleistocene (0.44Ma).

- 4) During contourite drift accumulation, glacial phases are evidenced by the occurrence of iceberg plough marks (PL40 and the GU).
- 5) Iceberg plough mark geometries and the internal architecture of glacial deposits (Unit 3) suggest disrupted thermohaline current activity during their formation.

#### *4.7.1. Sedimentary processes and slope evolution*

The interpretation of 3D seismic data for this study has resulted in the identification and analysis of a number of features which would have not been possible using 2D seismic data alone. Three of these highlights are: (1) the identification of a distinct and previously unrecognised downslope depositional system within the WSD Slope section; (2) a newly discovered sediment wave field; and (3) iceberg plough marks on the surface of PL 40. The significance of each of these findings is discussed in turn, and summarised in Figure 4.13..

##### *4.7.1.1. Downslope processes*

The identification of significant downslope depositional elements within the WSD Slope section directly above the INU signifies a distinct change in the sedimentary regime of the West Shetland slope from alongslope current erosion (Stoker, 1999; Stoker, 2003) to significant downslope deposition. The proposal that the formation of the INU was related to tilting of the West Shetland Margin (Stoker, 1999, Stoker, 2003; Japsen and Chalmers, 2000) provides a potential mechanism for the initiation of the downslope system within Unit 1a, and may also imply that downslope channelling began during the formation of the INU.

Aggradational channel complexes of the type found within Unit 1a form in settings usually associated with point sourced fine grained clastic systems and often associated with sea level lowstands (Reading and Richards, 1994). A major sea level fall is observed for the period following the formation of the INU (Fig 4.2, Haq et al., 1987), and could be related to the initiation of the Unit 1a downslope system. Thin distal sheet fans are often associated with these channel complexes, but have not been identified in association with Unit 1a, in which the channels appear to die-out downslope (Fig. 4.8). The interpretation of alongslope current influence within Unit 1a could account for the lack of base of slope deposition within Unit 1a. The reported continuity of drift deposits and conformity of the INU in the basin axis observed on seismic profiles and in samples from well 214/4-1 (Davies et al., 2001; Knutz



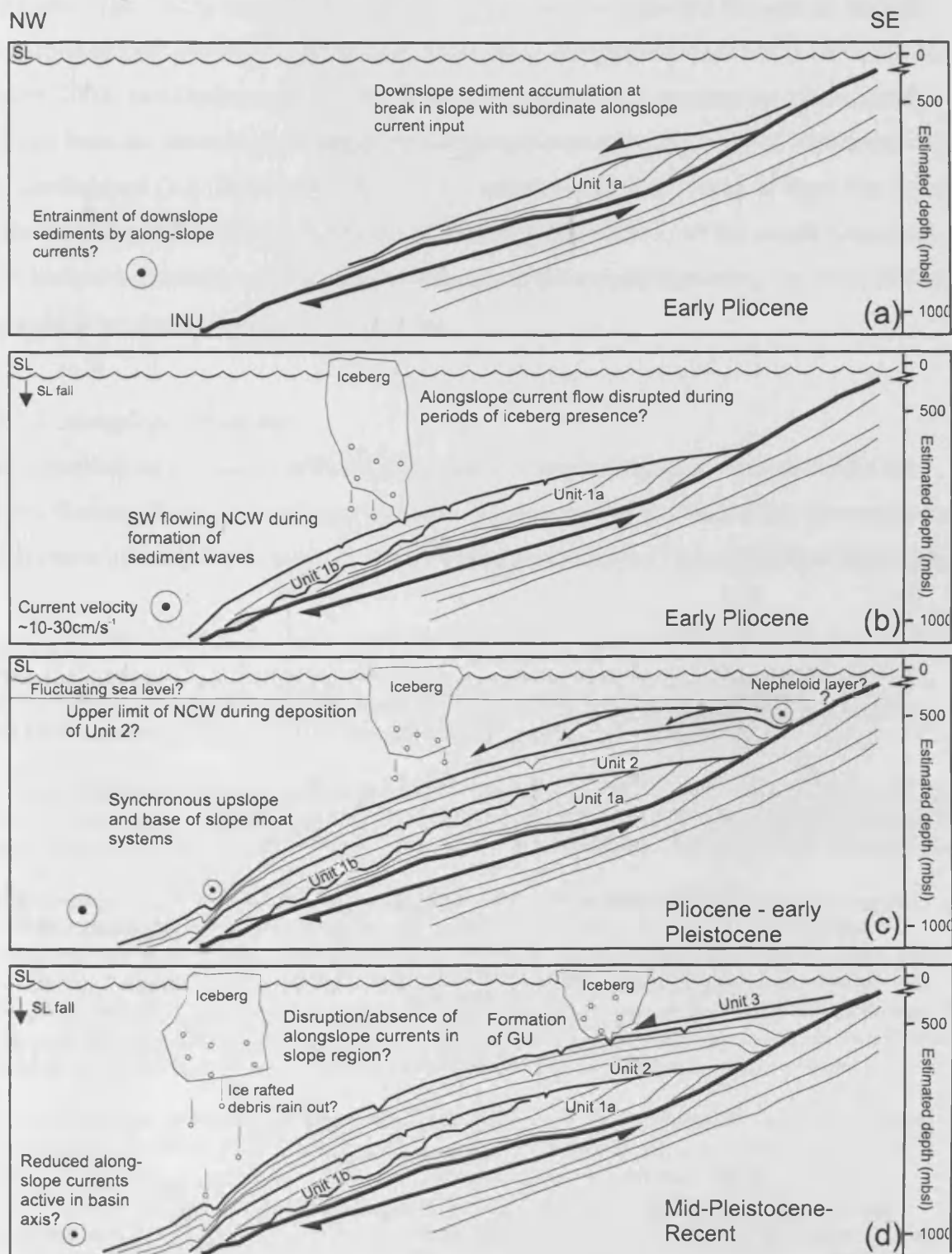


Figure 4.13

and Cartwright, 2003), suggests alongslope currents were continuous through the time of deposition of Unit 1a (at least in the deep basin axis), a suggestion previously advanced by Stoker (2003) and Davies et al. (2001). Therefore, dilution and entrainment of sediments sourced from the downslope channels by alongslope currents may have inhibited terminal fan development (e.g. Stow et al., 2002). The limited extent of the break of slope that formed the locus of deposition for the WSD Slope section (particularly Unit 1a) would potentially have limited the development of fans, with material potentially bypassing the break of slope and continuing further basinward (Fig. 13a).

#### 4.7.1.2. *Alongslope processes*

The deposition of contourite drifts and formation of regional erosion surfaces within the Faeroe Shetland Basin since at least the early Oligocene (Davies et al., 2001) illustrates the significance of alongslope currents on sedimentation within the Faeroe Shetland Basin. The

---

#### **Figure 4.13**

Schematic summarising the proposed evolution of the WSD Slope section. Water depth (mbsl) on each panel represents present day values and not depositional water depths, which are thought to have been a maximum of 500m shallower than the present day water depths.

**(a)** Accumulation of Unit 1a at a break in slope on the INU surface via downslope processes during the early Pliocene. It is likely that alongslope currents were active resulting in subordinate contourite deposition and the possible entrainment of downslope sediments resulting in a lack of fan deposition.

**(b)** Deposition of Unit 1b by SW flowing Northern Component Water (NCW) during the early Pliocene, resulting in the formation of the sediment waves and contourite drift deposits and representing the onset of SW flowing alongslope currents as the dominant depositional force on the West Shetland margin. The formation of seismic marker PL40 by alongslope current erosion was followed by iceberg turbation of the seabed, interpreted to represent a period of glaciation during which it is proposed alongslope current flow was disrupted. Sea level fluctuation would be expected with growth and decay of large ice sheets deemed to have been the source of the icebergs.

**(c)** Continued flow of Northern Component Water during the Pliocene-early Pleistocene, resulting in the deposition of Unit 2 combined with the development of base of slope and upper slope moat systems. Occasional iceberg presence is also recorded during this interval. Arrows pointing downslope from the upslope moat system represent Coriolis related deflection of SW flowing alongslope currents, potentially distributing sediment supplied by nepheloid layers further upslope.

**(d)** Final phase of the WSD evolution, represented by the shelf transgression of ice sheets to form the Glacial Unconformity (GU), and the subsequent deposition of Unit 3 during the mid-Pleistocene to Recent. Unit 3 shows no seismically identifiable evidence of alongslope currents, and it is proposed that at this time (440-18Ka, Stoker, 1999) alongslope current activity on the West Shetland Slope was reduced, and if any, limited to the deep basin. Significant sea level fall would have accompanied the growth of regional ice sheets.

first evidence within the WSD Slope section of alongslope current activity following the formation of the INU is SW downlapping reflections intercalated with/blanketing the channel-levee complex of Unit 1a (Fig. 4.6), deposited during the early Pliocene. The progressive SW downlap is taken as evidence for a SW depositional current (Faugères et al., 1999). The switch from formation of the INU by alongslope current erosion to downslope deposition on the West Shetland slope suggests a significant change in the alongslope current intensity. However, the interpretation of alongslope current influence during the phase of downslope deposition suggests that the alongslope currents which formed the INU were reduced but still active throughout this time (early Pliocene).

The formation of the PL20 sediment waves represents the onset of an alongslope current dominated sedimentary regime (Fig. 4.13b). During this time it is interpreted that a SW flowing water mass impinged on the West Shetland slope. The palaeo-water depth in which the PL20 sediment waves formed is difficult to constrain due to the probable impact of Late Neogene subsidence of the margin. We tentatively suggest that this subsidence amounted to several hundred metres (max 500m, section 4.3.2) which would place the likely minimum depth range of formation of the sediment waves as between c.500-800 mbsl. At these depths the present day West Shetland slope is influenced by SW flowing currents (Turrell et al., 1999; Hansen and Østerhus, 2000), and similar sediment waves are present, formed by SW flowing currents (Masson, 2001).

In order not to imply a pathway or source area (e.g. Faeroe-Shetland Channel Bottom Water, Turrell et al., 1999) for the SW flowing current(s) responsible for deposition of the sediment waves and contourites within the WSD slope section, the water mass responsible is simply referred to as the Northern Component Water (NCW, sensu Broecker and Peng 1982 (Fig. 4.13b). Preliminary velocity estimates of between 9-30cm/s are proposed for the Northern Component Water during formation of the sediment waves based on observed velocity ranges for generation and migration of large fine grained bottom current sediment waves (Flood, 1988; Wynn and Stow, 2002).

The depositional effects of alongslope currents are known to vary with current speed and sediment load, among other factors (Stow et al., 2002). Velocities of only 10-15cm/s are

needed to deposit fine grained contourite drifts (McCave and Tucholke, 1986) and therefore, deposition of minor contourite drifts (upper Unit 1b) most likely represent a change in flow characteristics and/or sediment load of the same Northern Component Water that formed the underlying sediment waves. Analysis of contourite drifts in core has shown that fluctuations in current velocity produce alternations in contourite deposition and seabed erosion on centimetre to metre scales (Stow and Holbrook, 1984; Howe et al., 1994; Viana et al., 2002). An increased flow velocity of the current responsible for deposition of Unit 1b is also invoked for the formation of PL40, subsequent to which the current resumed contourite deposition with the formation of Unit 2.

The progressive SW downlap of internal reflections within Unit 2 combined with presence of the mid-upper slope moats and the base of slope moat system (Knutz and Cartwright 2004) suggests that the entire WSD was principally affected by SW flowing depositional currents. The presence of a boundary between the opposing water masses, which is at present known to be turbulent and a site of nepheloid layer generation (Van Raaphorst et al., 2001; Bonnin et al., 2002), upslope of the WSD Slope section may have contributed a supply of sediment (Fig. 4.13c).

The SW flow direction inferred from analysis of the sediment wave field complements the proposals of SW flow from the SW downlapping reflections intercalated with the levee complex of Unit 1a below, SW downlapping reflections and gross thinning toward the SW of Unit 2 above, and the occurrence of the base of slope moat system interpreted by Knutz and Cartwright (2003) to have been deposited by SW flowing currents. It is the combination of these flow indicators which lead to the proposal of a SW flowing depositional current for the alongslope deposits of Unit 1 and 2, and most likely for the erosion which occurred during the formation of the INU and PL40. Domination of the West Shetland slope to within 600m of the sea surface at present (Turrell et al., 1999; Bonnin et al., 2002; Masson, 2002) demonstrates that the proposed SW depositional flow regime proposed for the Pliocene is entirely feasible.

The sedimentary environment of the present sea floor in the Faeroe Shetland Basin is dominated by alongslope currents, and a mixture of minor alongslope and downslope

deposition in some areas is combined with non-deposition/erosion in others (Masson, 2002). A large variety of sedimentary bedforms including scour marks, furrows and sediment drifts are also present (Masson et al., 2005), which would be sub-seismic resolution on paleo-surfaces. These observations show that the Faeroe Shetland Basin is dominated by alongslope currents during periods of reduced glaciation, which in turn deposit contourite drifts and associated features. Global sea level reconstructions suggest a rise in sea level of >100m during the early Pliocene (Fig 4.2, Haq et al., 1987) which suggests a warming of the climate and could account for the transition from downslope to alongslope sedimentation on the West Shetland Slope based on the assumption that convection and generation of deep waters north of the Faeroe Shetland Basin is most active during periods of reduced glaciation (e.g. Alley et al., 1999).

#### 4.7.1.3. Glacial influences

The identification of iceberg plough marks on the PL40 surface is taken as strong evidence of significant glaciation affecting the Faeroe Shetland Basin and surrounding region during the deposition of the WSD. This is supported by large scale fluctuations in eustatic sea level which are related to growth and decay of polar ice sheets (Fig 4.2, Haq et al., 1987).

Glaciation was also proposed by Knutz and Cartwright (2004) as the cause of Pliocene/Pleistocene slope instability on the West Shetland Slope. Present day icebergs sourced from glaciers and ice shelves are not generally seen to scour the sea bed in water depths greater than 100 and 300-400m respectively (Lygren, 1997; Polyak, 1997; Wadhams, 2000). Iceberg scours on the Lomonosov Ridge in the Arctic Ocean were formed in water depths in excess of 900m during the Pleistocene (Polyak et al., 2001) and other scours in water depths up to 800m on high latitude continental margins are interpreted to be relict plough marks which were formed during recent glacial periods by very large icebergs calved from ice sheets during low sea level (Barrie, 1980). In addition, the width and depth of a plough mark is a function of the size of the iceberg which formed it, which in turn is controlled by the size of the ice sheet from which the iceberg was calved (Clark et al., 1989), and plough marks created by modern icebergs are reported to have average depths 0.5-5m (Bass and Woodworth-Lynas, 1988; Vogt et al., 1994). The plough marks on PL40 are found at 750-1000mbsl at present. The possibility of up to 500m of post PL40 subsidence (see section 4.3.2) allows us to estimate an upper limit of 250-750±100m water depth,

including 100m eustatic sea level fluctuation, for the formation of the iceberg plough marks. From this we suggest that the icebergs which scoured PL40 in water depths of perhaps 500m or more and that produced plough marks up to 200m wide were most probably calved from ice sheet related ice bodies and not smaller scale valley glaciers. This argument, although based on uncertain estimates of post PL40 subsidence, suggests that the iceberg plough marking occurred during a period of significant glaciation resulting in icesheet development. This interpretation fits with proposed Pliocene-Pleistocene eustatic sea level fluctuations, related to ice sheet growth and decay (Fig 4.2, Haq et al., 1987)

The recognition of major iceberg plough marking in likely deep water conditions at PL40 raises the important question of the likely source ice sheet. The most likely source of such potentially large icebergs is thought to have been relatively local to the Faeroe Shetland Basin. Ice-rafted debris provenance of Pleistocene sediments from the Norwegian margin suggests that the icebergs which dropped the debris were most likely sourced from the Eurasian Ice Sheet (Thiede et al., 1998). Iceberg plough marks of late Pliocene-Early Pleistocene have been identified on the Northern Margin of the Faeroe Islands within contourite drift sediments and are at present 800mbsl (Nielsen & Van Weering, 1998). Other plough marks of late Pliocene age have been identified on the Haltenbanken off Mid-Norway (Long and Praeg, 1997). These additional examples of Pliocene iceberg activity lead us to suggest that the plough marks on the PL40 surface may represent an early major iceberg calving event in the Faeroe Shetland Basin/Southern Norway region during the Pliocene. This would fit with estimates of glacial expansion in the region proposed by other authors (Jansen et al., 1988; Poole and Vorren, 1993; Jansen and Sjöholm, 1991; Hjelstuen et al., 2005).

The formation of the Glacial Unconformity during the mid-Pleistocene (0.44Ma) by transgressing Northern Hemisphere ice sheets (Stoker, 1995, Stoker, 1999) marks the top of Unit 2, and is coincident with a major sea level fall (Fig 4.2, Haq et al., 1987). Analysis of iceberg plough marks on the Glacial Unconformity surface as imaged on 3D seismic gives mixed transport directions for the icebergs, similar to those observed on PL40. Similarly, a minimum estimate of c.300m paleo-water depth can be applied to the formation of the plough marks on the Glacial Unconformity (based on a maximum of 500m subsidence).

Seismically discernable evidence of alongslope current activity is absent within Unit 3, which implies alongslope-directed current activity along the upper slope was low and any activity which did occur was limited to the deep basin (Fig. 4.13d), as suggested by Stoker (1999).

#### *4.7.2. Palaeoceanographic development of the West Shetland Margin*

Based on our interpretation of depositional processes and approximate ages for Units 1-3 of the WSD Slope section, it is now possible to propose a preliminary paleoceanographic development of the West Shetland slope during the Pliocene-Pleistocene. The interpretation of a series of alongslope current related processes interspersed with indicators of glaciation within the WSD Slope section strongly indicates that its depositional history was influenced by episodes of increased and decreased glaciation.

Phases of glaciation during the deposition of the WSD Slope Section are interpreted to be accompanied by a disruption of thermohaline current activity on the West Shetland slope, evidenced by multidirectional iceberg plough marking and a lack of seismic characteristics synonymous with alongslope currents within known glaciation-process derived deposits (e.g. Unit 3). The formation of sea ice in the Norwegian-Greenland Sea/Arctic Ocean during glacial periods is believed to inhibit production of deep water to the north of the Greenland Scotland Ridge and as a result the thermohaline circulation which is active in the Faeroe Shetland Basin during interglacial periods (including the present day) breaks down (Alley et al., 1999; Rahmstorf, 2002). Reduced thermohaline circulation in the North Atlantic/Nordic Seas during glacial maxima has been proposed from a wide range of proxies (Duplessey et al., 1980; Oppo and Lehman, 1993; Keigwin and Lehman, 1994; Bond and Lotti, 1995; Manighetti and McCave, 1995; Adkins et al., 1997; Kissel et al., 1997; Paillard, 2001; Akhurst et al., 2002 & Groger et al., 2003). North Atlantic thermohaline circulation is thought to be active in three modes: modern (full thermohaline circulation), glacial (no deep water formation in the Norwegian Greenland Sea) and Heinrich (deep water formation virtually inhibited), which are discussed fully by Alley et al., (1999). Therefore, bottom currents in the Northern Hemisphere (and thus the Faeroe Shetland Basin) are most active during interglacials, when the global thermohaline circulation is in full operation (Rahmstorf, 1997; Alley et al., 1999; Marotzke, 2000). The exact behaviour of the water



masses within the Faeroe Shetland Basin during periods of glaciation is unknown, but there is evidence that there may be intra-basinal currents which flow around the basin and possible NE flow in the deep basin axis (pers comm. Doug Masson).

In light of these inferences, it is tentatively suggested that Unit 1a may have been deposited during a period of glaciation in the Northern Hemisphere (or Global) resulting in reduced thermohaline circulation (*sensu* Alley et al., 1999) which slowed the flow of rapid alongslope currents through the Faeroe Shetland Basin, halting the formation of the INU and promoting the development of a downslope sedimentary system (Fig. 4.13a). Global sea level and climate are known to have fluctuated during the late Miocene-early Pliocene (Haq et al., 1987, Fig. 4.2), and thermohaline circulation fluctuations are recorded during this time (Kennett, 1986; Fronval and Jansen, 1996; St John and Krissek, 2002). Therefore it is possible that the formation of the INU was the result of climatic changes resulting in vigorous thermohaline circulation through the Faeroe Shetland Basin (Wright and Miller, 1996), potentially enhanced by tectonic adjustments (Stoker, 1999), and other global changes such as the closure of the Panama Isthmus at 4.6Ma (Lear et al., 2003). The initiation of downslope deposition may also correlate to the proposed cooling. Downslope depositional systems are often formed during periods of glaciation as a result of denudation of the continents by ice (Reading, 1986). The lack of direct indicators of glaciation, such as iceberg plough marks, may suggest that the Faeroe Shetland Basin was not subjected to localised glaciation directly, but was influenced by a eustatic sea level fall.

In contrast, the deposition of Units 1b and 2 during the Pliocene-mid Pleistocene by Northern Component Water may correlate with fluctuating degrees of glaciation in the Northern Hemisphere. Coeval accumulation of the WSD Slope and Basin sections at this time suggests large scale SW flow of deep waters from the Nordic Seas into the North Atlantic (Figs. 4.13b & c), perhaps similar to that observed today. Similar past circulation patterns to that of the present have been proposed by previous authors (Damuth and Olsen, 2001; Knutz and Cartwright, 2003). The apparent continuous sedimentation of the base of slope moat system from the early Pliocene onwards also suggests that thermohaline circulation may occur through the Faeroe Shetland Basin during periods of glaciation, but is restricted to the deeper basin. The formation of PL40 by initial alongslope current erosion

followed by a period of iceberg presence which suggests a disruption of thermohaline circulation may represent the interruption of relatively icesheet free conditions and contourite deposition by a period of glaciation (Figs 4.13b&c). The occurrence of rare and isolated plough marks within Unit 2 hints at the possibility of numerous fluctuations in climate and/or thermohaline circulation during its deposition, and climatic fluctuations have been proposed from other proxies during the Pliocene and early Pleistocene (Raymo et al., 1989; Thiede et al., 1998). Further evidence for glaciation during the deposition of Unit 2 are ice rafted debris accumulations in synchronous basinal sediments (Stoker, 1999) and debris flows within the WSD Basin section. Headwall scarps associated with these slope failures are present within Unit 2, and the slope instability is linked to glaci-eustatic sea level fluctuations during Pliocene-Pleistocene ice sheet growth and retreat (Knutz and Cartwright, 2004). These direct glacial indicators correlate well to fluctuations in eustatic sea level throughout the same time interval related to ice sheet fluctuation (Fig 4.2, Haq et al., 1987).

Based on the resolution of the data available to this study it is not possible to comment upon the nature of the periods of glaciation which affected the basin throughout the late Neogene. Instead this work is intended to supply evidence for glaciation within the basin and surrounding region throughout the late Neogene, and to comment upon the resultant effect on sediment deposition. Coring and geophysical logging of the WSD Slope section would shed further light on the initial interpretations presented here.

## 4.8. Conclusions

- 1) The WSD Slope section consists of a plastered contourite drift that was deposited coevally with the WSD Basin section during the Pliocene-Pleistocene by SW flowing Northern Component Water thought to be comparable to the present day SW flowing deep waters within the Faeroe Shetland Basin.
- 2) The WSD Slope section is comprised of 3 Units with initial downslope channel and levee formation subsequently overwhelmed by alongslope currents and contourite deposition during the early Pliocene.

- 3) Throughout the Pliocene-Pleistocene, the West Shetland margin was significantly influenced by thermohaline currents (Units 1b and 2), inferred to have been flowing toward the SW at velocities between c.10-30cm/s<sup>-1</sup>.
- 4) Thermohaline current flow along the West Shetland margin during the Pliocene-Pleistocene was punctuated by glacial periods during which thermohaline current activity appears to be perturbed (i.e. PL40). Contourite drift deposition is thought to have occurred predominantly during interglacial periods.
- 5) The WSD Slope section may potentially contain a record of the switching between distinct modern/glacial/Heinrich modes of the North Atlantic Ocean circulation, represented seismically by glacial indicators such as iceberg plough marks within contourite drift deposits.
- 6) Coring and detailed analysis of the WSD Slope section is needed to test the interpretations made during this study, as industrial sampling of non-prospective intervals does not supply the required resolution or accuracy.
- 7) 3D seismic data is an extremely useful tool for extracting paleoceanographic information from contourite drifts. It is particularly applicable to identification and analysis of small scale architectural elements exemplified by the discovery of the PL20 sediment wave field and the PL40 iceberg plough marks.

## Chapter Five: Discussion

### 5.1. Introduction

A combination of industrial seismic and well data have been used during this study to investigate and characterise the Cenozoic sedimentary succession of the Faeroe-Shetland Basin in order to reconstruct the history of thermohaline current circulation through this key oceanic gateway. The comprehensive database available to the study allowed the interpretation of features over a range of scales from regionally extensive depositional units over 100's km to small scale architectural elements with vertical and horizontal dimensions of 10's-100's m. As a result of the multi-scale approach to the investigation, the thesis is broken down into three main chapters which consider the initiation (*chapter 2*), evolution (*chapter 3*) and detail (*chapter 4*) of contourite sedimentation within the basin.

The first aim of this chapter is to synchronize the observations and interpretations of the previous 3 chapters in order to produce a comprehensive synthesis of the evolution of the Faeroe-Shetland Basin as an oceanic gateway throughout the Cenozoic. Secondly, this chapter aims to comment on the efficacy of industrial seismic data as a tool for contourite research both specifically within the Faeroe-Shetland Basin and in general. This section will also compare the data and interpretations of previous seismic data based investigations within the basin to the results from this study in order to highlight the significance of advances in seismic acquisition, processing and manipulation. The issue of limitations pertaining to the use of industrial data for contourite research specifically within the Faeroe-Shetland Basin and also in general is then tackled in order to highlight some of the limits associated with the research method. Finally, future avenues of research are discussed, both within the Faeroe Shetland Basin and more regionally. The discussion begins with a summary of the research results from the three key chapters.

## 5.2. Results summary

### *5.2.1. Chapter Two: Eocene contourite drifts and initiation of overflow across the Greenland Scotland Ridge*

The primary aim of chapter 2 was to identify the earliest evidence for contourite drift deposition within the Faeroe Shetland Basin in order to establish the time at which the basin was established as an oceanic gateway, represented sedimentologically by the transition between the slope process-dominated regime of the Eocene and contourite sedimentation of the Oligocene-Neogene. The combination of high resolution seismic data and BGS core 99/3 resulted in the identification of a significant contourite drift at the southern end of the basin, which was deposited between the early middle Eocene (Lutetian) and at least the late Eocene (Priabonian) (Fig. 5.1). Deposition of the 800m thick drift throughout this time was used as evidence for a significant, long lived flow of deep waters from the Norwegian Greenland Sea through the Faeroe Shetland Basin and into the North Atlantic. This interpretation suggests that the initiation of formation of deep water, through thermal densification of surface inflow waters, within the Norwegian Greenland Sea began far earlier than the early Oligocene, which was previously thought to represent the onset of contourite deposition within the basin.

### *5.2.2. Chapter Three: Late Palaeogene and Neogene contourites and palaeoceanographic evolution of the Faeroe Shetland Basin*

Chapter 3 was intended to form a continuation of chapter 2 in determining the role of the Faeroe Shetland Basin as a conduit for the passage of deep water currents from the Norwegian Greenland Sea into the North Atlantic throughout the Oligocene and Neogene. In order to achieve this, the stratigraphy of the basin was divided into units on the basis of identification of key marker reflections, which were in turn calibrated with existing stratigraphic nomenclatures in order to reconcile the various stratigraphic divisions of the basin. The study concluded that the Faeroe Shetland Basin acted as a conduit for SW flowing deep waters throughout the Oligocene, Miocene and Pliocene (Fig. 5.1), and that the water mass structure within the basin was likely similar to that at present. Furthermore, the contourite deposition within the basin was punctuated by at least two major episodes of erosion, the first during the Miocene during which erosion was limited to the basin of the

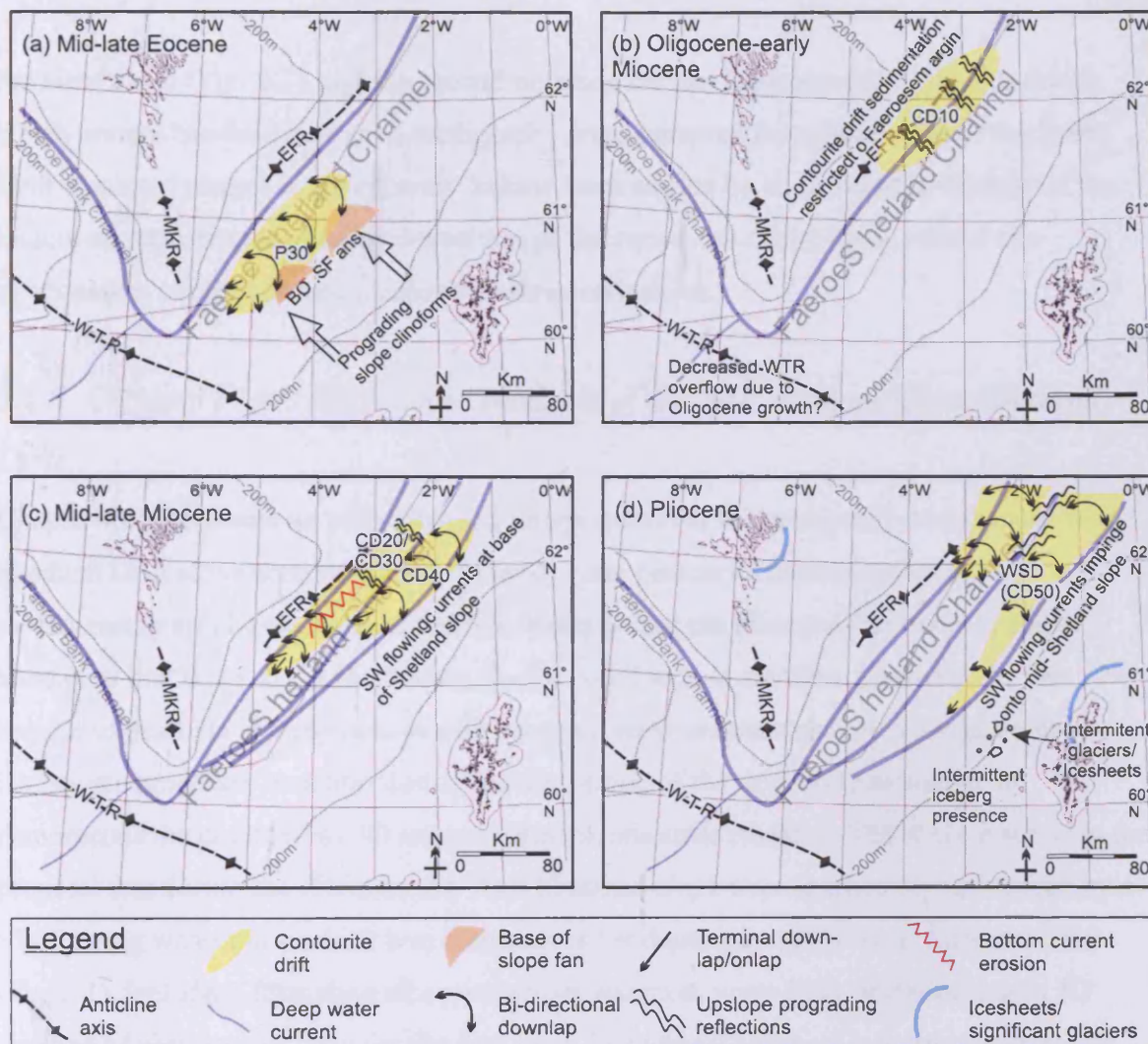


Figure 5.1

Palaeogeographic map time series to illustrate sedimentological and palaeoceanographic history of the Faeroe Shetland Basin. Abbreviations: WTR, Wyville Thompson Ridge; MKR, Munkagrunnar Ridge; EFR, East Faeroes Ridge.

(a) Southwesterly flow of Northern Component Water through the basin as part of the North Atlantic Conveyor Belt began in the mid-Eocene (Lutetian) and resulted in the deposition of the P30 elongate mounded contourite drift (*Chapter 2*) within the southern basin axis. Contemporaneous slope progradation from the Shetland Margin resulted in intercalation of contourite drift and base of slope fans (B.O.S fans). The depositional currents are thought to have exited through the Faeroe Bank Channel with potentially significant overflow of the nascent Wyville Thompson Ridge. (b) Oligocene early Miocene contourite sedimentation was concentrated on the Faeroese margin (CD10, *Chapter 3*), characterised by combined upslope prograding contourite drifts with sheeted drifts. Note restriction of bottom currents to the Faeroese margin. Overflow across the Wyville Thompson Ridge may have been reduced due to growth on the structures during the Oligocene.

(c) During the mid-late Miocene, both upslope prograding and mounded elongate contourite drifts were deposited on the Faeroese margin (CD20 and CD30, *Chapter 3*), with sedimentation and currents influenced by the newly formed East Faeroes Ridge. Rapid middle Miocene bottom currents caused erosion of the base of the Faeroes slope (UC1, *Chapter 3*), particularly in the area of the East Faeroes Ridge. CD40 was deposited as a mounded elongate drift in the basin axis during the mid-late Miocene, signifying the increase in distribution of SW flowing bottom currents within the basin as far as the base of the Shetland slope.

(d) During the Pliocene, following the formation of the INU during the late Miocene-early Pliocene, SW flowing bottom currents reached the mid-Shetland Slope, and deposited the West Shetland Drift (WSD, *Chapter 4*). The WSD basin section was characterised by sheeted, infilling drifts, while the WSD slope section formed a tapering elongate plastered drift. During this time rapid, non depositional SW current flow is envisaged on the Faeroese margin. At intermittent periods, icesheets discharged icebergs into the basin, during which times alongslope current activity was reduced.

Faeroese slope (Fig. 5.1), and the second between the late Miocene-early Pliocene during which several hundred metres of stratigraphy were removed from large areas of the basin. Both erosional phases are interpreted to have been caused by an increase in velocity of the bottom currents responsible for deposition of the contourite drifts, likely related to a combination of climatic and localised tectonic influences.

### *5.2.3. Chapter Four: 3D seismic analysis of the late Neogene West Shetland Drift*

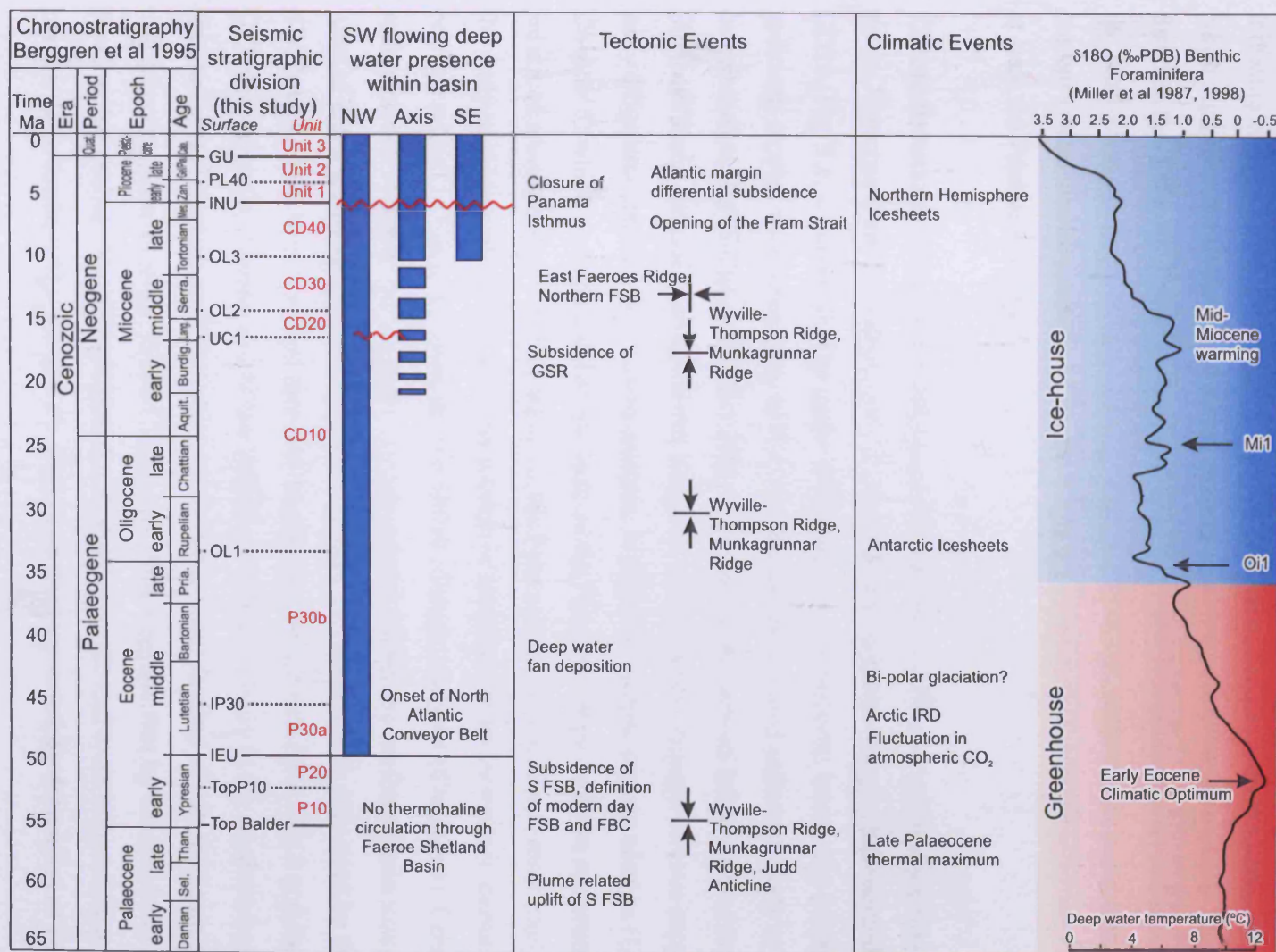
Chapter 4 concentrates on more detailed interpretation of the previously documented West Shetland Drift slope section in order to investigate contourite sedimentation and palaeoceanographic conditions within the basin during the Pliocene-Pleistocene, and to attempt to link these to the fluctuating glacial conditions at the time. Furthermore, the chapter utilised 3D seismic data to analyse small scale architectural elements in order to investigate processes in action during the deposition of the drift body as well as to demonstrate the potential of 3D seismic data to contourite research. The study resulted in the proposal that during the Pliocene the West Shetland slope was significantly influenced by a SW flowing water mass which was responsible for deposition of the West Shetland Drift (Fig. 5.1), including formation of a spectacular sediment wave field, and resulting in 3D imaging of such a wave field for the first time. The identification of iceberg plough marks also allowed for the interpretation that the flow of alongslope currents through the basin is disrupted during periods of glaciation.

## 5.3. Cenozoic evolution of the Faeroe Shetland Basin

### *5.3.1. Summary of alongslope current sedimentation*

The preceding three chapters of this thesis each tackle a specific interval of time and scale of study which provide the constituent components of the history of bottom current flow and contourite sedimentation within the Faeroe Shetland Basin. Therefore, this section aims to combine and summarise the main results from each chapter, thus providing an overview of the palaeoceanographic history of the Faeroe Shetland Gateway. The sedimentological and palaeoceanographic history of the basin is related to local and regional tectonic events and climatic fluctuations in Figure 5.2.





**Figure 5.2**  
Cenozoic event history diagram summarising sedimentological and palaeoceanographic evolution of the Faeroe Shetland Basin and key associated tectonic and climatic events. Note that the Faeroe Shetland Basin was present in a form similar to its modern day expression prior to contourite deposition. The two erosion events within the basin (UC1 and INU, represented by red wavy lines at the mid Miocene and the late Miocene-early Pliocene respectively) correspond to tectonic events (subsidence and folding) and climatic events revealed by the  $\delta^{18}\text{O}$  curve. Note also that the distribution of SW flowing deep waters within the basin increases throughout the Cenozoic in relation to global climatic cooling. Abbreviations: FSB- Faeroe Shetland Basin; FBC- Faeroe Bank Channel; GSR- Greenland Scotland Ridge. References for all events documented within chapter.

The earliest indicators of Cenozoic bottom current flow through the Faeroe Shetland Basin are provided by the Intra Eocene Unconformity and the Unit P30 contourite drift located in the Judd Basin area of the southern Faeroe Shetland Basin (Figs. 5.1 & 5.2, *Chapter 2*). It is proposed that subsidence of the Judd Anticline coincident with the withdrawal of the proto-Icelandic plume from the base of the crust during the early Eocene (Turner and Scrutton, 1993; White and Lovell, 1997; Nadin et al., 1999; Smallwood and Gill, 2002) permitted the initiation of through-flow of deep waters formed in the Norwegian-Greenland Sea into the North Atlantic via the Faeroe Shetland Basin. The initiation of the deep water connection is dated as the Ypresian/Lutetian boundary (Fig. 5.2), and is represented by erosion that formed the Intra Eocene Unconformity in water depths of c.450m, followed by a stabilisation of the current system and deposition of the thick Unit P30 contourite drift between the Lutetian and at least the Priabonian (Fig. 5.1).

Contourite sedimentation was continuous through the late Eocene and early Oligocene, with early Oligocene contourite deposition shifting to the Faeroese margin, represented by Unit CD10 (Fig. 5.1, *Chapter 3*). The cause of the shift in depositional locus may be related to sediment supply, with reworking of Eocene downslope derived sediment likely to have contributed to the formation of Unit P30, while sediment derived from north of the Faeroe Shetland Basin including a significant biogenic component is thought to have supplied the early Oligocene drift on the Faeroes margin. A phase of bottom current erosion (UC1, *Chapter 3*) which was focussed at the base of the Faeroese slope and was apparently enhanced around newly forming folds on the Faeroese margin occurred most likely during the early-mid Miocene (Fig. 5.2). The erosion is attributed to an increase in current velocity, perhaps related to basin tectonics and/or global climatic changes (*Chapter 3*). Contourite sedimentation resumed on the Faeroese margin and within the northern basin axis in the form of Units CD20 and CD30, which are interpreted to have been deposited by the same SW flowing deep water current that previously deposited Units P30, CD10 and formed the UC1 unconformity. Deposition of the infilling CD30 drift body in the northern basin axis resulted in burial of topography created by contractional folding within the basin during the mid Miocene (Davies et al., 2004; *Chapter 3*). This suggests that by the mid Miocene, SW flowing deep waters had spread from the Faeroese margin and were influencing a wider portion of the basin (Figs. 5.1 & 5.2). This is further supported by deposition of Unit CD40

during the late Miocene, which forms an elongate mounded drift body deposited within the basin axis and strongly suggests the impingement of SW flowing deep waters onto the lower Shetland slope (Figs. 5.1 & 5.2, *Chapter 3*).

The proposal of increased spatial influence of SW bottom currents throughout the Neogene is based on contourite distribution and is strongly supported by the formation of the Intra Neogene Unconformity during the late Miocene-early Pliocene (Fig. 5.2). The unconformity, which extends throughout the basin and represents erosion of several hundred metres of stratigraphy from the both margins and the southern basin axis (*Chapter 3*), is interpreted to have been caused by the action of SW flowing bottom currents distributed throughout the basin with a water mass structure similar to that at present (*Chapter 3*). Contourite deposition resumed following the erosion phase, resulting in deposition of the West Shetland Drift system (*Chapter 4*). Deposition during the Pliocene-recent was concentrated on the Shetland Margin, with SW flowing deep water impinging the mid-Shetland slope (Figs. 5.1 & 5.2, *Chapter 4*), similar to the present day situation where the boundary between SW deep waters and NE surface waters lies at 400-600m (Turrell et al., 1999; Masson, 2001).

In summary, the Faeroe Shetland Basin became a conduit for the passage of deep waters from the Norwegian Greenland Sea into the North Atlantic during the early middle Eocene. From this time the deep waters have been focussed on the Faeroese margin as a result of the Coriolis Force. However, throughout the Miocene and Pliocene, the extent of deep water influence has grown, resulting in the development of the present day water mass structure by the late Miocene-early Pliocene.

### *5.3.2. Correlation with Cenozoic global change*

#### *5.3.2.1. Development of the Faeroe Shetland Basin as an oceanic gateway*

It is possible to correlate key events in the evolution of the Faeroe Shetland Basin to extra-basinal events, both local to the basin and global. The onset of bottom current flow between the Norwegian Greenland Sea and the North Atlantic through the Faeroe Shetland Basin represents the birth of the basin as an oceanic gateway. The timing of the event appears to be the result of a combination of factors which combined during the early middle Eocene. During the Palaeocene the Faeroe Shetland Basin consisted of a well defined deep water

basin (Mitchell et al., 1993; Lamers and Carmichael, 1999) and because the Wyville Thompson Ridge was yet to form (Boldreel and Andersen, 1993) was probably opened to the south into the Rockall Trough/North Atlantic. Therefore, at this time the basin could have acted as a conduit for deep waters. However, the early Palaeogene was characterised by global greenhouse conditions, with warm polar sea surface temperatures and a low latitudinal temperature gradient (Barron, 1987; Miller et al., 1987; Zachos et al., 1993, Zachos et al., 2001; Lear et al., 2003). Furthermore, the Fram Strait was closed, forming a barrier between the Arctic Ocean and the Norwegian Greenland Sea (Lawver, 1990), which combined with the climatic conditions would have resulted in diminished potential for deep water generation north of the Faeroe Shetland Basin. Late Palaeocene-early Eocene uplift of the Faeroe Shetland Basin (Nadin et al., 1997; Doré et al., 1999; Naylor et al., 1999) resulted in sub-aerial exposure of the southern end of the basin (Smallwood and Gill, 2002), which is interpreted to have formed an emergent land bridge characterised by a delta top depositional environment (*Chapter 1, coals in wells*) and providing a route for the migration of land mammals between the Eurasian and North American continents (Nielsen, 1983). Consequently, this land bridge would have formed a barrier to deep water connection between the Norwegian Greenland Sea and North Atlantic, thus removing the potential for deep water mass exchange. Subsidence of the uplifted southern Faeroe Shetland Basin during the early Eocene (Mitchell et al., 1993; Naylor et al., 1999; Smallwood and Gill, 2002) was coincident with a cooling of high latitude sea surface temperatures and an increase in latitudinal temperature gradient (Barron, 1987; Zachos et al., 1993, Zachos et al., 2001; Lear et al., 2003) that would have permitted the formation of deep waters by thermal densification in the Norwegian Greenland Sea. Therefore, the coincidence of tectonic adjustment and global climatic conditions appear to have resulted in the initial establishment of the Faeroe Shetland Basin as a deep water gateway during the middle Eocene.

#### 5.3.2.2. *Palaeoceanographic evolution*

Throughout the Oligocene and Miocene, the area of the basin influenced by SW flowing deep waters is proposed to have increased, based on the locus of contourite deposition, from apparent restriction to the Faeroese margin during the Oligocene to influencing the entire basin during the late Neogene. The restriction of SW flowing depositional currents to the western side of the basin is as a result of the Coriolis Force. An increased volume of SW

flowing deep water throughout the Oligocene and Miocene as a result of increased deep water production in the Norwegian Greenland Sea could account for the increase in distribution of SW flowing water within the basin throughout this time.

A theoretical argument for a potential cause of an increase in deep water flux through the basin between the Oligocene and the Pliocene can be presented as follows. The production of deep water at present relies on a latitudinal temperature gradient between the tropics and the pole, thus permitting cooling of warmer surface waters at high latitudes and resulting in thermal densification and sinking (Broecker and Denton, 1990; Broecker, 1991; Rahmstorf, 2002). In turn, the generation and sinking of deep water translates a vertical pressure gradient into a lateral pressure gradient at depth, resulting in lateral flow of deep water as bottom currents (Pickard and Emery, 1990, Broecker, 1991). Therefore, an increased rate of deep water production would result in increased lateral pressure gradients and increased deep water flux. The rate of heat loss from the surface waters to the atmosphere thus exerts a control on the rate of deep water formation, along with additional factors such as salinity. Exchange of heat from the surface waters to the atmosphere is achieved through long wave radiation, conduction and evaporation. Estimation of the values of palaeo-radiation and evaporation is not possible due to the unknown variation in factors which affect their rate, such as humidity, wind regime, cloud cover and solar insolation. However, loss of heat from the sea surface to the air via thermal conduction ( $Q_h$ ) can be commented on as it is proportional to the temperature gradient between the sea surface and the air ( $dt/dz$ ), heat conductivity ( $A_h$ ) and the specific heat of air at a constant pressure ( $C_p$ ) (Pickard and Emery, 1990) as:

$$Q_h = - C_p * A_h * dt/dz$$

The rate of heat loss via conduction is proportional to the temperature gradient between the sea surface and the air. Therefore, assuming the heat conductivity and specific heat of air are constants, as the temperature gradient increases (i.e. the sea surface temperature increases relative to the air temperature), the rate of heat loss will increase.

During the Oligocene to early/mid Miocene, polar sea surface temperatures (and adjacent air temperatures) averaged c.4C°, and further cooling during the mid/late Miocene resulted in

polar sea surface temperatures of  $<2^{\circ}\text{C}$  (Fig. 5.2, Zachos et al., 2001; Lear et al., 2003). Conversely, tropical sea surface temperatures remained relatively stable throughout the Cenozoic at near modern values ( $23\text{--}27^{\circ}\text{C}$ , Barron, 1987; Zachos et al., 1993). As a result, the latitudinal temperature gradient would have increased, leading to increased transport of warm tropical surface waters to polar regions. This in turn would lead to an increase in the temperature gradient between the sea surface and the air, based on an increase in the tropical sea surface temperature relative to the polar air temperature, resulting in an increased rate of conductive heat loss from the sea to the atmosphere. As documented above, thermal densification of surface waters leads to generation of deep waters and an increased rate of heat loss would lead to increased cooling and thus increased deep water generation. In turn, increased deep water generation would induce stronger vertical and lateral pressure gradients, and thus an increase in deep water flux. This increase in deep water volume could account for the proposed increase in deep water flux through the Faeroe Shetland Basin based on observations of increased distribution of contourite drifts within the basin throughout the Oligocene and Neogene.

The same principal would account for the dominance of contourite deposition on the Shetland margin during the Pliocene and at present. The present day interglacial conditions are thought to be optimal for deep water production within the Norwegian Greenland Sea and consequent SW current flow through the Faeroe Shetland Basin. As described above, deep water formation in the Norwegian Greenland Sea is most prevalent during periods of greatest latitudinal temperature gradient between the tropics and the poles. However, during glacial periods, deep water formation is shut off to the north of the Faeroe Shetland Basin as a result of sea ice coverage, and shifts south of Iceland (Alley et al., 1999; Rahmstorf, 2002). Conversely, periods of global greenhouse conditions during which polar sea surface temperatures are much warmer than at present and thus the latitudinal temperature gradient is diminished are characterised by lower rates of deep water formation (Huber et al., 2003). The present day interglacial conditions of warm tropics and ice at the poles therefore provide the optimum conditions for deep water formation in the Norwegian Greenland Sea and Arctic Ocean. The Pliocene epoch was characterised by fluctuating degrees of glaciation and icesheet volume in the Northern Hemisphere (Raymo et al., 1992; Billups et al., 1998; Zachos et al., 2001; Draut et al., 2003). Analysis of the West Shetland Drift slope section

(Chapter 4) reveals that during periods of significant sea ice presence, the alongslope current regime within the basin appears to have been diminished, particularly on the Shetland slope. As a result, the West Shetland Drift slope section contourites are interpreted to have formed in interglacial and interstadial periods (Chapter 4). Therefore, the shift in SW bottom current locus from the Faeroese margin to the west Shetland slope between the Oligocene and Pliocene could be accounted for by a change in global climatic conditions which resulted in an increase in latitudinal temperature gradients, increasing the rate of heat transfer to the atmosphere, and thus increasing the rate of deep water production.

It is fully acknowledged that the evolution of the climate system throughout the Cenozoic and the formation and circulation of deep waters are extremely complex and variable, and therefore that the estimates based on thermal conduction are grossly simplified. Instead, the concept is intended as speculation on the potential causality of the changing patterns of bottom current circulation within the Faeroe Shetland Basin proposed to have occurred through the Cenozoic. Further comment would require estimations of sedimentation rates, sediment composition and high resolution internal reflection configurations as well as more precise dating which are beyond the scope of this study.

#### 5.3.2.3. Formation of the Intra-Neogene Unconformity

The formation of the Intra-Neogene Unconformity (INU) constitutes the most significant single event within the Neogene history of the Faeroe Shetland Basin in terms of its extent, magnitude, and palaeoceanographic significance, excluding perhaps the onset of deep water circulation. The general increase in deep water flux through the basin can account to some extent for the distribution and mechanism for erosion. However, the lack of other regional, large magnitude erosion events suggest that formation of the INU was an extraordinary event within the basins history. Furthermore, timing of formation of the INU is coincident with other global events which may have influenced its formation (Fig. 5.2). It has been previously suggested that the formation of the INU was associated with differential subsidence of the Faeroe Shetland Basin in association with fluctuations of the Iceland plume (Wright and Miller, 1996; Stoker, 1999; Stoker, 2003, Stoker et al., 2005), and the final closure of the Panama Isthmus (Fig. 5.2) which is thought to have resulted in increased flow of warm saline surface waters northward into the Norwegian Greenland Sea (Lear et



al., 2003; Knutz and Cartwright, 2004). Differential basin subsidence and margin uplift is invoked for the European Atlantic margin during the late Neogene (Cloetingh et al., 1990; Doré and Jensen, 1996, Doré et al., 1999; Stoker, 2003), and may have influenced deep water circulation patterns through the Faeroe Shetland Basin (Stoker, 2002, Stoker, 2003). Furthermore, a connection between the Arctic Ocean, which at present is a site of prolific deep water formation and a major contributor to deep water flow through the Faeroe Shetland Basin (Turrell et al., 1999; Hansen and Østerhus, 2000) and the Norwegian Greenland Sea is reported to have existed from the late Miocene at around 7.5Ma (Fig. 5.2, *Chapter 2*, Lawver et al., 1990, Kristofferson et al., 1990). This timing coincides with the late Miocene-early Pliocene timing suggested for the formation of the INU (*Chapter 2*), and likely formed a significant contribution to deep water within the Norwegian Greenland Sea. The formation of the INU is therefore thought to have resulted from a combination of coincidental events, some of which were localised to the basin, and others global.

## 5.4. Utilisation of industrial data for contourite research

### 5.4.1. *Advantages of industrial seismic data*

Definitive identification of contourite deposits on land or in core is notoriously difficult, largely due to the predominantly large scale of contourite drifts and the interaction of alongslope and downslope processes, resulting in intercalation of contourite sediments with other facies such as hemipelagite, between which it can be difficult to distinguish (Faugères 1993; McCave, 1995b; Stow et al., 2002). In contrast, a documented range of criteria can be readily used to identify contourite drifts using seismic data (Faugères et al., 1999; Rebesco and Stow, 2001; Stow et al., 2002). In particular, the capacity to determine unit thickness distributions and internal reflection configurations has resulted in identification of a range of contourite drift morphologies, resulting in seismic data becoming the primary tool for contourite research. As a result, contourites have been identified around the globe using seismic data (e.g. Heezen et al., 1966; Faugères et al., 1993; Hollister, 1993; Marani et al., 1993; Niemi et al., 2000; Faugères et al., 2002; Lu et al., 2003; Wong et al., 2003 and *Sedimentary Geology* Vol. 82, 1993).

Contourite research is often based on seismic data either acquired specifically for the study or seismic data acquired by national geological surveys usually for the purpose of shallow section investigation in conjunction with petroleum exploration (e.g. Boldreel and Andersen, 1998; Stoker, 1998; Stoker, 2003). However, other studies have utilised the often vast seismic databases acquired for the purposes of petroleum exploration to specifically study contourite drifts (Bulat and Long, 2001; Davies et al., 2001; Knutz and Cartwright, 2003, Knutz and Cartwright, 2004). Industrial seismic datasets are particularly well suited to contourite research for a number of reasons:

1) Industrial datasets provide the coverage and depth of penetration necessary to investigate large scale and/or long lived contourite depositional systems, such as that present in the Faeroe Shetland Basin. The datasets commonly contain a combination of regional 2D seismic profiles and more localised 3D or high resolution 2D seismic surveys, providing the opportunity to delineate regional scale depositional systems and then identify and interpret small scale features in order to add detail to the regional picture.

2) The availability of 3D seismic data volumes allows detailed mapping and slicing of architectural elements in addition to attribute analysis which allow a far more detailed interpretation of contourite geometries and depositional systems than is possible with standard 2D data. High resolution 2D data provides the opportunity to investigate internal drift geometries with a vertical resolution of sub-10m which also increases the level of detail in the interpretation.

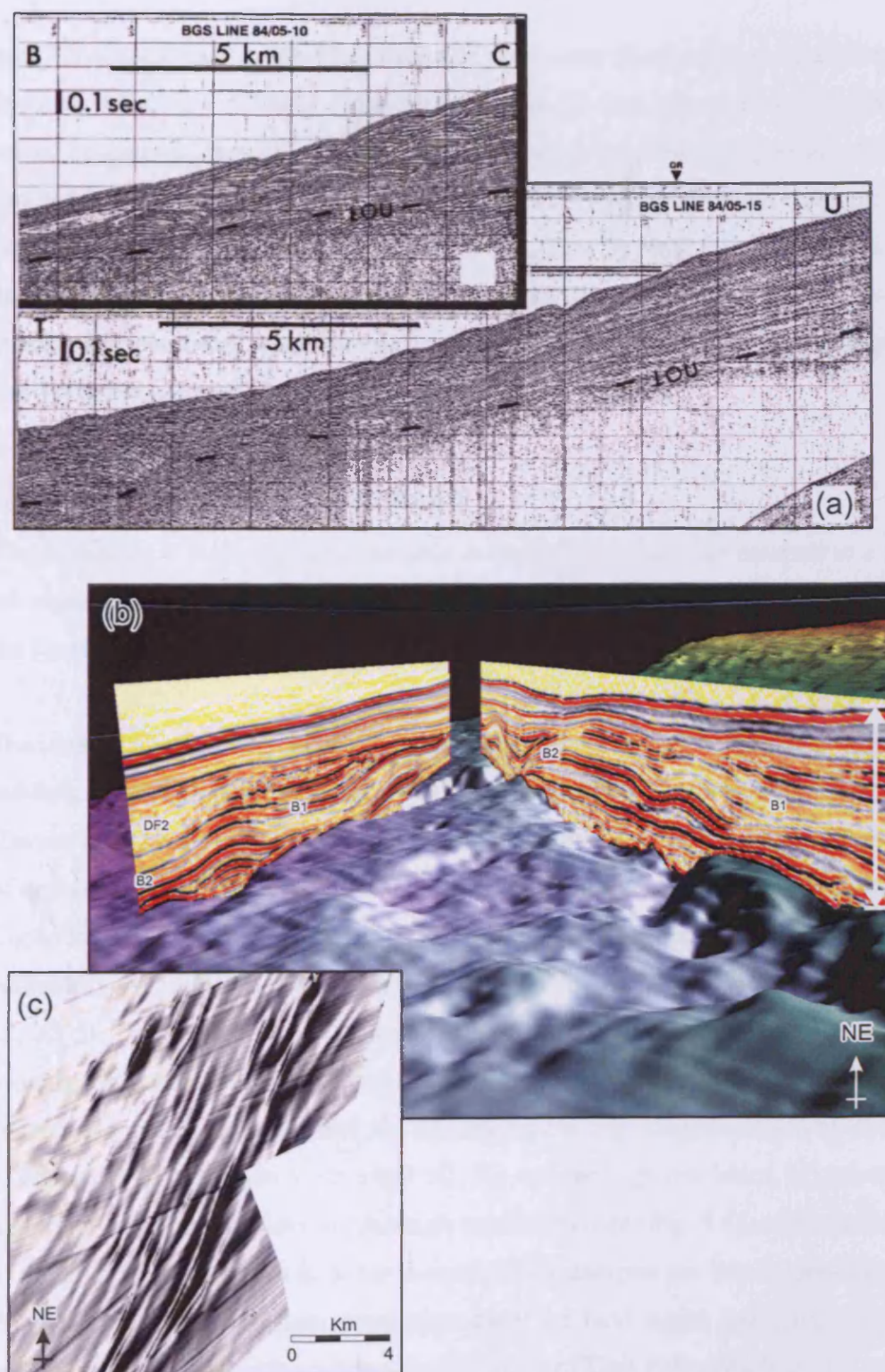
3) Recent advances in computer memory and visualisation has allowed the amalgamation of individual 3D seismic surveys into 'seismic mega-surveys' which provide continuous 3D seismic coverage over tens of thousands of km<sup>2</sup> (e.g. Central North Sea PGS mega-survey covers over 60000km<sup>2</sup>). This would therefore allow 3D seismic interpretation of large scale contourite systems, with the potential for regional attribute analysis. In addition to standard 2D and 3D seismic surveys which generally exhibit frequencies of a few 10's to c.150Hz, high resolution seismic with frequencies within the kHz range and seabed sidescan sonar are also acquired for the purposes of shallow section geohazard and rig placement assessment. These data provide very detailed information regarding the upper few hundred metres of the sediment pile, and the seabed, and allow detailed analysis of recent/shallow buried contourite drifts. Therefore, seismic databases collected for the

purposes of petroleum exploration can provide the range of scales, depths of penetration and resolution necessary for full investigation of contourite successions.

#### *5.4.2. Previous studies within the Faeroe Shetland Basin*

A number of previous studies document the occurrence of contourite drifts within the Faeroe-Shetland Basin based on interpretation of seismic data, much of it acquired by or allied to the petroleum industry. A specific example of advancements of understanding of the contourite drifts within the Faeroe Shetland Basin through increased quality and quantity of seismic data is presented below. Damuth and Olsen (1993) analysed the Neogene-Recent succession of the Faeroe Shetland Basin utilising high resolution 2D seismic profiles acquired by the BGS in collaboration with the petroleum exploration industry in a study carried out in conjunction with interpretation of the underlying Palaeogene succession in order to identify features within the Neogene which may be analogous to features in the prospective but less well imaged Palaeogene succession. In addition to a late Oligocene unconformity of bottom current origin, the post-Oligocene succession was found to contain a combination of downslope (mass flow) and alongslope deposits. A series of upslope prograding sediment waves at the base of the Shetland slope provided the best evidence for contourite sedimentation (Fig. 5.3a), but due to the limited 2D coverage, it was not possible to confidently determine the waves as contourite rather than turbidite in origin.

These features were also identified using GLORIA sonograph (Kenyon, 1987) but due to a lack of subsurface penetration could not be assigned an origin (Damuth and Olsen, 2001). A re-investigation of the stratigraphy by Damuth and Olsen (2001) utilising the entire BGS high resolution 2D seismic grid was designed to build upon the previous work. With the additional seismic profiles it was possible to reveal that the base of slope sediment waves were parallel to the slope, and thus were interpreted as of alongslope current origin, although it was still not possible to map the individual wave crests. Internal reflection configurations were used to suggest both SW and NE flowing depositional currents. The acquisition of a 3D seismic volume across the area of the waves which was released for academic study allowed detailed mapping and analysis of the waves resulting in effectively combining the seafloor and subsurface reflection mapping and analysis in a way that had not previously been possible (Knutz and Cartwright, 2003, Knutz and Cartwright, 2004). Bulat and Long (2001)



**Figure 5.3**

Comparison of imaging of upslope migrating sediment waves at the base of the Shetland Slope. Damuth and Olsen (1993, 2001) utilised BGS seismic profiles to identify the features (Fig. 5.3a), but were unable to interpret the features in detail or make maps of the seabed or subsurface reflections. The utilisation of 3D seismic data by Knutz and Cartwright (2004) allowed the mapping and 3D visualisation of the sediment waves (Fig. 5.3b), in addition to detailed mapping of the seabed expression (Fig. 5.3c) allowing a more confident interpretation of the features.

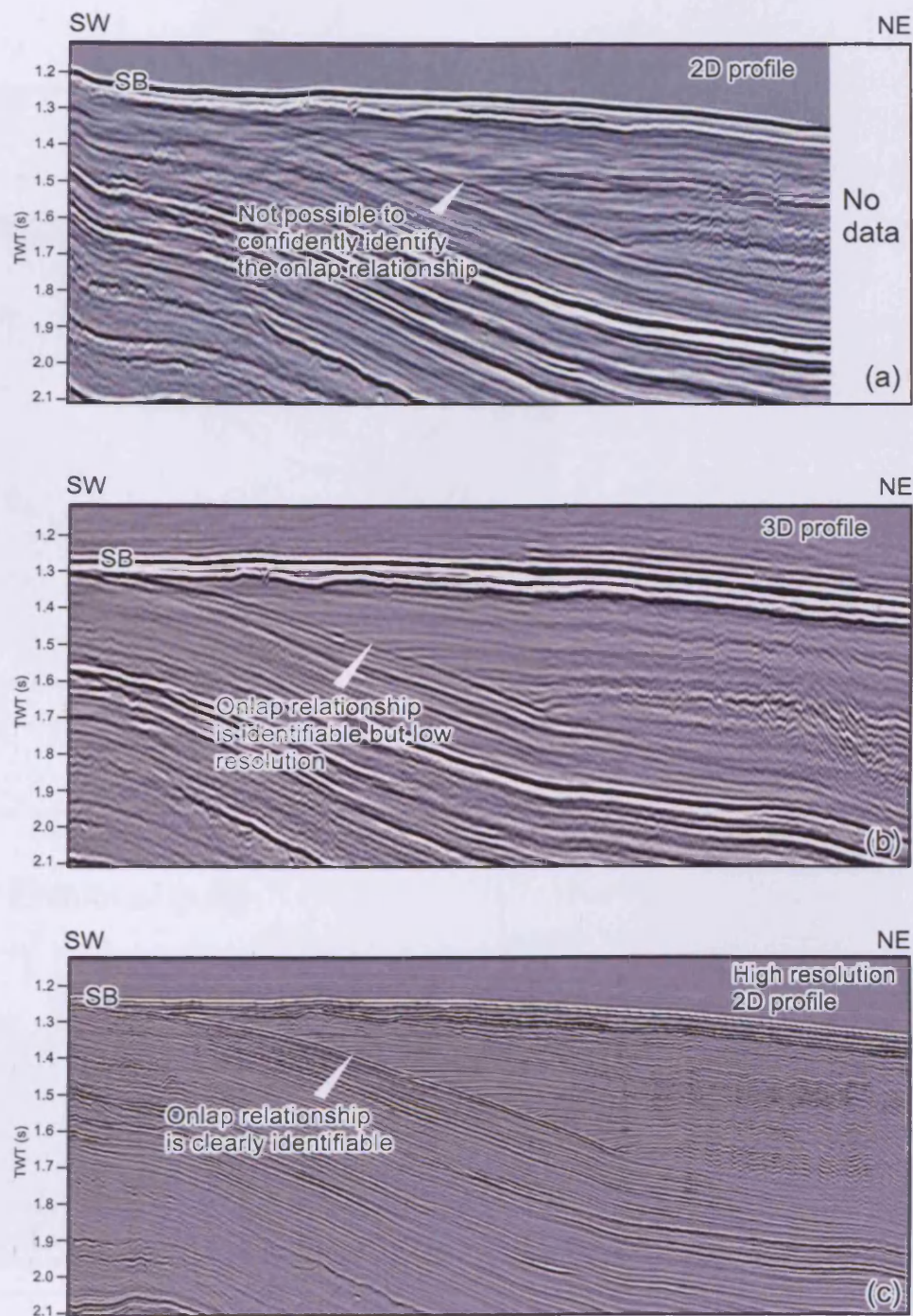
used 3D seismic data to map the seabed of the Faeroe Shetland Basin and identified the same features, referring to them as contourite mounds. 3D data was also used to visualise buried palaeo-seabed surfaces (Fig. 5.3b) and their modern day seabed expression (Fig. 5.3c) and resulted in the interpretation that the sediment waves were deposited by southwesterly flowing currents (Knutz and Cartwright, 2004). This increase in observational detail and understanding of the contourite waves at the base of the Shetland slope is directly related to increased seismic data quantity and quality, and demonstrates the value of high resolution and 3D industrial seismic data to future contourite research.

#### 5.4.3. *Advances made by this study*

The utilisation of industrial seismic data as part of this study has resulted in a number of advances in the understanding of contourite drifts and the history of bottom currents within the Faeroe Shetland Basin.

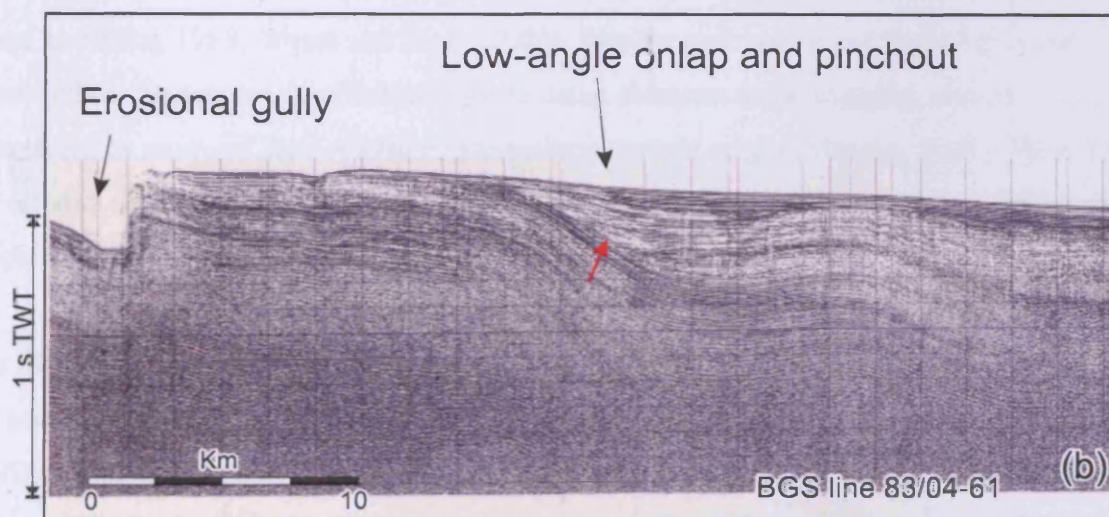
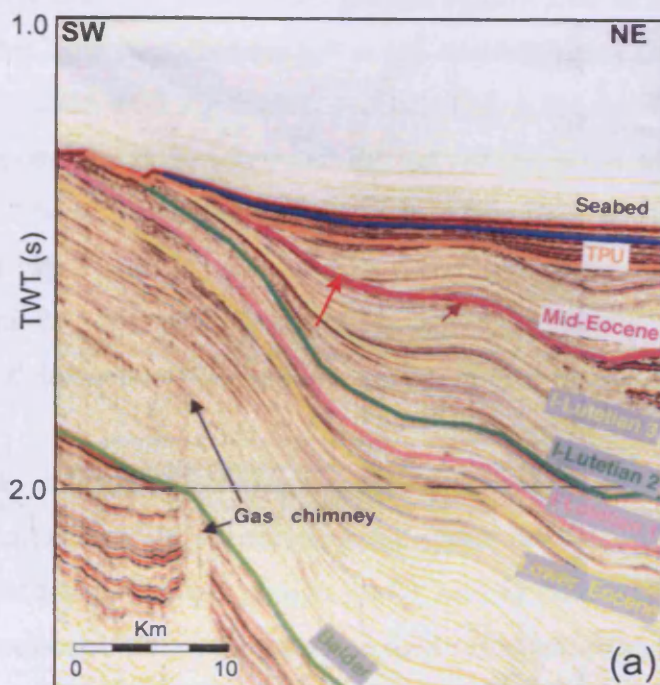
The identification of a middle Eocene contourite drift as part of this study suggests that published early Oligocene estimates for the onset of SW deep water flow through the basin (Davies et al., 2001) are far too young, and that Eocene estimates based on identification of unconformities within the North Atlantic (Berggren and Hollister, 1974; Miller and Tucholke, 1983) are closer to an accurate timing of onset than more recent Miocene estimates (e.g. Eldholm, 1990; Wold, 1994; Wright and Miller, 1996; Stoker, 2003, Stoker et al., 2005). The availability of high resolution seismic data was critical to this interpretation, proving the vertical resolution (sub-10m) necessary to confidently identify diagnostic reflection configurations such as the upslope aggrading onlap exhibited by the P30 drift (Chapter 2). Comparison of standard 2D, 3D and the high resolution 2D seismic data highlight the detail provided by the high resolution data (Fig. 5.4), and reveal the necessity of the high resolution data in order to confidently interpret the key onlapping relationship. Previously published seismic interpretations of the Judd region had identified the upslope prograding onlap that characterises the SW limit of Unit P30 using both the same data set (Smallwood, 2004) and high resolution BGS profiles (Howe et al., 2002) (Fig. 5.5). While Smallwood (2004) described a package that exhibited ‘smooth bi-directional (climbing) onlapping reflector geometries’ which he dated as middle Eocene in age (Fig. 5.5a), he did not recognise that the reflection geometry was characteristic of contourite drifts and thus did





**Figure 5.4**

Comparison of the quality and resolution of the standard 2D, 3D and high resolution 2D seismic data used in this study. The profile images the discrete onlap surface exhibited by the Eocene contourite drift within the basin (Unit P30, *Chapter 2*), and clearly shows that without the high resolution data it would not have been possible to identify the reflection configuration and thus interpret the contourite drift with such a high level of confidence.



**Figure 5.5**

Previous identification of the Eocene contourite drift Unit P30 (*Chapter 2*), indicated by red arrow. Smallwood (2004) identifies the upslope prograding onlap relationship exhibited by the contourite drift, but fails to identify it as such (Fig. 5.5a). Howe et al. (2002) identify the relationship as indicative of contourite drift deposition (Fig. 5.5b), but do not comment further on the age of the drift body and therefore its significance.



not identify the palaeoceanographic significance of the package. Howe et al., (2002) on the other hand identified the SW onlap relationship of Unit P30 as a contourite drift using high resolution BGS 2D seismic profiles (Fig. 5.5b), but did not comment on the age of the deposit or and therefore also did not recognise the palaeoceanographic significance of the drift body. The coupling of BGS borehole 99/3, which provided biostratigraphic dating, and the high resolution seismic data was critical in finally recognising the significance of the Unit P30 drift body. The result is that the onset of SW flowing deep water is estimated to predate the previous earliest estimate (Early Oligocene, Davies et al., 2001) by c. 15Ma.

The utilisation of 3D seismic data in *chapter 4* resulted in the identification and analysis of small scale architectural elements within the WSD Slope section, namely the sediment wave field and the iceberg plough marks, neither of which had been identified or analysed previously. The sediment wave field is distinct from that which is interpreted at the base of slope and is interpreted to be more akin to large mudwave fields discovered over vast areas of the deep ocean basins (Hollister et al., 1974; Embley et al., 1980; Normark et al., 1980; Flood and Shor, 1988; Wynn and Stow, 2002). Similar sediment wave fields have been identified on the present day Shetland slope using sidescan sonar imaging, and are interpreted as mud and sand waves of alongslope current origin (Masson, 2001). Therefore, 3D seismic data allows morphological comparison of ancient bottom current sediment wave fields with recent wave fields.

The identification of the iceberg plough marks within the drift body also provides detail on the accumulation of the drift body which it would not be possible to glean from 2D seismic profiles. The interpreted interruption of alongslope current flow during times when large icebergs (draft of several hundred metres) were present within the basin supports the proposal that deep water formation may shift south of the Greenland Scotland ridge during global cool periods (Alley and Clark, 1999, Rahmstorf, 2002). It also suggests the possibility that the deposition of intercalated alongslope and glacial deposits within the basin (e.g. Stoker et al., 1998, Stoker et al., 2002) may be broadly alternate and not synchronous within the basin.

## 5.5. Limitations and further study

### 5.5.1. Limitations of industrial data

#### 5.5.1.1. General limitations of industry data

The usage of industry seismic and well data for contourite research does have some limitations which are explored here. The issues are divided into two sections, firstly those concerning obtaining industrial data which record the presence of contourite drifts and secondly issues surrounding the quality of the data. Most importantly, industrial data is limited to areas of petroleum exploration, which means that contourite deposition and petroleum accumulation need to co-exist if industrial data is to be used to analyse contourite drifts. Fortunately, continental margins of ocean basins are often prospective petroleum provinces, and are also commonly associated with contourite deposition.

However, vast areas of contourite drift accumulation on the abyssal plains of the worlds oceans (e.g. Ewing et al., 1971; Embley et al., 1980) are largely out of reach of petroleum exploration, which has been limited to water depths of less than c.2km (Hurst et al., 2005), and/or are non-prospective. This results in large areas of contourite drift accumulation that are not covered by industry seismic data. Put differently, analysis of contourite drifts using industrial seismic data relies on the coincidence of contourite drifts and areas of seismic acquisition. Assuming contourites are present within a seismic dataset, the proprietary nature of the data can lead to problems in gaining access to the data and if granted, publishing of interpreted data. Furthermore, industrial seismic surveys, and in particular 3D surveys, are often very memory intensive (i.e. several Gigabytes) which can lead to data storage and management issues. In turn, storage and interpretation of industrial seismic data requires specialist hardware and software which are costly to purchase and maintain.

The primary objective of industrial exploration seismic and well data is to allow interpretation of prospective intervals, which, particularly on rifted continental margins, are often buried beneath a considerable thickness of ‘overburden’ of no economic interest. As a result, the processing of seismic data is tuned to give optimum imaging and resolution at the depths of prospective intervals, and lithological and geophysical information, in the form of logs and core, is acquired only through the intervals of interest. In most instances, the

utilisation of very large drill bits to complete the shallow section of the well resulting in very large diameter holes (c.60cm) renders the acquisition of geophysical logs impossible even if desired. As a result, the overburden, which is often the interval of contourite accumulation, is characterised by a potentially lower resolution seismic data with sparse well calibration.

#### *5.5.1.2. Limitations of industry data within the Faeroe-Shetland Basin*

The above issues firstly with the presence of contourite drift deposits within industry data sets and secondly with the potential for poorer data quality and quantity in the intervals commonly of interest for contourite research result in potential limitations to the application of industrial data to contourite research. However, the Faeroe-Shetland Basin provides an ideal location for the utilisation of industry data for the study of contourites through a combination of fortunate circumstances. Firstly, the basin is both an area of prolific petroleum exploration, resulting in the acquisition of a vast industrial seismic and well database, and a key present day oceanic gateway which has accumulated contourite drift sediments for the past 50Ma. Secondly, hydrocarbons have accumulated at multiple levels within the sedimentary succession, with accumulation in Eocene fans within c.1000m of the seabed, resulting in high quality seismic data coverage of the shallow section and a number of wells using a remotely operated vehicle to obtain sediment samples to calibrate the shallow section (see Davies et al., 2001; Davies and Cartwright, 2002). However, there are a number of limitations which affect the interpretation of Cenozoic contourites within the Faeroe Shetland Basin. The first main issue is the preferential distribution of seismic and well data toward the Shetland margin. Tilted fault block plays that are easier to access in the shallow water of the Shetland shelf and slope area (e.g. the Foinaven, Schiehallion and Clair fields, Mitchell et al., 1993; Lamers and Carmichael, 1999, Cooper et al., 1999), result in large amounts of seismic and well data on the West Shetland margin. Conversely, a relative lack of exploration of the Faeroese margin results from the presence of thick basalts which overlie the prospective interval and hamper seismic imaging (Smallwood et al., 2001) combined with deep water found in the basin axis result in a relative lack of seismic and well data within the basin axis and on the Faeroese margin. Secondly, the basinal Cenozoic succession within the Faeroe-Shetland Basin, which forms the predominant locus for contourite accumulation, is poorly calibrated by exploration wells resulting in a lack of detailed lithological and biostratigraphic constraint for the contourite deposits. Furthermore,

imaging of detailed reflection configurations associated with smaller scale features such as the sediment wave field (PL20, *Chapter 4*) and the detailed onlap relationships (Unit P30, *Chapter 2*) requires increased vertical resolutions which are afforded only by high resolution seismic surveys that are shot over smaller, specific areas. As high resolution seismic data is only available over select areas within the Faeroe Shetland Basin, it is not possible to fully analyse features such as the sediment wave field that are not present in the area of high resolution coverage.

### *5.5.2. Future study*

#### *5.5.2.1. Investigation of the onset of the North Atlantic Conveyor Belt*

In order to test the hypothesis proposed by this study that a circulation system analogous to the North Atlantic Conveyor Belt has been in action since the mid Eocene and throughout the Neogene, it would be logical to investigate other geographical areas that are key to the function of the North Atlantic Conveyor Belt at present. Based on investigation of published accounts on the evolution of the Greenland Scotland Ridge during this study, it is thought unlikely that deep waters were able to cross the ridge at locations other than the Faeroe Shetland Basin during the early middle Eocene.

Therefore, investigation of the northern Iceland Basin into which at present deep waters exit from the Faeroe bank Channel, and the northern Rockall Trough which receives some deep waters that overflow the Wyville Thompson Ridge may provide evidence for the flow of SW deep waters into the North Atlantic during the Eocene. Petroleum exploration has led to the acquisition of 2D seismic surveys within the Faeroe Bank Channel, thus providing potential data to begin to investigate these areas. Previous studies of the Gardar and Feni sediment drifts in the Rockall Trough and Iceland basin suggest that the drifts began accumulating during the Eocene-Oligocene as a result of overflow of Norwegian Sea Deep Water across the Greenland Scotland Ridge (Kidd and Hill, 1987), thus apparently supporting the interpretations drawn during this study. Therefore, further investigation of these drift bodies may provide supporting evidence for an Eocene onset of deep water exchange between the Norwegian Greenland Sea and the North Atlantic. The inflow of warm surface waters into the Norwegian Greenland Sea is also an integral part of the North Atlantic Conveyor. At present, these currents flow from the Gulf of Mexico along the eastern seaboard of North

America before crossing the Atlantic and flowing into the Norwegian Greenland in the form of the Gulf Stream and North Atlantic Drift (Broecker 1991, Rahmstorf 2002). Therefore, investigation into the onset of surface water currents along the Atlantic margin of southern North America may provide the evidence for the inflow waters which ultimately supply the circulation system at present.

#### *5.5.2.2. Further study within the Faeroe Shetland Basin*

##### *Chronological and lithological calibration*

An important aspect of the evolution of the Faeroe Shetland Basin as an oceanic gateway that was not possible as part of this study is a robust and detailed chronological and lithological calibration of the drift bodies. This is required in order to test and add detail to the interpretations of this study. Tighter chronological constraint would allow closer relation of the drift deposition to changes in climate and ocean circulation revealed by other higher resolution proxies, such as isotope analysis. Lithological samples, and in particular core, would allow rapid alternations in current activity to be identified as well as potential provenance analysis based on mineral and microfossil analysis.

##### *3D seismic mapping*

Interpretation of a '3D mega-survey' which has been created within the Faeroe Shetland Basin and consists of 30000km<sup>2</sup> of full fold continuous 3D seismic coverage would allow the mapping and analysis of the drift bodies identified as part of this study. Advantages of 3D coverage would include continuous coverage across areas of widely spaced 2D profiles (particularly on the Faeroese margin) and the potential for manipulation of the data including attribute analysis which could potentially be used to reveal intricacies of sediment type distribution.

##### *Correlation with adjacent basins*

The current system that flows through the Faeroe Shetland Basin at present also influences the Norwegian basin and margin to the North, and the Rockall Trough and associated margins to the south. These adjacent basins are also areas of petroleum exploration, which provides the potential for correlation of the key sediment bodies and reflections identified within the Faeroe Shetland Basin into the neighbouring basins. This would allow assessment

of to what degree the current system and sedimentation may have been localised to the Faeroe Shetland Basin, and may allow identification of current pathways in order to provide a more detailed understanding of the regional palaeocurrent circulation.



## Chapter Six: Conclusions

This study has analysed the Cenozoic succession of the Faeroe Shetland Basin using petroleum industry seismic data in order to assess the basins history as an oceanic gateway. The outcome has been the identification of contourite drifts which are consistently present within the basin from the middle Eocene onwards, revealing that the basin has acted as a deep water oceanic gateway since the middle Eocene. This chapter is intended to summarise the key findings of this research and does so firstly by drawing some general conclusions followed by concluding remarks from each of the chapters.

### 6.1. General conclusions

1. The Faeroe Shetland Basin has acted as a conduit for SW flowing deep waters from the Norwegian Greenland Sea into the North Atlantic across the Greenland Scotland Ridge since the middle Eocene.
2. This exchange of cool deep waters between the Norwegian Greenland Sea and the North Atlantic through the Faeroe Shetland Basin is interpreted to be analogous to the modern day North Atlantic Conveyor Belt Circulation, suggesting that this system was initiated during the middle Eocene. A combination of global climatic and regional tectonic factors is thought to have permitted the development of the circulatory regime.
3. Throughout the Palaeogene and Neogene, a general increase in the flux of deep water through the basin is postulated based on the increased distribution and eastward migration of contourite deposition, from the Faeroese margin during the Oligocene-early Miocene to the basin axis and onto the Shetland margin during the Neogene. This increased flux is also thought to have resulted from a combination of increasingly favourable climatic conditions promoting deep water formation and tectonic controls permitting greater flow through the basin.
4. Formation of deep water unconformities within the basin are attributed to an increase in alongslope current velocity resulting from climatic and/or tectonic factors, and are postulated to have an inverse relationship to shelfal sea level related unconformities with respect to timing of formation.

5. Alongslope current activity and contourite deposition within the basin is thought to be most active during interglacial/interstadial periods, and is disrupted and reduced during glacial periods, due to a probable shift in deep water formation south of the Greenland Scotland Ridge.
6. Petroleum industry seismic data have provided an excellent means to investigate the history of the Faeroe Shetland Basin as an oceanic gateway. The combination of regional 2D coverage, 3D mapping and visualisation and the high degree of vertical resolution afforded by high resolution 2D seismic data along with lithologic and biostratigraphic calibration by an extensive well and borehole data set permits the investigation of all aspects of contourite deposition within the basin.

## 6.2. Concluding remarks from Chapter Two

1. Identification and analysis of a large elongate contourite drift in the southern Faeroe Shetland Basin dates the onset of SW deep water circulation through the basin as middle Eocene.
2. Prior to the onset of contourite deposition, the southern Faeroe Shetland Basin was characterised by deltaic sedimentation during continuous subsidence to water depths of c.500m which is thought ultimately to have permitted the through-flow of deep waters through the basin.
3. The onset of deep water circulation is thought to be related to both tectonic control and the increasing latitudinal temperature gradient between the tropical and high latitudes. Indeed, the proposed existence of significant northern hemisphere ice-sheets during the middle Eocene provides further evidence that a cooling northern hemisphere climate resulted in the initiation of deep water formation in the Norwegian Greenland Sea, which combined with subsidence of the southern Faeroe Shetland Basin constituted the conditions required for formation and transport of deep waters between the Norwegian Greenland Sea and the North Atlantic.
4. Previous early Oligocene and Miocene estimates for the onset of deep water circulation through the basin are thought to be too conservative, and the presence of an Eocene deep water connection between the North Atlantic and the Norwegian Greenland Sea has implications for climate/ocean circulation modelling of the Cenozoic greenhouse to icehouse transition.

5. The intercalation of contourite drifts with base of slope fans demonstrates that during the Eocene, both alongslope and downslope sedimentary processes were active contemporaneously, demonstrating that the transition from slope process domination during the early Palaeogene to alongslope process domination during the late Palaeogene and Neogene was gradual.
6. The availability of high resolution industrial seismic data to this study was crucial in the confident determination of the sediment body as a contourite drift which would not have been possible if based on conventional 2D and 3D seismic data.

### 6.3. Concluding remarks from Chapter Three

1. The Oligocene to Recent succession of the Faeroe Shetland Basin is divided into five seismic-stratigraphic units, each interpreted as having been deposited or significantly influenced by SW flowing deep water currents. As a result, the Faeroe Shetland Basin is interpreted to have continued to facilitate the exchange of deep waters from the Norwegian Greenland Sea into the North Atlantic as part of a modern style North Atlantic Conveyor Belt circulation that was initiated in the middle Eocene.
2. The chapter provides a comprehensive overview of key published stratigraphic nomenclatures for the basin, outlining the nature and reliability of each and the method of dating used, and relating them fully to the division proposed by this study. The study also confirms the status of well 214/4-1 as the key source of lithologic and biostratigraphic information for the late Palaeogene and Neogene succession of the basin.
3. Throughout the Oligocene to Recent an increased flux of deep water is hypothesised based on the increased distribution of contourite drifts from the Faeroese margin to the Shetland margin.
4. Deep water erosion phases are interpreted to have been related to changes in climatic and tectonic regime, resulting in vigorous bottom current erosion and removal of tens-hundreds of meters of sediment.
5. Contourite drift and erosional unconformity distribution are used to propose that the water mass structure throughout the late Palaeogene-Neogene was similar to that observed at present.

6. A range of contourite drift types (*sensu* Faugères et al., 1999) have been identified within the Oligocene-Recent succession, and have been used to make inferences regarding the characteristics depositional current.
7. The chapter utilises the presence of an Opal A/CT transition in a novel approach to estimating erosional magnitude of unconformity surfaces where seismic resolution and imaging prohibit truncated reflection projection.

#### 6.4. Concluding remarks from Chapter Four

1. Analysis of the West Shetland Drift Slope section using recently available 3D seismic data results in confirmation of the sediment body as a plastered contourite drift which was deposited synchronously with the basinal sheeted drift (WSD Basin section) following the formation of the Intra-Neogene Unconformity.
2. Deposition of the WSD Slope section was initiated by downslope processes including channel and levee formation. During this time, subordinate alongslope currents are thought to have been active, which subsequently increased in influence and ultimately took control of deposition on the West Shetland slope during the early Pliocene.
3. The lower-mid West Shetland slope is interpreted to have been influenced by SW flowing alongslope currents with velocities of 10-30cm/s throughout the Pliocene. This interpretation was aided by the identification and interpretation of a significant bottom current sediment wave field within the drift, which was presented here for the first time.
4. The identification and analysis of significant iceberg plough marks within the West Shetland Drift Slope section suggests that contourite deposition was interrupted by glacial episodes during which ice bergs scoured the sea floor in several hundred meters of water depth,
5. Plough mark geometries are used to suggest that alongslope currents within the basin were disrupted during episodes of significant glaciation and iceberg presence.
6. It is proposed that contourite sedimentation within the Faeroe Shetland Basin occurs primarily during periods of reduced icesheet presence, and that the West Shetland Drift contains a sedimentological record of fluctuations in glaciation that affected the Faeroe Shetland Basin and surrounding region during the Pliocene and Pleistocene.

7. 3D seismic data have been shown to provide an excellent means for contourite interpretation, allowing the identification of small scale architectural elements, such as the spectacular sediment wave field, which would not be possible using a coarsely spaced 2D seismic grid.

## Bibliography

- Adkins, J. F., Boyle, E. A., Keigwin, L., & Cortijo, E., 1997. Variability of the North Atlantic thermohaline circulation during the last interglacial period. *Nature*. v 390. 154-156.
- Akhurst, M.C., Stow, D.A.V., & Stoker, M.S., 2002. Late Quaternary glacigenic contourite, debris flow and turbidite process interaction in the Faroe-Shetland Channel, NW European Continental Margin. *In*: Stow, D.A.V., Pudsey, C.J., Howe, J.A., Faugères, J.C., and Viana, A.R., (Eds), *Deep-Water Contourite Systems: Modern Drifts and Ancient Series, Seismic and Sedimentary Characteristics*. Geological Society London. *Memoirs*, 22. 73-84.
- Alley, R.B., & Clark, P.U., 1999. The deglaciation of the Northern Hemisphere: A Global Perspective. *Annual Review of Earth and Planetary Science*. v. 27, 149-182.
- Alley, R.B., Clark, P.U., Keigwin, L.D., & Webb, R.S., 1999. Making sense of Millennial-Scale Climate Change. *Mechanisms of Global Climate Change at Millennial Time Scales*. *Geophysical Monograph* 112. 385-394.
- Andersen, M.S., Nielsen, T., Sorensen, A.B., Boldreel, O.L., & Kuijpers, A., 2000. Cenozoic sediment distribution and tectonic movements in the Faroe region. *Global and Planetary Change*. v. 24. 239-259.
- Austin, B., 2004. Integrated use of 3D seismic in field development, engineering and drilling: examples from the shallow section. *In*: Davies, R.J., Cartwright, J.A., Stewart, S.A., Lappin, M and Underhill, J.R., (Eds), *3D Seismic Technology: Applications to the Exploration of Sedimentary Basins*. Geological Society, London, *Memoirs*, 29. 279-296.
- Bacon, S., 1997. Circulation and Fluxes in the North Atlantic between Greenland and Ireland. *Journal of Oceanography*. v. 27. 1420-1435.
- Badley, M.E., 1985. *Practical Seismic Interpretation*. International Human Resources Development Corporation, Boston, USA.
- Barrie, J.V., 1980. Iceberg-Seabed Interaction (Northern Labrador Sea). *Annals of Glaciology*. v. 1. 71-76.
- Barron, E.J., 1987. Eocene equator-to-pole surface ocean temperature. A significant climate problem? *Paleoceanography*. v. 2. 729-739.
- Bass, D.W., & Woodworth-Lynas, C., 1988. Iceberg crater marks on the sea floor, Labrador Shelf. *Marine Geology*. v. 79. 243-260.

Bell, B. R. & Jolley, D. W., 1997. Application of palynological data to the chronology of the Palaeogene lava fields of the British Province: implications for magmatic stratigraphy. *Journal of the Geological Society, London*. v. 154. 701-708.

Benn, D.I., & Evans, D.J.A., 1998. *Glaciers and Glaciation*. Hodder Headline Group. London.

Berggren, W.A., & Hollister, C.D., 1974. Paleogeography, Paleobiogeography and the history of circulation in the Atlantic Ocean. *In*: Hay, W.W., (Ed), *Studies in Paleooceanography*. SEPM Special Publication No 20. 126-186.

Berggren, W.A., & Schnitker, W.A., 1983. Cenozoic marine environments in the North Atlantic and Norwegian-Greenland Sea. *In*: Bott, M.H.P., Saxov, S., Talwani, M and Thiede, J., (Eds), *Structure and Development of the Greenland-Scotland Ridge*. Plenum Press, New York. 495-548.

Berggren, W.A., Kent, D.V., Swisher III, C.C., & Aubry, M.-P., 1995. A revised Cenozoic geochronology and chronostratigraphy. *In*: Berggren, W.A., Kent, D.V., Aubry, M.-P., & Hardenbol, J., (Eds.), *Geochronology, Time Scales and Stratigraphic Correlation: Framework for an Historical Geology*. SEPM Special Publication No 54. 129-212.

Bice, K. L., & Marotzke, J., 2002. Could changing ocean circulation have destabilized methane hydrate at the Palaeocene/Eocene boundary? *Paleoceanography*. v. 17. 1018-1034.

Bigg, G.R., 1996. *The Oceans and Climate*. Cambridge University Press, UK, 266p.

Billups, K., A. C. Ravelo & J. C. Zachos., 1998. Early Pliocene Deep Water Circulation in the Western Equatorial Atlantic: Implications for High Latitude Climate Change. *Paleoceanography*. v. 13. 84-95.

Billups, K., 2002. Late Miocene through early Pliocene deep water circulation and climate change viewed from the sub-Antarctic Southern Ocean. *Palaeoecology, Palaeogeography, Palaeoclimatology*. v. 185. 287-307.

Bohrmann, G., Abelman, A.M.S., Gersonde, R., Hubberten, H., & Kuhn, G., 1994. Pure siliceous ooze, a diagenetic environment for early chert formation: *Geology*, v. 22. 207-210.

Boldreel, L. O. & Andersen, M. S., 1993: Late Paleocene to Miocene compression in the Faroe-Rockall area. *In*: Parker, J. R., (Ed), *Petroleum Geology of Northwest Europe: Proceedings of the 4th Conference*. 1025-1034.

Boldreel, L.O. & Andersen, M.S., 1995. The relationship between the distribution of Tertiary sediments, tectonic processes and deep-water circulation around the Faeroe



Islands. *In*: Scrutton, R.A., Shimmield, G.B., Stoker, M.S., & Tudhope, A.W. (Eds), *The Tectonics, Sedimentation and Paleooceanography of the North Atlantic Region*. Geological Society, London, Special Publication. 90, 145-158.

Boldreel, L.O., Andersen, M.S., 1998. Tertiary compressional structures on the Faroe-Rockall Plateau in relation to northeast Atlantic ridge push and Alpine foreland stresses. *Tectonophysics*. v. 300. 13-28.

Bond, G.C., & Lotti, R., 1995. Iceberg discharges into the North Atlantic on millennial time scales during the last glaciation. *Science*. v. 267. 1005-1010.

Bonnin, J., Van Raaphorst, W., Brummer, G.J., Van Haren, H., & Malschaert, H., 2002. Intense mid-slope resuspension of particulate mater in the Faeroe-Shetland Channel: short-term deployment of near-bottom sediment traps. *Deep-Sea Res. I*. v. 49. 1485-1505.

Bott, M.H.P., 1983. Deep structure and geodynamics of the Greenland Scotland Ridge: An introductory review. *In*: Bott, M.H.P., Saxov, S., Talwani, M., & Theide, J. (Eds), *Structure and development of the Greenland-Scotland Ridge – new methods and concepts*. Plenum. New York. 549-589.

Bott, M.H.P., 1984. Deep structure and origin of the Faeroe-Shetland Channel. *In*: Spencer, A.M. (Ed), *Petroleum Geology of the North European Margin*, Norwegian Petroleum Society. Graham and Trotman. 341-347.

Brass, G.W., Southam, J.R., & Peterson, W.H., 1982. Warm, saline bottom water in the ancient ocean. *Nature*. v. 296. 620-623.

Broecker, W.S., & Peng, T.H., 1982. *Tracers in the Sea*. ELDIGIO Press, New York.

Broecker, W.S., & Denton, G.H., 1990. The role of ocean-atmosphere reorganizations in glacial cycles. *Quaternary Science Reviews*. v. 9. 305-341.

Broecker, W.S. (1991). "The Great Ocean Conveyor". *Oceanography*. v. 4. 79-89

Brown, L. F., and Fisher, W. L., 1977, Seismic-stratigraphic interpretation of depositional systems: Examples from Brazilian rift and pull-apart basins, *In*: Payton, C. E., (Ed), *Seismic Stratigraphy - Applications to Hydrocarbon Exploration*. American Association of Petroleum Geologists Memoir 26. 213-248.

Bujak, J., Mudge, D., 1994. A high-resolution North Sea Eocene dinocyst zonation. *Journal of the Geological Society, London*. v. 151. 449-462.

Bulat, J., Long, D., 2001. Images of the seabed in the Faroe-Shetland Channel from commercial 3D seismic data. *Marine Geophysical Researches*. v. 22. 345-367.

- Bulat, J. (2005) Some considerations on the interpretation of seabed images based on commercial 3D seismic in the Faroe-Shetland channel. *Basin Research*. v. 17. 21–42.
- Buntebarth, G., 1984. *Geothermics: An introduction*. Springer-Verlag, Berlin. pp 125.
- Cartwright, J.A., 1992. *The Application of Seismic Stratigraphic Methods in Structural Interpretation*. Joint Association of Petroleum Exploration Courses, Course Notes. Geological Society, London.
- Cartwright, J. A. & Dewhurst, D., 1998. Layer-bound compaction faults in fine-grained sediments. *Geological Society of America Bulletin*. v. 110, No 10. 1242-1257.
- Clark, J.I., Chari, T.R., Landva, J., & Woodworth-Lynas, C.M.T., 1989. Pipeline Route Selection in an Iceberg-Scoured Seabed. *Marine Geotechnology*. v. 8. 51-67.
- Cloetingh, S., Gradstein, F.M., Kooi, H., Grant, A.C., & Kaminski, M., 1990. Plate reorganization: a cause of rapid late Neogene subsidence and sedimentation around the North Atlantic. *Journal of Geological Society, London*. v.147. 495-506.
- Cloke, I., Line, C., Davies, R. J., Ferrero, C., McLachlan, K., Bingham, J., & Hornafius, S. 1999, (abstract). The Role of Inversion in the Development of the Petroleum System of the Faroe-Shetland Basin.
- Cooper, M.M., Evans, A.C., Lynch, D.J., Neville, G., & Newley, T., 1999. The Foinaven Field: managing reservoir development uncertainty prior to start-up. *In: Fleet, A.J., & Boldy, S.A.R., (Eds), Petroleum Geology of Northwest Europe: Proceedings of the 5th Conference*. 675-682.
- Crossen, K.J., 1991. Structural control of deposition by Pleistocene tidewater glaciers, Gulf of Maine. *Geological Society of America. Special Paper* 261. 127-135.
- Crowley, T.J., 1992. North Atlantic Deep Water cools the southern hemisphere. *Paleoceanography*. v. 7. 489-497.
- Dahlgren, K.I.T., Vorren T.O., & Laberg, J.S., 2002. Late Quaternary glacial development of the mid-Norwegian margin - 65°-68°N. *Marine and Petroleum Geology*. v. 19. 1089-1113.
- Damuth, J.E., Olson, H.C., 1993. Preliminary observations of Neogene-Quaternary depositional processes in the Faeroe-Shetland Channel revealed by high-resolution seismic facies analysis. *In: Parker, J.R. (Ed), Petroleum Geology of North West Europe: Proceedings of the 4th Conference*. Geological Society. London. 1035-1045.
- Damuth, J.E., Olson, H.C., 2001. Neogene-Quaternary contourite and related deposition on the West Shetland Slope and Faeroe-Shetland Channel revealed by high-resolution seismic studies. *Marine Geophysical Research*. v. 22. 369-399.

Davies, R.J., Cartwright, J.A., Pike, J., & Line, C., 2001. Early Oligocene initiation of North Atlantic Deep Water formation. *Nature*. v. 410. 917-920.

Davies, R.J., & Cartwright, J.A., 2002. A fossilized Opal A to Opal C/T transformation on the northeast Atlantic margin: support for a significantly elevated Palaeogeothermal gradient during the Neogene? *Basin Research*. v. 14. 467-486.

Davies, R.J., Cloke, I., Cartwright, J.A., Robinson, A.M., & Ferrero, C., 2004. Post-breakup compression of a passive margin and its impacts on hydrocarbon prospectivity: An example from the Tertiary of the Faeroe-Shetland Basin, United Kingdom. *AAPG Bulletin*. v. 88, No. 1. 1-20.

Davies, R.J., 2005. Differential compaction and subsidence in sedimentary basins due to silica diagenesis: A case study. *Geological Society of America Bulletin*. v. 117, No. 9. 1146-1155.

Dean, K., McLachlan, K., & Chambers, A., 1999. Rifting and development of the Faeroe-Shetland Basin. *In*: Fleet, A.J., & Boldy, S.A.R. (Eds), *Petroleum Geology of Northwest Europe: Proceedings of the 5th Conference*. Geological Society. London. 533-54

Deegan, C.E., Scull, B.J., 1977. A proposed standard lithostratigraphic nomenclature for the Central and Northern North Sea. Report of the Institute of Geological Sciences, No 77/25; *Bulletin of the Norwegian Petroleum Directorate*. No.1.

Dickson, R.R., Brown, J., 1994. The production of North Atlantic Deep Water: Sources, rates and pathways. *Journal of Geophysical Research*. v. 9, No. 6. 12319-12341.

Doré, A.G., Jensen, L.N., 1996. The impact of late Cenozoic uplift and erosion on hydrocarbon exploration: offshore Norway and some other uplifted basins. *Global and Planetary Change*. v. 12. 415-436.

Doré, A.G., Lundin, E.R., 1996. Cenozoic compressional structures on the NE Atlantic margin: Nature, origin and potential significance for hydrocarbon exploration. *Petroleum Geoscience*. v. 22. 299-311.

Doré, A.G., Lundin, E.R., Birkeland, O., Eliassen, P.E., & Jensen, L.N., 1997. The NE Atlantic margin: implications of Late Mesozoic and Cenozoic events for Hydrocarbon prospectivity. *Petroleum Geoscience*. v. 3. 117-131.

Doré, A.G., Lundin, E.R., Jensen, L.N., Birkeland, Ø., Eliassen, P.E., & Fichler, C., 1999. Principal tectonic events in the evolution of the northwest European Atlantic margin. *In*: Fleet, A.J., & Boldy, S.A.R. (Eds), *Petroleum Geology of Northwest Europe: Proceedings of the 5th Conference*. Geological Society. London. 41-61.

Duplessy, J.C., Moyes, J., & Pujol, C., 1980. Deep water formation in the North Atlantic Ocean during the last ice age. *Nature*. v. 286. 479-482.

Draut, A.E., Raymo, M.E., McManus, J.E., & Oppo, D.W., 2003. Climate stability during the Pliocene warm period. *Paleoceanography*. v. 18, No. 4. 1078-1090.

Ebdon, C. C., Grainger, P. J., Johnson, H. D. & Evans, A. M. 1995. Early Tertiary evolution and sequence stratigraphy of the Faroe-Shetland Basin: implications for hydrocarbon prospectivity. *In*: Scrutton, R. A., Stoker, M. S., Shimmield, G. B., & Tudhope, A. W., (Eds). *The Tectonics, Sedimentation and Palaeoceanography of the North Atlantic Region*. Geological Society, London, Special Publication 90. 51-69.

Eldholm, O., & Thiede, J., 1980. Cenozoic continental separation between Europe and Greenland. *Palaeogeography, Palaeoclimatology, Palaeoecology*. v. 30. 243-259.

Eldholm, O., 1990. Paleogene North Atlantic magmatic-tectonic events: environmental implications. *Memorie Societa Geologica Italiana*. v. 44. 13-28.

Embley, R.W., Hoose, P.J., Lonsdale, P., Mayer, L., & Tucholke, B.E., 1980. Furrowed mud waves on the western Bermuda Rise. *Geological Society America Bulletin*, Part 1, v. 91. 731-740.

Emery, D., & Myers, K.J. (Eds), 1996. *Sequence Stratigraphy*. Blackwell Science. pp 279

Ercilla, G., Alonso, A., Wynn, R.B., & Baraza, J., 2002. Turbidity current sediment waves on irregular slopes: observations from the Orinoco sediment-wave field. *Marine Geology*. v. 192. 171-187.

Ewing, M, Eittrheim, S.L., Ewing, J.I., & Le Pichon, X., 1971. Sediment transport and distribution in the Argentine Basin, 3, Nepheloid-layer processes of sedimentation. *Physics & Chemistry of the Earth*. v. 8. 51-77.

Faugères, J.C., Gonthier, E., & Stow, D.A.V., 1984. Contourite drift molded by deep Mediterranean outflow. *Geology*. v. 12. 296-300.

Faugères, J.C., Mézeraïs, M.L., & Stow, D.A.V., 1993. Contourite drift types and their distribution in the North and South Atlantic Ocean basins. *Sedimentary Geology*. v. 82 (1-4). 182-203.

Faugères, J.C., Stow, D.A.V., Imbert, P., & Viana, A., 1999. Seismic features diagnostic of contourite drifts. *Marine Geology*. v.162. 1-38.

Faugères, J.C., Gonthier, E., Mulder, T., Kenyon, N., Cirac, P., Griboulard, R., Bernè, S., & Lesuavè, R., 2002. Multi-process generated sediment waves on the Landes Plateau (Bay of Biscay, North Atlantic). *Marine Geology*. v.182. 279-302.

Fisher, P., 1992. Non-tectonic structures caused by differential compaction over buried sandbodies, southern Sacramento Basin. *American Association Petroleum Geologists Bulletin*. v. 76. 418-419.

Flood, R.D., 1988. A lee wave model for deep-sea mudwave activity. *Deep-Sea Research, A*. v. 35. 973-983.

Flood, R.D. & Shor, A.N., 1988, Mud waves in the Argentine Basin and their relationship to regional bottom circulation patterns. *Deep-Sea Research*. v. 35. 943-971.

Flood, R.D., 1994. Abyssal bedforms as indicators of changing bottom current flow: Examples from the U.S. East Coast continental rise. *Paleoceanography*. v. 9. 1049-1060.

Flood, R.D., & Giosan, L., 2002. Migration history of a fine-grained abyssal sediment wave on the Bahama Outer Ridge. *Marine Geology*. v. 192. 259-273.

Fronval, T., & Jansen, E., 1996. Late Neogene paleoclimates and paleoceanography in the Iceland-Norwegian Sea: Evidence from the Iceland and Vøring Plateaus. *In*: Theide, J., Myhre, A.M., Firth, J.V., Johnson, G.L., & Ruddiman, W.F. (Eds), *Proceedings of the Ocean Drilling Program, Scientific Results*. v. 151. 455-467.

Gatliff, R.W., Hitchen, J.D., Ritchie, J.D., & Smythe, D.K., 1984. Internal structure of the Erland Tertiary volcanic complex, north of Shetland, revealed by seismic reflection. *Journal of the Geological Society, London*. v. 141. 555-562.

Gorsline, D.S., 1985. Some thoughts on fine-grained sediment transport and deposition. *Sedimentary Geology*. v. 41. 113-130.

Grabau, A.W., 1905. Physical character and history of some New York Formations. *Science*. v. 22. 534

Greenwood, D.R., & Wing, S.L., 1995. Eocene continental climates and latitudinal temperature gradients. *Geology*. v. 23. 1044-1083.

Groger, M., Henrich, R., & Bickert, T., 2003. Glacial-Interglacial variability in lower North Atlantic Deep Water: Inference from silt grain-size analysis and carbonate preservation in the western equatorial Atlantic. *Marine Geology*. v. 201. 321-332.

Hansen, B., & Østerhus, S., 2000. North Atlantic-Nordic Seas exchanges. *Progress in Oceanography*. v. 45. 109-208.

Haq, B.U., Hardenbol, J., & Vail, P.R., 1987. Chronology of Fluctuating Sea Levels Since the Triassic. *Science*. v. 235. 1157-1167.

Hardenbol, J., Thierry, J., Farley, M.B., Jacquin, T., De Graciansky, P.-C., & Vail, P.R., 1998. Cenozoic Biochronostratigraphy. *In*: De Graciansky, P.-C., Hardenbol, J., Jacquin,

T., Vail, P.R. (Eds), Mesozoic and Cenozoic sequence stratigraphy of European basins, SEPM Special Publication 60.

Heezen, B.C., Hollister, C.D., & Ruddiman, W.F., 1966. Shaping the continental rise by deep geostrophic contour currents. *Science*. v. 152. 502-508.

Hesse, R., 1990, Origin of chert: Diagenesis of biogenic siliceous sediments. *In*: McIlreath, I.A., & Morrow D.W., (Eds), Diagenesis. Geoscience Canada Reprint Series 4. pp 338

Hitchen, K., & Ritchie, J.D., 1987. Geological review of the West Shetland area. *In*: Brooks, J., & Glennie, K. (Eds), Petroleum Geology of North West Europe. Graham and Trotman. 737-749.

Hjelstuen, B.O., Sejrup, H.P., Haflidason, H., Nygård, A., Ceramicola, S., & Bryn, P., 2005. Late Cenozoic glacial history and evolution of the Storegga Slide area and adjacent slide flank regions, Norwegian continental margin. *Marine and Petroleum Geology*. v. 22. 57-69.

Hohbein, M.W., & Cartwright, J.A., in prep (a). A Middle-Eocene onset of the North Atlantic Conveyor Belt: evidence from the Faeroe-Shetland Basin. In preparation for *Palaeoceanography*.

Hohbein, M.W., & Cartwright, J.A., in prep (b). Late Palaeogene-Neogene contourite drifts and palaeoceanographic evolution of the Faeroe Shetland Basin. In preparation for *Marine Geology*.

Hollister, C.D., & Heezen, B.C., 1972. Geologic effects of ocean bottom currents. *In*: Gordon, A.L (Ed), *Studies in Physical Oceanography – A tribute to George Wust on his 80th Birthday*. Gordon and Breach, New York. 2. 37-66.

Hollister, C.D., 1993. The concept of deep-sea contourites. *Sedimentary Geology*. v. 82. 5-11.

Howe, J.A., Stoker, M.S., & Stow, D.A.V., 1994. Late Cenozoic sediment drift complex, NE Rockall Trough, North Atlantic. *Paleoceanography*. v. 9. 989-999.

Howe, J.A., 1996. Turbidite and contourite sediment waves in the Northern Rockall Trough, North Atlantic Ocean. *Sedimentology*. v. 43. 219-230.

Howe, J.A., Stoker, M.S., & Woolfe, K.J., 2001. Deep-marine seabed erosion and gravel-lags in the northwestern Rockall Trough, North Atlantic Ocean. *Journal of the Geological Society*, London. v.158. 427-438.

Howe, J.A., Stoker, M.S., Stow, D.A.V., & Akhurst, M.C., 2002. Sediment drifts and contourite sedimentation in the northeastern Rockall Trough and Faroe-Shetland

Channel, North Atlantic Ocean. *In*: Stow, D.A.V., Pudsey, C.J., Howe, J.A., Faugères, J.C., & Viana, A.R. (Eds), Deep-Water Contourite Systems: Modern Drifts and Ancient Series, Seismic and Sedimentary Characteristics. Geological Society, London Memoirs. 22. 73-84.

Huag, G.H., & Tiedemann, R., 1998. Effect of the formation of the Isthmus of Panama on Atlantic Ocean thermohaline circulation. *Nature*. v. 393. 673-676

Huber, M., & Sloan, L.C., 2001. Heat transport, deep waters, and thermal gradients: Coupled simulation of an Eocene Greenhouse Climate. *Geophysical Research Letters*, v. 28, No. 18. 3481-3484

Huber, M., Sloan, L.S., & Shellito, C., 2003. Early Paleogene oceans and climate: A fully coupled modelling approach using the NCAR CCSM. *In*: Wing, S.L., Gingerich, P.D., Schmitz, B., & Thomas, E (Eds), Causes and Consequences of Globally Warm Climates in the Early Paleogene: Boulder, Colorado, Geological Society of America Special Paper 369. 25-47.

Hurst, A., Fraser, A.J., Fraser, S.I., & Hadler-Jacobsen, F., 2005. Deep-water clastic reservoirs: a leading global play in terms of reserve placement and technological challenges. *In*: Dore, A.G., Vining, B.A., (Eds), Petroleum Geology: North-West Europe and Global Perspectives – Proceedings of the 6th Petroleum Conference. 1111-1120

Isaksen, D., & Tonstad, K., 1989. A revised Cretaceous and Tertiary lithostratigraphic nomenclature for the Norwegian North Sea. *Bulletin of the Norwegian Petroleum Directorate*. No. 5.

Jansen, E., Bleil, U., Henrich, R., Kringstad, L., & Slettemark, B., 1988. Paleoenvironmental changes in the Norwegian Sea and the Northeast Atlantic during the last 2.8m.y. Deep Sea Drilling Program Sites 610, 642, 643, 644. *Paleoceanography*. v. 3. 356-581.

Jansen, E., & Sjøholm, J., 1991. Reconstruction of glaciation over the past 6 Myr from ice-borne deposits in the Norwegian Sea. *Nature*. v. 349. 600-603.

Japsen, P. & Chalmers, J.A., 2000. Neogene uplift and tectonics around the North Atlantic: overview. *Global and Planetary Changes*. v. 24. 165-173.

Johnson, R. G., 1997: Ice age initiation by an ocean-atmospheric circulation change in the Labrador Sea, *Earth And Planetary Science Letters*, 148, 367-379.

Jolley, D. W. 1997. Palaeosurface palynofloras of the Skye lava field and the age of the British Tertiary volcanic province. *In*: M. Widdowson (ed), Palaeosurface: Recognition, Reconstruction and Palaeoenvironmental Interpretation. Geological Society, London, Special Publication 120, 67-94.



Jolley, D. W. & Bell, B. R. 2002. The evolution of the North Atlantic Igneous Province and the opening of the Northeast Atlantic rift. *In*: Jolley, D. W., & Bell, B. R., (Eds), The North Atlantic Igneous Province: Stratigraphy, Tectonic, Volcanic and Magmatic Processes, Geological Society, London, Special Publication 197. 1-14.

Jones, E.J., Ewing, M., Ewing, J.I., & Eitrem, S.L., 1970. Influences of Norwegian Sea overflow water on sedimentation in the northern North Atlantic and Labrador Sea. *Journal of Geophysical Research*. v. 75. 1655-1680.

Kaneps, A.G., 1979. Gulf Stream: Velocity fluctuations during the late Cenozoic. *Science*. v. 204. 297-301.

Keigwin, L.D., & Lehman, S.J., 1994. Deep circulation change linked to HEINRICH event 1 and Younger Dryas in a mid-depth North Atlantic core. *Paleoceanography*. v. 9, No. 2. 185-194.

Keller, G., Herbert, T., Dorsey, R., D'Hondt, S., Johnsson, M., & Chi, W.R., 1987. Global distribution of Paleogene hiatuses. *Geology*. v. 18. 199-203.

Kennet, J.P., & Shackelton, N.J., 1976. Oxygen isotopic evidence for the development of the psychrosphere 38Myr ago. *Nature*. v. 260. 513-515.

Kennet, J.P., 1986. Miocene to Early Pliocene oxygen and carbon isotope stratigraphy in the SW Pacific, deep sea drilling project leg 90. *In*: Kennet J.P., von der Borch, C.C. (Eds), Initial reports DSDP 90 (part 2), 1383-1411. U.S. Government Printing Office, Washington D.C.

Kennett, J.P., Stott, L.D., 1990. Proteus and Proto-Oceanus: Ancestral Paleogene oceans as revealed from Antarctic stable isotopic results. ODP Leg 113, Proceedings of the Ocean Drilling Program. v. 113. 865-880

Kenyon, N.H., 1987. Mass-wasting features on the continental slope of northwest Europe. *Marine Geology*. v. 74. 57-77.

Kidd, R.B., & Hill, P.R., 1987. Sedimentation on Feni and Gardar sediment drifts. Initial Reports of the Deep Sea Drilling Project. v. XCIV, Part 2. Sites 606-611. National Science Foundation. 1217-1244.

Kiørboe, L. 1999. Stratigraphic relationships of the Lower Tertiary of the Faeroe Basalt Plateau and the Faeroe-Shetland Basin. *In*: Fleet, A. J., & Boldy, S. A. R., (Eds), Petroleum Geology of Northwest Europe: Proceedings of the 5th Conference, Geological Society, London, 559-572.

Kissel, C., Laj, C., Lehman, B., labyrie, L., & Bout-Roumzeilles, V., 1997. Changes in the strength of the Iceland-Scotland Overflow Water in the last 200,000 years: Evidence

from magnetic anisotropy analysis of core SU90-33. *Earth & Planetary Science Letters*. v. 152. 25-36.

Kneller, B., 1995. Beyond the turbidite paradigm: physical models for deposition of turbidites and their implications for reservoir prediction. *In*: Hartley, A.J., & Prosser, D.J., (Eds), *Characterisation of Deep Marine Clastic Systems*. Geological Society Special Publication No. 94. 31-49.

Knott, D. S., Burchell, M. T., Jolley, E. J., & Fraser, A. J. 1993. Mesozoic to Cenozoic plate reconstructions of the North Atlantic and the tectonostratigraphic history of the UKCS Western Margin. *In*: Parker, J. R., (Ed), *Petroleum Geology of Northwest Europe: Proceedings of the 4th Conference*, Geological Society, London. 953-974.

Knox, R.W.O'B, Morton, A.C., Nielsen, O.B., & King, C., 1988. The North Sea, central Viking Graben (Beryl-Frigg area, including Norwegian territories). *In*: Vinken, R. (Compiler) *The Northwest European Tertiary Basin*. *Geologisches Jahrbuch*. 100A. 18-21.

Knox, R.W.O'B., & Holloway, S., 1992. Paleogene of the Central and Northern North Sea, in: Knox, R.W.O'B., Cordey, W.G. (Eds), *Lithostratigraphic nomenclature of the UK North Sea*. BGS. Nottingham.

Knox, R.W.O'B., Holloway, S., Kirby, G.A., & Bailey, H.E., 1997. Stratigraphic nomenclature of the UK North West Margin. 2. Early Paleogene lithostratigraphy and sequence stratigraphy. BGS. Nottingham.

Knutz, P.C., & Cartwright, J.A., 2003. Seismic stratigraphy of the West Shetland Drift: Implications for late Neogene paleocirculation in the Faeroe-Shetland gateway. *Paleoceanography*. v. 18, No. 4, 1093.

Knutz, P.C., & Cartwright, J.A., 2004. 3D anatomy of late Neogene contourite drifts and associated mass flows in the Faroe-Shetland Basin. *In*: Davies, R.J., Cartwright, J.A., Stewart, S.A., Lappin, M & Underhill, J.R. (Eds), *3D Seismic Technology: Applications to the Exploration of Sedimentary Basins*. Geological Society, London, *Memoirs*, 29, 63-71.

Kristoffersen, Y., 1990. On the tectonic evolution and paleoceanographic significance of the Fram Strait gateway. *In*: Bleil, U., Theide, J (Eds). *Geological History of the Polar Oceans: Arctic Versus Antarctic*. Dordrecht (Kluwer Academic Publishing.). 63-76.

Kuijpers, A., Hansen, B., Hühnerbach, V., Larsen, B., Nielsen, T., & Werner, F., 2002. Norwegian Sea Overflow through the Faroe-Shetland gateway as documented by its bedforms. *Marine Geology*. v. 188, 147-164.

Kump, L.R., 2005. Foreshadowing the glacial era. *Nature*. v. 436, 333-334.

Kuramoto, S., Tamaki, K., Langseth, M.G., Nobes, D.C., Tokuyama, H., Pisciotto, K.A. & Taira, A. (1992). Can Opal A/Opal-C/T BSR be an indicator of the thermal structure of the Yamato basin, Japan Sea? *In*: Tamaki, K., Suyehiro, K., Allan, J., & McWilliams., (Eds), *Proceedings of the Ocean Drilling Program, Scientific Results*, v. 127–128. 1145–1151.

Laberg, J.S., Stoker, M.S., Dahlgren K.I.T., de Haas, H., Ceramida, S. Haflidason, H., Hjelstuen, B.O., Nielsen, T., Shannon, P., Vorren, T.O. & van Weering, T.C.E., 2005. Cenozoic alongslope processes and sedimentation along the NW European Atlantic margin. *Marine and Petroleum Geology*. v. 22, issue 9-10. 1069-1088

Lamers, E. & Carmichael, S. M. M. 1999. The Palaeocene deepwater sandstone play west of Shetland. *In*: Fleet, A.J., & Boldy, S. A. R., (Eds), *Petroleum Geology of Northwest Europe: Proceedings of the 5th Conference*, Geological Society, London. 645-659.

Lawver, L.A., Müller, R.D, Srivastava, S.P., & Roest, W., 1990. The opening of the Arctic Ocean. *In*: Bleil, U., & Theide, J (Eds), *Geological History of the Polar Oceans: Arctic Versus Antarctic*. Dordrecht (Kluwer Academic Publishing). 29-62.

Lear, C.H., Elderfield, H., & Wilson, P.A., 2000. Cenozoic Deep-Sea Temperatures and Global Ice Volumes from Mg/Ca in Benthic Foraminiferal Calcite. *Science*. v. 287. 269-272

Lear, C.H., Rosenthal, Y., & Wright, J.D., 2003. The closing of a seaway: ocean water masses and global climate change. *Earth and Planetary Science Letters*. v. 210. 425-436.

Long, D., & Praeg, D., 1997. Buried Ice-Scours: 2D vs 3D-Seismic Geomorphology, *in*: Davies, T.A., Bell, T., Cooper, A.K., Josenhans, H., Polyak, L., Stoker, M.S., & Stravers, J.A. (Eds), *Glaciated Continental Margins: An atlas of acoustic images*. Chapman and Hall. 142-143.

Lu, H., Fulthorpe, C., & Mann, P., 2003. Three-dimensional architecture of shelf-building sediment drifts in the offshore Canterbury basin, New Zealand. *Marine Geology*. v. 193. 19-47.

Lundin, E., & Doré, A.G., 2002. Mid-Cenozoic post-breakup deformation in the ‘passive’ margins bordering the Norwegian-Greenland Sea. *Marine and Petroleum Geology*. v. 19. 79-93.

Lygren, T.H., Berg, M.N., & Berg, K., 1997. Sub-Glacial Features Interpreted from 3D-Seismic. *In*: Davies, T.A., Bell, T., Cooper, A.K., Josenhans, H., Polyak, L., Stoker, M.S., & Stravers, J.A. (Eds), *Glaciated Continental Margins: An atlas of acoustic images*. Chapman and Hall. 60-61.

Mariani, M., A. Argnani, M. Roveri, & F. Trincardi., 1993. Sediment drifts and erosional surfaces in the central Mediterranean: Seismic evidence of bottom-current activity. *Sedimentary Geology*. v. 82: 207–220.

Marotzke, J., 2000. Abrupt climate change and thermohaline circulation: Mechanisms and predictability. *Proceedings of the National Academy of Sciences (U.S.A.)*. v. 97. 1347-1350.

Manighetti, B., & McCave, I.N., 1995. Late Glacial and Holocene paleocurrents around Rockall Bank, NE Atlantic Ocean. *Paleoceanography*. v. 10. 611-626.

Manley, P.L., & Caress, D.W., 1994. Mudwaves on the Gardar Sediment Drift, NE Atlantic. *Paleoceanography*. v. 9, No. 6. 973-988.

Masson, D.G., 2001. Sedimentary processes shaping the eastern slope of the Faeroe-Shetland Channel. *Continental Shelf Research*. v. 21. 825-857.

Masson, D.G., Howe, J.A., & Stoker, M.S., 2002. Bottom-current sediment waves, sediment drifts and contourites in the northern Rockall Trough. *Marine Geology*. v. 192. 215-237.

Masson, D.G., Wynn, R.B., & Bett, B.J., 2005. Sedimentary environment in the Faroe-Shetland Faroe Bank Channels, north-east Atlantic, and the use of bedforms as indicators of bottom current velocity in the deep ocean. *Sedimentology*. v. 51. 1207-1241.

McCave, I.N., & Tucholke, B.E., 1986. Deep current-controlled sedimentation in the western North Atlantic. *In: Vogt, P.R., & Tucholke, B.E. (Eds), The Geology of North America. Volume M, The Western North Atlantic Region. Geological Society of America. Boluder, Colorado. 451-468*

McCave, I.N., Manighetti, B., & Robinson, S.G., 1995a. Sortable silt and fine sediment size/composition slicing: parameters for paleocurrent speed and paleoceanography. *Paleoceanography*. v. 10. 593-610.

McCave, I.N., 1995b. Sedimentary processes and the creation of the stratigraphic record in the late Quaternary North Atlantic Ocean. *Philosophical Transactions of the Royal Society of London. B*. v. 348. 229-241.

Mitchell, S. M., Beamish, G. W. J., Wood, M. V., Malacek, S. J., Armentrout, J. A., Damuth, J. E. & Olsen, H. C. 1993. Palaeogene sequence stratigraphic framework of the Faeroe Basin. *In: Parker, J. R., (Ed), Petroleum Geology of Northwest Europe: Proceedings of the 4th Conference. Geological Society, London. 1011-1023.*

Mitchum, R.M., Vail, P.R., & Thompson, S., 1977. Seismic Stratigraphy and Global Changes of Sea Level, Part 2: The Depositional Sequence as a Basic Unit for Stratigraphic Analysis. *In: Payton, C.E. (Ed), Seismic Stratigraphy – applications to*

hydrocarbon exploration. American Association of Petroleum Geologists, Memoir 26. 53-82.

Miller, K.G., & Tucholke, B.E., 1983. Development of Cenozoic abyssal circulation South of the Greenland-Scotland Ridge. *In: Bott, M.H.P., Saxov, S., Talwani, M., & Theide, J. (Eds), Structure and development of the Greenland-Scotland Ridge – new methods and concepts.* Plenum. New York. 549-589.

Miller, K.G., & Fairbanks, R.G., 1985. Oligocene to Miocene carbon isotope cycles and abyssal circulation changes. *In: Sunquist, E.T., and Broecker, W.S., (Eds), The Carbon Cycle and Atmospheric CO<sub>2</sub>: Natural Variations Archean to Present.* Geophysical Monograph Series. v. 32. AGU, Washington, D.C. 469-486.

Miller, K.G., Wright, J.D., & Fairbanks, R.G., 1991. Unlocking the ice house: Oligocene-Miocene oxygen isotopes, eustasy and margin erosion. *Journal Geophysical Research.* v. 96, No. B4. 6829-6894

Miller, K.G., Mountain, G.S, Browning, J.V., Kominz, M., Sugarman, P.J., Christie-Blick, N., Katz, M.E., & Wright, J.D., 1998. Cenozoic global sea-level, sequences, and the New Jersey Transect: Results from Coastal Plain and Slope Drilling. *Reviews of Geophysics.* v. 36. 569-601.

Moron, V., Vautard R., & Ghil M., 1998: Trends, in decadal and interannual oscillations in global sea surface temperatures. *Climate Dynamics.* v. 14. 545-569.

Mountain, G.S. & Tucholke, B.E., 1985. Mesozoic and Cenozoic Geology of the U.S. Atlantic Continental Slope and Rise. *In: Poag, C.W., (Ed), Geologic Evolution of the U.S. Atlantic Margin.* Van Nostrand Reinhold, Stroudsburg, Pa. 293-341.

Mudge, D. C. & Rashid, B. 1987. The geology of the Faeroe Basin area. *In: J. Brooks, J., & Glennie, K. W., (Eds), Petroleum geology of NW Europe.* Heyden & Son, London, 751-763.

Nadin, P. A., Kuszniir, N. J. & Cheadle, M. J. 1997. Early Tertiary plume uplift of the North Sea and Faroe-Shetland Basins. *Earth and Planetary Science Letters.* v. 148, 109-127.

Naylor, P.H., Bell, B.R., Jolley, D.W., Durnall, P., & Fredsted, R., 1999. Paleogene magmatism in the Faeroe-Shetland Basin: influences on uplift history and sedimentation. *In: Fleet, A.J., & Boldy, S.A.R. (Eds), Petroleum Geology of Northwest Europe: Proceedings of the 5th Conference.* Geological Society. London. 545-588.

Niemi, T.M., Ben-Avraham, Z., Hartnady, C.J.H., & Reznikov, M., 2000. Post- Eocene seismic stratigraphy of the deep ocean basin adjacent to the southeast African continental margin: a record of geostrophic bottom current systems. *Marine Geology.* v. 162. 237-258

- Nilsen, T.H., 1983. Influence of the Greenland-Scotland Ridge on the geological history of the North Atlantic and Norwegian-Greenland Sea areas. *In*: Bott, M.H.P., Saxov, S., Talwani, M., & Theide, J. (Eds), Structure and development of the Greenland-Scotland Ridge – new methods and concepts. Plenum. New York. 457-478.
- Nielsen, T., & van Weering, T.C.E. 1998. Seismic stratigraphy and sedimentary processes at the Norwegian Sea Margin northeast of the Faroe Islands. *Marine Geology*. v. 152. 141-157.
- Normark, W.R., Hess, G.R., Stow, D.A.V., & Bowen, A.J., 1980. Sediment waves on the Monterey Fan levee: a preliminary physical interpretation. *Marine Geology*. v. 37. 1-18.
- O'Grady, D. B., & Syvitski, J.P.M., 2002. Large-scale morphology of Arctic continental slopes: the influence of sediment delivery on slope form. *In*: Dowdeswell, J.A., Ó Cofaigh, C (Eds), Glacier-Influenced Sedimentation on High-Latitude Continental Margins. Geological Society of London. Special Publication. 203. 11-31.
- Oppo, D.W., & Lehman, S.J., 1993. Mid-depth circulation of the subpolar North Atlantic during the last glacial maximum. *Science*. v. 259. 1148-1152.
- Paillard, D., 2001. Glacial hiccups. *Nature*. v. 409. 147-148.
- Pak, D.K., & Miller, K.G., 1992. Paleocene to Eocene benthic foraminiferal isotopes and assemblages: implications for deep water circulation. *Paleoceanography*. v. 7, No.4. 405-422.
- Parker, G., Fukushima, Y., & Pantin, H.M., 1984. Self-accelerating turbidity currents. *Journal of Fluid Mechanics*. v. 171. 145-181.
- Pearson, D.G., Emeleus, C.H., Kelley, S.P., 1996.  $^{40}\text{Ar}/^{39}\text{Ar}$  age for the initiation of Palaeogene volcanism in the Inner Hebrides and its regional significance. *Journal of the Geological Society, London*. v. 153. 815-818.
- Pearson, P. N. & Palmer, M. R., 2000. Atmospheric carbon dioxide concentrations over the past 60 million years. *Nature*. v. 406. 695–699
- Pickard, G.L., & Emery, W.J., 1990. Descriptive Physical Oceanography: an introduction. 5th Edition. Pergamon Press, UK. pp 320.
- Pickering, K.T., Stow, D.A.V., Watson, M., & Hiscott, R., 1986. Deep-water facies, processes and models: review and classification scheme for modern and ancient sediments. *Earth-Science Reviews*. v. 23. 75-174.

Pickering, K.T., 2000. The Cenozoic world. *In*: Culver, S.J., Rawson, P.F (Eds), *Biotic Response to Global Change: the late 145 Million years*. Cambridge University Press, UK. 20-34.

Polyak, L., 1997. Ice-keel Scouring. *In*: Davies, T.A., Bell, T., Cooper, A.K., Josenhans, H., Polyak, L., Stoker, M.S., & Stravers, J.A. (Eds) *Glaciated Continental Margins: An atlas of acoustic images*. Chapman and Hall. 136-137.

Polyak, L., Edwards, M.H., Coakley, B.J., & Jakobsson, M., 2001. Ice shelves in the Pleistocene Arctic Ocean inferred from glaciogenic deep-sea bedforms. *Nature*. v. 410. 453-456.

Poole, D.A.R., & Vorren, T.O., 1993. Miocene to Quaternary paleoenvironments and uplift history on the mid Norwegian shelf. *Marine Geology*. v. 115. 173-205.

Powell, A.J., (Ed), 1992. *A Stratigraphic Index of Dinoflagellate Cysts*. British Micropalaeontological Society Publication Series. Chapman and Hall, London. 290 pp

Rahmstorf, S., 1997. Risk of sea-change in the Atlantic. *Nature*. v. 388. 825-826.

Rahmstorf, S., 2000. The thermohaline ocean circulation - a system with dangerous thresholds? *Climatic Change*. v. 46, 247-256.

Rahmstorf, S., 2002. Ocean circulation and climate during the last 120000 years. *Nature* v. 419. 207-214.

Ramsay, A.T.S., Smart, C.W., & Zachos, J.C., 1998. A model of early middle Miocene deep ocean circulation for the Atlantic and Indian Oceans. *In*: Cramp, A., MacLeod, C.J., Lee, S.V., & Jones, E.J.W., (Eds), *Geological Evolution of Ocean Basins: Results from the Ocean Drilling Program*. Geological Society, London, Special Publication 131. 55-70.

Raymo, M.E., Ruddiman, W.F., Backman, J., Clement, B.M., & Martinson, D.G., 1989. Late Pliocene variation in Northern Hemisphere ice sheets and North Atlantic Deep Water circulation. *Paleoceanography*. v. 4, No. 4. 413-446.

Raymo, M.E., D. Hodell, & E. Jansen, 1992. Response of deep ocean circulation to the initiation of northern hemisphere glaciation (3-2 M.Y.). *Paleoceanography*. v. 7. 645-672.

Raymo, M.E., 1994. The initiation of Northern Hemisphere glaciation. *Annual Reviews of Earth and Planetary Science*. v. 22. 353-383.

Reading, H.G. (Ed), 1986. *Sedimentary Environments and Facies*. Second Edition. Blackwell Scientific Publications. London. pp 615



Reading, H.G., & Richards, M., 1994. Turbidite Systems in Deep-Water Basin Margins Classified by Grain Size and Feeder System. *American Association of Petroleum Geologists Bulletin*. v. 78, No. 5. 792-822.

Rebesco, M., & Stow, D.A.V., 2001. Seismic expression of contourites and related deposits: a preface. *Marine Geophysical Research*. v. 22, No. 5-6. 303-308.

Riding, J.B., 1999. BGS Borehole 99/3 internal report. Report Number: WH/2000/8C

Ritchie, J.D., Johnson, H., & Kimbell, G.S., 2003. The nature, age and origin of Cenozoic contractional deformation within the NE Faroe-Shetland Basin. *Marine and Petroleum Geology*. v. 20. 399-409.

Roberts, D.G., 1975. Marine Geology of the Rockall Plateau and Trough. *Philosophical Transactions of the Royal Society, London. Series. A*. v. 278. 447-509.

Roberts, D.G., Montadert, L., & Searle, R.C., 1979. The western Rockall Plateau: stratigraphy and crustal evolution. *In: Initial Reports of the Deep Sea Drilling Project*. v. 48. Washington, D.C, U.S. Government Printing Office. 1061-1088.

Roberts, D.G., Thompson, M., Mitchener, B., Hossack, J., Carmichael, S., & Bjørnseth, H.-M., 1999. Palaeozoic to Tertiary rift and basin dynamics: mid-Norway to the Bay of Biscay—a new context for hydrocarbon prospectivity in the deepwater frontier. *In: Fleet, A.J., Boldy, S.A.R. (Eds.), Petroleum Geology of Northwest Europe: Proceedings of the Fifth Conference*. Geological Society, London. 7-40.

Robinson, A.M., 2004. Stratigraphic development and controls on the architecture of Eocene Depositional Systems in the Faroe-Shetland Basin. PhD Thesis. Cardiff University. Wales. U.K.

Robinson, A.M., Cartwright, J.A., Burgess, P.M., & Davies, R.J., 2004. Interactions between topography and channel development from 3d seismic analysis: an example from the Tertiary of the Flett Ridge, Faroe-Shetland Basin, UK. *In: Davies, R.J., Cartwright, J.A., Stewart, S.A., Lappin, M & Underhill, J.R. (Eds), 3D Seismic Technology: Applications to the Exploration of Sedimentary Basins*. Geological Society, London, Memoirs, 29, 63-71.

Rosby, T., 1996: The North Atlantic Current and Surrounding Waters: At the Crossroads. *Review of Geophysics*. v. 34. 463-481

Ruddiman, W.F., 1972. Sediment redistribution on the Reykjanes Ridge: seismic evidence. *Geological Society of America Bulletin*. v. 86. 1499-1510.

Rumph, B., Reaves, C.M., Orange, V.G., & Robinson, D.L., 1993. Structuring and transfer zones in the Faroe Basin in a regional tectonic context. *In: Parker, J.R. (Ed),*

Petroleum geology of NW Europe: Proceedings of the 4th Conference. Geological Society. London. 999-1009.

Schmitz, W.J. 1995. On the interbasinal-scale thermohaline circulation. *Reviews of geophysics*. v. 33, No.2. 151-173.

Schnitker, D, 1980. Global Paleooceanography and Its Deep Water Linkage to the Antarctic Glaciation. *Earth Science Reviews*. v. 16. 1-20.

Schut, E.W., & Uenzelmann-Neben, G, 2005. Cenozoic bottom current sedimentation in the Cape Basin, South Atlantic. *Geophysical Journal International*. v. 161, No2. 325-333.

Scrutton, R.A., & Stow, D.A.V., 1984. Seismic evidence for early Tertiary bottom-current controlled deposition in the Charlie Gibbs Fracture Zone. *Marine Geology*. v. 56. 325-334.

Shackleton, N.J., & J.P. Kennett. 1975. Paleotemperature history of the Cainozoic and the initiation of antarctic glaciation: Oxygen and carbon analysis in DSDP sites 277, 279 and 281. *In*: Kennett, J.P., & Houtz, r., (Eds.), Initial reports of the deep sea drilling project. v. 29. Washington, D.C. U.S. Government Printing Office.

Shackleton, N., & Boersma, A., 1981. The climate of the Eocene Ocean. *Journal of the Geological Society*, London. v. 138. 153-157.

Shanmugam, G., 1988. Origin, Recognition and Importance of Erosional Unconformities in Sedimentary Basins. *In*: Kleinspehn, K.L., Paola, C (Eds), *New Perspectives in Basin Analysis*. Springer Verlag, New York. 83-108.

Sheriff, R. E. 1977. Limitations on resolution of seismic reflections and geological detail derivable from them. *In*: Payton, C. E., (Ed), *Seismic Stratigraphy – Applications to Hydrocarbon Exploration*. American Association of Petroleum Geologists, Memoir 26. 3-14.

Shipboard Scientific Party, 2005. Arctic Coring Expedition (ACEX): paleoceanographic and tectonic evolution of the central Arctic Ocean. IODP Preliminary Report. v. 302. <http://www.ecord.org/exp/acex/302PR.pdf>.

Shor, A.N., & Poore, R.Z., 1979. Bottom currents and ice rafting in the North Atlantic: Interpretation of Neogene depositional environment of Leg 49 cores. *In*: Luyendyk, B.P., Cann, J.R (Eds), *Initial Reports of the Deep Sea Drilling Project*. v. 49. U.S. Government. Printing Office. Washington D.C. 859-872.

Skogseid, J., Pedersen, T., Eldholm, O. & Larsen, B. T. 1992. Tectonism and magmatism during NE Atlantic continental break-up: the Vøring Margin. *In*: Storey, B. C., Alabaster, T., & Pankhurst, R. J., (Eds), *Magmatism and the causes of Continental Break-up*. Geological Society, London, Special Publication 68, 305-320.

Sloan, L.C., Walker, J.C.G., & Moore, T.C., 1995. Possible role of oceanic heat transport in early Eocene climate. *Paleoceanography*. v. 10, No2. 347-356

Smallwood, J.R., Towns, M.J., & White R.S., 2001. The structure of the Faeroe Shetland Trough from integrated deep seismic and potential field modelling. *Journal of the Geological Society, London*. v. 158. 409-412.

Smallwood, J. R. & Gill, C. E. 2002. The rise and fall of the Faroe-Shetland Basin: evidence from seismic mapping of the Balder Formation. *Journal of the Geological Society, London*. v 159. 627-630.

Smallwood, J.R., 2004. Tertiary inversion in the Faroe-Shetland Channel and the development of major erosional scarps. *In*: Davies, R.J., Cartwright, J.A., Stewart, S.A., Lappin, M & Underhill, J.R. (Eds), *3D Seismic Technology: Applications to the Exploration of Sedimentary Basins*. Geological Society, London, *Memoirs*, 29, 197-198.

Sørensen, A.B., 2003. Cenozoic basin development and stratigraphy of the Faroes area. *Petroleum Geoscience*. v. 9. 189–207.

Stewart, T.G., 1991. Glacial marine sedimentation from tidewater glaciers in the Canadian High Arctic. *Geological Society of America. Special paper* 261. 95-105.

St John, K.E.K., & Krissek, L.A., 2002. The Late Miocene to Pleistocene ice-rafting history of southeast Greenland. *Boreas*. v. 31. 28-35.

Stoker, M.S., Hitchen, K., & Graham, C.C., 1993. United Kingdom offshore regional report: the geology of the Hebrides and West Shetland shelves and adjacent deep-water areas. London: HMSO for the British Geological Survey

Stoker, M.S. 1995. The influence of glacial sedimentation on slope-apron development on the continental margin off Northwest Britain. *In*: Scrutton, R.A., Stoker, M.S., Shimmield, G.B., Tudhope, A.W., (Eds), *The Tectonics, Sedimentation and Paleooceanography of the North Atlantic Region*. Geological Society, London, *Special Publication*. 90. 159-177.

Stoker, M.S., Akhurst, M.C., Howe, J.A., & Stow, D.A.V., 1998. Sediment drifts and contourites on the continental margin off northwest Britain. *Sedimentary Geology*. v. 115. 33–51.

Stoker, M.S., 1999. Stratigraphic nomenclature of the UK North West Margin. 3. Mid- to late Cenozoic Stratigraphy. British Geological Survey, Edinburgh.

Stoker, M.S., Neilsen, T., van Weering, T.C.E., & Kuijpers, A., 2002a. Towards and understanding of the Neogene tectonostratigraphic framework of the NE Atlantic margin between Ireland and the Faroe Islands. *Marine Geology*. v. 188. 233-248.

Stoker, M.S., 2002b. Late Neogene development of the UK Atlantic margin. *In*: Doré, A.G.D., Cartwright, J., Stoker, M.S., Turner, J.P., & White, N. (Eds), *Exhumation of the North Atlantic Margin: Timing, Mechanisms and Implications for Petroleum Exploration*. Geological Society, London. Special Publication 196. 313-329.

Stoker, M.S. (Compiler), 2003. Neogene evolution of the glaciated European margin. STRATAGEM Project.

Stoker, M.S., Praeg, D., Hjelstuenc, B.O., Laberg, J.S., Nielsen, T., & Shannon, P.M., 2005. Neogene stratigraphy and the sedimentary and oceanographic development of the NW European Atlantic margin. *Marine and Petroleum Geology*. v. 22, Issues 9-10. 977-1005

Stow, D.A.V., 1979. Distinguishing between fine-grained turbidites and contourites on the Nova Scotian deep water margin. *Sedimentology*. v. 26. 371-387.

Stow, D.A.V., Holbrook, 1984. North Atlantic contourites: an overview. *In*: Stow, D.A.V., Piper, D.J.W (Eds), *Fine-Grained Sediments: Deep-Water Processes and Facies*. Geological Society Special Publication No.15. 245-256.

Stow, D.A.V., Faugères, J.C., Howe, J.A., Pudsey, C.J., & Viana, A.R., 2002. Bottom currents, contourites and deep-sea sediment drifts: current state-of-the-art. *In*: Stow, D.A.V., Pudsey, C.J., Howe, J.A., Faugères, J.C., & Viana, A.R. (Eds), *Deep-Water Contourite Systems: Modern Drifts and Ancient Series, Seismic and Sedimentary Characteristics*. Geological Society, London, Memoirs. 22. 73-84.

Talwani, M., & Eldholm, O., 1977. Evolution of the Norwegian-Greenland Sea. *Geological Society of America Bulletin*. v. 88. 969-999

Tearpock, D.J., & Bischke, R.E., 2002. *Applied subsurface geological mapping*. Prentice-Hall PTR.

Thiede, J., & Eldholm, O., 1983. Speculations about the paleodepth of the Greenland Scotland Ridge during late Mesozoic and Cenozoic times. *In*: Bott, M.H.P., Saxov, S., Taiwan, M., Thiede, J. (Eds.), *Structure and Development of the Greenland-Scotland Ridge*. Plenum Publishing Corporation, New York. 445-456.

Thiede, J., & Myhre, A.M., 1996. Introduction to the North Atlantic –Arctic Gateways: plate tectonic-palaeoceanographic history and significance. *In*: Thiede, J., Myhre, A.M., Firth, J.V., Johnson, G.L., & Ruddiman, W.F (Eds), *Proceedings of the Ocean Drilling Program, Scientific Results Leg 151: College Station, TX (Ocean Drilling Program)*. 3-23.

Thiede, J., Winkler, A., Wolf-Welling, T., Eldholm, O., Myhre, A., Baumann, K.H., Henrich, R., & Stein, R., 1998. Late Cenozoic history of the Polar North Atlantic: Results from Ocean Drilling. *Quaternary Science Reviews*. v. 17. 185-208.

Todd, B.J., Lewis, C.F.M., & Ryall, P.J.C., 1988. Comparison of trends of iceberg scour marks with iceberg trajectories and evidence of paleocurrent trends on the Skaglek Bank, northern Labrador Shelf. *Canadian Journal of Earth Sciences*. v. 25. 1374-1383.

Tripathi, A., Backman, J., Elderfield, H., & Ferretti, P. 2005. Eocene bipolar glaciation associated with global carbon cycle changes. *Nature*. v. 436, 341-346.

Turner, J. D. & Scrutton, R. A. 1993. Subsidence patterns in western margins: evidence from the Faroe-Shetland Basin. *In*: Parker, J. R., (Ed). *Petroleum Geology of Northwest Europe: Proceedings of the 4th Conference*, Geological Society, London, 975-983.

Turrell, W.R., Slessor, G., Adams, R.D., Payne, R., & Gillibrand, P.A., 1999. Decadal variability in the composition of Faroe Shetland Channel bottom water. *Deep-Sea Res. I*. v. 46. 1-25.

Uenzelmann-Neben, G. 2001. Seismic characteristics of sediment drifts: An example from the Agulhas Plateau, southwest Indian Ocean. *Marine Geophysical Researches*. v. 22. 223-243.

Van Raaphorst, W., Malschaert, H., Van Haren, H., Boer, W., & Brummer, G.J., 2001. Cross-slope zonation of erosion and deposition in the Faeroe-Shetland Channel, North Atlantic Ocean. *Deep-Sea Res. I*. v. 48. 567-591.

Vail, P.R., & Mitchum, R.M. (Compilers) 1977. Seismic Stratigraphy and Global Changes of Sea Level. *In*: Payton, C.E. (Ed) *Seismic Stratigraphy – applications to hydrocarbon exploration*. American Association of Petroleum Geologists Memoir 26. 47-205.

Velde, B., 1996. Compaction trends of clay-rich deep sea sediments. *Marine Geology*. v. 133. 193-201.

Vellinga, M., & Wood, R.A., 2002. Global climatic impacts of a collapse of the Atlantic thermohaline circulation. *Climate Change*. v. 54. 251-267.

Viana, A.R., Hercos, C.M., De Almeida, W., Magalhães, J.L.C., & De Andrade, S.B., 2002. Evidence of bottom current influence on the Neogene to Quaternary sedimentation along the northern Campos Slope, SW Atlantic Margin. *In*: Stow, D.A.V., Pudsey, C.J., Howe, J.A., Faugères, J.C., & Viana, A.R. (Eds), *Deep-Water Contourite Systems: Modern Drifts and Ancient Series, Seismic and Sedimentary Characteristics*. Geological Society of London Memoirs, 22. 249-259.

Vogt, P.R., 1972. The Faeroe-Iceland-Greenland aseismic ridge and the Western Boundary Undercurrent. *Nature*. v. 239. 79-81.

Vogt, P.R., Perry, R.K., Feden, R.H., Fleming, H.S., & Cherkis, N.Z., 1981. The Greenland-Norwegian Sea and Iceland environment: Geology and Geophysics. *In*: Nairn, A.E.M., Churkin, M., & Stehli, F.G (Eds), *The Ocean Basins and Margins (Vol 5), The Arctic Ocean*: New York (Plenum). 493-598

Vogt, P.R., Crane, K., & Sundvor, E., 1994. Deep Pleistocene iceberg plowmarks on the Yermak Plateau: Sidescan and 3.5kHz evidence for thick calving ice fronts and a possible marine ice sheet in the Arctic Ocean. *Geology*. v. 22. 403-406.

Volpi, V., Camerlenghi, A., Hillenbrand, C.-D., Rebesco, M., & Ivaldi, R., 2003. Effects of biogenic silica on sediment compaction and slope stability on the Pacific margin of the Antarctic Peninsula. *Basin Research*. v. 15, No. 3. 339-363

Waagstein R. 1988: Structure, composition and age of the Faeroe basalt plateau. Geological Society, London, Special Publication 39. 225-238.

Wade, B.S., & Kroon, D., 2002. Middle Eocene regional climate instability: Evidence from the western North Atlantic. *Geology*. v.30, No.11. 1011-1014.

Wadhams, P., 2000. *Ice in the ocean*. Gordon and Breach Science Publishers.

White, R. S. 1989. Initiation of the Iceland Plume and Opening of the North Atlantic. *In*: A. J. Tankard & H. R. Balkwill (Eds), *Extensional Tectonics and Stratigraphy of the North Atlantic Margins*. American Association of Petroleum Geologists, Memoir 46, 149-154.

White, R. S. & McKenzie, D. 1989. Magmatism at rift zones: The generation of volcanic continental margins and flood basalts. *Journal of Geophysical Research*. v. 94, 7685-7729.

White, N. & Lovell, B. 1997. Measuring the pulse of a plume with the sedimentary record. *Nature*. v. 387, 888-891.

Williams, G.L., Brinkhuis, H., Pearce, M.A., Fensome, R.A., & Weegink, J.W., 2004. Southern Ocean and Global dinoflagellate cyst events compared: Index events for the Late Cretaceous-Neogene. *In*: Exon, N.F., Kennett, J.P., Malone, M.J. (Eds), *Proceedings of the Ocean Drilling Program, Scientific Results Volume 189*. 3-49.

Wold, C.N. 1994. Cenozoic sediment accumulation on drifts in the northern North Atlantic. *Paleoceanography*. v. 9. 917-941.

Wong, H. K., Lüdmann, T., Baranov, B. V., Ya. Karp, B., Konerding, P., & Ion, G., 2003. Bottom current controlled sedimentation and mass wasting in the northwestern Sea of Okhotsk. *Marine Geology*. v. 201, No.4. 287-305.

Wright, J.D., Miller, K.G., and Fairbanks, R.G., 1992. Early and middle Miocene stable isotopes: Implications for deepwater circulation, climate and tectonics, *Paleoceanography*. v. 7. 357-389.

Wright, J.D., Miller, K.G., 1996. Control of North Atlantic Deep Water circulation by the Greenland-Scotland Ridge. *Paleoceanography*. v. 11, 157-170.

Wright, J.D., 1998. The Role of the Greenland-Scotland Ridge in Cenozoic Climate Change. *In*: Crowley, T.J., & Burke, K., (Eds), *Tectonic Boundary Conditions for Climate Reconstructions*, Oxford University Press. 192-211.

Wynn, R.B., & Stow, D.A.V., 2002. Classification and characterisation of deep-water sediment waves. *Marine Geology*. v. 192. 7-22.

Zachos, J.C., Lohmann, K.C., Walker, J.C.G., & Wise, S.W., 1993. Abrupt Climate Change and Transient Climates during the Paleogene: A Marine Perspective. *The Journal of Geology*. v. 101. 191-213.

Zachos, J., Pagani, M., Sloan, L., Thomas, E., & Billups, K., 2001. Trends, rhythms, and aberrations in global climate 65 Ma to present. *Science*. v. 292, 686–693.

Ziegler, P. A. 1990. *Geological Atlas of Western and Central Europe*. Geological Society, London. pp 239



## Appendix 1: Seismic database

2D seismic surveys used in this study:

Survey Name	Number of Lines
AHL94-202	29
C92	48
C93	23
DEL93	19
GA95-NSB	40
NWSHET2D	19
NWZ96	14
OF94	37
SFE95	21
WEST SHET	21
WG84-RR	8
WS94	64
WS_MASTER, Comprised of:	370
AUK92-AH	
DGS95	
E-84	
M90-WS	
M91-FT6	
M92-FT6	
NEST-90	
NSB-96	
OF-95	
RM90-WS	
RM91-FT6	
RM92-FT6	
SF94	
WG-RR-84	
WSD-91	
WSD-92	
92-07	

High resolution 2D seismic data used in this study:

BPHR00	26
--------	----

3D seismic surveys used in this study:

<b>Survey Name</b>	<b>Area (km<sup>2</sup>)</b>
REPRO-SF96	2540
SF96	3680
SF97-3D	1790
T4-S	1300
T4-WSH3D	1090
T61/T62	2900
T6	7450
W95001_2	680

## Appendix 2. Well Database

Wells available for this study are listed below. Wells which are referenced directly in the study are marked in red. List of wells compiled by A. Robinson.

### Quadrant 202

Well Name	X location	Y location	Composite Log	Velocity Log	Biostratigraphic Report	Year drilled	Current Owner	TD
202/02- 1	408936.7423	6635392.942	Y	Y	Y	1974	ExxonMobil	1219.81m
202/03- 1A	415210.5757	6637011.514	Y	Y	Y	1974	BP	1775.52m
202/03- 2	416165.7613	6644671.556		Y	Y	1977	BP	1524.51m
202/03a- 3	412528.8429	6652273.716	Y			1987	BP	2553.34m
202/08- 1	414017.0942	6629403.981	Y			1974	Shell	1685.54m
202/09- 1	427010.6682	6629284.448	Y	Y		1987	ExxonMobil	1665.12m
202/18- 1	418230.3438	6583399.641	Y			1991	Total	3102.86m
202/19- 1	422873.0213	6578134.499	Y			1984	Shell	3188.82m

### Quadrant 204

Well Name	X location	Y location	Composite Log	Velocity Log	Biostratigraphic Report	Year drilled	Current Owner	TD
204/19- 1	425696.9469	6695460.223		Y		1986	BP	4683.25m
204/19- 2	429529.5925	6694909.028	Y	Y	Y	1991	BP	967.98m
204/22- 1	409318.4363	6678205.027	Y	Y	Y	1989	BP	2774.29m
204/22- 2	404567.2121	6684724.037		Y		1994	BP	3711.0m
204/23- 1	417155.7799	6679141.945	Y	Y	Y	1987	BP	3881.99m
204/24- 1A	430067.757	6687121.622	Y	Y	Y	1990	BP	3019.8m
204/24A-2Y	425908.2901	6685841.315		Y		1992	BP	954.12m
204/25- 1	441068.1734	6688583.449	Y	Y		1991	Amerada	2904.74m
204/27a- 1	408162.3556	6671083.802	Y	Y		1990	BP	2179.69m
204/28- 1	414900.4888	6670815.408	Y	Y		1981	BP	1974.0m
204/29- 1	424741.495	6664614.168	Y	Y		1986	Talisman	2243.33m
204/30- 1	438532.8396	6663552.34	Y	Y	Y	1975	Amerada	1981.81m
204/30a- 2	443655.6327	6653401.599	Y	Y		1991	Amerada	3442.11m

## Quadrant 205

Well Name	X location	Y location	Composite Log	Velocity Log	Biostratigraphic Report	Year drilled	Current Owner	TD
205/09- 1	479717.1108	6741448.283	Y	Y	Y	1989	BP	4748.78m
205/10- 1A	496841.2137	6735383.939	Y			1981	BP	2453.6m
205/10- 2B	496950.0404	6736438.887	Y	Y		1984	BP	998.52m
205/10- 3	499491.0229	6736333.923	Y	Y		1985	BP	2790.39m
205/14- 1	482755.9945	6711555.364	Y			1990	Shell	2738.33
205/16- 1	452282.7054	6690972.638	Y	Y		1986	BP	4313.0m
205/20- 1	493622.9671	6702898.024	Y	Y	Y	1974	Total	623.32m
205/21- 1A	453235.4768	6672190.859	Y	Y	Y	1974	Shell	1367.94m
205/21- 2	450962.9591	6678554.399	Y	Y		1990	Shell	3646.93m
205/22- 1A	457570.7403	6681758.735	Y			1974	BP	3229.0m
205/23- 1	476168.7222	6674154.126	Y	Y	Y	1975	ExxonMobil	2743.2m
205/25- 1	495120.0189	6670626.929	Y		Y	1977	ConocoPhillips	2600.25m
205/26- 1	449540.0614	6664324.598	Y		Y	1975	BP	2136.04m
205/26a- 2	450184.6008	6654175.332	Y	Y	Y	1982	BP	2467.97m
205/26a- 3	444385.397	6656747.813	Y			1990	Amerada	2875.36m
205/27a- 1	460631.2363	6659552.138	Y			1982	Shell	2626.77m
205/30- 1	490118.8164	6665801.184	Y	Y	Y	1974	Talisman	2194.56m

## Quadrant 206

Well Name	X location	Y location	Composite Log	Velocity Log	Biostratigraphic Report	Year drilled	Current Owner	TD
206/01- 1A	508849.309	6746237.071	Y	Y		1985	BP	3032.15m
206/01- 2	506507.2186	6758919.017	Y	Y		1986	Shell	4532.68m
206/02- 1A	513026.8746	6762473.595	Y	Y	Y	1980	Shell	4493.97m
206/03- 1	530408.8905	6749528.343	Y	Y		1985	BP	4940.81m
206/04- 1			Y			1996	ConocoPhillips	4149.24m
206/05- 1	544941.8528	6756610.937	Y	Y	Y	1976	Total	4145.28m
206/08- 1A	524393.9367	6727888.273	Y	Y		1977	BP	2327.0m
206/08- 2	528298.6861	6733620.947	Y			1978	BP	1890.0m
206/08- 3	527185.299	6729190.62	Y			1978	BP	1945.0m
206/08- 3Z	527114.204	6729252.955	Y	Y		1978	BP	2577.0m
206/08- 4	527283.1307	6726592.24	Y	Y		1979	BP	3008.01m
206/08- 5	524515.3335	6727789.631	Y			1980	BP	2135.0m
206/08- 6A	522430.8349	6734233.352	Y	Y		1980	BP	2739.3m
206/08- 7	524528.6704	6727356.759	Y	Y		1985	BP	2334.4m
206/08- 8	524982.9821	6728647.311	Y	Y		1991	BP	2499.36m
206/08- 9Z	524931.2626	6728623.671	Y	Y		1992	BP	3725.88m
206/09- 1	538705.7679	6738301.258	Y	Y		1977	BP	2777.95m
206/09- 2	534455.0593	6739127.524		Y		1978	ExxonMobil	2464.92m
206/10a- 1	546274.4663	6741609.269	Y	Y		1980	ExxonMobil	2989.48m
206/11- 1	503147.26	6719272.333	Y			1977	BP	4620.01m
206/12- 1	512766.5381	6718026.045	Y			1972	Amerada	1727.0m
206/12- 2	513907.003	6723106.152	Y	Y		1977	Amerada	2563.98m

## Quadrant 207

Well Name	X location	Y location	Composite Log	Velocity Log	Biostratigraphic Report	Year drilled	Current Owner	TD
207/01- 1	557948.4161	6762313.157	Y	Y		1977	ChevronTexaco	1466.7m
207/01- 2	560237.868	6757891.48	Y	Y	Y	1977	ChevronTexaco	1761.74m
207/01- 3	558666.896	6759705.753	Y	Y		1977	ChevronTexaco	1434.39m
207/01a- 4Z	555919.0653	6751440.597	Y			1990	ChevronTexaco	2682.24m
207/02- 1	568410.647	6761157.097	Y	Y		1974	Shell	2058.92m

## Quadrant 208

Well Name	X location	Y location	Composite Log	Velocity Log	Biostratigraphic Report	Year drilled	Current Owner	TD
208/15- 1A	602361.2791	6836923.912	Y		Y	1979	BP	3165.17m
208/15- 2			Y			1995	BP	2549.56m
208/17- 1	564527.6831	6814401.036	Y	Y	Y	1985	BP	4846.32m
208/17- 2			Y			1995	BP	3702.84m
208/19- 1	587635.5754	6816214.017	Y	Y	Y	1983	BP	3334.51m
208/21- 1	562524.7673	6793723.684	Y	Y		1985	Total	3610.33m
208/22- 1	568717.209	6788148.501	Y	Y	Y	1986	ExxonMobil	2286.0m
208/23- 1	579867.8135	6782858.554	Y		Y	1983	ENI	2066.85m
208/24- 1A	588653.1071	6785344.585	Y	Y		1986	BP	2159.51m
208/26- 1	563558.1588	6776670.174	Y			1983	BP	3901.99m
208/27- 1	569106.2451	6773831.986	Y			1979	BP	1525.52m
208/27- 2	572857.727	6778686.23	Y	Y		1982	BP	1401.78m

## Quadrant 209

Well Name	X location	Y location	Composite Log	Velocity Log	Biostratigraphic Report	Year drilled	Current Owner	TD
209/03- 1A	627532.6291	6860776.88	Y			1980	ExxonMobil	2316.48m
209/04- 1A	641860.7152	6868561.066	Y			1985	ENI	4051.71m
209/06- 1	612727.4001	6839641.388	Y		Y	1980	ChevronTexaco	3902.66m
209/09- 1	640148.0576	6850752.333	Y			1980	BP	2699.92m

## Quadrant 213

Well Name	X location	Y location	Composite Log	Velocity Log	Biostratigraphic Report	Year drilled	Current Owner	TD
213/23- 1	476306	6788177	Y	Y	Y	1999	ExxonMobil	4374.79m

## Quadrant 214

Well Name	X location	Y location	Composite Log	Velocity Log	Biostratigraphic Report	Year drilled	Current Owner	TD
214/04- 1	540175.13	6870659.85	Y	Y	Y	1999	ExxonMobil	4349.5m
214/17- 1	511909	6800924	Y	Y	Y	1998	ExxonMobil	2698.39m
214/19- 1			Y			1996	Shell	4867.0m
214/26- 1	509192.17	6776311.91	Y	Y	Y	1996	ConocoPhillips	2743.2m
214/27- 1	518747.2494	6770299.237	Y	Y	Y	1985	ChevronTexaco	5030.72m
214/27- 2	513722.1947	6776197.527	Y	Y	Y	1986	ChevronTexaco	4425.7m
214/28- 1	527376.3534	6775721.239	Y	Y	Y	1984	ExxonMobil	5124.3m
214/29- 1	541015.7927	6768409.936	Y	Y	Y	1985	Total	5032.71m
214/30- 1	548343.2414	6781254.688	Y	Y	Y	1984	BG	3323.84m

## BGS Boreholes

Well Name	X location	Y location	Composite Log	Velocity Log	Biostratigraphic Report	Year drilled	Current Owner	TD
99/3	409047.46	6699788.17			Y	1999	BGS	166.5m
99/6	371966.87	6696922.79			Y	1999	BGS	36m

